

The anatomical description of the erector spinae, paravertebral and epidural block for post-operative pain management in paediatric care.

SABASHNEE GOVENDER
11083647

Ph.D. (Anatomy)

Supervisor: Albert-Neels Van Schoor¹
Co-supervisor: Adrian Bosenberg²

¹ Department of Anatomy, University of Pretoria


² Department Anaesthesiology and Pain Management, University
Washington and Seattle Children's Hospital, Seattle, WA, USA

2018 – 2020

In the school of Medicine, Faculty of Health Sciences,
University of Pretoria, Pretoria, South Africa

Declaration

I declare that the dissertation that I am hereby submitting to the University of Pretoria for the PhD degree in Anatomy, is my own work and that I have never before submitted it to any other tertiary institution for any degree.



Ms S Govender

21st October 2020

Acknowledgements

To the families of the cadaveric donors used in this research, I would like to express my sincerest gratitude for your selfless act. Through your contribution, we can make strides in the field of medical research and improve the future quality of patient care.

I would like to thank my supervisor, Prof. Albert-Neels van Schoor for all his valued insights, contributions, time and effort put into this thesis. I am extremely fortunate to have had a supervisor who has been so passionate about my work, which motivated me, to do even better. Your support, advice and guidance were tremendously valued through every step of the way.

To my co-supervisor, Prof. Adrian Bosenberg: Thank you for your guidance and recommendation for every article that was published. Your knowledgeable, worldly insights were extremely appreciated.

To Dr Dwayne Mohr: Thank you for your patience and commitment. Your availability and willingness to assist were greatly appreciated.

To Dr Alfred Musekiwa: Thank you for all the statistical analyses that were done in this thesis.

To Prof. Suleman and Prof. Lockhart from the Radiology Department at Steve Biko Academic Hospital: Thank you for your assistance with the procurement of the scans used in this study.

I would also like to thank the talented Miss Jade Naicker, who drew and recreated images used in this thesis.

A special thanks also to Mr Daniël van Tonder, who assisted with the data collection.

To my friends, who are my cheerleaders: Thank you for your encouragement and the distractions when it was needed. A special mention goes to Mr Paul Akkerman who

assisted me with the interpretation of various components into the late hours of the morning.

To Mrs Pillay-Addinall, my partner in crime: Thank you for being my 24/7 soundboard. Your support and motivation are deeply cherished.

To Dr Llewelyn Davies, my person: Thank you for your patience and equanimity at all times. Your continuous encouragement and constant motivation were truly treasured.

To my parents, my pillars of strength: Your constant support and unconditional love have always been my light throughout life. Thank you for standing by me through this journey. I am grateful for your selfless love, care and sacrifices that shaped my life.

To my brother: Growing up, you have constantly challenged me to do and be better. You have always been a role model, setting your own path. Thank you for your constant positivity, random jokes and motivational speeches. Your advice, support and reassurance were sincerely appreciated throughout this journey.

Summary

The anatomical description of the erector spinae -, paravertebral - and epidural block for post-operative pain management in paediatric care

S Govender

Supervisor: Prof AN van Schoor

Co-supervisor: Prof AT Bosenberg

Department of Anatomy: Clinical Anatomy, School of Medicine, Faculty of Health Sciences, University of Pretoria, South Africa

The fundamental indicative constituent for any successful clinical procedure is patient satisfaction, which is directly related to post-operative analgesia. In paediatric care, due to the nature of the patient – and depending on the age group – it is often difficult, or even impossible, to fully understand the extent of pain perceived, leading to insufficient pain management. A variety of regional anaesthetic techniques have been thoroughly investigated for the ease of administration, as well as enhanced patient satisfaction. Coupled with image modalities, these blocks can be safe and efficient. However, these investigations mainly apply to an adult population. Paediatric procedures may be inaccurately extrapolated from an adult population, when the anatomical discrepancies that exist between population groups are not taken into consideration. Until recently, the gold standard for paediatric truncal procedures relied solely on paravertebral and epidural blocks. With the discovery of the novel interfascial erector spinae plane block, however, this is no longer the case. This block is hypothesised to target the ventral and dorsal rami of spinal nerves, as local anaesthetic is deposited into the erector spinae fascial plane space. The therapeutic effect of the block is attributed to the cranio-caudal spread of anaesthetic over multiple vertebral levels within the tissue plane. This ‘happily accidental’ block serves as a “paravertebral block by proxy” and is an alternative approach, targeting similar nerves as in the paravertebral and epidural blocks. However, the anatomy of the erector spinae plane block is not fully understood. This study aimed to investigate the anatomical differences of these three blocks for the management of post-operative pain

in paediatric care, based on observations and measurements from a fresh paediatric cadaver sample, as well as ultrasound and computed tomography scans. Apart from the easily identifiable bony landmarks, together with the distant application of the erector spinae plane block, the block offers a higher safety profile with various clinical advantages such as improved pre- and post-operative pain management, as well as reduced opioid requirement. In conclusion, it is vital to acknowledge the anatomical differences that exist in a paediatric population for the safe and successful administration of any regional technique to improve the management of pain in a vulnerable population.

Keywords: Erector spinae plane block, paravertebral block, epidural block, interfascial block, paediatric, regional anaesthesia, pain management

Contents

Declaration.....	
Acknowledgements.....	
Summary	
List of Figures	
List of Tables	
Chapter 1 – Introduction	1
Chapter 2 – Erector spinae plane (ESP) block	4
2.1 Anatomy	6
2.2 Ultrasound anatomy.....	8
a) Transverse approach	8
b) Parasagittal approach	10
2.3 Aim	11
2.4 Research objectives	12
2.5 Material and methods	12
a) Ultrasound component.....	13
b) Retrospective CT component.....	15
c) CT component (real-time spread of contrast medium)	17
d) Cadaveric component	17
2.6 Statistical analysis	21
2.7 Results.....	22
a) Ultrasound component.....	23
b) Retrospective CT component.....	28
c) CT component (real-time spread of contrast medium)	41
d) Cadaveric component	42
2.8 Discussion	47
a) Block measurements.....	47

b) Injectate spread.....	49
2.9 ESP block compared to other neuraxial blocks.....	67
2.10 Advantages and disadvantages.....	73
2.11 Strength and limitations.....	75
a) Practical implications.....	75
b) Limitations.....	76
c) Future studies.....	77
2.12 Conclusion.....	78
Chapter 3 – Paravertebral block.....	79
3.1 Anatomy.....	81
3.2 Ultrasound anatomy.....	83
a) Transverse plane/technique.....	83
b) Paramedian plane/technique.....	85
3.3 Aim.....	86
3.4 Research objectives.....	86
3.5 Material and Methods.....	86
a) Ultrasound component.....	86
b) Retrospective CT component.....	88
3.6 Statistical analysis.....	89
3.7 Results.....	89
a) Ultrasound component.....	90
b) CT component.....	96
3.8 Discussion.....	111
a) Block measurements.....	111
b) Injectate spread.....	114
3.9 Paravertebral blocks versus ESP blocks.....	119

3.10	Advantages and disadvantages.....	121
3.11	Limitations.....	122
3.12	Conclusion.....	122
Chapter 4 – Epidural block		123
4.1	Anatomy	126
4.2	Ultrasound anatomy.....	128
	a) Midline approach.....	129
	b) Paramedian approach.....	129
4.3	Aim	131
4.4	Research objectives	132
4.5	Materials and Methods	132
	a) Ultrasound component.....	132
	b) Retrospective CT component.....	133
4.6	Statistical analysis	134
4.7	Results.....	135
	a) Ultrasound component.....	135
	b) CT component.....	139
4.8	Discussion	147
	a) Block measurements.....	148
	b) Injectate spread.....	152
4.9	Epidural blocks versus ESP blocks.....	156
4.10	Advantages and disadvantages.....	158
4.11	Limitations.....	159
4.12	Conclusion.....	159
Chapter 5 – Conclusion of the thesis		161
References		163

Appendix A	185
Appendix B	188
Appendix C	192
Appendix D	200
Appendix E	201
Appendix F.....	202
Appendix G.....	203

List of Figures

- Figure 1: The erector spinae fascial plane space and the structures that contribute to its borders. Key: a – spinal nerve, b – ventral rami, c – dorsal rami, d – transverse process, e – lamina, f – spinous process, g – superior costotransverse ligament, h – intertransverse ligament, i – injectate inserted into the erector spinae fascial plane space, green arrows – spread of injectate8
- Figure 2: The ultrasound anatomy as seen on the ultrasound screen of a transverse section scan taken at vertebral level T5.....9
- Figure 3: The ultrasound anatomy as seen on the ultrasound screen of a parasagittal section scan taken at vertebral level T5. The muscular complex consists of the levatores costarum, rotatores spinae and external intercostal muscles.....11
- Figure 4: The ultrasound bony landmarks in a transverse (A) and parasagittal orientation (B) taken at vertebral level T5. The green dotted arrow represents the needle course in a transverse alignment, while the white arrows represent the needle course in a parasagittal alignment.14
- Figure 5: A transverse ultrasound image showing the various measurements taken. Measurements that were taken include; A – the distance from the spinous process to the lateral tip of the transverse process; B – the depth from the skin to the erector spinae fascial space (tip of the transverse process); C – the depth from the skin to the most superficial point of the erector spinae muscle; D – the depth from the skin to the most superficial point of the rhomboid major muscle; E – the depth from the skin to the most superficial point of the trapezius muscle.15

Figure 6: An axial CT image through the thorax at vertebral level T5. Measurements that were taken include; A – the distance from the spinous process to the lateral extent of the transverse process; B – the depth from the skin to the ESFP space (tip of the transverse process); C – the depth from the skin to the most superficial point of the erector spinae muscle; D – the depth from the skin to the most superficial point of the rhomboid major muscle; E – the depth from the skin to the most superficial point of the trapezius muscle.16

Figure 7: Photographic images showing A – the skin reflected to reveal the trapezius muscle, B – the rhomboid muscles, C – the individual bands of the erector spinae muscle, D & E – the cleaned vertebra, F – removal of the transverse process and the articulating rib to reveal the spinal cord and rami deep to it (indicated by the stars)20

Figure 8: Bar graph showing the results from the paired t-test for the statistically significant measurements between the left and right sides. The error bar represents the standard error in relation to the mean.....30

Figure 9: Scatter plot displaying the correlation between T5StoESFPS in cm to age in months (top image), T8StoESFPS in cm to age in months (middle image), T8SPtoTP in cm to age in months (bottom image).....39

Figure 10: Lateral view of a three-dimensional volume-rendered CT reconstruction of contrast injectate spread in a fresh neonate. Green arrows represent the craniocaudal spread within the erector spinae fascial plane space when introducing contrast material at vertebral level T8. Yellow arrows represent the craniocaudal spread within the erector spinae fascial plane space and posterior to the erector spinae muscle at the spinous and transverse processes of vertebral level T1042

Figure 11: Photographic images displaying the A – surface staining of the superficial muscles of the back. B – extensive craniocaudal spread both deep and superficial to the erector spinae fascial plane C – methylene blue dye found over the posterior aspect of the lamina and transverse process near the neural/intervertebral foramina D – methylene blue dye in the epidural space and surrounding the spinal nerves as

they come off the spinal cord E – methylene blue dye staining the ganglion (i), dorsal rami (ii) and ventral rami (iii)	44
Figure 12: The anatomy of the thoracic paravertebral space and the structures that contribute to the borders of the space.	82
Figure 13: Image displaying the probe orientation, a transverse plane of the expected anatomy at vertebral level T5, as well as a transverse ultrasound image at vertebral level T5 during a paravertebral block.	84
Figure 14: Images showing the needle course as it makes contact with the transverse process (A & B), before being ‘walked-off’ the inferior edge of the transverse process (C) into the paravertebral space.	85
Figure 15: A transverse ultrasound image showing the various measurements taken. Measurements included: A – the distance from the spinous process to the lateral tip of the transverse process; B – the distance from the spinous process to the hypothetical needle insertion site; C – the depth from the skin to the transverse process; D – the depth from the skin to the paravertebral space; E – the depth from the skin to the anterior border of the rib.....	87
Figure 16: An axial thoracic CT image at vertebral level T5. Measurements included: A – the distance from the spinous process to the hypothetical needle insertion site; B – the distance from the spinous process to the lateral tip of the transverse process; C – the depth from the skin to the transverse process; D – the depth from the skin to the paravertebral space; E – the depth from the skin to the anterior border of the rib.	89
Figure 17: Scatter plot displaying the correlation between SPtoNeedle (top image - T8 in orange and T5 in blue) and SPtoTP (bottom image - T8 in orange and T5 in blue) in cm and weight in kg	94

Figure 18: Bar graph showing the results from the paired t-test for the statistically significant measurements. The error bar represents the standard error in relation to the mean.....98

Figure 19: Bar graph showing the results from the paired t-test for the statistically significant measurements. The error bar represents the standard error in relation to the mean.....101

Figure 20: Scatter plot displaying the correlation between: T5SkintoRib in cm to age in months (top/first image), T8SPtoTP in cm to age in months (middle/second image), T8SkintoTP in cm to age in months (middle/third image), T8SkintoTP in cm to age in months (bottom/last image).109

Figure 21: A right lateral view of the epidural space, with the right side of the vertebral arch removed. Anterior, posterior parts and its related borders.128

Figure 22: Ultrasound image displaying the paramedian plane of the thoracic epidural block.131

Figure 23: A median sagittal ultrasound image of the vertebral column showing the various measurements taken. Measurements taken: A – the distance from the skin to the anterior border of the ligamentum flavum; B – the distance from the skin to the anterior border of the ligamentum flavum at an incline; C – the distance from the inferior borders of the adjacent spinous process.133

Figure 24: A CT scan of a sagittal section through the vertebral column. From this view, the 5th and 8th vertebral levels can be identified. Measurements taken: A – the distance from the skin to the anterior border of the ligamentum flavum; B – the distance from the skin to the anterior border of the ligamentum flavum at an incline; C – the distance from the inferior border of the upper spinous process of the interspinous space and the superior border of the lower spinous process.134

Figure 25: Scatter plot displaying the correlation between T8Skintolig in cm to age in months.....142

List of Tables

Table 1. Results of the paired t-test of the erector spinae plane measurements taken from the neonatal ultrasound scans.....	24
Table 2. Descriptive statistics summary after pooling the right and left sides for the ultrasound component for the neonatal group.	25
Table 3: Results from the linear regression analysis displaying the correlation between the measurements and variables.....	26
Table 4. Multivariant regression analysis for determining the depth to the erector spinae fascial plane space in a preterm neonatal sample.	27
Table 5. Results of the paired t-test of the erector spinae plane measurements taken from the neonatal CT scans (group 1).	29
Table 6. Results of the paired t-test of the erector spinae plane measurements taken from the infant CT scans (group 2).	31
Table 7. Results of the paired t-test of the erector spinae plane measurements taken from the children CT scans (group 3).	32
Table 8. Descriptive statistics summary after pooling the right- and left sides for the CT component (group 1).....	33
Table 9. Multivariant regression analysis for determining the depth from the skin to the erector spinae fascial plane space using the data from the CT component (group 1).	34
Table 10. Descriptive statistics summary after pooling the right- and left sides for the CT component (group 2).....	35

Table 11. Multivariant regression analysis for determining the depth from the skin to the erector spinae fascial plane space using the data from the CT component (group 2).	36
Table 12. Descriptive statistics summary after pooling the right- and left sides for the CT component (group 3).....	37
Table 13. Multivariant regression analysis for determining the depth from the skin to the erector spinae fascial plane space using the data from the CT component (group 3).	40
Table 14. Summary of the results obtained when replicating the erector spinae plane block in the neonatal cadavers.	46
Table 15. List of authors who have performed the erector spinae plane block on a paediatric sample.	59
Table 16. Results of the paired t-test of the paravertebral measurements taken from the neonate ultrasound scans.....	91
Table 17. Descriptive statistics summary after pooling the right- and left sides for the ultrasound component.	92
Table 18. Multivariant regression analysis for determining the depth to the paravertebral space in the ultrasound component.....	95
Table 19. Results of the paired t-test of the paravertebral measurements taken from the neonatal CT scans (group 1).	96
Table 20. Results of the paired t-test of the paravertebral measurements taken from the infant CT scans (group 2).	99
Table 21. Results of the paired t-test of the paravertebral measurements taken from the children CT scans (group 3).	100

Table 22. Descriptive statistics summary after pooling the right- and left sides for the CT component (group 1).....	102
Table 23. Multivariant regression analysis for determining the depth to the paravertebral space (group 1).	103
Table 24. Descriptive statistics summary after pooling the right- and left sides for the CT component (group 2).....	104
Table 25. Multivariant regression analysis for determining the depth from the skin to the erector spinae fascial plane space using the data from the CT component (group 2).	105
Table 26. Descriptive statistics summary after pooling the right- and left sides for the CT component (group 3).....	106
Table 27. Multivariant regression analysis for determining the depth from the skin to the erector spinae fascial plane space using the data from the CT component (group 3).	110
Table 28. Descriptive statistics summary of the epidural measurements taken from the neonate ultrasound scans.....	135
Table 29. Multivariant regression analysis for determining the depth to the epidural space in a preterm neonatal sample.....	137
Table 30. Descriptive statistics summary of the epidural measurements taken from the neonatal CT scans.....	139
Table 31. Descriptive statistics summary of the epidural measurements taken from the infant CT scans.....	140
Table 32. Descriptive statistics summary of the epidural measurements taken from the children CT scans.....	140

Table 33. Multivariant regression analysis for determining the depth to the epidural space (group 1).	143
Table 34. Multivariant regression analysis for determining the depth to the epidural space (group 2).	145
Table 35. Multivariant regression analysis for determining the depth to the epidural space (group 3).	146
Table 36. Skin-to-epidural space distance formulae as described in the literature from previous authors.	151

Chapter 1 – Introduction

The fundamental indicative constituent for any successful clinical procedure is patient satisfaction, which is directly related to post-operative analgesia. Pain can be highly subjective and dependent on patient experience (Garcia *et al.*, 2017). In paediatric care, due to the nature of the patient – and depending on the age group – it is often difficult, or even impossible, to obtain a definite understanding of the extent of pain perceived, possibly leading to insufficient pain management. Furthermore, insufficient treatment of pain in paediatric patients may lead to amplified physiological and behavioural responses to future noxious events, or even high mortality rates (Keech, 2015). Results show that paediatric patients younger than four years of age may lack the cognitive ability or vocabulary to express their symptoms, whereas patients older than four years of age can formulate appropriate retorts. Additionally, paediatric patients between six and eight years of age are able to use visual analogue pain scales to indicate their pain levels (Diedericks, 2006).

The American Academy of Paediatrics released a paper in which they reported on the barriers to pain control management in children. The report consists of a summary of six points that need to be considered when treating paediatric patients. These points include the myth that children, especially infants, do not feel pain the way adults do, or if they do, there is no untoward consequence; the lack of assessment and reassessment for the presence of pain; the misunderstanding of how to conceptualise and quantify a subjective experience; the lack of knowledge of pain treatment. The report also addressed the notion that treating pain in children is tiring and time-consuming with the constant fear of adverse effects of analgesic medications (Committee on Psychosocial Aspects of Child and Family Health and Task Force on Pain in Infants, Children, and Adolescents, 2001).

Before practitioners can perform any clinical procedure, surgeons or anaesthesiologists evaluate the negative and positive outcomes for each approach to best determine which would provide the most effective results, with the patient's safety being the main focus. Factors such as location, ease of access, availability of equipment, peri- and post-operative analgesia, reduced opioid consumption and quicker hospital recovery time, influence the decision (Garcia *et al.*, 2017).

It is important to be aware of variations in the anatomy and pharmacology in the paediatric population, prompting the need to adjust techniques and dosage accordingly. Additionally, paediatric central neuraxial techniques can be challenging to anaesthetists' mostly because these techniques are performed under general anaesthesia, eliminating the safety of routine 'awake placement' employed in adults (Wong and Lim, 2019).

In recent years, interfascial plane blocks have become increasingly popular. The addition of readily available ultrasound technology and the production of longer-lasting amide local anaesthetics has had an impact on this exponential growth in fascial plane block research (Pourkashanian *et al.*, 2019). The development of fascial plane blocks allows for the anaesthetic to be injected into a tissue plane rather than directly around the nerve(s), permitting a passive spread within the tissue plane or adjacent tissue compartments (Chin, 2019). The use of ultrasound guidance makes it easier to identify fascial planes and to gain access to the targeted area(s). Due to the direct visualisation, there is no need to rely on tactile "pops" and "clicks" to confirm needle placement (Elsharkawy *et al.*, 2018). Ultrasound guidance has proved to increase success rates and reduce the risk of complications, as the surrounding structures can be avoided (Gerrard and Roberts, 2012).

Either paravertebral - or epidural nerve blocks are currently highly recommended as the gold standard for paediatric truncal surgery. Recently, Forero *et al.* (2016) developed and discussed a novel technique – the erector spinae plane (ESP) block – that can be administered for surgeries in the cervical-, thoracic -and abdominal regions. However, this has struck controversy due to the similarities between this relatively new interfascial plane block and the paravertebral block. Several questions, such as "Is the multilevel spread dependent on the volume of anaesthesia used?", "Is the ESP block another name for the paravertebral block?", "Will the ESP block provide sufficient post-operative analgesia coverage?", "Is the anaesthetic spread confined to the erector spinae fascia only?", have been raised.

Currently, only a few papers report on the clinical aspects of ESP blocks in paediatric patients (Muñoz *et al.*, 2017; Ueshima and Otake, 2018). Fewer still have examined and described the anatomy of this block in the paediatric population. This study, therefore, aims to shed light on the anatomy of the erector spinae fascial space to understand the

ESP block, as well as to compare the anatomy with that of the more established paravertebral - and epidural nerve blocks.

The focus of this thesis is the novel ESP block. This thesis is structured into various chapters. Each chapter will encompass various subheadings relative to each block, as well as a comparative section related to the more recent ESP block.

Chapter 2 – Erector spinae plane (ESP) block

The ESP block is a novel ultrasound-guided interfascial technique serendipitously discovered while treating thoracic neuropathic pain in an adult patient (Forero *et al.*, 2016). This interfascial block is hypothesised to target the ventral - and dorsal rami of spinal nerves, as the block is performed in a tissue plane deep to the erector spinae muscle (López *et al.*, 2018; Balaban *et al.*, 2019; Roy *et al.*, 2020). Local anaesthetic is deposited deep to the erector spinae muscle, yet superficial and lateral to the tips of the transverse processes (Govender *et al.*, 2020a) (Appendix A).

The therapeutic effect of the ESP block is attributed to the craniocaudal spread of anaesthetic over multiple vertebral levels within the tissue plane (Govender *et al.*, 2020b) (Appendix B). Absorption and diffusion of anaesthetic across intersecting tissue planes also play a role in the extent and quality of the block (Pourkashanian *et al.*, 2019). Furthermore, the block has been reported to successfully manage acute and chronic pain for truncal procedures as it blocks both visceral and somatic pain (Aksu *et al.*, 2019a; Balaban *et al.*, 2019; Bang, 2019; Godlewski, 2019; Karaca, 2019; Mostafa *et al.*, 2019; Nair *et al.*, 2019; Lima *et al.*, 2020; Sahin *et al.*, 2020).

This 'happily accidental' block serves as a "paravertebral by proxy" and is an alternative approach, targeting similar nerves as the paravertebral- and epidural blocks (Muñoz *et al.*, 2017; Cesur *et al.*, 2018; Costache *et al.*, 2018; De la Cuadra-Fontaine *et al.*, 2018; Vidal *et al.*, 2018; Aksu and Gürkan, 2019a; Govender *et al.*, 2020a; Zhang *et al.*, 2020) (Appendix A). The block has been described to provide thoracic- and abdominal analgesia when performed at vertebral levels T5 and T8, respectively (Abdelhamid *et al.*, 2020; Sakae *et al.*, 2020).

Although the ESP block has been successful in the adult population, there is only a limited number of documented cases in neonates, infants and children (Gaio-Lima *et al.*, 2018; Aksu and Gurkan, 2019a; Aksu and Gürkan, 2019b; Altıparmak *et al.*, 2019; Balaban *et al.*, 2019; Elkoundi *et al.*, 2019a; Karaca, 2019; Mostafa *et al.*, 2019; Tulgar *et al.*, 2019a). Despite the increasing number of indications for the ESP block, the anatomy, mechanism of action, concentration and volume of anaesthetic is yet to be determined, especially in

neonates and children (Aksu and Gürkan, 2019b; Balaban *et al.*, 2019; Barrios *et al.*, 2020).

To date, this block has been used for open thoracic surgery (Leyva *et al.*, 2017; De la Cuadra-Fontaine *et al.*, 2018; Aksu and Gürkan, 2019c), thoracic lipoma and tumours (Muñoz *et al.*, 2017), cardiac surgery (De la Cuadra-Fontaine *et al.*, 2018), appendectomy, biliary atresia, congenital defects, gallbladder surgery, gastroschisis, bow chest, abnormal pathways/malformation of the trachea and oesophagus (Cesur *et al.*, 2018), vascular ring repair (Wyatt and Elattary, 2019), pectus excavatum (Ueshima and Otake, 2018), nephrectomy (Aksu and Gürkan, 2018a), inguinal hernias (Aksu and Gürkan, 2018b; Cesur *et al.*, 2018; Hernandez *et al.*, 2018; Aksu and Gürkan, 2019a), laparoscopic cholecystectomy (Aksu and Gürkan, 2019d, 2019e; Karaca, 2019), hip dysplasia (Elkoundi *et al.*, 2019a), axillary hidradenitis suppurativa resection (De Haan *et al.*, 2018), ovarian surgery, breast surgery, anoplasty, colostomy and circumcision (Aksu and Gurkan, 2019b). Its use has also been reported for pain management in palliative care (Baca *et al.*, 2019).

Apart from its growing establishment in hospitals, the ESP block has also been reported in the aeromedical retrieval environment (Ibbotson *et al.*, 2020). A possible contraindication for this block in a paediatric sample is the lack of parental consent. As this block is fairly new, it is understandable that fear may accompany a block with no supporting statistics. Moreover, infections may arise at the site of needle insertion and it may be associated with anticoagulation (Cesur *et al.*, 2018; Krishnan and Cascella, 2020).

2.1 Anatomy

Fascia is composed of loose- and dense fibrous connective tissue – containing collagen – that forms tunnels or planes throughout the entire body (Adstrum *et al.*, 2017). These planes can be divided into superficial and deep fascial planes. Deep fascial planes form potential spaces, paths or pockets allowing for a lesser resistant route for anaesthesia to travel. The continuity of the planes allows for multiple access points and wider distribution.

The biomechanical properties of fascia further assist with the distribution of fluid-like substances. These properties include movement of the planes due to muscle tendons attaching onto deep fascial planes, therefore, contraction of these muscles results in stretching of deep fascia and the consequent movement of the planes. Secondly, fascia contains contractile elements which play a role in generating force, therefore, permitting motion. Lastly, fascia acts as an energy reserve that absorbs, stores and releases energy. This is important, as the anaesthetic solution can be absorbed and stored within the fascia and gradually released (Elsharkawy *et al.*, 2019).

The interfascial ESP block is performed at the level deep to the erector spinae muscle (Forero *et al.*, 2016). The erector spinae muscle forms part of the intermediate layer of the intrinsic muscles of the back. It consists of three longitudinal columns of muscles. From lateral to medial, these muscles are known as the iliocostalis-, longissimus- and spinalis muscles. These muscles lie posterolateral to the vertebral column between the spinous processes, medially, and the angle of the ribs, laterally. They act as a unit to stabilise the vertebral column during flexion and extension, as well as to maintain posture. Located between adjacent transverse processes, is an intertransverse connective tissue complex which consists of a series of ligamentous structures and small muscles. This complex is formed by two ligaments – the superior costotransverse- and intertransverse ligaments – together with the levatores costarum-, rotatores spinae- and intercostales externi- and intercostales interni muscles (Govender *et al.*, 2020c) (Appendix C).

Depending on the level at which the block is performed, various musculoskeletal and neurovascular structures can be found overlying the posterior aspect of the erector spinae muscle. Structures from superficial to deep at vertebral level T5 to T6 include the trapezius-, rhomboids-, serratus posterior superior-, erector spinae-, external intercostal-

and internal intercostal muscles, endothoracic fascia, intercostal neurovascular bundle and the parietal pleura of the lungs (Chin *et al.*, 2017). An ESP block at this level will provide full dermatomal coverage for surgery of the thoracic region.

Structures from superficial to deep at vertebral level T7 to T11 include the trapezius-, erector spinae-, external intercostal- and internal intercostal muscles, thoracolumbar fascia, endothoracic fascia, intercostal neurovascular bundle and the parietal pleura of the lungs. An ESP block at this level will provide full dermatomal coverage for surgery of the abdominal region. Therefore, the rhomboid muscles – which terminate at the root of the scapula spine and the inferior angle of the scapula – serves as an important landmark on an ultrasound scan, as it will distinguish between the thoracic- and abdominal regions. Additionally, it can be used to confirm that the T7 transverse process is viewed (Chin *et al.*, 2017).

Govender and co-workers described the erector spinae fascial plane space, which is sandwiched superiorly and inferiorly between the heads and necks of adjacent ribs as follows; it is bordered anteriorly by the transverse processes of the relevant vertebrae and the superior costotransverse ligament, posteriorly by the deep fascia of the erector spinae muscle, medially by the laminae and spinous processes of the relevant vertebrae and laterally by the distal part of the costotransverse ligament and the rib (Govender *et al.*, 2020c) (Appendix C) (Figure 1).

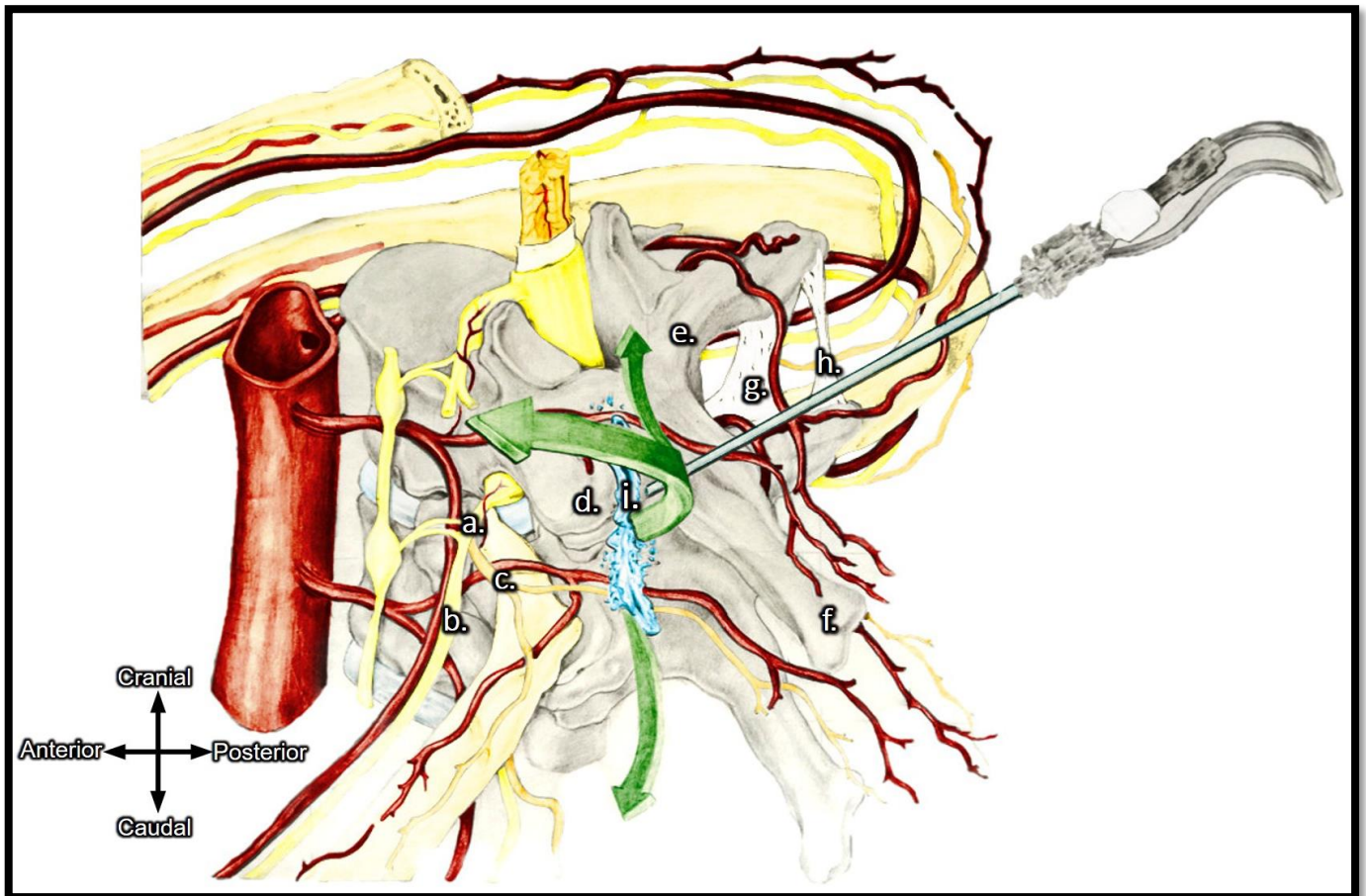


Figure 1: The erector spinae fascial plane space and the structures that contribute to its borders. Key: a – spinal nerve, b – ventral rami, c – dorsal rami, d – transverse process, e – lamina, f – spinous process, g – superior costotransverse ligament, h – intertransverse ligament, i – injectate inserted into the erector spinae fascial plane space, green arrows – spread of injectate (Govender *et al.*, 2020c).

2.2 Ultrasound anatomy

There are two common approaches to performing the ESP block: A transverse approach and a parasagittal/longitudinal approach.

a) ***Transverse approach***

If the transducer is positioned transversely (perpendicular to the vertebral column), the anatomical structures will appear as follows: the transverse processes of the vertebra can

be identified as flattened, square-like, hypoechoic structures. Following the transverse process medially, the spinous process can be identified as a triangular, hypoechoic structure connected to the transverse process by the hypoechoic arch-shaped lamina. Immediately superior to the transverse process and lateral to the spinous process, the erector spinae muscle appears as hyperechoic bands in direct contact with the bony structures (Figure 2).

Filling the arch-shaped space lateral to the spinous process, covering part of the transverse process, is the spinalis muscle. Lateral to that, immediately posterior to the remainder of the transverse process, is the longissimus thoracis muscle. Superficial to the longissimus thoracis muscle is another band-like muscular structure, the rhomboid major muscle. Superficial to the rhomboid major muscle, extending laterally from the tip of the spinous process over the muscle, is another band-like muscular structure, the trapezius muscle (Govender *et al.*, 2020c) (Appendix C) (Figure 2).

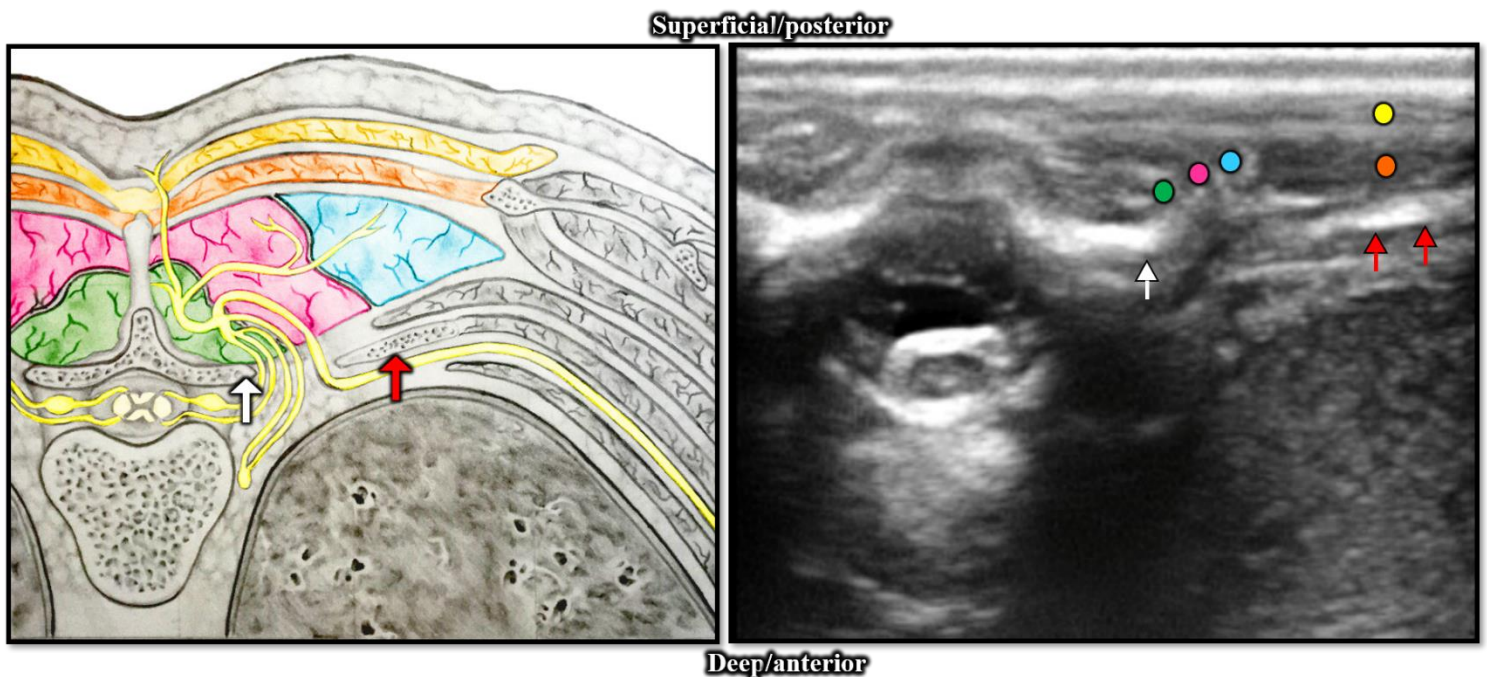


Figure 2: The ultrasound anatomy as seen on the ultrasound screen of a transverse section scan taken at vertebral level T5. Key: green – spinalis muscles, pink – longissimus muscle, blue – iliocostalis muscle, orange – rhomboid major muscle, yellow – trapezius muscle, white arrow – transverse process of T5, red arrows – rib (Govender *et al.*, 2020c).

b) ***Parasagittal approach***

If the transducer is positioned parasagittally (parallel to the vertebral column), the anatomical structures will appear as follows: the transverse processes of the adjacent vertebrae can be identified as rhomboid-shaped hypoechoic structures in a vertical line. Immediately inferior to each transverse process, the corresponding rib can be observed as an oval hypoechoic structure (Figure 3). Running from the superior border of the transverse process to the superior border of the adjacent transverse process is the intertransverse ligament, which can be identified as a hyperechoic line. Filling the spaces between the transverse processes of the adjacent vertebrae is a hyperechoic mass that is formed by a collection of structures. Running from the superior border of the transverse process to the inferior border of the adjacent rib in a cranial to caudal direction is the obliquely arranged superior costotransverse ligament which divides this space into a superior and inferior triangle (Figure 3).

The superior triangle is bordered laterally by the intertransverse ligament, medially by the superior costotransverse ligament and caudally by the transverse process of the adjacent transverse process. The superior triangular space is occupied by a group of muscles, namely the levatores costarum, rotatores spinae and the external- and internal intercostal muscles. The inferior triangle is bordered laterally by the superior costotransverse ligament, cranially by the transverse process and its corresponding rib and medially by the pleura. This triangular space is known as the paravertebral space. Superior to the intertransverse ligaments are three hypoechoic muscular bands, the erector spinae-, rhomboid major- and trapezius muscles (Figure 3).

The three distinct muscular bands are equal in size and can be traced cranially and caudally. Superficial to these muscles is a layer of fat, which appears hyperechoic on the ultrasound screen. If the transducer is placed too far laterally, the ribs will be viewed instead of the transverse processes. The ribs can be recognized as rounded hyperechoic shadows with an intervening hyperechoic pleural line (Figure 3). If the transducer is placed too far medially, the laminae, which appear as flat hyperechoic lines, will be visualized.

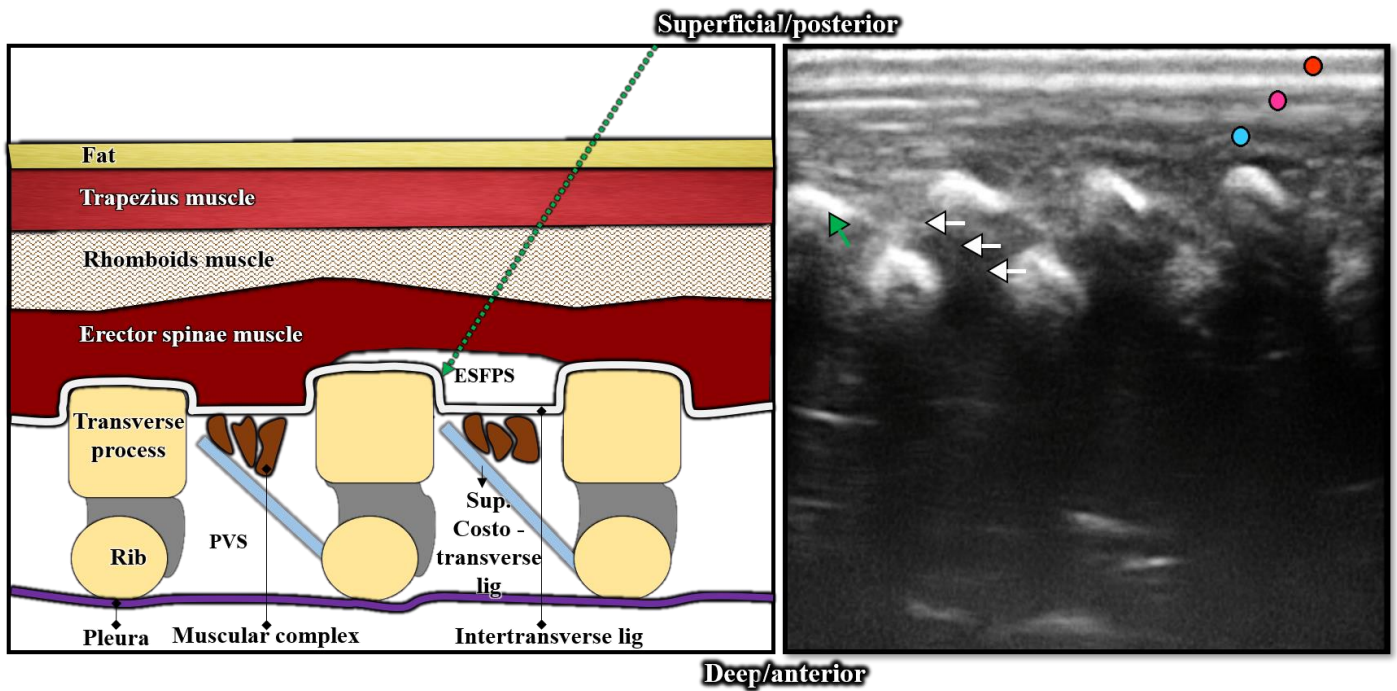


Figure 3: The ultrasound anatomy as seen on the ultrasound screen of a parasagittal section scan taken at vertebral level T5. The muscular complex consists of the levatores costarum, rotatores spinae and external intercostal muscles. Key: green arrow on the ultrasound scan – the transverse process of T5, green arrow on the diagram – needle insertion, white arrows – superior costotransverse ligament, orange circle – trapezius muscle, pink circle – rhomboids muscle, blue circle – erector spinae muscle, ESPFS – erector spinae fascial plane space, PVS – paravertebral space (Govender *et al.*, 2020c).

2.3 Aim

The aim of this chapter was to investigate the anatomy and action mechanism of the erector spinae plane block using fresh cadavers, ultrasound and CT scans.

2.4 Research objectives

- I. To investigate the macro and ultrasound anatomy of the erector spinae fascial plane space when replicating the ESP block in a fresh neonatal sample, by determining the surface landmarks with regards to; the average distance from the surface landmark of the spinous process (point A) to the corresponding surface landmark of the transverse process (point B) and the average depth – from the skin to the lateral tip of the transverse process deep to it (point C) – for the needle to be inserted in different paediatric age groups.
- II. To determine the relationship between the depth to the erector spinae fascial plane space and the demographic features of the sample by using simple and multiple regression analysis.
- III. To determine whether the spread of contrast is affected by the needle direction – cephalad to caudal versus caudal to cephalad – and needle entry site – at the angle of the transverse process or between the transverse processes – in the erector spinae fascial plane space.

2.5 Material and methods

This study was approved by the PhD and Research Ethics Committee (ethics reference number 94/2019), University of Pretoria, South Africa. Eleven fresh, unembalmed preterm, neonatal cadavers subject to cryopreservation were obtained through the National Tissue Bank from the University of Pretoria and Sefako Makgatho Health Sciences University. All cadaveric material was handled in accordance with the South African National Health Act, 61 of 2003. Permission was also obtained from the Head of the Department of Radiology and CEO of Steve Biko Academic Hospital, to retrospectively source CT scans from patient archives. All records obtained were kept confidential as to keep patient identity anonymous. For simplicity, this study was divided into three components: ultrasound scans, CT scans (present vs retrospective) and cadaveric dissections.

a) ***Ultrasound component***

The ESP block was replicated bilaterally, at vertebral level T5 on the right hand side and T8 on the left hand side, in eleven fresh neonates with the aid of ultrasound guidance. An Edge™ ultrasound machine (ref: P15000-11, SN-03P55Z) with a 6 – 13 MHz linear array probe (footprint size of 2.5 cm) covered with a protective plastic sheath, was used in all procedures. For this component, the contrast material used was a methylene blue mixture which consisted of 10 ml of iodinated contrast material, diluted in 85 ml of 0.9% sodium chloride. The height of each cadaver was documented used a standard measuring tape, while the weight was determined with the use of a body scale.

The procedure began by identifying the spinous process of the C7 vertebra with the cadaver placed in a prone position. The transducer was then placed sagittally over the spinous process in the neck region to further confirm C7. The spinous processes of T5 and T8 and their corresponding transverse processes were identified by counting inferiorly from the spinous process of C7. The trapezius and erector spinae muscles were visualized superficial to the acoustic shadow of the transverse processes. The absence of the rhomboid muscle was used to confirm visualization of the transverse process below vertebral level T6. Ultrasound scans were taken with the transducer orientated in both a transverse and parasagittal alignment to identify the anatomical structures.

When replicating the ESP block, the transducer was placed either transversely or parasagittally over the transverse process of T5 and T8, about 1 cm lateral to the spinous process. Vertebral levels T5 and T8 were selected in order to track the thoracic and abdominal spread separately. Using the in-plane approach, a 100mm 21g needle was inserted midway between the transverse processes and then directed in a cephalad to a caudal direction (and vice versa) towards the superficial tip of the transverse process (Figure 4). Once the tip of the needle reached the transverse process (the endpoint), 0.05 ml of saline solution was injected to confirm the position of the needle tip. The erector spinae fascial plane space was further confirmed as the erector spinae muscle bundle was hydro-dissected off the underlying bony structures. In cadavers with low body mass index, the lifting of the erector spinae muscles presented on the skin as a temporary raised protrusion/lump. Methylene blue dye, 0.1 ml/kg was then injected while observing the

anechoic spread of the dye within the deep tissue plane. Thirty minutes subsequently, dissections were performed.

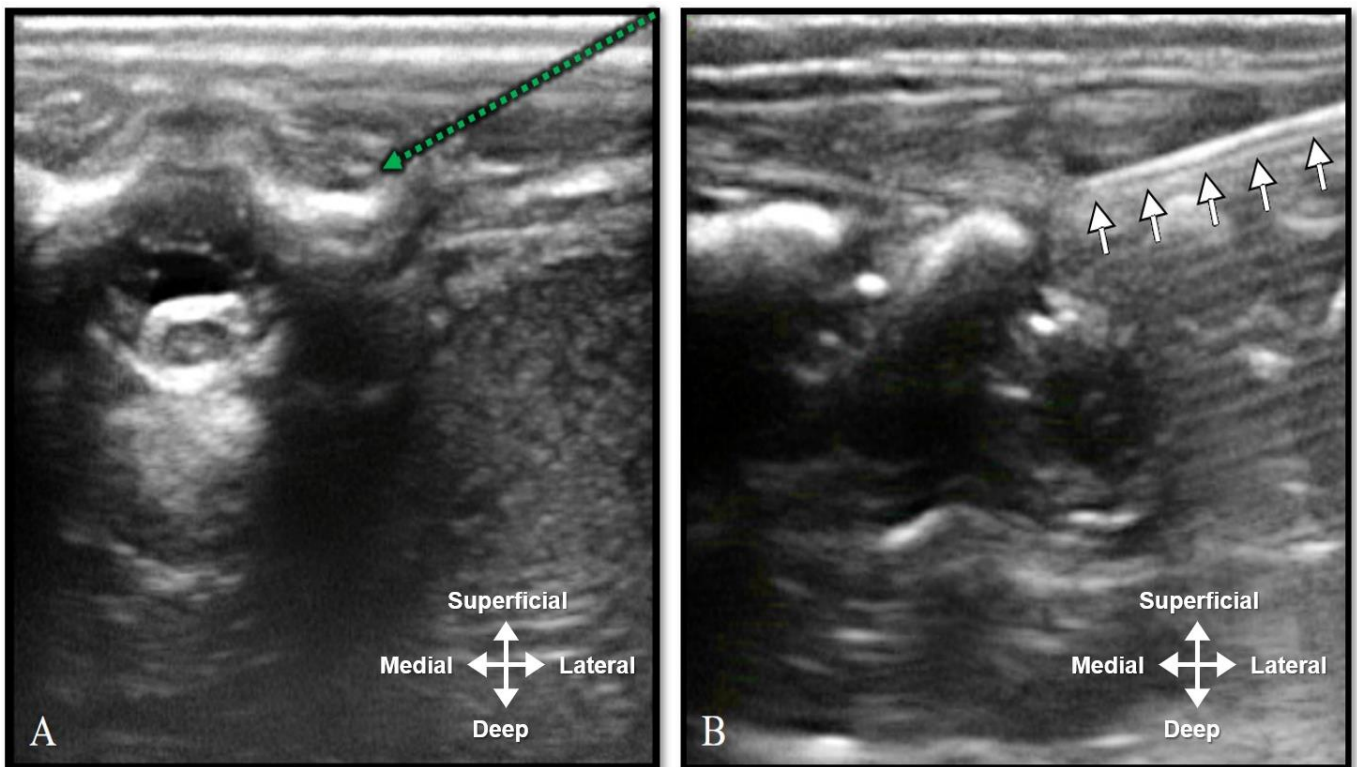


Figure 4: The ultrasound bony landmarks in a transverse (A) and parasagittal orientation (B) taken at vertebral level T5. The green dotted arrow represents the needle course in a transverse alignment, while the white arrows represent the needle course in a parasagittal alignment.

After obtaining the scan images, the format was converted and then uploaded onto RadiAnt, a Digital Imaging and Communication in Medicine (DICOM) viewer, from which various measurements were taken bilaterally at vertebral levels T5 and T8. These measurements include A – the distance from the spinous process to the transverse process; B – the depth from the skin to the erector spinae fascial space (tip of the transverse process); C – the depth from the skin to the most superficial point of the erector spinae muscle; D – the depth from the skin to the most superficial point of the rhomboid major muscle; E – the depth from the skin to the most superficial point of the trapezius muscle (Figure 5).

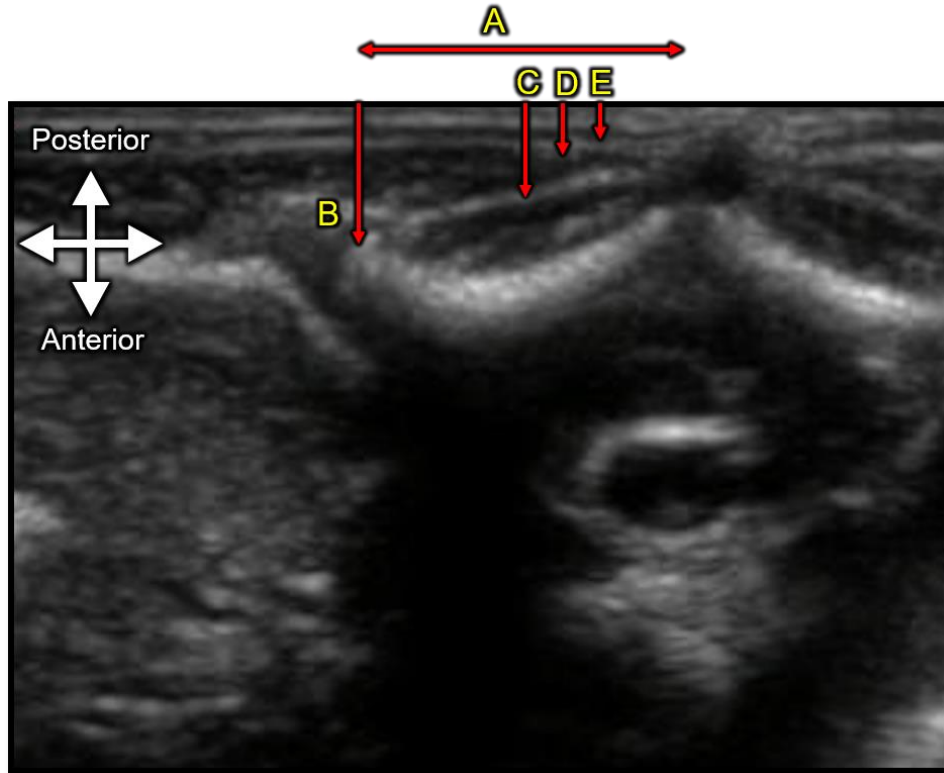


Figure 5: A transverse ultrasound image showing the various measurements taken. Measurements that were taken include; A – the distance from the spinous process to the lateral tip of the transverse process; B – the depth from the skin to the erector spinae fascial space (tip of the transverse process); C – the depth from the skin to the most superficial point of the erector spinae muscle; D – the depth from the skin to the most superficial point of the rhomboid major muscle; E – the depth from the skin to the most superficial point of the trapezius muscle.

b) ***Retrospective CT component***

One hundred and fifty CT scans were retrospectively selected from the database of radiographic images at the Department of Radiology, Steve Biko Academic Hospital. Demographic information such as age and sex were recorded. Scans were grouped according to age groups: neonates (0 – 2 months), infants (>2 months – 2 years) and children (>2 – 12years). Scans with abnormal vertebral column development such as kyphosis and scoliosis, visceromegaly or space-occupying lesions, as diagnosed by the consulting radiologist, were excluded from this study.

RadiAnt, DICOM viewer was then used to analyse the CT scans. Using the on-screen measuring function, calibrated for each image, various measurements were taken at vertebral levels T5 and T8 in a transverse section. Measurements included: A – the distance from the spinous process to the lateral tip of the transverse process; B – the depth from the skin to the erector spinae fascial space (tip of the transverse process); C – the depth from the skin to the most superficial point of the erector spinae muscle; D – the depth from the skin to the most superficial point of the rhomboid major muscle; E – the depth from the skin to the most superficial point of the trapezius muscle (Figure 6).

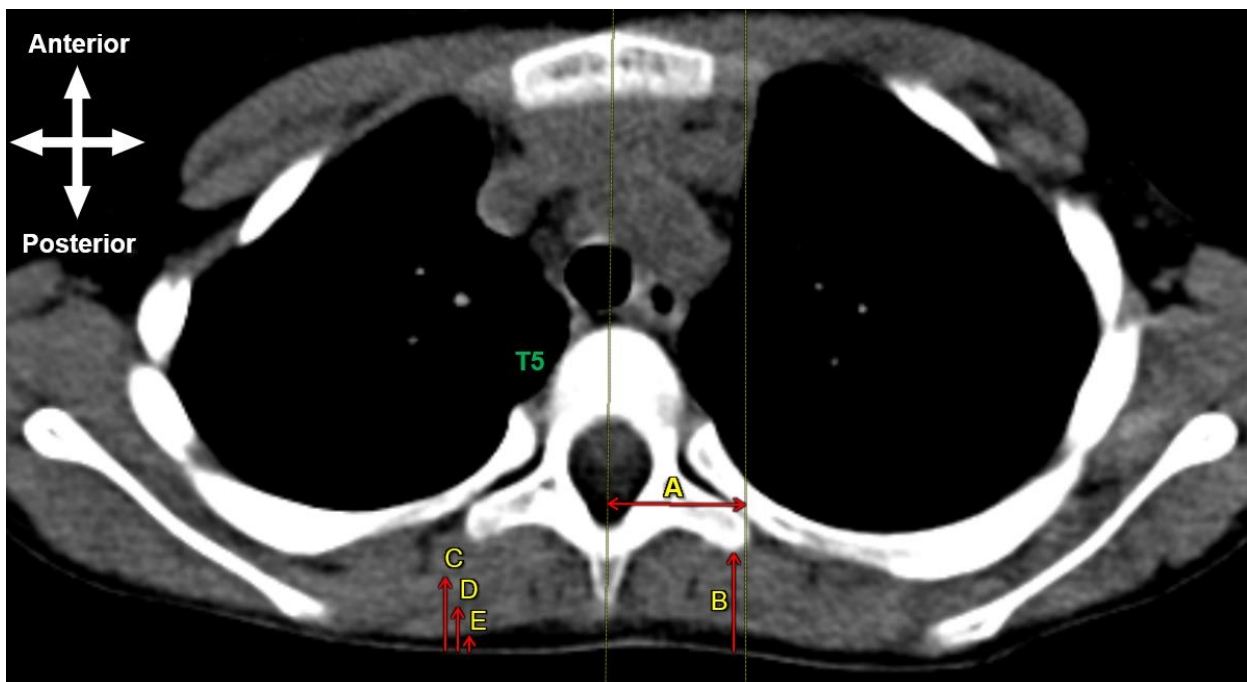


Figure 6: An axial CT image through the thorax at vertebral level T5. Measurements that were taken include; A – the distance from the spinous process to the lateral extent of the transverse process; B – the depth from the skin to the ESFP space (tip of the transverse process); C – the depth from the skin to the most superficial point of the erector spinae muscle; D – the depth from the skin to the most superficial point of the rhomboid major muscle; E – the depth from the skin to the most superficial point of the trapezius muscle.

c) ***CT component (real-time spread of contrast medium)***

For this component, the sample size consisted of one cadaver. The procedure began by using ultrasound guidance to identify the spinous process and its corresponding transverse process of T8 and T10 as mentioned in 2.5.a. Prior to introducing the contrast solution, test injections were done on the lower limb to determine the concentration of the solution that would be used. This depended on the amount of scatter – a combination of dark and light streaks between objects such as bone – seen on the Philips CT machine (parameters: 100 Kvp, 75 mAs, 7.2 scan time).

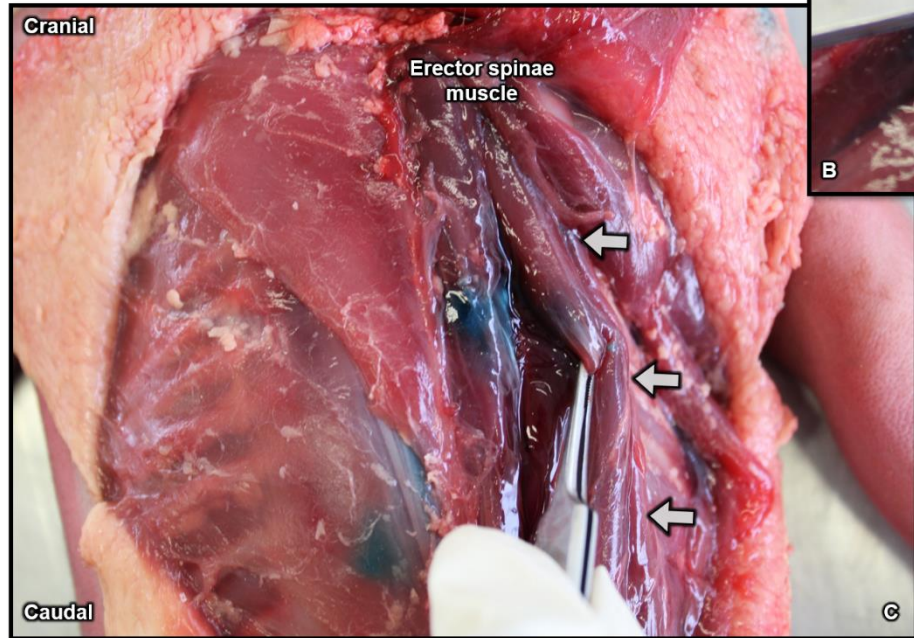
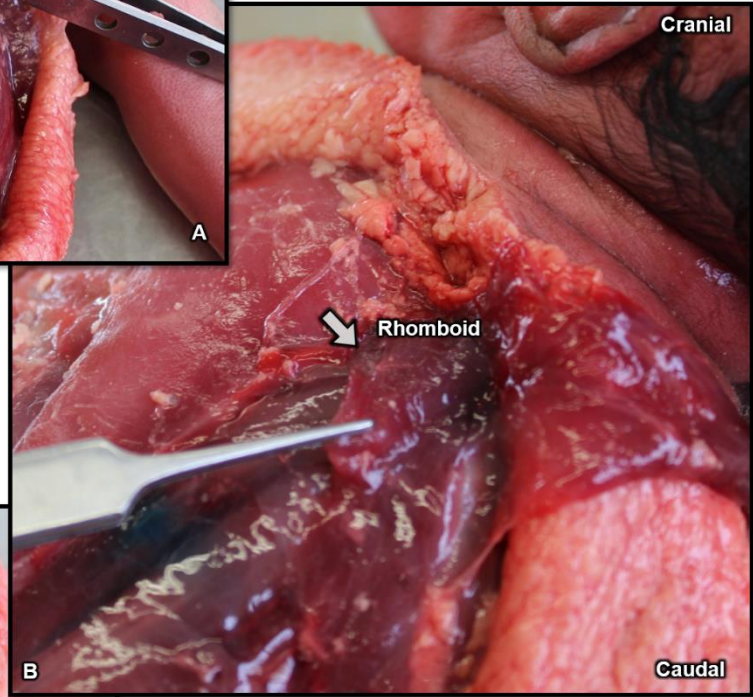
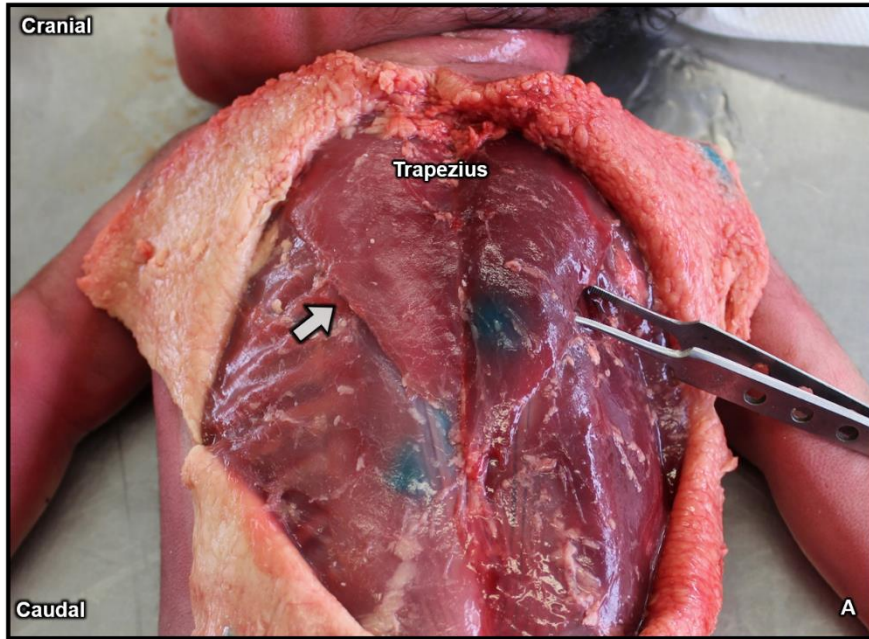
Two millilitres of pure concentrated contrast dye was injected into the right leg, while two millilitres of diluted contrast dye was injected into the left leg. The contrast material was injected into the fascial planes between the gastrocnemius muscles. Upon scanning, the right side was difficult to interpret as the quality of the image was distorted by scattering artifacts. Therefore, we decided to use 30 ml of 30% urografin (cot 85588036) diluted in 200 ml of 0.9% sodium chloride (cot 9030801) as the contrast medium. The contrast medium, 1 ml/kg was then injected as described in section 2.5.a. on the right hand side at vertebral level T8 and on the left hand side at vertebral level T10. The contrast medium was allowed to spread for 20 minutes prior to turning the cadaver in a supine position for CT scanning. The images were then reconstructed to provide a three-dimensional (3D) view of the trunk in an attempt to fully delineate the spread of the contrast dye. Important to mention is that this cadaver was not dissected as CT contrast material does not stain musculoskeletal or neurovascular structures.

d) ***Cadaveric component***

Subsequently, to the spread of the contrast medium (in the remaining eleven cadavers), a vertical skin incision was made along the midline over the spinous processes of C7 to L2, followed by bilateral horizontal incisions from the spinous process of T1, laterally towards the acromion of the scapula. Bilateral horizontal incisions were also made at vertebral level T10, laterally towards the midaxillary line. The skin was then reflected laterally to expose the posterior aspect of the scapular-, thoracic- and lumbar regions. The surface staining of the methylene blue dye on the muscular structures was noted before further dissection (Figure 7A).

The trapezius, rhomboid major, rhomboid minor and latissimus dorsi muscles (superficial muscles of the back) were individually identified and reflected laterally to reveal the serratus posterior superior and inferior – which was removed – and the erector spinae muscle (Figure 7A-C). Again, surface staining of the muscles was noted before further dissection. Each band of the erector spinae, as well as the multifidus and rotatores muscles, was cut and reflected from its insertion sites to reveal the bony structures deep to it (Figure 7D & E).

The lamina and transverse process of the vertebra, as well as the head, neck and tubercle of the corresponding rib, were cleaned to further view the spread of dye. The bony structures were then cut and removed to expose the ventral and dorsal rami of the spinal nerves within the intercostal space to determine whether they were stained by the contrast material (Figure 7F). The craniocaudal and lateral extent of the spread of dye across vertebral levels were noted and counted from the point of insertion in all procedures. The spread was described from the T1 to L2 vertebra.



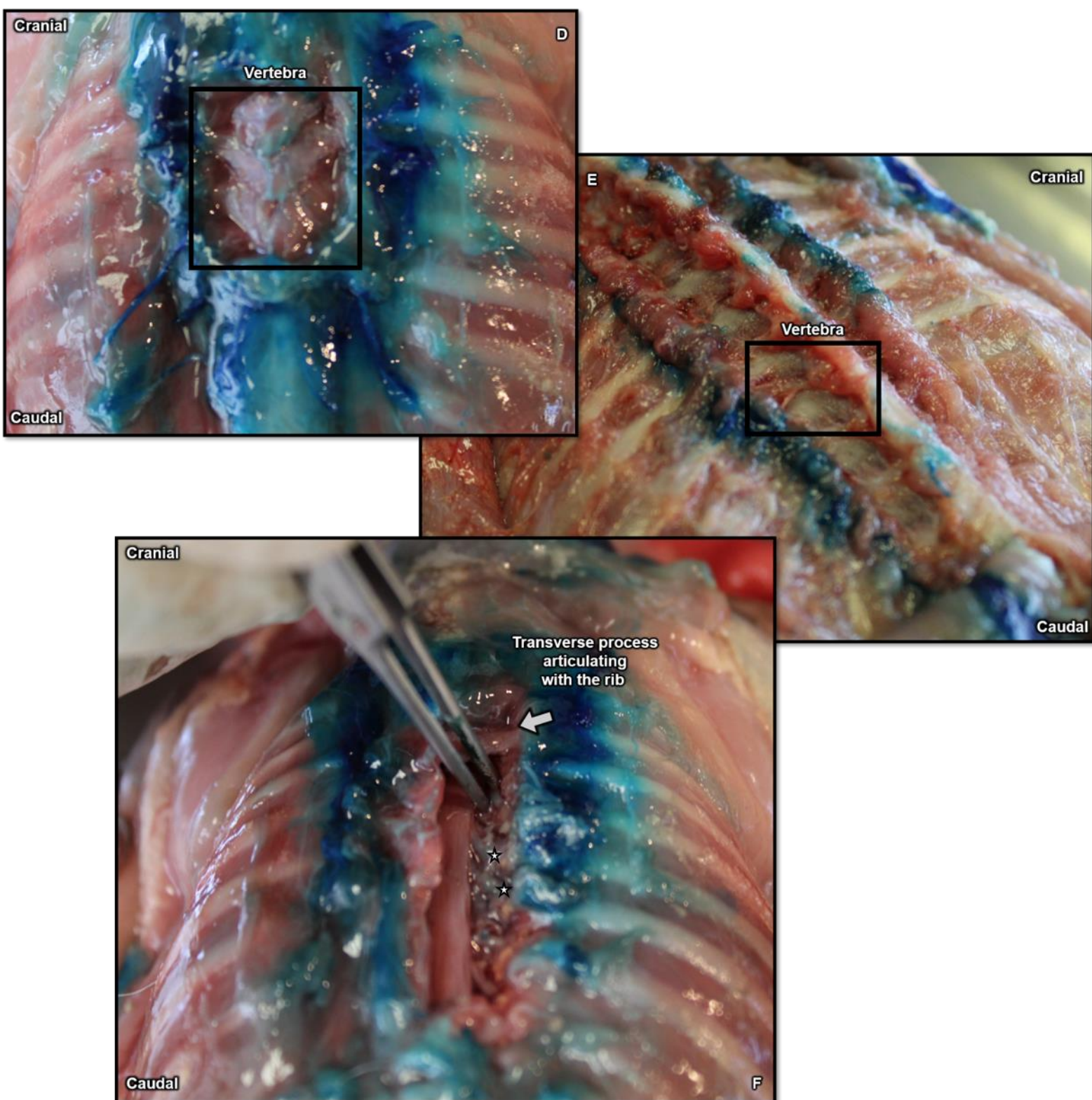


Figure 7: Photographic images showing A – the skin reflected to reveal the trapezius muscle, B – the rhomboid muscles, C – the individual bands of the erector spinae muscle, D & E – the cleaned vertebra, F – removal of the transverse process and the articulating rib to reveal the spinal cord and rami deep to it (indicated by the stars) (Govender *et al.*, 2020a).

2.6 Statistical analysis

All measurements were loaded into a Microsoft Excel spreadsheet. Further statistical analysis of the measurements, as well as the subsequent comparisons of those measurements with the available demographic profile for each component of the study, was performed using Statistic Data Analysis (STATA), version 16.

Comparisons included left versus right side measurements, as well as descriptive statistics – means, standard deviations and 95% confidence intervals – taken from the different paediatrics groups from the ultrasound and CT component. Due to the limited sample size and the different variables between these two components, it was decided to keep the data sets separate. These sample sets will then be used as an extensive anatomy reference data set for a South African paediatric population. In order to ensure the validity and accuracy of the results obtained, intra- and inter-observer reliability checks were conducted. The primary investigator repeated 25% of the initial measurements, while an independent researcher repeated 20% of the initial measurements.

The data set was first tested for normality, prior to further statistical testing. Results revealed the data sets to be normally distributed, allowing the statistician to continue with parametric testing. Subsequently, a paired t-test was performed in order to determine whether there was a statistical significant difference between the right and left sides, by producing a t-value. The t-value compares a sample mean(s) to the null hypothesis and incorporates both the sample size and the variability in the data. Every t-value has a corresponding p-value. The lower the p-value, the better it indicates that the data did not occur by chance and is attributed to parameters. A p-value of < 0.05 is regarded as statistically significant. Measurements that were not statistically significant, were pooled together to create averages before continuing with the statistical analysis.

Linear regression models were then performed to establish whether a linear relationship/correlation existed between the dependent variables – the measurements – and the independent variables – age, sex, height or weight. The test produced a p-value, R^2 -value and an adjusted R^2 -value which were used to determine the strength of the relationship. The R^2 -value analyses how the differences in the dependent variables can be explained by the differences in the independent variables. In other words, the R^2 -value

gives a percentage variation in the dependent variable that can be explained by the independent variable. A p-value of < 0.05 is regarded as statistically significant, while R^2 – and adjusted R^2 -values less than 0.3 indicated a weak correlation between the variables. Values greater than 0.7 were considered to be a strong correlation between the variables. Any value between 0.3 and 0.7 was considered a weak to strong correlation and therefore had a slight significant effect on the variables.

Lastly, multilinear regression models were run to generate formulas that could be used to perform the block while taking known parameters into account. The models were performed for measurements at vertebral levels T5 and T8. The right- and left values were calculated separately if there was a significant difference between the sides. Multilinear regression models for the CT component used sex and age, as this was the only demographic information available, whereas, for the ultrasound component age, sex, height and weight were used.

A biostatistician from the School of Health Systems and Public Health from the University of Pretoria was consulted throughout the study design, statistical analyses and statistical interpretation of this thesis.

2.7 Results

Upon intra- and inter-observer analysis, a student t-test was performed to compare the two sets of data in order to ensure that the measurements obtained, were valid. The statistical results revealed a p-value greater than 0.05 for both the intra- and inter-reliability checks, which indicated that there was no statistical significant difference between the data sets. The initially obtained data measurements were thus considered to be correct.

Additionally, the macro and ultrasound anatomy corroborated with the previously described anatomy.

a) ***Ultrasound component***

From the data obtained, paired t-tests were performed to test for statistical significance between the right and the left side measurements. Normality was further confirmed, as the mean for each measurement was twice the standard deviation. Overall, there were a total of nine comparisons, which justified the adoption of the Bonferroni correction method.

The Bonferroni method is used to adjust the p-value when numerous dependent or independent statistical tests are being performed simultaneously on a single data set. The Bonferroni correction method reduces the chances of obtaining false-positive results (type I errors) when multiple paired tests are performed on a single set of data. This test is done by dividing the critical p-value (α/α) by the number of comparisons being made. For this component it was $0.05/9 = 0.0056$, Therefore, a p-value smaller than 0.0056 was considered significant. Table 1 below summarises the results of the paired t-test.

Table 1. Results of the paired t-test of the erector spinae plane measurements taken from the neonatal ultrasound scans.

Measurement on the right side	n	Mean (cm)	SD	Measurement on the left side	n	Mean (cm)	SD	p-value
T5SPtoTP	10	2.33	2.7	T5SPtoTP	10	1.41	0.40	0.33
T5StoESFPS	10	0.95	0.42	T5StoESFPS	10	0.95	0.45	0.98
T5StoES	10	0.67	0.29	T5StoES	10	0.67	0.31	0.90
T5StoRh	10	0.39	0.17	T5StoRh	10	0.39	0.17	0.77
T5StoTrap	10	0.20	0.10	T5StoTrap	10	0.20	0.11	0.52
T8SPtoTP	9	1.56	0.23	T8SPtoTP	9	1.52	0.25	0.19
T8StoESFPS	9	0.99	0.29	T8StoESFPS	9	0.99	0.38	0.93
T8StoES	9	0.58	0.18	T8StoES	9	0.55	0.18	0.09
T8StoTrap	9	0.25	0.08	T8StoTrap	9	0.25	0.80	0.86

KEY: **n** – sample size, **SD** – standard deviation, **T5** – vertebral level T5, **T8** – vertebral level T8, **SPtoTP** – Spinous process to the Transverse process, **StoESFPS** – Skin to the Erector spinae fascial plane space, **StoES** – Skin to the Erector spinae muscle, **StoRh** – Skin to the Rhomboid muscle, **StoTrap** – Skin to Trapezius muscle.

From the total sample size, 5 scans belonged to females while the remaining 5 belonged to males. After evaluating the p-values, there was no statistical significant difference between right and left side measurements in this component. Therefore, the data were pooled to create averages for each measurement with a new standard deviation (Table 2).

Table 2. Descriptive statistics summary after pooling the right and left sides for the ultrasound component for the neonatal group.

Measurement	n	Minimum (cm)	Maximum (cm)	Mean (cm)	SD
T5 Spinous process to the transverse process	10	0.75	1.79	1.88	0.39
T5 Skin to the Erector spinae fascial plane space	10	0.41	1.71	0.95	0.42
T5 Skin to the Erector spinae muscle	10	0.29	1.18	0.67	0.30
T5 Skin to the Rhomboid muscle	10	0.20	0.71	0.39	0.17
T5 Skin to Trapezius muscle.	10	0.10	0.44	0.20	0.11
T8 Spinous process to the Transverse process	9	1.10	1.84	1.54	0.23
T8 Skin to the Erector spinae fascial plane space	9	0.54	1.54	0.99	0.33
T8 Skin to the Erector spinae muscle	9	0.37	0.86	0.56	0.18
T8 Skin to Trapezius muscle.	9	0.10	0.39	0.25	0.08

KEY: **n** – sample size, **SD** – standard deviation, **T5** – vertebral level T5, **T8** – vertebral level T8. The data obtained were taken from 11 individuals, however, the mean represents the average of the 20/18 measurements (right and left sides).

Using linear regression analysis, each measurement – the dependent variable – was further tested for correlation against fixed factors such as sex, age, height and weight – the independent variables. Due to the quantity of the data, the adjusted R^2 -value was used instead of the R^2 -value to predict the correlation. The adjusted R^2 -value is a modified version of the R^2 -value that has been adjusted for the number of predictors in the model. It thus provides a more precise view of that correlation by taking into account how many independent variables are added to a particular model against which the data is measured. These additions usually increase the reliability of the model. Moreover, the adjusted R^2 -value quantifies how well a model fits the data. Results revealed a weak correlation between the dependant and independent variables, as the adjusted R^2 -values were < 0.5 (Table 3).

Table 3: Results from the linear regression analysis displaying the correlation between the measurements and variables

Measurement	Variable	Adjusted R ² value
T5 Spinous process to the transverse process	Sex	0.244
	Height	0.189
	Weight	0.74
T5 Skin to the Erector spinae fascial plane space	Sex	-0.123
	Height	-0.201
	Weight	-0.387
T5 Skin to the Erector spinae muscle	Sex	-0.125
	Height	-0.272
	Weight	-0.482
T5 Skin to the Rhomboid muscle	Sex	-0.125
	Height	-0.156
	Weight	-0.343
T5 Skin to Trapezius muscle.	Sex	-0.106
	Height	-0.058
	Weight	-0.199
T8 Spinous process to the Transverse process	Sex	-0.118
	Height	-0.319
	Weight	-0.445
T8 Skin to the Erector spinae fascial plane space	Sex	-0.093
	Height	-0.134
	Weight	0.488
T8 Skin to the Erector spinae muscle	Sex	-0.139
	Height	-0.095
	Weight	-0.222
T8 Skin to Trapezius muscle.	Sex	-0.098
	Height	-0.217
	Weight	-0.363

A multivariant regression analysis was performed to assess the overall effect of the independent variables on the dependent variables as a whole. Subsequently, the multivariant regression model for the skin to erector spinae fascial plane space measurement was then used to create a standard equation that can be utilised when performing the ESP block in a preterm neonatal paediatric sample (Table 4).

Table 4. Multivariant regression analysis for determining the depth to the erector spinae fascial plane space in a preterm neonatal sample.

Level	Parameter	Coefficient	SE	t	p-value	95% confidence interval	
						Lower	Upper
T5	Sex	0.203	0.440	0.462	0.660	-0.873	1.280
	Height (mm)	0.002	0.004	0.453	0.666	-0.008	0.011
	Weight (kg)	0.078	0.321	0.244	0.815	-0.707	0.864
	-constant	-0.235	1.748	-0.134	0.897	-4.510	4.041
T8	Sex	0.364	0.177	2.054	0.109	-0.873	1.280
	Height (mm)	0.001	0.002	0.719	0.512	-0.007	0.011
	Weight (kg)	0.325	0.122	2.660	0.056	-0.707	0.864
	-constant	-0.428	0.815	-0.525	0.627	-4.510	4.041

Key: **SE** – standard error, **T5** – vertebral level T5, **T8** – vertebra level T8.

Sex was determined with numeric values. Males were assigned the number 0, while females were assigned the number 1 that could be inserted into the equations. Although none of the variables was statistically significant ($p > 0.05$), as well as the weak correlation (adjusted R^2 -value < 0.3), formulae were still created for this component. These formulae included the standard error of the estimate to indicate the accuracy of the predictions.

The formulae were as follows:

- T5 skin to the erector spinae fascial plane space:
 - Depth in cm = $0.002(\text{height in mm}) + 0.078(\text{weight in kg}) + 0.203(\text{sex}) - 0.235$
 \pm the standard error of estimate (0.590)
- T8 skin to the erector spinae fascial plane space:

- $\text{Depth in cm} = 0.001(\text{height in mm}) + 0.325(\text{weight in kg}) + 0.364(\text{sex}) - 0.428$
+/- the standard error of estimate (0.211)

The adjusted R^2 -value for the formulae were -0.38 and 0.49 for vertebral level T5 and T8, respectively. Overall, the approximate distance from the spinous process to the insertion site at vertebral level T5 was 1.88 cm with a standard deviation of 0.39, while the distance at vertebral level T8 was 1.54 cm with a standard deviation of 0.23. While the average depth from the skin to the erector spinae fascial plane space was 0.95cm with a standard deviation of 0.42 at vertebral level T5 and 0.99cm with a standard deviation of 0.33 at vertebral level T8.

b) ***Retrospective CT component***

Paired t-tests were performed to test for statistical significance between the right-side versus the left-side measurements. Normality was further confirmed as the mean for each measurement was twice the standard deviation. Overall, there were a total of 9 comparisons per age group (group 1 – neonates, group 2 – infants, group 3 – children). After adopting the Bonferroni correction method, the new p-value was 0.0056. Table 5 to 7 summarise the results of the paired t-test for each of the three age groups.

Table 5. Results of the paired t-test of the erector spinae plane measurements taken from the neonatal CT scans (group 1).

Measurement on the right side	n	Mean (cm)	SD	Measurement on the left side	n	Mean (cm)	SD	p-value
T5SPtoTP	45	1.28	0.20	T5SPtoTP	45	1.28	0.20	0.73
T5StoESFPS	45	1.41	0.40	T5StoESFPS	45	1.52	0.40	0.004*
T5StoES	44	0.64	0.23	T5StoES	44	0.65	0.17	0.39
T5StoRh	44	0.43	0.16	T5StoRh	44	0.43	0.16	0.86
T5StoTrap	44	0.24	0.09	T5StoTrap	44	0.26	0.10	0.02
T8SPtoTP	44	1.25	0.19	T8SPtoTP	44	1.26	0.20	0.23
T8StoESFPS	44	1.03	0.28	T8StoESFPS	44	1.13	0.28	0.009
T8StoES	43	0.47	0.16	T8StoES	43	0.49	0.16	0.0006*
T8StoTrap	43	0.24	0.09	T8StoTrap	43	0.24	0.09	0.13

KEY: **n** – sample size, **SD** – standard deviation, **T5** – vertebral level T5, **T8** – vertebral level T8, **SPtoTP** – Spinous process to the Transverse process, **StoESFPS** – Skin to the Erector spinae fascial plane space, **StoES** – Skin to the Erector spinae muscle, **StoRh** – Skin to the Rhomboid muscle, **StoTrap** – Skin to Trapezius muscle, * – represents statistically significant values as the p-value was less than 0.0056.

From the total sample size, 22 scans belonged to females while the remaining 23 belonged to males. Based on the p-values, a significant difference was noted between the right and left sides for T5 skin to erector spinae fascial plane space, as well as the right and left sides of T8 skin to erector spinae muscle in the neonatal group (even though measurements were assessed for outliers). Statistically significant measurements were then plotted on a bar graph reflecting the mean and standard error (Figure 8).

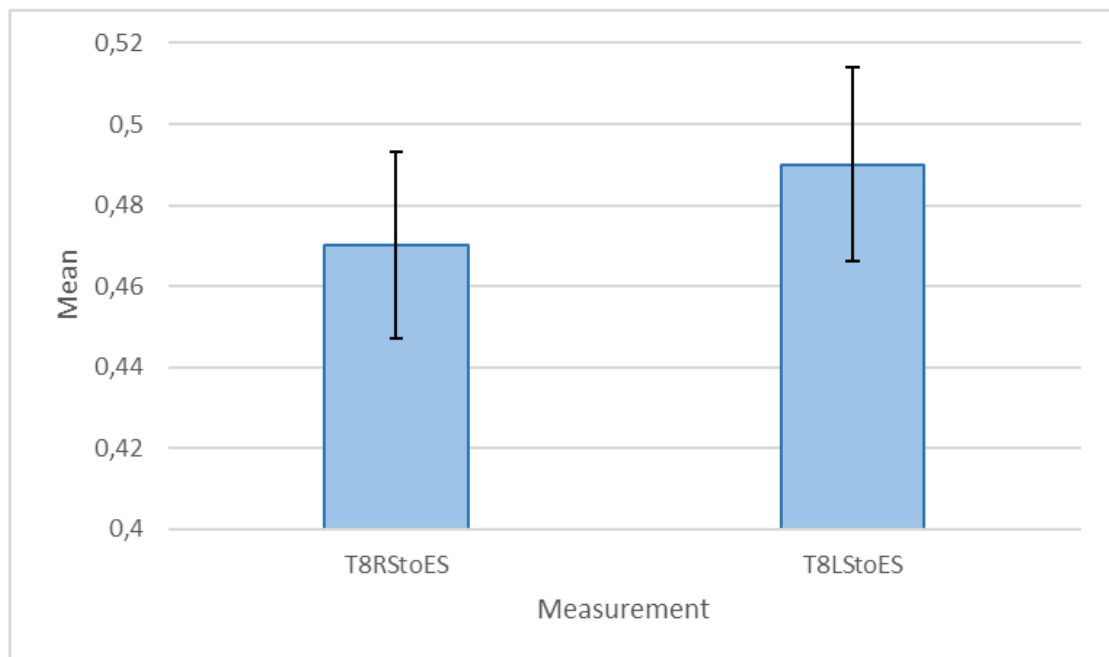
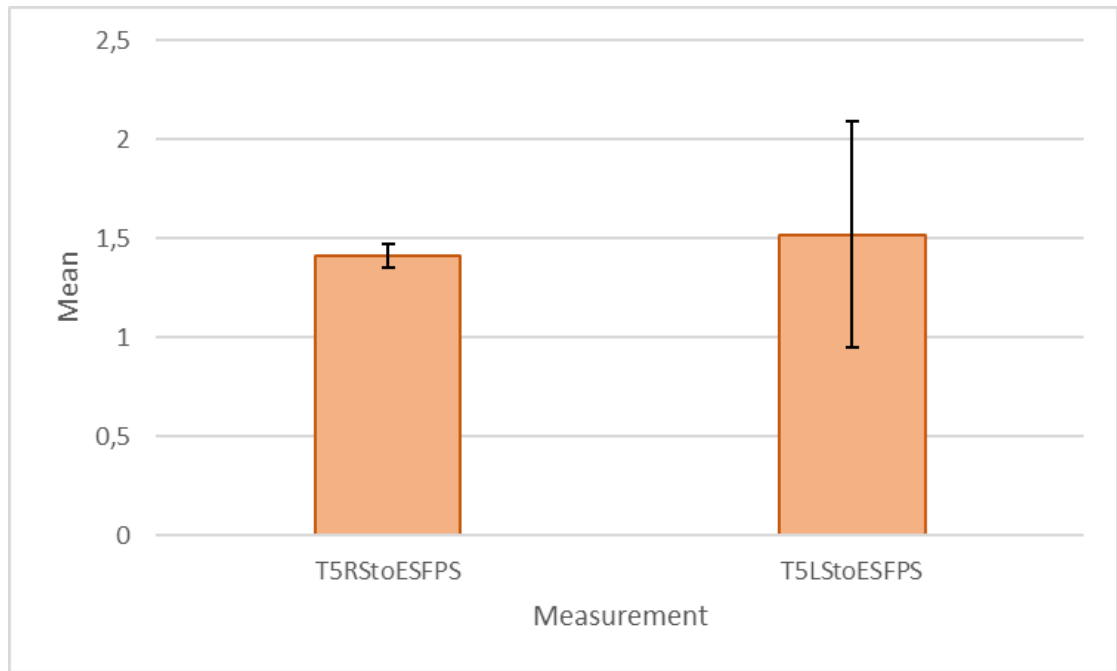


Figure 8: Bar graph showing the results from the paired t-test for the statistically significant measurements between the right and left sides. The error bar represents the standard error in relation to the mean.

As seen in figure 8, the measurements from the skin to the erector spinae fascial plane at vertebral level T5, were greater on the left side than on the right side. Likewise, the measurements from the skin to the erector spinae muscle at vertebral level T8 were greater on the left side than on the right side. The error bar represents the standard error

of the mean. The standard error is used to measure the accurateness with which a sample distribution represents a population by using the standard deviation. Error bars indicate the spread of data around the mean or how accurately the mean of the measurements represents the data set (i.e., the variability). The error around the mean is larger on the left side for both measurements.

Furthermore, standard error bars can be used to estimate whether or not a difference is truly significant depending on the overlapping of the bars – or lack thereof. If standard error bars overlap as indicated in the top image in orange (T5 skin to erector spinae fascial plane space), the difference is less likely to be statistically significant, whereas the overlapping of bars as seen on the bottom image in blue (T8 skin to erector spinae muscle), indicates that there is a probability that the difference is statistically significant. Overall, there is statistical significance between the measurements. However, the actual difference between the right and left sides is small.

Table 6. Results of the paired t-test of the erector spinae plane measurements taken from the infant CT scans (group 2).

Measurement on the right side	n	Mean (cm)	SD	Measurement on the left side	n	Mean (cm)	SD	p-value
T5SPtoTP	49	1.61	0.27	T5SPtoTP	49	1.62	0.28	0.54
T5StoESFPS	49	1.50	0.43	T5StoESFPS	49	1.56	0.49	0.03
T5StoES	46	0.78	0.75	T5StoES	46	0.69	0.30	0.42
T5StoRh	42	0.47	0.19	T5StoRh	42	0.48	0.21	0.23
T5StoTrap	49	0.39	0.49	T5StoTrap	49	0.31	0.12	0.25
T8SPtoTP	49	1.58	0.25	T8SPtoTP	49	1.62	0.32	0.07
T8StoESFPS	49	1.21	0.35	T8StoESFPS	49	1.20	0.38	0.62
T8StoES	46	0.52	0.15	T8StoES	46	0.58	0.40	0.29
T8StoTrap	49	0.26	0.09	T8StoTrap	49	0.26	0.09	0.66

KEY: **n** – sample size, **SD** – standard deviation, **T5** – vertebral level T5, **T8** – vertebral level T8, **SPtoTP** – Spinous process to the transverse process, **StoESFPS** – Skin to the Erector spinae fascial plane space, **StoES** – Skin to the Erector spinae muscle, **StoRh** – Skin to the Rhomboid muscle, **StoTrap** – Skin to Trapezius muscle.

Table 7. Results of the paired t-test of the erector spinae plane measurements taken from the children CT scans (group 3).

Measurement on the right side	n	Mean (cm)	SD	Measurement on the left side	n	Mean (cm)	SD	p-value
T5SPtoTP	57	1.91	0.26	T5SPtoTP	57	1.92	0.25	0.33
T5StoESFPS	57	1.66	0.47	T5StoESFPS	57	1.68	0.46	0.37
T5StoES	50	0.77	0.73	T5StoES	50	0.69	0.25	0.44
T5StoRh	50	0.37	0.16	T5StoRh	50	0.39	0.16	0.04
T5StoTrap	53	0.24	0.17	T5StoTrap	53	0.24	0.16	0.79
T8SPtoTP	57	1.91	0.26	T8SPtoTP	57	1.93	0.25	0.08
T8StoESFPS	57	1.37	0.39	T8StoESFPS	57	1.39	0.40	0.49
T8StoES	49	0.51	0.19	T8StoES	49	0.52	0.19	0.72
T8StoTrap	51	0.21	0.09	T8StoTrap	51	0.26	0.34	0.30

KEY: **n** – sample size, **SD** – standard deviation, **T5** – vertebral level T5, **T8** – vertebral level T8, **SPtoTP** – Spinous process to the Transverse process, **StoESFPS** – Skin to the Erector spinae fascial plane space, **StoES** – Skin to the Erector spinae muscle, **StoRh** – Skin to the Rhomboid muscle, **StoTrap** – Skin to Trapezius muscle.

No significant difference was noted between any of the measurements for age groups 2 (28 females and 21 males) and 3 (31 females and 26 males). Subsequently, comparative analysis was performed between groups to determine if there was a significant difference between individual measurements and the age group before pooling the data. Results revealed a significant difference (p-value > 0.05) between; spinous process to transverse process, skin to erector spinae fascial plane space and age groups. Due to the statistical difference between groups, the data were not pooled, and further statistical testing was performed on the groups individually.

Measurements from group 1 that was not statistically significant were pooled create averages for each measurement with a new standard deviation (Table 8). The T5 skin to erector spinae fascial space and T8 skin to erector spinae muscle was excluded from the pooled data.

Table 8. Descriptive statistics summary after pooling the right and left sides for the CT component (group 1).

Measurement	n	Minimum (cm)	Maximum (cm)	Mean (cm)	SD
T5 Spinous process to the Transverse process	45	0.73	1.84	1.28	0.20
T5 Skin to the Erector spinae muscle	45	0.28	1.46	0.63	0.20
T5 Skin to the Rhomboid muscle	45	0.16	1.04	0.42	0.16
T5 Skin to Trapezius muscle	45	0.10	0.58	0.24	0.09
T8 Spinous process to the Transverse process	45	0.81	1.78	1.25	1.95
T8 Skin to the Erector spinae fascial plane space	45	0.50	2.04	1.08	0.26
T8 Skin to Trapezius muscle.	45	0.06	0.58	0.24	0.94

KEY: **n** – sample size, **SD** – standard deviation, **T5** – vertebral level T5, **T8** – vertebral level T8

Regression analysis was then performed to evaluate the correlation between the measurements – the dependent variable – and fixed factors such as sex and age – the independent variables. From the results, a weak correlation – adjusted R^2 -value ≤ 0.3 – was found between the measurements and sex. Likewise, a weak correlation – adjusted R^2 -value ≤ 0.3 – was found between the measurements and age.

Subsequently, a multivariate regression analysis was performed to create a standard equation that can be utilised when performing the ESP block in age group 1. For the analysis, factors such as sex and age were used, as these were the only demographic information available from the CT scans. Since the T5 right and left sides for the skin to erector spinae fascial plane space measurement was significantly different, a separate equation was created for each side. While one formula was created for T8 skin to erector spinae fascial plane space (Table 9). The equations/formulae highlight the depth at which the block needle can be inserted at different vertebral levels, should the block be performed using the ‘blind’ technique in age group 1 (0 – 2 months).

Table 9. Multivariant regression analysis for determining the depth from the skin to the erector spinae fascial plane space using the data from the CT component (group 1).

Level	Parameter	Coefficient	SE	t	p-value	95% confidence interval	
						Lower	Upper
T5 Left	Sex	0.125	0.129	0.969	0.338	-0.135	0.385
	Age	-0.058	0.155	-0.375	0.710	-0.371	0.254
	-cons	1.529	0.189	8.099	0.0001	1.145	1.910
T5 Right	Sex	0.168	0.120	-1.403	0.168	-0.149	0.252
	Age	-0.038	0.144	-0.265	0.793	-0.228	0.228
	-cons	1.370	0.176	7.804	0.000001	0.756	1.345
T8	Sex	0.051	0.099	0.518	0.606	-0.149	0.252
	Age	-0.012	0.119	-0.107	0.914	-0.254	0.228
	-cons	1.050	0.145	7.211	0.0000001	0.756	1.345

Key: **SE** – standard error, **T5** – vertebral level T5, **T8** – vertebra level T8.

Sex was determined with numeric values that could be inserted into the equations. Males were assigned the number 0, while females were assigned the number 1. As displayed in Table 9, the constants were the only statistically significant variables. Formulae created, included the standard error of estimates to further validate the formula.

The formulae for age group 1 were as follows:

- T5 skin to the erector spinae fascial plane space (left side):
 - Depth in cm = 1.559 + 0.125(sex) - 0.058(age in months) +/- the standard error of estimate (0.407)
- T5 skin to the erector spinae fascial plane space (right side):
 - Depth in cm = 1.370 + 0.168(sex) - 0.038(age in months) +/- the standard error of estimate (0.379)
- T8 skin to the erector spinae fascial plane space:
 - Depth in cm = 1.050 + 0.051(sex) - 0.012(age in months) +/- the standard error of estimate (0.272)

The adjusted R²-value for the formulae were as follows: at vertebral level, T5 left -0.25 and T5 right 0.0001. While the adjusted R²-value for vertebral level T8 was -0.047. Overall, the distance from the spinous process to the transverse process in group 1 at vertebral level T5 was 1.28 cm with a standard deviation of 0.20, while the distance at vertebral level T8 was 1.25 cm with a standard deviation of 1.95.

The same tests were conducted for the remaining groups. Since group 2 and 3 displayed no significant differences between left- and right-side measurements, the data was pooled create averages for each measurement with a new standard deviation (Table 10 to 13).

Table 10. Descriptive statistics summary after pooling the right and left sides for the CT component (group 2).

Measurement	n	Minimum (cm)	Maximum (cm)	Mean (cm)	SD
T5 Spinous process to the Transverse process	50	0.64	2.59	1.59	0.30
T5 Skin to the Erector spinae fascial plane space	50	0.64	3.11	1.52	0.46
T5 Skin to the Erector spinae muscle	47	0.27	3.01	0.73	0.43
T5 Skin to the Rhomboid muscle	43	0.17	1.67	0.52	0.28
T5 Skin to Trapezius muscle	50	0.09	1.67	0.37	0.29
T8 Spinous process to the Transverse process	49	0.98	2.59	1.59	0.27
T8 Skin to the Erector spinae fascial plane space	49	0.63	2.39	1.20	0.35
T8 Skin to the Erector spinae muscle	46	0.19	1.69	0.54	0.23
T8 Skin to Trapezius muscle.	49	0.07	0.50	0.25	0.09

KEY: **n** – sample size, **SD** – standard deviation, **T5** – vertebral level T5, **T8** – vertebral level T8

Regression analysis was then performed to evaluate the correlation between the measurements – the dependent variable – and fixed factors such as sex and age – the independent variables. From the results, a weak correlation was found between the measurements and sex or age. All regression models produced an adjusted R²-value of ≤ 0.1.

Subsequently, a multivariate regression analysis was performed to create a standard equation that can be utilised when performing the ESP block in age group 2. Since the data was pooled together, one formula was created for each vertebral (Table 11). Again, the equations/formulae highlight the depth at which the block needle can be inserted at different vertebral levels, should the block be performed using the 'blind' technique in age group 2 (2 months – 2 years).

Table 11. Multivariate regression analysis for determining the depth from the skin to the erector spinae fascial plane space using the data from the CT component (group 2).

Level	Parameter	Coefficient	SE	t	p-value	95% confidence interval	
						Lower	Upper
T5	Sex	-0.163	0.133	-1.217	0.229	-0.432	0.106
	Age	0.004	0.008	0.469	0.641	-0.013	0.020
	-cons	1.556	0.159	9.743	7.345	1.234	1.877
T8	Sex	-0.100	0.100	-0.996	0.324	-0.302	0.102
	Age	0.003	0.006	0.517	0.607	-0.009	0.015
	-cons	1.214	0.119	10.20	2.15	0.975	1.454

Key: **SE** – standard error, **T5** – vertebral level T5, **T8** – vertebra level T8.

Sex was determined with numeric values that could be inserted into the equations. Males were assigned the number 0, while females were assigned the number 1. None of the variables were statistically significant as shown in table 11.

The formulae for age group 2 were as follows:

- T5 skin to the erector spinae fascial plane space:
 - Depth in cm = 1.556 - 0.163(sex) + 0.004(age in months) +/- the standard error of estimate (0.469)
- T8 skin to the erector spinae fascial plane space:
 - Depth in cm = 1.214 - 0.100(sex) + 0.003(age in months) +/- the standard error of estimate (0.394)

The adjusted R²-value for the formulae at vertebral level T5 and T8 was -0.005 and -0.015. Overall, the distance from the spinous process to the transverse process in group 2 at vertebral level T5 was 1.59 cm with a standard deviation of 0.30, while the distance at vertebral level T8 was 1.59 cm with a standard deviation of 0.27.

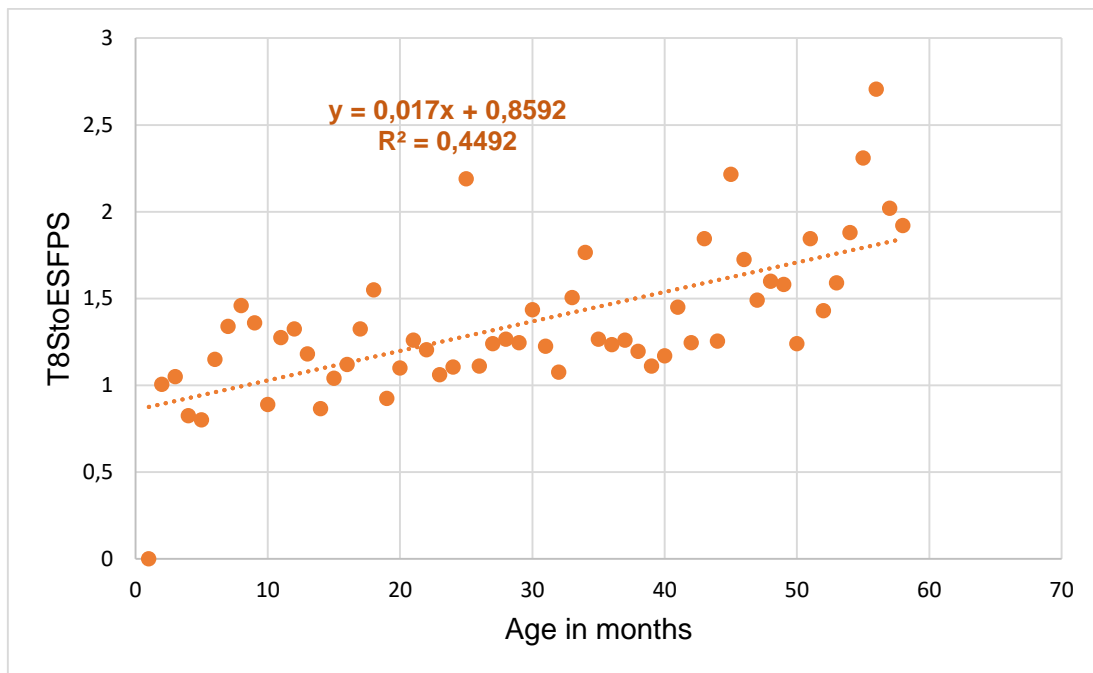
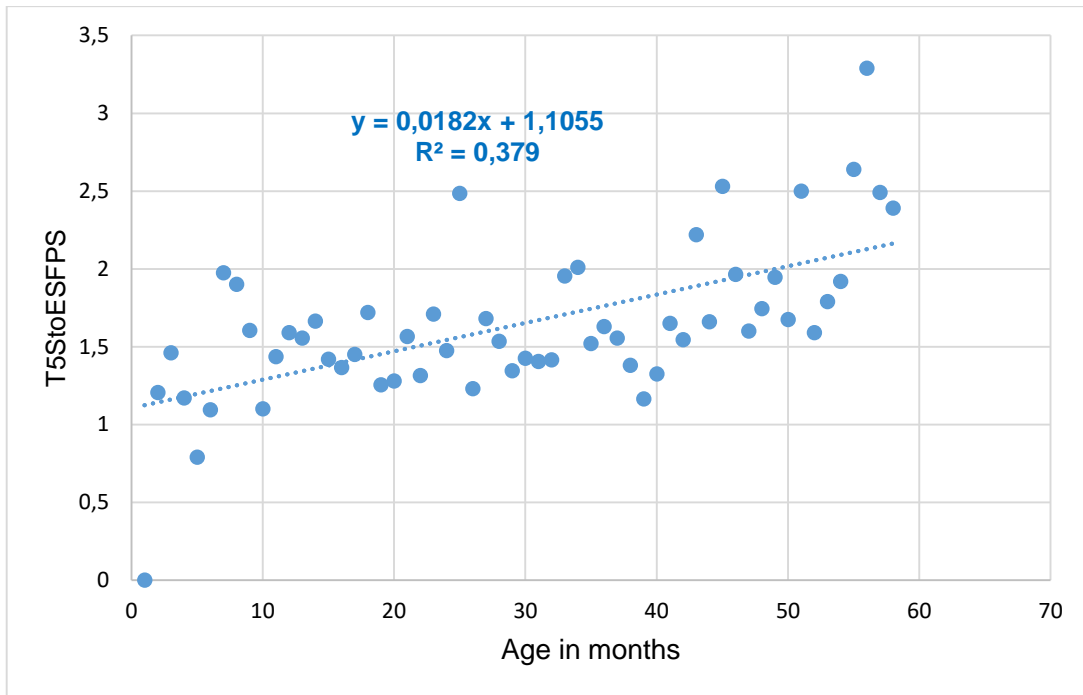
Table 12. Descriptive statistics summary after pooling the right and left sides for the CT component (group 3).

Measurement	n	Minimum (cm)	Maximum (cm)	Mean (cm)	SD
T5 Spinous process to the Transverse process	57	1.39	2.68	1.91	0.25
T5 Skin to the Erector spinae fascial plane space	57	0.79	3.29	1.67	0.45
T5 Skin to the Erector spinae muscle	50	0.37	3.06	0.73	0.42
T5 Skin to the Rhomboid muscle	50	0.11	0.97	0.38	0.15
T5 Skin to Trapezius muscle	53	0.07	1.30	0.24	0.17
T8 Spinous process to the Transverse process	57	1.40	2.54	1.92	0.25
T8 Skin to the Erector spinae fascial plane space	57	0.80	2.70	1.38	0.39
T8 Skin to the Erector spinae muscle	50	0.22	1.30	0.51	0.19
T8 Skin to Trapezius muscle.	52	0.06	1.41	0.24	0.19

KEY: **n** – sample size, **SD** – standard deviation, **T5** – vertebral level T5, **T8** – vertebral level T8

Regression analysis was then performed to evaluate the correlation between the measurements – the dependent variable – and fixed factors such as sex and age – the independent variables. From the results, no correlation was found between any of the measurements and sex. A moderate correlation was found between the following measurements; T5 skin to erector spinae fascial space and age (adjusted R²-value of 0.38), T8 skin to erector spinae fascial space and age (adjusted R²-value of 0.45), T8 spinous process to transverse process (adjusted R²-value of 0.42).

Measurements with a moderate correlation were then further plotted on a scatter plot to display the relationship of the correlation (Figure 9).



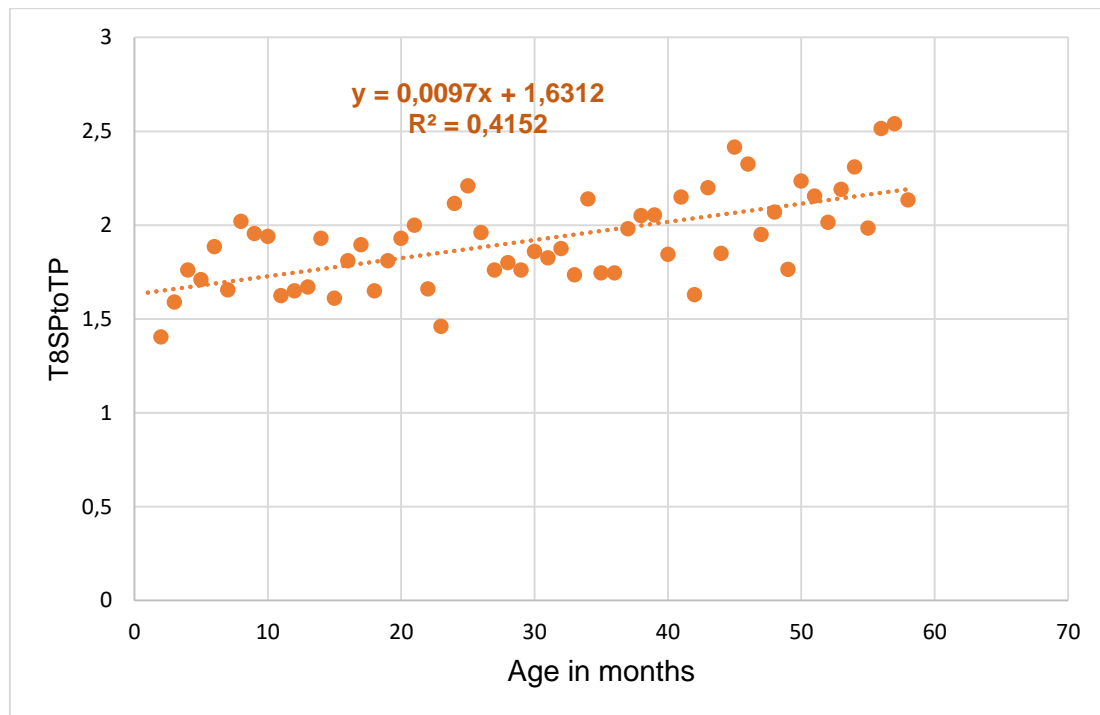


Figure 9: Scatter plot displaying the correlation between T5StoESFPS in cm to age in months (top image), T8StoESFPS in cm to age in months (middle image), T8SPtoTP in cm to age in months (bottom image).

As shown in figure 9, the adjusted R^2 -values indicate how much of the attribution is caused by age. Therefore, the skin to the erector spinae fascial plane space at vertebral level T5 and T8, 38% and 45% respectively, of the variations can be explained by age or is caused by age. While for T8 spinous process to transverse process, 42% of the variation can be explained by age or is caused by age.

Subsequently, a multivariate regression analysis was performed to create a standard equation that can be utilised when performing the ESP block in age group 3. Since the data was pooled together, one formula was created for each vertebral (Table 13). The equations/formulae highlight the depth at which the block needle can be inserted at different vertebral levels, should the block be performed using the 'blind' technique in age group 3 (2 – 12 years).

Table 13. Multivariant regression analysis for determining the depth from the skin to the erector spinae fascial plane space using the data from the CT component (group 3).

Level	Parameter	Coefficient	SE	t	p-value	95% confidence interval	
						Lower	Upper
T5	Sex	-0.013	0.095	-0.136	0.892	-0.205	0.178
	Age	0.008	0.001	5.887	2.580	0.005	0.011
	-cons	0.928	0.156	6.317	5.260	0.633	1.223
T8	Sex	-0.065	0.076	-0.851	0.398	-0.219	0.088
	Age	0.008	0.001	6.86	6.86	0.005	0.010
	-cons	0.716	0.117	6.077	1.280	0.480	0.953

Key: **SE** – standard error, **T5** – vertebral level T5, **T8** – vertebra level T8.

Sex was determined with numeric values that could be inserted into the equations. Males were assigned the number 0, while females were assigned the number 1. Again, none of the variables were statistically significant.

The formulae for age group 3 were as follows:

- T5 skin to the erector spinae fascial plane space:
 - Depth in cm = $0.928 - 0.013(\text{sex}) + 0.008(\text{age in months}) \pm$ the standard error of estimate (0.359)
- T8 skin to the erector spinae fascial plane space:
 - Depth in cm = $0.716 - 0.065(\text{sex}) + 0.008(\text{age in months}) \pm$ the standard error of estimate (0.288)

The adjusted R²-value for the formulae at vertebral level T5 and T8 was -0.369 and -0.452. Overall, the distance from the spinous process to the transverse process in group 3 at vertebral level T5 was 1.91 cm with a standard deviation of 0.25, while the distance at vertebral level T8 was 1.92 cm with a standard deviation of 0.25.

c) ***CT component (real-time spread of contrast medium)***

Using the multi-slice CT and 3D volume rendering function on radiant DICOM viewer, we were able to determine the craniocaudal spread over multiple vertebral levels. Contrast material was found over three dermatomal levels on the right hand side (T6 to T9) when introduced at vertebral level T8 and over four dermatomal levels on the left hand side (T9 to the interspinous space of T11/12) when introduced at vertebral level T10. The contrast material was also found over the costotransverse ligament and further lateral from the lateral border of the erector spinae muscle into the intercostal space. Dye spread was also seen in the paravertebral space, however, no spread was seen in the epidural space. Additionally, contrast dye was seen anterior to the erector spinae muscle from vertebral levels T6 to T11/12, yet posterior to the muscle from vertebral levels T9 to T11/12 (Figure 10). Results from this section suggested that the dose per kilogram per dermatome was 0.65 ml.



Figure 10: Lateral view of a three-dimensional volume-rendered CT reconstruction of contrast injectate spread in a fresh neonate. Green arrows represent the craniocaudal spread within the erector spinae fascial plane space when introducing contrast material at vertebral level T8. Yellow arrows represent the craniocaudal spread within the erector spinae fascial plane space and posterior to the erector spinae muscle at the spinous and transverse processes of vertebral level T10 (Govender *et al.*, 2020b).

d) ***Cadaveric component***

The ESP block was replicated bilaterally in nine, and unilaterally in two fresh neonatal cadavers (n = 20). Dissections were performed 30 minutes subsequent to performing the block. From the total sample size, 16 of the blocks were successfully placed, while the remaining injections were either incomplete (n = 1) or failed blocks (n = 3). An incomplete block was defined as a block in which contrast material was only seen at the vertebral

level in which the dye was introduced, with no craniocaudal spread, whereas, a failed block was defined as a block with the complete absence of contrast material infiltration. The failed blocks were then excluded from the results. Therefore, the final sample size was 17 blocks. It was discovered that two cadavers had been frozen prior to performing the block which may have affected the spread (failed blocks).

Upon dissection, extensive dye spread was seen in a craniocaudal direction, both superficial and deep to the erector spinae fascial plane (Figure 11B). Surface staining was noticed on the trapezius-, rhomboid-, latissimus dorsi and erector spinae muscles in all cadavers (Figure 11A). Slight staining was also noted over the external intercostal muscles. Methylene blue dye was found at the lamina and over the posterior aspect of the transverse process, in close proximity to the costotransverse ligament/foramen, as well as around the neural/intervertebral foramina in 8 cadavers (Figure 11C). Deeper staining was also found at the level of the dorsal and ventral roots or ganglions of the spinal nerves in the paravertebral gutters in all successfully placed blocks (n = 17) (Figure 11D & E).

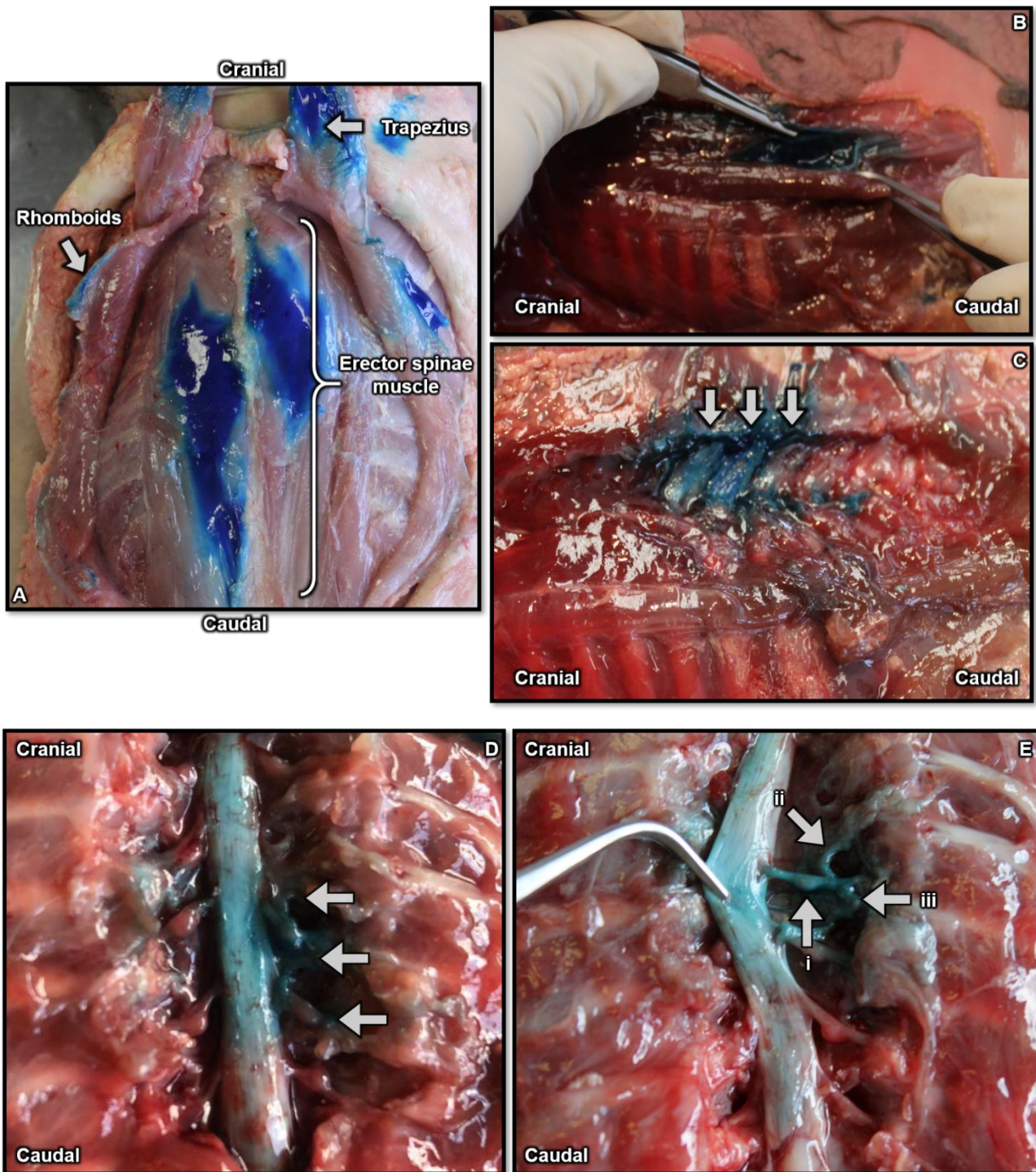


Figure 11: Photographic images displaying the A – surface staining of the superficial muscles of the back. B – extensive craniocaudal spread both deep and superficial to the erector spinae fascial plane C – methylene blue dye found over the posterior aspect of the lamina and transverse process near the neural/intervertebral foramina D – methylene blue dye in the epidural space and surrounding the spinal nerves as they come off the spinal cord E – methylene blue dye staining the ganglion (i), dorsal rami (ii) and ventral rami (iii) (Govender *et al.*, 2020a, 2020b).

Paravertebral and neural/intervertebral foramina spread was noted in 17 and 16 blocks respectively, as the dye spread to the spinal roots, intercostal spread was seen in 15 blocks, whereas epidural spread was only noted in 11 blocks. With regard to the intercostal spread, the number of vertical vertebral levels covered, correlated with the number of horizontal intercostal spaces in all but three blocks ($n = 3$). The epidural spread was further confirmed by the staining of the dura mater surrounding the spinal cord. Table 14 provides a detailed summary of the number of blocks replicated, including the volume used per cadaver, the craniocaudal spread of dye, and the number of dermatomal levels covered.

The average spread of dye was 5 (range 3-7) vertebral levels in the thorax and the abdomen, while the dose per kilogram per dermatome ranged from 0.02 – 0.13 ml (Table 14). Moreover, we were also able to determine that by inserting the needle from cranial to caudal ($n = 2$) versus caudal to cranial ($n = 15$), did not alter the distribution of dye within the fascial space. Similarly, introducing the dye between adjacent transverse processes ($n = 2$) as opposed to at the angle of the transverse process ($n = 15$), did not affect the overall spread. The ESP block produced consistent results in terms of injectate distribution.

Table 14. Summary of the results obtained when replicating the erector spinae plane block in the neonatal cadavers. (Govender *et al.*, 2020c)

n	Weight (kg)	Volume (ml)	Injection level	Injectate spread								
				Vertebral levels	Number of dermatomes	Dose/kg/dermatome (ml)	Paravertebral space	Epidural space	Intercostal space	Neural/inter vertebral foramina		
1	1.6	0.5	T5	T3 – T6	4	0.13	✓	✓	✓	✓		
2	0.6	0.2	T8	T7 – T11	5	0.04	✓	✓	✓	✓		
3♦	2.95	0.3	T8	T6 – T9	4	0.08	✓	-	✓	✓		
			T10	T6 – T12	7	0.04	✓	-	T9 – T11	✓		
4•	2.60	0.3	T5	T4 – T8	5	0.06	✓	✓	✓	✓		
			T8	T7 – T11	5	0.06	✓	✓	✓	✓		
5	1.7	0.2	T8	T5 – T9	5	0.04	✓	✓	✓	✓		
			T10	T11 – L2	4	0.05	✓	✓	✓	✓		
6	1.35	0.3	T5	T2 – T7	6	0.05	✓	-	T4 – T6	✓		
			T8	T6 – T11	6	0.05	✓	✓	✓	✓		
7	2	0.3	T5	T2 – T5	4	0.08	✓	✓	✓	✓		
			T8★	Incomplete	-	-	✓	-	-	-		
8	0.7	0.1	T5	T2 – T6	5	0.02	✓	✓	T4 – T6	✓		
			T8	T7 – T9	3	0.03	✓	✓	✓	✓		
9	1.2	0.2	T5	T2 – T7	6	0.03	✓	✓	✓	✓		
			T8	T6 – T10	5	0.04	✓	-	✓	✓		
10	3.4	0.3	T8	T7 – T9	3	0.1	✓	-	-	✓		
			T10	Failed spread	Blocks were replicated; however, upon dissection, the dye was not found/seen. These cadavers were discovered to have been frozen prior to replicating the block.							
11	1.8	0.2	T5	Failed spread								
			T8	Failed spread								

Key: ♦ - Needle was inserted cranial to caudal, • - Needle was insertion mid-way between adjacent transverse processes, ★ - Contrast material was only found at the vertebral level in which the injection was inserted.

2.8 Discussion

The ESP block is a novel interfascial technique that can be used for various truncal procedures in both adults and paediatrics (Costache *et al.*, 2018; De la Cuadra-Fontaine *et al.*, 2018; Vidal *et al.*, 2018; Aksu and Gürkan, 2019a; Govender *et al.*, 2020a) (Appendix A). Although this block is relatively new, it has sparked interest in clinicians due to its relative ease of administration and clinical efficacy. This study aimed to investigate the spread of contrast material and the subsequent dermatomal coverage by replicating the procedure in eleven fresh neonatal cadavers. Results from the different components in this study revealed that injecting contrast material – 0.1 ml/kg or 1 ml/kg – into the erector spinae fascial plane space at vertebral levels T5 and T8 (T10) will provide an average of 4-5 levels of coverage for the thoracic and abdominal regions respectively.

The discussion will be broken down into two sections, reporting on the measurements and spread separately.

a) **Block measurements**

To date, only one case study had been conducted on the means and standard deviations for the various measurements when performing an ESP block in different paediatric age groups.

From the results of the ultrasound component, in which preterm neonates were evaluated, no statistical significance was found between left sides, nor any correlation between dependent and independent variables. It can only be assumed that the limited sample size of this component contributed to the uneventful results. Overall, the approximate depth to perform the ESP block was 0.95 cm and 0.99 cm at vertebral levels T5 and T8, respectively, with a standard deviation of 0.42 and 0.33. The distance from the spinous process to the needle insertion site (transverse process) for vertebral levels T5 and T8 was 1.42 cm and 1.54 cm, respectively, with a standard deviation of 0.39 and 0.23.

The CT component revealed a significant difference between right and left measurements in age group 1 for T5 skin to erector spinae fascial plane space and T8 skin to erector spinae muscle. Even though these measurements were statistically significant, the difference was rather small, while the residual measurements for age groups 2 and 3 displayed no significant difference between the right and left sides. The average depth for performing the block in age group 1 was between 1.67 cm to 1.08 cm (standard deviation of 0.40/+ 0.03 and 0.26), while for age groups 2, the depth was 1.52 cm with a standard deviation of 0.46 at vertebral level T5 and 1.20 cm with a standard deviation of 0.35 at vertebral level T8. The average depth for group 3 was 1.67 cm with a standard deviation of 0.45 at vertebral level T5 and 1.38 cm with a standard deviation of 0.39 at vertebral level. Overall, the low standard deviations indicated little variations within the age groups.

Karaca (2019) noted that for children above the age of 10 years old, the needle should be inserted 1.5-2 cm lateral to the midsagittal region. Results from this study are similar to those of Karaca, as our predicted value falls within their predicted range. However, Karaca's estimation included children up to the age of 14 years, whereas our study only included children up to 12 years. Moreover, the mean distance reported in this study was specified to vertebral levels T5 and T8, whereas, Karaca's estimation was specific to vertebral level T7.

Additionally, this study noted the skin to muscle distance in various age groups. Results revealed that changes in body habitus, which is directly related to the age group, affects the overall size of muscular structures. This in turn directly relates to the depth at which the needle can be inserted in various age groups.

Based on the regression models, no correlation was found between any of the CT measurements and sex, while a moderate to strong correlation was found between measurements T5 and T8 skin to erector spinae fascial plane space, T8 spinous process to transverse process and age. The models that displayed a moderate to strong correlation revealed that as age in months increases, so does the measurement in cm. Lastly, the multivariate regression analysis was performed to create estimation formulae that could be used to help administer the block. A total of six formulae were

created. To our knowledge, this was the only study to produce formulae for calculating the needle depth when performing an ESP block in a paediatric population.

b) ***Injectate spread***

Hamilton and Manickam (2017) stated that the anatomy of the erector sheath is the reason for the success of the ESP block. They suggested that the individual muscles of the erector spinae muscle, together with their associated sheaths, exhibit a complex three-dimensional cylindrical anatomical structure. Each cylinder is surrounded by retinacular fascia which separates its contents from other muscular compartments in the region. Anteriorly, the fascial sheath is incomplete due to multiple varied apertures or perforations. Furthermore, the sheath is intermittently tethered anteromedially to the bony structures – the spinous and transverse processes – along its course.

Findings from this study substantiate suggestions by other authors that the success of this block is attributed to the diffusion of anaesthetic through soft tissue gaps (Luftig *et al.*, 2017; López *et al.*, 2018). Additionally, Hamilton and Manickam (2017) hypothesized that the craniocaudal spread is assisted by the thoracolumbar fascia, as it contributes to the sheath found around the erector spinae muscle (López *et al.*, 2018). Supporting both Hamilton and Manikam, we believe that the erector sheath and the thoracolumbar fascia combine to form a continuous tissue plane over multiple vertebral levels, allowing for the craniocaudal spread of dye.

The anterior perforations within the sheath explain the mechanism of anterior spread through the intertransverse connective tissue into the paravertebral-, epidural- and intercostal spaces, as seen in this study and supported by others (Nair *et al.*, 2018; Elkoundi *et al.*, 2019a). Anterior diffusion through the costotransverse foramen (as the dye is inserted nearby), allows for the injectate to be deposited in the vicinity of the spinal nerve roots (Cornish, 2019). As the dye penetrates through the costotransverse foramen, it creates a tunnel between the paravertebral space and the erector spinae fascial plane, which acts as a local anaesthetic depot (Sahin *et al.*, 2020). This allows for the anaesthetic to be retained and released over a longer period of time.

Dissection revealed staining in the overlying muscular structures – the trapezius and rhomboid muscles – posterior to the erector spinae muscle from vertebral levels T2 and T6. A study conducted by Barker and Briggs (1999), reported that part of the thoracolumbar fascia fuses with the muscular fascia of the trapezius and rhomboid muscles, which would explain the staining as seen in a study by Govender *et al.*, 2020a (Appendix A). Muscular staining was also noted in the erector spinae muscle between vertebral levels T1 and L2. Contrary to another cadaveric study, the spread was seen in the paravertebral-, intercostal- and epidural spaces in most cadavers (Ivanusic *et al.*, 2018). The intercostal spread was assessed laterally towards the midscapular line. The vertebral level spread, however, did not match the intercostal space spread.

Upon investigation, factors such as needle direction and entry site most likely does not affect the spread of contrast material. Results revealed that inserting the needle in a cephalad to caudal direction versus caudal to cephalad, did not alter the distribution of dye within the fascial space (in 1 cadaver). It was recommended that the ESP block should be performed by inserting the needle in a cephalad to caudal direction at the superior aspect of the transverse process to avoid the anterior costotransverse ligament (Cornish, 2019). Furthermore, introducing the dye between adjacent transverse processes, as opposed to at the superficial lateral tip of the transverse process, also did not affect the overall spread in the fascial plane (in 1 cadaver). However, the anaesthesiologist did note that there was more resistance/pushback when performing the block midway between the transverse processes.

Results from the CT component somewhat contradicted results from the cadaveric component, even though a larger volume dose was introduced. Extensive craniocaudal spread was seen, with a limited paravertebral and intercostal spread. The intercostal spread extended laterally towards the tubercle of the ribs (at vertebral levels T6 – T9). Lastly, no epidural spread was seen at any of the vertebral levels. Studies that used imaging modalities such as magnetic resonance imaging and fluoroscopic guidance seem to display more favourable results than our study (Adhikary *et al.*, 2018; Jadon *et al.*, 2018; Schwartzmann *et al.*, 2018; Diwan and Nair, 2020). Although these studies show encouraging results, which included epidural spread, it is important to note that certain imaging techniques offer a higher spatial resolution than others. Furthermore, the type of contrast material used may also result in discrepancies in the spread

between soft tissue gaps (Aponte *et al.*, 2019). Govender *et al.* suggested that contrast material have different physicochemical properties than local anaesthetic agents, therefore, affecting the overall spread (Appendix B).

Two techniques for the ESP block, namely a superficial and a deep approach (Jain *et al.*, 2018). The superficial approach involved injecting anaesthetic between the rhomboid and erector spinae muscle, whereas the deep approach involved introducing anaesthetic deep to the erector spinae muscle. Forero *et al.* (2016), described both approaches upon the discovery of the block. Results revealed a much greater spread with the deep approach. The spread included the area deep to the intercostal muscles, through the costotransverse foramina and intervertebral foramina approaching the spinal nerve roots. Subsequent ESP studies adopted the deep approach (Adhikary *et al.*, 2018; Darling *et al.*, 2018; Ivanusic *et al.*, 2018; Schwartzmann *et al.*, 2018; Vidal *et al.*, 2018; Aksu and Gürkan, 2019c; Aponte *et al.*, 2019; Choi *et al.*, 2019; Pourkashanian *et al.*, 2019; Tulgar *et al.*, 2019b).

Adult anatomical studies, which included cadaveric and imaging modalities done by various authors, reported dissimilarities with regard to the spread of injectate. Ivanusic *et al.* (2018) reported extensive craniocaudal spread to the dorsal rami of spinal nerves, however, limited anterior spread to the ventral rami of spinal nerves. Additional blockage of the lateral cutaneous branches of intercostal nerves was noted at the angle of the ribs. Similar results were reported by Aponte *et al.* (2019) who conducted an anatomical evaluation of the extent of spread in an ESP block using both CT scanning and fresh cadavers. Results from the CT scans showed a wide craniocaudal distribution and a lateral extension towards the costotransverse area, affecting all three bands of the erector spinae muscle. No radiocontrast dye, however, was found in the paravertebral or epidural space. These results contradicted the results of the current study as paravertebral spread was seen in the CT component. Additionally, cadaveric results revealed extensive craniocaudal spread and spread to the dorsal rami of spinal nerves, as well as lateral spread from the costotransverse region to the lateral margin of the iliocostalis muscles at the costal angle. No staining was found in the paravertebral space or the ventral rami of spinal nerves. Comparable results were reported by Visoiu and Scholz (2019). Contrary to the findings of both these studies,

the current study found dye staining the paravertebral, epidural and intercostal spaces in most of the samples in the cadaveric component.

Adhikary and others relayed anterior spread into the paravertebral space, lateral spread into the neural/intervertebral foramina, as well as spread to the epidural space and ipsilateral sympathetic chain (Adhikary *et al.*, 2018; Pourkashanian *et al.*, 2019; Tulgar *et al.*, 2019a). Similar findings were described by other authors (Yang *et al.*, 2018; Choi *et al.*, 2019). Vidal *et al.* (2018) reported evident spread posterior to the transverse process, as well as in the paravertebral and intercostal spaces. No spread was noted in the neural/intervertebral foramina or epidural space. Vidal *et al.* (2018) further stated that the dye covered more intercostal spaces than expected for the amount of injectate. This could be due to the multiple planes the injectate has to penetrate to eventually reach the paravertebral space and it further explains the technique's analgesic but non-anaesthetic effect. Two magnetic resonance imaging studies by Adhikary *et al.* (2018) and Schwartzmann *et al.* (2018) reported anterior spread into the paravertebral-, epidural- and intercostal space, as well as the neural/intervertebral foramina.

Darling *et al.* (2018) was the first to report on a single case study which utilized an ESP block in the thoracic region as an alternative to a lumbar plexus block for hip dysplasia. Results reveal that lower thoracic ESP blocks provide successful lumbar dermatomal coverage. They further went on to note the directional features of an ESP block. Inserting a catheter/needle in a cephalad orientation provides thoracic and upper abdominal dermatomal analgesia (Wong *et al.*, 2018), while inserting a catheter/needle in a caudal orientation provides effective lumbar coverage (Munshay *et al.*, 2018b). They also noted that lumbar ESP blocks are more challenging to perform due to the increased thickness in the erector spinae muscle and the corresponding depth of the intermuscular plane in the lumbar levels (Darling *et al.*, 2018, Aygun *et al.*, 2020a). The shamrock technique is a technique used for scanning of the lumbar plexus or nerve(s). The nerve(s) are confirmed after identifying the shamrock or clover-shaped muscular complex around the vertebra. Therefore, a modification of the shamrock technique which involves the patient being placed in the lateral decubitus position, with the side of the block in a higher position, might be an easy-to-perform option for the lumbar region (Aksu and Gürkan, 2019a; Tulgar *et al.*, 2019a). Additionally, the shamrock

technique requires a convex probe rather than a linear ultrasound probe (De Cassai *et al.*, 2019).

Multiple studies reported on the vertical spread of contrast material – by highlighting the number of vertebral levels – using both cadaveric and imaging modality analysis. Choi *et al.* (2019) reported on the paravertebral spread after an ESP block was achieved using endoscopic and anatomical evaluation. The ESP block was performed on 12 cadavers bilaterally – using 10 ml or 30 ml per side – at vertebral level T5. Upon insertion of the endoscope, staining of the superior costotransverse ligament was noted in the majority of the cases. Results from the ESP blocks that used 10 ml of dye solution revealed staining of the superior costotransverse ligament from vertebral levels T4 to T6, yet no paravertebral spread. For the ESP blocks using 30 ml of dye solution, staining of the superior costotransverse ligament from vertebral levels T2 to T8 was seen. Furthermore, staining of thoracic spinal nerves – and thus the paravertebral space – at the intervertebral foramina was noted from vertebral levels T3 to T7.

In anatomical dissections, dye solution was found in the fascial layer of the erector spinae muscle group and the external intercostal muscles in all ESP blocks. Specific to the 30 ml dye solution group, dye was found posterior to the fascial layer of the erector spinae muscle in a craniocaudal direction, however, dye was barely observed in the retrolaminar plane medially and vertically. Lateral spread to the posterior layer of the thoracolumbar fascia and external intercostal muscle was observed. No dye was located deep to the external intercostal muscle, therefore, the intercostal nerves which are found in the space between the internal and innermost intercostal muscle were not stained in any of the ESP blocks, regardless of the volume. Sympathetic chain and epidural spread were found in one case (30 ml). These results contradicted the results of the current study as intercostal spread was observed. Choi and co-workers (2019) concluded that ESP blocks are volume dependent, therefore, more volume will lead to a more extensive spread.

Bilateral ESP blocks were performed at vertebral level T9 in four embalmed cadavers by Altinpulluk and colleagues (2019). Upon dissection, methylene blue spread was found through the costotransverse foramen, which stained the dorsal rami at different

vertebral levels (T5 – T12). Dye also spread to the ventral rami and spinal ganglion between vertebral levels T8 to T11. Additionally, dye was found inside the intervertebral foramina and extended to the vertebral canal at vertebral level T9. The dura of the spinal cord, the subdural space and epidural space were stained at T9.

To examine the true effect of dye diffusion, Ohgoshi *et al.* (2019) conducted a cadaveric study to investigate whether injections at the costotransverse notch facilitated superior paravertebral spread. To regulate the limitations of cadaveric material, the authors decided to use two cadavers which were subject to different embalming processes, Thiel and formaldehyde. The injections were performed at two sites, the first at the transverse process and the second at the notch of the costotransverse joint. Injections were done bilaterally at three vertebral levels T4, T7 and T10, using different colours of contrast material.

Five of the six costotransverse notch injections displayed contrast spread in the paravertebral space (three in the Thiel-embalmed cadaver and two in the formaldehyde embalmed cadaver), whereas no paravertebral spread was found after any of transverse process injections. From the five successful costotransverse notch injections, the contrast material spread over one intercostal space in the Thiel-embalmed cadaver and over two intercostal spaces in the formaldehyde embalmed cadaver. Results from this study showed that the site of injection largely influences the spread of contrast material and can, therefore, significantly influence the performance of ESP blocks. By injecting closer to the costotransverse notch, paravertebral spread can be easily achieved with a relatively low dose of injectate. Additionally, tissue structure and consistency influence the spread of injectate.

After performing an ESP block at vertebral level T5 on a patient with carcinoma of the right lung by Diwan and Nair (2020), CT scans were taken to track the spread of the injection. Favourable results revealed radio-opaque contrast spread deep to the erector spinae muscle, medially in the retrolaminar space, posteriorly in the epidural space and the paravertebral space through the intervertebral foramina at all levels. Spread was also observed longitudinally up to the lateral epidural space at all levels. Additionally, contrast material was found over the costotransverse foramen, which attributes to its mechanism of pathway blockade. After an assessment, the level of

dermatomal analgesia achieved was from vertebral level T2 and vertebral level T7 on the right hand side.

Using contrast magnetic resonance imaging to report on their experiences, Ahiskalioglu and colleagues (2020) performed an ESP block in the lumbar region as the main anaesthetic method for patients undergoing hip surgery. Subsequent to performing the block at vertebral level L4, patients were placed in a supine position and scans were taken. Significant contrast spread was observed between vertebral levels T12 and L5 around the transverse processes and erector spinae muscle. Muscular staining of the multifidus and iliocostalis muscles was seen between vertebral levels L2 and L4.

Contrast material was observed anterior to the transverse processes, penetrating the paravertebral-, foraminal- and epidural spaces, as well as the area around which the lumbar nerves enter the psoas major muscle. Contrast material was also found around the upper segment of the sacral plexus. Being one of the few reports on interfascial plane blocks being used as the main anaesthetic methods, the authors recommended the technique as a good alternative to lumbar plexus blocks citing many advantages. Distant needle application and less neurovascular damage were a few that were mentioned. The ESP block has also been used as the main anaesthetic for kyphoplasty (Verduzco, 2020).

In another magnetic resonance study (Schwartzmann *et al.*, 2020), the spread of local anaesthetic was documented after performing the ESP block in patients with chronic pain. Using a gadolinium- containing solution, the ESP block was performed unilaterally at vertebral level T10 in six patients. Extensive spread to the paraspinal muscles, intercostal spaces and neural/intervertebral foramina was seen. Although the spread to the intercostal spaces (ranging from 5 to 11 vertebral levels) was consistent in all patients, the craniocaudal spread was highly variable, while the neural/intervertebral foramina spread ranged between 2 and 6 levels. Furthermore, the lateral spread of the intercostal spaces did not reach the angle of the rib in any patient. Epidural spread was seen in two of the six patients. Muscular staining was also seen within the erector spinae and trapezius muscles. The consistent spread through the intercostal spaces, neural/intervertebral foramina and erector spinae muscle seen in

this study, contributes to the sensory findings in the ventral and dorsal thoracic and abdominal walls (Schwartzmann *et al.*, 2020).

The ESP block was also reported on by highlighting its clinical efficacy by Zhang *et al.* (2020). The ESP block was used in a single case study for hip dysplasia. Results revealed anterior penetration through the intertransverse connective tissue into the paravertebral space. There was no mention, however, of epidural or lateral spread. Furthermore, the authors commented on the decreased opiate exposure, decreased time in the post-anaesthesia recovery room, decreased hospital stay and increased satisfaction of the patient with regard to the block (Elkoundi *et al.*, 2019a). Contrary to the abovementioned studies, the sensory loss and decline in cutaneous cold sensation were investigated on a group of healthy volunteers. After performing unilateral ESP blocks at vertebral level T5, results revealed a significant block of the ipsilateral dorsal cutaneous sensory nerves. The cold sensation declination ranged from vertebral level T1 to L4. The anaesthetic concentration was found between vertebral levels T4 and T11, extending laterally towards the posterior axillary line. After an assessment, it was noted that the anterior and lateral chest walls, as well as the abdominal wall, was not affected. Authors concluded their study by affirming that the ESP block only affects dorsal branches of the ipsilateral spinal nerve, as no evidence of the block affecting the paravertebral space or the intercostal nerve, including the lateral branches, were seen (Zhang *et al.*, 2020).

In a separate study by Tsui *et al.* (2018) a bilateral continuous ESP block was used for a cardiopulmonary bypass. Successful results lead the authors to state that the arrival of ESP blocks has brought about a new era for cardiac regional anaesthesia. That has the potential to reduce intraoperative opioid use, facilitate early extubating and to improve the morbidity in cardiac patients. The ESP block has also been described as an avascular plane block which allows for a longer duration of action of local anaesthesia, which results in lower plasma levels due to reduced uptake of the local anaesthetic (de Haan *et al.*, 2018).

Although authors expressed their concern regarding the effect of weight, specifically in obese patients, on the performance of the block, there have been case reports reflecting positive outcomes. Piliego and co-workers (2020) reported on a case study

in which they selected an overweight patient to perform an ESP block for the pain management in laparoscopy nephrectomy. Using a convex ultrasound probe, the block was performed unilaterally at vertebral level T9, using 20 ml of anaesthetic (the standard amount used in previous studies). The procedure was uneventful, allowing the practitioners to spare the use of opioids and reducing the length of hospital stay. The authors concluded that even in overweight patients, the ESP block makes mini-invasive procedures such as laparoscopic nephrectomy, even less invasive.

Yang *et al.* (2018) proposed that the discrepancies in the composition of the ligaments neighbouring the costovertebral joint along the vertebral column play a role in the dispersal patterns of solutions. It was noted that the posterior costovertebral ligament is absent from vertebral levels T1 to T6, yet well developed between vertebral levels T7 to T10 (Adhikary *et al.*, 2018). This could explain the varying distribution and diffusion of injectate into the paravertebral space as seen in certain studies (Aponte *et al.*, 2019). Other explanations for variations in the spread include the anatomic complexity of the thoracolumbar fascia, the complex 3-dimensional geometry of the erector spinae muscle group and differences in operator technique (Hamilton, 2019a).

The spread of the ESP block has also been determined in paediatrics. Muñoz and co-workers (2017) noticed an extensive multi-dermatomal sensory block of the anterior, posterior and lateral thoracic walls in a patient undergoing oncological thoracic surgery. Upon assessment, injectate was seen in the paravertebral space. Similar spread was also noted by Ueshima and Hiroshi (2018), who used fluoroscopy to track the spread of anaesthetic. Neither author commented on the intercostal or epidural spread.

Aksu and Gürkan (2018b) reported positive results in four separate case studies in which patients, ranging from 6 months to 10 years were scheduled for inguinal hernia repair and nephrectomy surgeries. They further commented on the opioid-sparing effects of an ESP block and described the block as a promising technique in the field of paediatric post-operative analgesia. In a study by Thomas and Tulgar (2018), somatic and visceral analgesia was achieved when performing an ESP block in an 11-year old patient for laparoscopic cholecystectomy. They also stated that the distant application of the block from neuraxial structures resulted in rare mechanical

complications. They concluded that the ESP block is an easy to perform peripheral block that should be considered as an option for multimodal analgesia in children.

A unilateral ESP block was performed at vertebral level T5 in a 2.5-year old child undergoing excision of a chest wall tumour. Positive results led the authors to deduce that the use of clonidine as an adjuvant to local anaesthetics, may prolong the duration of analgesia and improve the quality of the block (Anju Gupta *et al.*, 2020). Ciftci *et al.* (2019b) performed a single shot ultrasound-guided ESP block for thoracic surgery in a 12-year old patient. The procedure, which was executed at vertebral level T5, was uneventful. The authors sought to test the effectiveness of a single dose pre-emptive ESP block, therefore, a catheter was not used. Overall, visual analog scale scores were low, with no requirement for rescue analgesia. They concluded that a pre-emptive single shot ESP block can be performed as part of a multimodal analgesic treatment for post-operative analgesia management in paediatric patients. Aksu and Gürkan (2020) described a sacral ESP with a longitudinal midline approach in a 6-month old patient undergoing distal hypospadias repair. After performing a single injection ESP block at the 4th median sacral crest, a bilateral effect was noted.

Kaushal *et al.* (2020) conducted a study on 80 paediatric patients to test their hypothesis that by administering bilateral ESP blocks after cardiac surgery, the post-operative analgesia would be improved. The study consisted of two groups: group B (receiving ESP blocks) and group C (without any intervention), with local anaesthetic being administered at vertebral level T3 in both groups. After negative aspiration, 1.5 ml/kg of ropivacaine was administered under ultrasound guidance. Results revealed that bilateral ESP blocks were effective in relieving the pain of post-sternotomy, with a longer duration of analgesia. Moreover, bilateral ESP blocks have also been reported to be effective in low birth-weight vulnerable infants as a regional anaesthetic technique to maintain cardiovascular stability (Basaran and Akkoyun, 2020).

Table 15 summarizes the number of documented ESP blocks that have been performed by various authors on a paediatric population, to date (July 2020). The table indicates the type of procedure, the volume used for the different ages and the overall spread of the injectate.

Table 15. List of authors who have performed the erector spinae plane block on a paediatric sample.

Author	Indication	Age	Volume	Level	Spread
<i>Hernandez et al. (2017)</i>	Lipoma	3 years	0.2 ml/kg	Unilateral T1	T1 – T9
<i>Muñoz et al. (2017)</i>	Tumor	7 years	×	Unilateral T8	T5 – T11
<i>Munshey et al. (2018a)</i>	Various	11 months – 17 years	0.4 ml/kg		×
<i>Munshey et al. (2018b)</i>	Pyeloplasty	11 months	0.3 ml/kg	Unilateral T8	×
<i>De la Cuadra-Fontaine et al. (2018)</i>	Open thoracic surgery	3 years	0.6 ml/kg	Unilateral T9	×
<i>Ueshima and Otake (2018)</i>	Funnel chest	6 and 8 years	0.6 ml/kg	Bilateral T6	×
<i>Kaplan et al. (2018)</i>	Lobectomy	7 months	0.3 ml/kg	Unilateral T6	T3 – T10
<i>Aksu and Gürkan (2018a)</i>	Nephrectomy	6 months and 7 years	0.5 ml/kg	Unilateral T12	
<i>Hernandez et al. (2018b)</i>	Inguinal hernia	2 months	0.4 ml/kg	Unilateral T6	T4 – L1
<i>Thomas and Tulgar (2018)</i>	Laparoscopic cholecystectomy	11 years	0.6 ml/kg	Bilateral T9	×
<i>Aksu and Gürkan (2019b)</i>	Inguinal hernia	2 and 5 years	0.5 ml/kg	×	×
<i>Bhoi et al. (2018)</i>	Decortication	12 years	Continuous infusion	×	×
<i>Wong et al. (2018)</i>	Sternotomy	17 years	Continuous infusion	Bilateral T7	×
<i>Darling et al. (2018)</i>	Hip dysplasia	11 years	Continuous infusion	Unilateral T8	T10 – L4
<i>de Haan et al. (2018)</i>	Axillary hidradenitis suppurativa resection	18 years	Continuous infusion	Unilateral T2	T1 – T10
<i>Moore et al. (2018)</i>	Exploratory laparotomy, duodenoduodenostomy	1 day	0.3 ml/kg	Bilateral T8 – T10	×

Author	Indication	Age	Volume	Level	Spread
Gaio-Lima <i>et al.</i> (2018)	Thoracotomy for paracardiac teratoma resection	15 months	0.45 ml/kg	Unilateral	×
Nardiello and Herlitz (2018)	Pectus carinatum, Pectus excavatum repair	13 years	0.3 – 0.4 ml/kg	Uni and Bilateral	×
<i>Mostafa et al.</i> (2019)	Splenectomy	3 – 10 years	0.3 ml/kg	Bilateral T7	×
Karaca (2019)	Cholecystectomy	10 – 14 years		T7	×
El-Emam and El motlb (2019)	Inguinal hernia	6 months – 3 years	0.5 ml/kg	Unilateral	×
Tulgar <i>et al.</i> (2019a)	Various				
Elkoundi <i>et al.</i> (2019b)	Hip dysplasia	4 years	0.3 ml/kg	Unilateral L2	L1-L4
Aksu and Gurkan (2019b)	Various (n =141)	< 15 years	0.1 – 0.5 ml/kg	Btw levels T4 – S4	×
Ince <i>et al.</i> (2019)	Abdominal surgery	13 years	Continuous infusion	Bilateral L2/3	×
Aksu and Gürkan (2019e)	Laparoscopic varicocelectomy	11 years	0.5 ml/kg	Bilateral	×
Baca <i>et al.</i> (2019)	Pain from lumbar spinal metastases from osteosarcoma	15 years	×	Bilateral	T12 – L1
Moore <i>et al.</i> (2019)	Primary liver transplant, redo liver transplant	8 and 12 years	0.3 ml/kg	Bilateral T8	×
Hagen <i>et al.</i> (2019)	Cardiothoracic surgeries	2.1 – 3 years	0.25 ml – 0.5 ml/kg	Uni and Bilateral	×
Patel <i>et al.</i> (2019)	Thoracotomy for lobectomy	6 years	0.5 ml/kg	Unilateral T5	
Wyatt and Elattary (2019b)	Thoracotomy for vascular ring	17 years	0.4 ml/kg	Unilateral T5	T5 – T9

Author	Indication	Age	Volume	Level	Spread
Aksu and Gürkan (2020)	Hypospadias	6 months	1 ml/kg	Unilateral S4	x
Özkalaycı <i>et al.</i> (2020)	Peroral endoscopic myotomy analgesia	x	x	x	x
Holland and Bosenberg (2020)	Intraoperative and/or post-operative analgesia	2 days – 9 years	0.1 – 0.5 ml/kg	x	x
Öksüz <i>et al.</i> (2020)	Anoplasty	7 months	x	x	x
Anju Gupta <i>et al.</i> (2020)	Chest wall tumour excision	2.5 years	x	Unilateral T5	x
Ekinci <i>et al.</i> (2020)	Extracorporeal shock wave lithotripsy	2 years	6 ml	Unilateral T10	x
Glazov and Mirgorodskaya (2020)	Pyothorax	1.5 years	x	Unilateral T7	T5 – T9
Basaran and Akkoyun (2020)	Meconium peritonitis	1 day	5 ml	Bilateral T7	x
Wellbeloved and Kemp (2020)	Removal of nephroblastoma	22 months	10 ml	Bilateral T7/8	x
<i>“Continuous Erector Spinae Block Versus Continuous Paravertebral Block,” (n.d.)</i>	Thoracotomy	6 months – 6 years	Continuous infusion	x	x
Lima <i>et al.</i> (2020)	Hip developmental dysplasia	10 months and 2 years	12 ml	Unilateral T12	x
	Bilateral valgus foot	14 years	10 ml	Bilateral L4	x

This table was last updated on the 28th of July 2020.

Key: x = not specified

Authors have recommended techniques or approaches based on their clinical experience and observations when performing an ESP block (single injection or continuous catheter placement). Aksu and Gürkan (2019) preferred the transverse approach while advancing the needle from the midline in a lateral direction. Narayanan and Venkataraju (2019) stated that lamination would occur between muscular fibres while executing a longitudinal approach, as compared to a favourable circumferential spread in a transverse approach. Furthermore, by advancing the needle away from the midline, concern regarding increased epidural spread can be reduced (Aksu and Gürkan, 2019e). Authors have expressed their concern when performing longitudinal bilateral ESP blocks. They explained multiple injections can be painful for some patients. They then modified the block technique to avoid multiple punctures. Placing the transducer in a transverse orientation, the block was performed using the out-of-plane approach, with a single needle entry from the midline over the spinous process. The needle was then directed to the right and left sides of the spinous process without withdrawing the needle (Yörükoğlu *et al.*, 2019).

As new data emerges, new approaches are being described as modifications to the ESP block, as the anaesthetic injection point is slightly deeper than that of the ESP block (Ohgoshi *et al.*, 2020b). Piraccini *et al.* (2020a) described the block at an alternative injection site or endpoint, which produced similar results as the classical approach. Authors injected local anaesthetic between the intertransverse and superior costotransverse ligaments as opposed to the long side of the transverse process. In another study, authors performed both the classical approach between the transverse process and muscular layers, as well as the modified approach between the ligaments, to increase the effectiveness of the ESP block (Coşarcan *et al.*, 2020).

In another study by Roy *et al.* (2020), it was noted that the spread of the drug mimicked the splaying of muscular layers which resulted in an inadequate blockade. Therefore, the authors modified the transverse approach by introducing the RACK approach. This approach was performed by identifying the structures that mimicked lying on a rack in a single line on an interspinous view. These structures included the vertebral column, articular process, posterior complex and the transverse process. Once the structures were identified, the needle was inserted using the in-plane technique, towards the area

below or deep to the erector spinae muscle, above the lateral transverse process. They stated that apart from the ease of administration ergonomically, the rack-like structures were easy to identify, making this modification to the transverse approach advantageous (Roy *et al.*, 2020).

In a cadaveric study using Thiel-embalmed cadavers, the modified ESP block was performed at the midpoint of the transverse process to investigate the pathway of paravertebral spread. Dye was injected into the thoracic intertransverse tissue complex, parallel to the superior costotransverse process. Paravertebral spread via the internal intercostal membrane was seen in all specimens. Furthermore, the dye spread up to the innermost intercostal muscle and was observed over the intercostal segment at which the dye was introduced. Authors concluded that dye penetration observed in the study was analogous to that of the intercostal nerve block. They believe that modified ESP blocks are more similar to intercostal blocks than the classic ESP block (Ohgoshi *et al.*, 2020b).

The concept of differential blockade may explain the disparities in efficacy between numerous studies performed. If low concentrations of local anaesthetic are applied to nerves, it will preferentially block C-nerve fibres over the larger A-delta and A-gamma fibres. C-fibres are responsible for the majority of nociception, A-delta fibres are responsible for transmitting fast-onset pain, while A-gamma fibres are involved with touch sensation, proprioception and motor function, however, not nociception. Therefore, it is plausible to assume that fascial plane blocks may produce analgesic coverage despite the absence or lack of sensory and motor blockade (Chin, 2019).

De Cassai and colleagues (2019) demonstrated that the median volume to cover one dermatome is equivalent to 3.4 ml when performing the ESP block. However, this is only applicable in an adult population. They further proposed the application of high volume and low concentration formula for interfascial plane blocks (De Cassai *et al.*, 2020). In a more recent review, the authors systemically analysed the available literature to establish the volume of injectate required to cover a single vertebral segment in an adult population. A total of 34 cadaveric studies and 35 radiologic studies were used for this review. After radiological assessment of the spread of

injectate for thoracic and lumbar ESP blocks, results revealed a median of 3.3 ml needed to cover one vertebral segment when looking at the vertebral column as a whole, whereas, only 2.5 ml and 5 ml of contrast material were needed to cover one vertebral segment in the thoracic and lumbar regions, respectively. Similar vertical spread was found when assessing cadaveric studies. A median of 3.5 ml of injectate was required to cover one vertebral segment. Furthermore, it was discovered that different volumes of injectate are needed in relation to the injection area. A median of 5 ml of injectate was needed to cover one vertebral segment in the lumbar region, whereas only 3.3 ml in radiology studies and 3.5 ml in cadaveric studies was needed for the thoracic region (De Cassai *et al.*, 2020).

Barrios *et al.* (2020) conducted a study to evaluate the sensory mapping of an ESP block by examining the extent of dermatomal blockade, using a standardized volume dose of 20 ml of injectate. The mean dermatomal spread was 9 vertebral segments (range: 8 to 11 segments). From the exploratory data examining volume require to block a single dermatome, it ranged between 1.81 to 2.5 ml. Although the volume per dermatome in this study is lower than that of De Cassai *et al.* (2019), it may be explained by the contrasting concentrations used (0.5% by Barrios *et al* versus 0.35% by De Cassie *et al*). To ensure complete segmental spread Aydin and co-workers (2019) suggested performing bi-level injections to guarantee extensive dorsal and ventral spread.

The volume-to-dermatome ratio in infants and children is yet to be determined. However, several authors hypothesize that the volume of 0.1 ml/kg should be enough to provide adequate spread in younger children (Wong *et al.*, 2018; Adler *et al.*, 2019; Aksu and Gurkan, 2019b; Govender *et al.*, 2020b, 2020c; Holland and Bosenberg, 2020) (Appendix B and C). Other authors suggest that a dosage between 0.2-0.5 ml/kg should be sufficient, as long as the maximum dosage for paediatric patients is not exceeded (Tulgar *et al.*, 2019a). In this study, it was found that, when using a 0.1 ml/kg dosage, the volume per kilogram per dermatome varied from 0.02 – 0.13 ml (Table 14).

Due to the vascular-rich muscular structures in the spinal region, local anaesthetic systemic toxicity should be kept in mind when deciding on the amount of volume to be used. Thus far, the choice of local anaesthetic has been reported to be bupivacaine, ropivacaine, levobupivacaine and ropivacaine. Concentrations depended on end goals of the block, surgical procedures or post-operative analgesia (López *et al.*, 2018; De Cassai *et al.*, 2019a; Tulgar *et al.*, 2019a, 2019c).

The question of anatomical differences between age groups arises due to the contradicting results from various cadaveric studies performed predominantly in adults (Willard *et al.*, 2012; Chin *et al.*, 2017; Hamilton and Manickam, 2017; Schwartzmann *et al.*, 2018; Aksu and Gürkan, 2019f). Apart from the variables such as weight, height and body shape, anatomical differences between neonates, infants, children and adults should also be considered. Factors such as the developmental formation of the vertebral curvatures may contribute to the differences in paravertebral tissue and muscle thickness observed between age groups. This would also affect the depth at which the ESP block is performed. Furthermore, the more elastic paediatric spine (Basu, 2012), together with the less dense ligaments and cartilaginous laminae, could allow for a more favourable spread, as seen in neonates and infants (Gupta and Usha, 2014). Incomplete myelination of nerve fibres in neonates and infants allows lower concentration and volume of anaesthetic required to perform the block (Ponde, 2019).

Apart from anatomical and physiological discrepancies, executing the ESP block in young paediatric patients also presents some technical challenges the thinner muscle layers, sliding fascial planes and loose connective tissue (Aksu and Gürkan, 2018b). Furthermore, due to the superficial nature of the block, a finer needle technique and stable patient positioning may be required when performing this block. Some authors suggest that, due to the superficial nature of the ESP block, combined with the distant neuraxial structures and relative ease of placement, the ESP block carries a higher risk profile when compared to paravertebral and epidural blocks (Hernandez *et al.*, 2017; Munshey *et al.*, 2018a; Tsui *et al.*, 2019; De Cassai *et al.*, 2020). Additionally, when combined with ultrasound guidance, the local anaesthesia spread can be tracked, allowing an adequate amount of anaesthetic for the desired extent of coverage, thereby reducing the risk of systemic toxicity (Hernandez *et al.*, 2017).

Regarding the results from cadaveric studies, it is understood that the extent of spread would be much greater in live patients than in cadaveric models (Schwartzmann *et al.*, 2020). Moreover, factors such as patient positioning, injection speed, needle gauge, injectate viscosity, ventilatory patterns, as well as muscle and ligament consistency, could theoretically modify and improve the spread during an ESP block (Barrios *et al.*, 2020). Schwartzmann and colleagues (2020) specifically pointed out that contraction of the ESP muscles and negative intrathoracic pressure during inspirations could potentially enhance the spread within live patients.

A major challenge during an interfascial block is the assessment of the block success. In a study evaluating the transverse abdominal plane, the authors noted that even though the cutaneous dermatomal coverage was limited, it still contributed to the analgesic efficacy. Likewise, no correlation was found between the analgesic efficacy and sensory distribution subsequent to performing an ESP block for a mastectomy (Ip *et al.*, 2019). Nair and Seelam (2019) cautioned the use of ESP blocks on coagulopathic patients and in patients on anti-platelet or anti-thrombotic agents. They expressed their concern regarding possible hematoma formations within the erector spinae fascial plane space.

Although this block is still in the trial-and-error phase, there have been a handful of documented cases with complications. These included pneumothorax, priapism, local anaesthetic systemic toxicity and unexpected motor weakness (Elkoundi *et al.*, 2019b; Hamilton, 2019b; Tulgar *et al.*, 2019a; Karaca and Pinar, 2020). Harlequin Syndrome following a unilateral ESP block at vertebral level T3, was the most recent complication to be associated with an ESP block. Authors concluded that the involvement of the sympathetic chain is the reason for this autonomic neuropathy (Sullivan *et al.*, 2019). Even though this block is easier and safer to perform, there is room for error should the tip of the needle not be visualized (Greenhalgh *et al.*, 2019). Motor weakness could also occur if the block is performed at lower thoracic or lumbar levels, resulting in the spread of local anaesthetic towards the lumbar plexus (Tulgar *et al.*, 2019c). Although motor weakness is not considered a complication, it is an unintended event (Tulgar *et al.*, 2019a).

Although this study focuses on the thoracic and abdominal coverage, various studies have reported on its success when performing this block for the cervical region (Hamadnalla *et al.*, 2019).

2.9 ESP block compared to other neuraxial blocks

The ESP block has been compared to numerous regional techniques, each reporting conflicting results. El-Emam and El motlb (2019) compared the efficacy of an ultrasound-guided ilioinguinal/iliohypogastric nerve block to the ESP block in a paediatric population (ranging from 6 months to 3 years) undergoing inguinal hernia repair. They concluded that the ESP block resulted in a more effective and longer duration of the post-operative analgesia.

In an adult study that had a cadaveric and clinical component, the pattern of dye distribution was compared between the costotransverse foramen block and ESP block (Shibata *et al.*, 2020). The authors described the costotransverse foramen block, whereby the injectate is distributed through the costotransverse foramen, as an alternative to thoracic paravertebral blocks. Injectate is introduced between the medial border of the superior costotransverse ligament and the lateral margin of the lamina of the vertebral arch, which is anterior to the intertransverse ligament. This allows the injectate to easily penetrate the gap in the paravertebral space without barriers. Six embalmed cadavers were used in the study. Both blocks were performed at vertebral level T4 bilaterally. Upon dissection, dye staining was found beneath the posterior layer of the thoracolumbar fascia that covered the erector spinae muscle with the ESP injection, whereas slight leakage was found along the costotransverse foramen injection path. For the ESP injections, intense craniocaudal spread, ranging from 5 to 6 levels, was found in the superficial and deep planes of the erector spinae muscle. This was much more extensive than the minimal spread after the costotransverse foramen injections, which ranged between 2 to 3 levels only, in 3 (out the 6) cadavers in the superficial and deep planes of the erector spinae muscle.

Minimal spread was seen within the transversospinalis muscle group in the costotransverse foramen injections, while no spread was seen in the ESP injections. Dye spread was noted to be more medially in the costotransverse foramen injections, towards the intertransverse ligament. Subsequent to deeper dissections, the dye did not penetrate the external intercostal muscle or internal intercostal membrane. Additionally, no dye spread was seen around the ventral rami of spinal nerves in all ESP injections. However, in all costotransverse foramen injections, the dye was observed in the paravertebral spaces via the costotransverse foramen between vertebral levels T3 to T6 and into the internal intercostal membrane and the costal part of the pleura.

For the costotransverse foramen block, results of the cadaveric component were consistent with the results of the sensory blockade in the case studies. The ESP results of the cadaveric component did not match the result of the case studies, as the sensory block was still produced at the level of the injection and adjacent levels, even though the blockade was equivocal and encompassed fewer dermatome levels. The authors concluded their study by recommending the costotransverse foramen block as an alternative to the paravertebral block, as there were consistent results for both the cadaveric and clinical portions of the study (anterior into the paravertebral space, involving thoracic spinal nerves). The ESP block displayed inconsistency in the spread of injectate and sensory blockade (Shibata *et al.*, 2020).

The ESP block has been reported to reduce post-operative opioid consumption for breast surgery when compared to other standard procedures (Pourkashanian *et al.*, 2019). When specifically compared to the pectoral nerve block, the ESP block displayed lower pain scores and less post-operative tramadol consumption (Gad *et al.*, 2019). Results from other studies favoured the pectoral nerve block, stating that lower post-operative opioid consumption, stress hormone levels and pain scores were observed with the pectoral nerve block than with the ESP block (Gad *et al.*, 2019; Shan *et al.*, 2020). Shan and co-workers (2020) further stated that in their opinion, the ESP block should not be routinely used for post-operative analgesia, as the mechanism of action is still controversial. Khorasanizadeh and colleagues (2020) concluded their study with remarks on both blocks. They stated that the pectoral nerve block

anaesthetizes the anterior cutaneous and medial branch of the intercostal nerve of the ipsilateral side, creating superior bilateral analgesia when compared to the ESP block. On the other hand, due to the proximity to the intrathecal and epidural space, the ESP block may be associated with more hemodynamic changes, yet less clinical impact.

De Cassai *et al.* (2018) questioned whether the pectoral nerve block, as well as the serratus plane block, can truly be compared to the ESP block. Both blocks offer analgesia to nerves that do not contribute to the brachial plexus and therefore, are not involved with the erector spinae plane. Ueshima and colleagues (2019) further advocated for De Cassai's concerns and suggested that the ESP block alone may be insufficient to achieve adequate analgesia to the anterior branches of intercostal nerves T2 to T6. Contrary to this, results from various studies report on the success of the ESP block in breast surgery, as well as the positive benefits of using this block (Adhikary *et al.*, 2018; Gürkan *et al.*, 2018).

Appreciating the potential of the ESP block, Gawęda *et al.* (2020) compared the efficacy of a normal ESP block with a combination of the ESP and pectoral nerve block in patients undergoing cardiac surgery. The authors stated that, although both blocks cover similar areas, their efficacy is still unclear. Furthermore, the ESP block produces unpredictable results. Outcomes from the combined group revealed significantly less oxycodone consumption, lower pain intensity and better patient satisfaction.

The ESP block has also been compared to the intercostal nerve block for the preservation of pulmonary function after video-assisted thoracoscopic surgery. Results showed significant preservation of lung volumes and lung capacities after video-assisted thoracoscopic surgery with patients who had ESP blocks, versus patients with intercostal nerve blocks. Furthermore, there was significant improvement in acute post-operative pain in the ESP group. Even after a two month follow up, patients had better pain scores at the chest tube- and port insertion site. Authors stated that the ESP block could balance the analgesic benefits with physiological homeostasis and reduce surgical stress, allowing the block to have the potential to be used as part of a multi-modal strategy for enhanced recovery (Chaudhary *et al.*, 2020).

In several studies in which patients underwent open cardiac surgery, the ESP blocks resulted in significantly lower post-operative adverse events, time to chest drain removal and time to first mobilization (Krishna *et al.*, 2019; Macaire *et al.*, 2019). Krishna *et al.* (2019) also mentioned that the ESP block offers a higher level of analgesia than systemic analgesia. Altinpulluk *et al.* (2019) stated that the ESP block was more effective than the oblique subcostal transverse abdominal plane block on post-operative tramadol requirement and pain scores in patients undergoing laparoscopic cholecystectomy. They also noted a greater dermatomal coverage in the ESP block as compared to the oblique subcostal transverse abdominal plane block.

Similarly, Tulgar *et al.* (2019b) compared a bilateral ESP block to a bilateral transverses abdominis plane block for the same procedure. However, their results revealed significantly lower numerical rest and dynamic pain scores in the first three post-operative hours and a lower 24-hour analgesic requirement for both blocks. Mostafa and co-workers (2019) evaluated various midline abdominal procedures and concluded that both techniques only provided somatic pain relief for abdominal wall structures from the wall to the peritoneum. They further stated that they believed the ESP block would be a better regional anaesthetic technique, as it provides both visceral and somatic pain relief.

Rincón and colleagues (2019) compared the transversus abdominis plane block and the quadratus lumborum block to the ESP block for post-caesarean delivery analgesia. They stated that a major limitation of the former two blocks was the lack of visceral analgesia, which is not this case for an ESP block, thereby suggesting that the ESP block is a preferred/superior technique for post-caesarean delivery analgesia. This was further supported by Boules and co-works (2020), who reported the longer duration of analgesia and reduced tramadol requirement when comparing the ESP block to the transversus abdominis plane block after elective caesarean sections.

In a single case study by Celik *et al.* (2019), a high-volume lumbar ESP block was hypothesized to produce similar effects to a lumbar plexus block when administering a transforaminal epidural injection. Positive results lead the authors to state that high-volume lumbar ESP blocks can be used as a less invasive procedure with similar

effects to alternative interventional pain procedures. When comparing the analgesic efficacy of lumbar ESP blocks for lower limb procedures such as hip- and femur surgery, the authors reported significantly lower pain scores within the first six hours and a lower total 24-hour tramadol requirement. However, when compared to a quadratus lumborum block, the ESP block revealed similar results (Tulgar *et al.*, 2018). In another study comparing a thoracic ESP block to a quadratus lumborum block for a caesarean section, unintended lower extremity motor blockade was experienced by the patient post-operatively. Although this was one of a few documented side-effects when performing an ESP block, similar side-effects were documented when performing a quadratus lumborum block for the same procedure (Selvi and Tulgar, 2018).

Elsharkawy and colleagues (2019) conducted an anatomical study to compare a lower ESP block to a quadratus lumborum block. Radiologic results for the ESP block revealed extensive craniocaudal spread, as well as lateral contrast spread towards the junction between the transverse process and its corresponding rib. Retrolaminar spread (spread related to just the lamina) was evident; however, partial spread was seen in the paravertebral space. No epidural-, intercostal-, intraperitoneal space- or transverse abdominal plane spread was seen. Upon dissection, lateral spread deep to the serratus anterior muscle was seen in few cases. Staining was noted over the dorsal rami of spinal nerves and the subcostal nerve in all cases. Retrolaminar spread was seen in one case, whereas staining in the paravertebral and intercostal space was noted in half of the cases. Epidural and neural/intervertebral foramen spread was seen in one case. None of the cadavers displayed spread to the pleura, intraperitoneal space or transverse abdominal plane. When compared to the quadratus lumborum block, the authors noted that, even though both blocks had unreliable spread to the paravertebral space and ventral rami of the spinal nerves, consistent dorsal rami spread was seen.

Onishi *et al.* (2019) compared the retrolaminar block to the ESP block, It was noted that, even though both blocks are compartmental, only the retrolaminar block can be performed using the landmark technique, whereas, the ESP block cannot, as the transverse process cannot always be detected by palpation. They then summarized the injectate distribution for the blocks into three patterns. Firstly, for the retrolaminar

block, the dye distribution was vertical beneath the transversospinalis muscle and the dorsal rami of spinal nerves. Secondly, for the ESP block, the dye spread laterally, covering the intercostal nerves and the lateral cutaneous branches. Lastly, the distribution into the paravertebral space was limited in both the retrolaminar and ESP block.

In a different study, the authors stated that the ESP block can be performed as landmarked-based (Vadera and Mistry, 2019). The retrolaminar block was again compared to the ESP block in a magnetic resonance study. Results revealed that, for a single shot injection, both blocks produced epidural and neural/intervertebral foramina diffusion across two to five vertebral levels. However, the ESP block dispersed more widely into the intercostal spaces. Authors stated that the ESP block could provide analgesia to the anterolateral thoracic and abdominal wall as an intercostal nerve block (Adhikary *et al.*, 2018). Similar findings were reported by (Yang *et al.*, 2018).

In a more recent study, the ESP block was compared to the mid-point transverse process to parietal pleura block and the costotransverse block. Findings from a study conducted by Ohgoshi *et al.* (2020b) suggested that the paravertebral spread after an ESP block progresses slowly in association with the local anaesthetic, as opposed to the mid-point transverse process to parietal pleura block and costotransverse block, which are more direct and quicker. They noted that a slight change in the angle of the needle tip could significantly influence the paravertebral spread. The injection depth for the mid-point transverse process to pleura and costotransverse blocks were deeper than the ESP blocks. They then concluded that the mid-point transverse process to pleura and costotransverse blocks are more effective than the ESP block, based on the paravertebral spread. They believe that the distance from the injection point to the costotransverse foramen, which is the gateway to the space, can provide information regarding the paravertebral spread (Ohgoshi *et al.*, 2020a). After a magnetic resonance imaging assessment, Celik *et al.* (2019) hypothesised that the ESP block provides similar effects as a transforaminal injection.

Even though the ESP block seems more appealing than existing neuraxial techniques, Piraccini (2020b) recommended an alternative to the ESP block for breast surgery. He suggested performing a bilateral rhomboid intercostal block. For this block, the local anaesthetic is injected between the rhomboid and intercostal muscles. Since the injection site is more peripheral than for the ESP block, injectate will spread mostly towards the lateral cutaneous branches of the intercostal nerve, rather than to the paravertebral or epidural space. Moreover, since the sympathetic chain blockade is not as deep with the ESP block, complications such as hypotension would be reduced. Generally according to the literature and the growing number of clinical studies, the ESP block seems to be a safer, preferred alternative to both the epidural and paravertebral blocks (Petsas *et al.*, 2018).

2.10 Advantages and disadvantages

The main appeal of the ESP block is the ease of application. With the aid of ultrasound guidance, bony landmarks and anatomical structures are easily identifiable (Ciftci and Ekinici, 2019a). The ease of identification reduces procedure time, as well as the potential for failed blocks. Furthermore, the entire course of the needle and eventual endpoint can be constantly viewed, allowing the practitioner to avoid important anatomical structures in the area (Govender *et al.*, 2020c) (Appendix C).

The ESP block carries a lower risk of clinical complications as the needle is inserted into a tissue plane that is a safe distance from that of the parietal pleura, neuroaxis and major neurovascular structures (Hernandez *et al.*, 2017; Jain *et al.*, 2018; Tukaç, 2019; Barrios *et al.*, 2020; Sakae *et al.*, 2020; Wellbeloved and Kemp, 2020). Additionally, by allowing the tip of the needle to make contact with the transverse process, it acts as a natural barrier and further provides a guide to the appropriate depth of insertion in children of different sizes, contributing to the safety of the block (Chaudhary and Singh, 2018; Ekinici *et al.*, 2020).

Since the block has the ability to cover multiple dermatomal levels from a single injection, the block can be performed at a different vertebral level than the level of the

surgical site, thereby avoiding wound dressing or surgical incision (Forero *et al.*, 2016; Muñoz *et al.*, 2017). This block also allows for the use of catheter insertion for intermittent boluses and continuous infusion of regional anaesthesia (Chin *et al.*, 2017; Leyva *et al.*, 2017; Luis-Navarro *et al.*, 2018).

The ESP block is linked to reduced opioid requirement, as there is ongoing analgesic coverage into the post-operative period (Ueshima and Hiroshi, 2018; Pirsaharkhiz *et al.*, 2020). Another advantage is that the patient can be positioned in various ways, including prone, lateral decubitus or leaning forward in a seated position and the recently described dry leaf technique (semi-lateral position) (Luis-Navarro *et al.*, 2018; Aygun *et al.*, 2020a). However, as with most regional blocks, there is a risk of systemic toxicity, for which authors suggest routinely adding epinephrine when introducing large doses of anaesthesia for this block (Leyva *et al.*, 2017).

Although there haven't been any reported incidences, Missair *et al.* (2019) put forward a theoretical possibility that the ESP block may negatively affect the spinal biomechanics and further impact stable, non-displaced vertebral fractures brought about by muscular relaxation from the block. Furthermore, the ESP block is not contraindicated for anti-coagulated patients, unlike the epidural block (Abdelhamid *et al.*, 2020).

2.11 Strength and limitations

a) **Practical implications**

The current study highlights the importance of the novel ESP block and its place in paediatric anaesthesia. When performed at vertebral levels T5 and T8, the ESP block potentially provides anaesthesia and analgesia to the thoracic and abdominal regions, respectively.

The literature, which includes case studies, cadaveric investigations, imaging modality reports and clinical trials, displays the positive outcomes and remarks when performing the block in both an adult and a paediatric population. Furthermore, authors have shown their preference for the block because of the ease of identification, the distant needle application and the longer duration of action (Forero *et al.*, 2016; Aksu and Gürkan, 2019e; Govender *et al.*, 2020b) (Appendix B). Moreover, the ESP block can be used in patients when techniques such as the paravertebral and epidural blocks are contraindicated due to the patient being on anticoagulant therapy or inexperience.

Despite limited information regarding its paediatric use, the ESP block can be performed for unilateral thoracotomies or thoracoscopies, as well as a variety of abdominal procedures in medically complex patients. These procedures include laparoscopic or open gastrostomies, subcostal incisions, peritoneal dialysis catheter placement, as well as lower pelvic and leg procedures inguinal hernia repair, hip dysplasia, anoplasty and bilateral valgus foot repair.

Please refer to the following published articles related to this thesis for more clinical implications:

- Govender, S., Mohr, D., Bosenberg, A. & Van Schoor, A. (2020) A cadaveric study of the erector spinae plane block in a neonatal sample. *Regional Anesthesia & Pain Medicine*, 45(5);386-388. (Journal impact factor 7.015)
- Govender, S., Mohr, D., Van Schoor, A. and Bosenberg, A. (2020) The extent of cranio-caudal spread within the erector spinae fascial plane space using

computed tomography scanning in a neonatal cadaver. *Pediatric Anesthesia*, 30(6); 667-670. (Journal impact factor 2.311)

- Govender, S., Mohr, D., Bosenberg, A. and Neels Van Schoor, A., 2020. The anatomical features of an ultrasound-guided Erector Spinae Fascial Plane block in a cadaveric neonatal sample. *Pediatric Anesthesia*. (Journal impact factor 2.311)

b) **Limitations**

The major limitation of this study was the small sample size, due to the sensitivity of the procurement procedure for neonatal cadavers. Another limitation was the use of cadaveric material to replicate the spread in a living model. This may be an inaccurate representation due to in vivo factors such as a lack of intrathoracic pressure changes, muscle tone or tissue tension, which may limit the spread of dye (Ivanusic *et al.*, 2018; Vidal *et al.*, 2018).

Other limitations include the speed of injection, the lack of gravitational effect on the spread of dye, as well as variability in the volume and mixture of dye used (Greenhalgh *et al.*, 2019; Chaudhary *et al.*, 2020). Additionally, temperature could affect the permeability of diffusion of the injectate (Shibata *et al.*, 2020). The temperature could also affect the biochemical changes of hyaluronic acid, which is a key substance controlling the viscosity of connective tissue and therefore, could influence the spread (Schwartzmann *et al.*, 2020). Furthermore, the physicochemical properties of the dye solution used, differs from local anaesthetics and may influence the spread.

The weight of the fresh neonatal cadavers used in this study was variable, ranging from 0.7 – 3.4kg, which could have influenced the spread. Additionally, the lack of information such as gestational age and preparation state made it difficult to fully evaluate the anatomical factors that may affect the spread of dye. When obtaining the ultrasound scans, probe pressure could have resulted in subcutaneous tissues compression, which may also have affected the measurements by making them appear smaller. Furthermore, measurements could differ from a live sample due to the absence of tissue perfusion.

Regarding the CT data, apart from the limited sample size, specifically due to the challenges faced when obtaining neonatal scans, there was a lack of information such as height and weight. The absence of these variables impeded a complete analysis, as the effects of these variables on measurements were not adequately addressed. As seen from the ultrasound component, these variables do influence the end result. Additionally, CT data obtained in this study were taken from CT scans while the patient was in a supine position. Most neuraxial techniques are performed with the patient in a lateral decubitus position. Previous studies have demonstrated that the spinal cord and cauda equina move with gravity, these structures also move ventrally with lower limb (specifically hip) flexion (Wani *et al.*, 2018).

Lastly, in terms of imaging modalities, magnetic resonance imaging is the most comprehensive imaging modality of the paraspinal- and intraspinal soft tissue and ligaments when compared to CT imaging (Wani *et al.*, 2017; Govender *et al.*, 2020b) (Appendix B). In this study, there was some difficulty in identifying the structures when performing measurements. As a result of estimation to the start or endpoint of structures from some scans, measurements may be inexact.

c) ***Future studies***

The following is proposed for future research regarding the ESP block:

1. To investigate the effect of volume on the craniocaudal spread of injectate.
2. To investigate the optimal patient positioning for a more favourable spread.
3. To compare the anaesthetic- and analgesic efficacy in an adult- versus a paediatric population.
4. To investigate the variability of sensory dermatomal block associated with injections at different transverse process levels.
5. To investigate whether making contact with the transverse process, which leads to manipulation of the fascial leaflets, influences the paravertebral spread.
6. To determine the appropriate concentration-to-volume ratio when performing the block in a paediatric population.

7. To determine the volume-per kilogram-per dermatome ratio with a larger sample size.
8. To create estimation formulae using age, sex, weight and height as parameters in a larger sample size.

2.12 Conclusion

The ESP block is a versatile technique that can be part of the multimodal post-operative analgesic strategy for truncal surgery. This study aimed to highlight the anatomical features when replicating an ESP block in a neonatal sample. The ESP block has been described as an alternative to paravertebral and epidural blocks as it targets the same nerves but at a further distance from neuraxial structures, therefore, offering a lower risk profile.

With the aid of imaging modalities, this block proves to be more efficient to perform, as the anatomical landmarks are easily identifiable. In this study, the methylene blue spread was found anteriorly in the paravertebral-, epidural- and intercostal spaces over multiple dermatomal levels, staining both the dorsal and ventral rami of the spinal nerves from vertebral levels T2 to L2. Results of this study revealed that the block can be performed at an average depth in age group of between 1.67 cm to 1.08 cm (standard deviation of 0.40+/+ 0.03 and 0.26), while for age groups 2, the depth was 1.52 cm with a standard deviation of 0.46 at vertebral level T5 and 1.20 cm with a standard deviation of 0.35 at vertebral level T8. The average depth for group 3 was 1.67 cm with a standard deviation of 0.45 at vertebral level T5 and 1.38 cm with a standard deviation of 0.39 at vertebral level.

This study thus postulates that the ESP block is a good alternative for practitioners who are wary of neuraxial techniques, due to the high risk of complication or the requirement for advanced skills, especially in a paediatric population.

Chapter 3 – Paravertebral block

Similar to the ESP block, the paravertebral block is performed to provide effective analgesic spread for truncal procedures. The anaesthetic solution is injected into the paravertebral space, which contains the dorsal and ventral rami of spinal nerves as they emerge from the intervertebral foramen (Luyet *et al.*, 2009). The paravertebral block results in ipsilateral somatosensory nerve block and sympathetic chain nerve block over multiple vertebral levels (Ng *et al.*, 2018). The block was originally described in 1905 by a German physician, after which it lost its popularity (Tighe *et al.*, 2010). It was then modified in 1979 by Eason and Wyatt to provide effective analgesia for both thoracic and abdominal surgeries in adults (Lönngqvist, 1992; Lönngqvist *et al.*, 1995; Tighe *et al.*, 2010). It was not until 1992, that the idea of adopting this technique for paediatric surgery came about when Lönngqvist (1992) performed a continuous paravertebral block on five children scheduled for renal surgery or cholecystectomies.

After intubating the patients, they were placed in a lateral position. A paediatric needle was then inserted 1 to 2 cm lateral to any of the spinous processes of vertebrae T7 to T9. The paediatric needle was then “walked” over the superior aspect of the transverse process before piercing the costotransverse ligament to enter the paravertebral space, a wedged-shaped space located between the head and neck of adjacent ribs and vertebrae. Results revealed an 80% success rate with effective post-operative analgesia and reduced opioid requirement. One block failed due to the difficulty of the needle manoeuvring and, as a result, the incorrect placement of the catheter. Although the study yielded positive results for paediatric paravertebral blocks, Lönngqvist concluded: “that even in the most experienced hands, the technique is very hazardous with few benefits”. Karmakar and co-workers (1996) further expanded on this field of research by demonstrating continuous paravertebral blocks for post-thoracotomy pain in young infants.

Since the paravertebral space is connected to epidural and intercostal spaces, anaesthetic can spread over numerous dermatomal layers following a single injection (D’Ercole *et al.*, 2018). Various cadaveric studies were performed to confirm the course of the anaesthetic spread. Saito and co-workers (1999) reported the lateral and cranial

spread to diffuse to the individual intercostal nerves, whereas the medial spread was limited by the vertebral body and did not travel beyond the midline. Caudally, contrast material was noted to reach the ipsilateral splanchnic nerves and the sympathetic trunk and its communicating nerves, extending as far down as the superior surface of the diaphragm.

In the following years, various authors continued to practice this technique in combination with ultrasound guidance in paediatric surgery. Direct visualisation of the paravertebral space increased success rates and reduced the rate of complications, as compared to classical landmark-based, loss of resistance, nerve stimulating or intercostal techniques (Cowie *et al.*, 2010; Saranteas *et al.*, 2010; Ng *et al.*, 2018). Furthermore, with the use of ultrasound guidance, alternative approaches such as landmark-based techniques or formulae can be derived for clinical application as an alternative due to the unavailability/absence of equipment. In 1992, Lönnqvist created a standard set of formulae to calculate the distance and depth, in millimetres, to the paravertebral space in the thoracic region. This formula, which can be used for all patients up to the age of 5 years, takes into consideration the body weight, in kilograms. However, age was not taken into consideration, thus leaving room for error. Currently, this is the only existing formula, and as age has proved to change the dimensions of the vertebral column and the paravertebral space as the vertebral column changes through developmental stages, this should be considered when updating the existing formulae (Ponde and Desai, 2012).

The paravertebral block can be used for most procedures of the thorax or abdomen, including thoracotomies and even lower abdominal procedures (Gerrard and Roberts, 2012). Although the block provides unilateral intra-operative and post-operative analgesia for surgical procedures, it is also used to provide analgesia for nonsurgical pain management (Ng *et al.*, 2018). Common relative contraindications include systemic sepsis, diaphragmatic paresis, previous spinal surgery and respiratory diseases, while absolute contraindications include infection at the needle insertion site, empyema (collection of pus) in the pleural cavity, allergy to the anaesthetic drugs, coagulopathy and patient refusal (Singh *et al.*, 2017; Ng *et al.*, 2018). Depending on the anatomical/clinical knowledge and experience of the practitioner, variations in the

normal anatomy can be avoided with the use of ultrasound guidance and is therefore no longer considered a contraindication.

More recently, a variety of paraspinal techniques have been described, including the ESP block. These blocks achieve local anaesthetic spread to the spinal nerves through the connective tissue gaps that surround the paravertebral space, without the need to enter this space (Forero *et al.*, 2016; Yang *et al.*, 2018; Tsui *et al.*, 2019; Nair *et al.*, 2020). These blocks have been described as ‘paravertebral by proxy’ blocks (Costache *et al.*, 2018). Furthermore, these blocks avoid needle placement close the parietal pleura and surrounding neuraxial structures, increasing the utilization of regional techniques (Pawa *et al.*, 2019).

3.1 Anatomy

The paravertebral space can be described as a triangular, wedge-shaped space found bilaterally along the vertebral column (Bouman *et al.*, 2017). The apex of the wedge lies laterally and allows for communication with the intercostal spaces. The base lies medially, adjacent to the vertebra body, between the lateral border of the vertebral body and the lateral extent of the transverse process (Pawa *et al.*, 2019). Medially the space forms a connection with the epidural space via the intervertebral foramen, allowing for the craniocaudal spread (Luyet *et al.*, 2009; D’Ercole *et al.*, 2018).

The paravertebral space is bordered anterolaterally by the parietal pleura and endothoracic fascia. In addition, the lateral border is completed by part of the internal intercostal membrane tapering off into the intercostal space. Posteriorly, the superior costotransverse and intertransverse ligaments, as well as the levator costarum, rotatores spinae- and intercostales externi- and intercostales interni muscles contribute to the borders of the space, while the vertebral body, the intervertebral disc and the intervertebral foramen form the medial border (Figure 12) (Cowie *et al.*, 2010; Bouman *et al.*, 2017; Page and Taylor, 2017; Pawa *et al.*, 2019; Nair *et al.*, 2020). The superior border is formed by the inferior aspect of the head of the rib, while the inferior border is the superior aspect of the head of the adjacent rib (Ng *et al.*, 2018). The space itself

is divided into an anterior and posterior fascial compartment by the endothoracic fascia (Tighe *et al.*, 2010; Nair *et al.*, 2020). The superior costotransverse ligament which is continuous with the internal intercostal membrane, is of anatomical importance, as the needle must penetrate this ligament for successful entry into the paravertebral space.

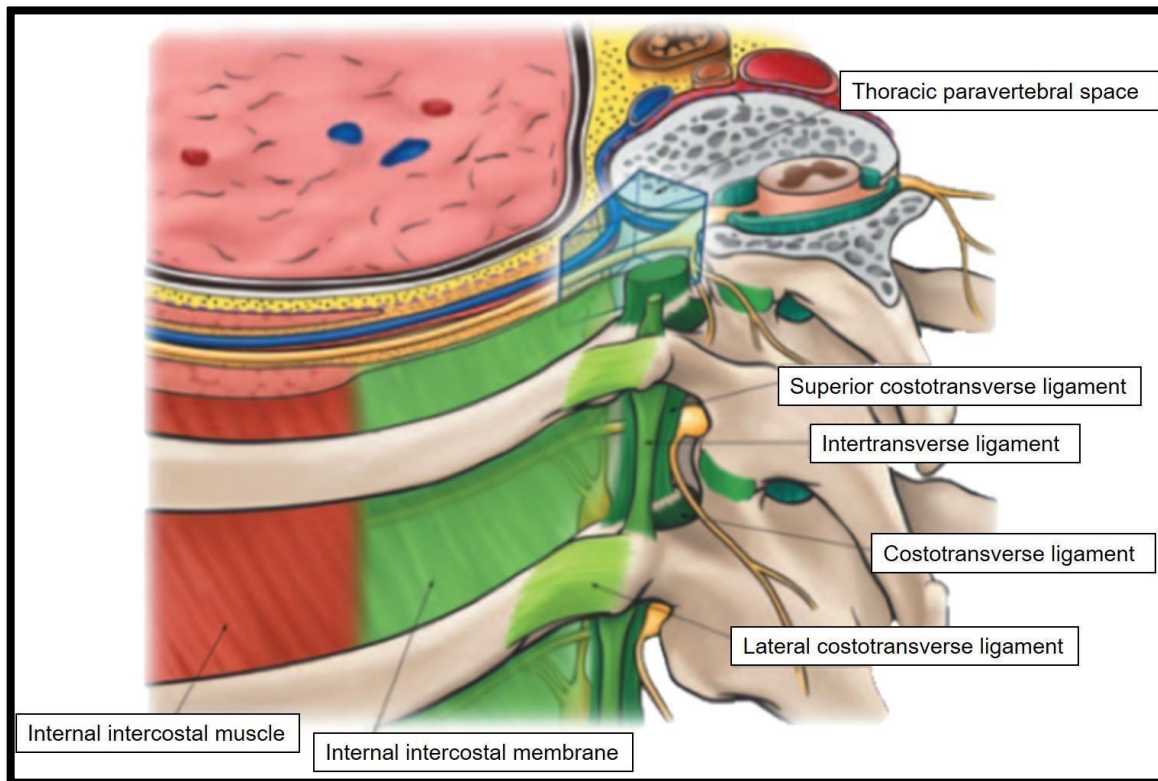


Figure 12: The anatomy of the thoracic paravertebral space and the structures that contribute to the borders of the space. Reproduced with permission from www.aic.cuhk.edu.hk/usgraweb.

The space contains fatty tissue, intercostal spinal nerves, intercostal vessels, the dorsal rami of the spinal nerve, rami communicantes, as well as the sympathetic chain. The spinal nerves lie freely dispersed in the space, while the intercostal neurovascular bundle (nerves and vessels) lie posterior to the endothoracic fascia. The sympathetic chain is located anterior to the endothoracic fascia (Nair *et al.*, 2020).

3.2 Ultrasound anatomy

The paravertebral block can be performed using two approaches, each producing similar results. The direct visualisation allows for the inserted needle to be directed towards the paravertebral space while avoiding relevant anatomical structures. This is extremely beneficial in cases of anatomical variations. The ultrasound probe can be placed in a transverse-, oblique- or paramedian (longitudinal) orientation.

a) ***Transverse plane/technique***

The probe should be placed just lateral to the midline over the transverse process (Figure 13). The tip of the transverse process should appear on the ultrasound screen as an obliquely elongated, oval, hypoechoic structure, deep to the paravertebral muscles (Karmakar *et al.*, 2012). Following the transverse process laterally, the corresponding rib should appear as a hyperechoic line extending from the transverse process. Directly inferior to the rib, the external and internal intercostal muscles can be seen as a grey/white hyperechoic band. This band is thick in width, making it difficult to distinguish between the separate intercostal muscles. Forming the inferior border of this band, the internal intercostal membrane appears as a lighter hyperechoic line.

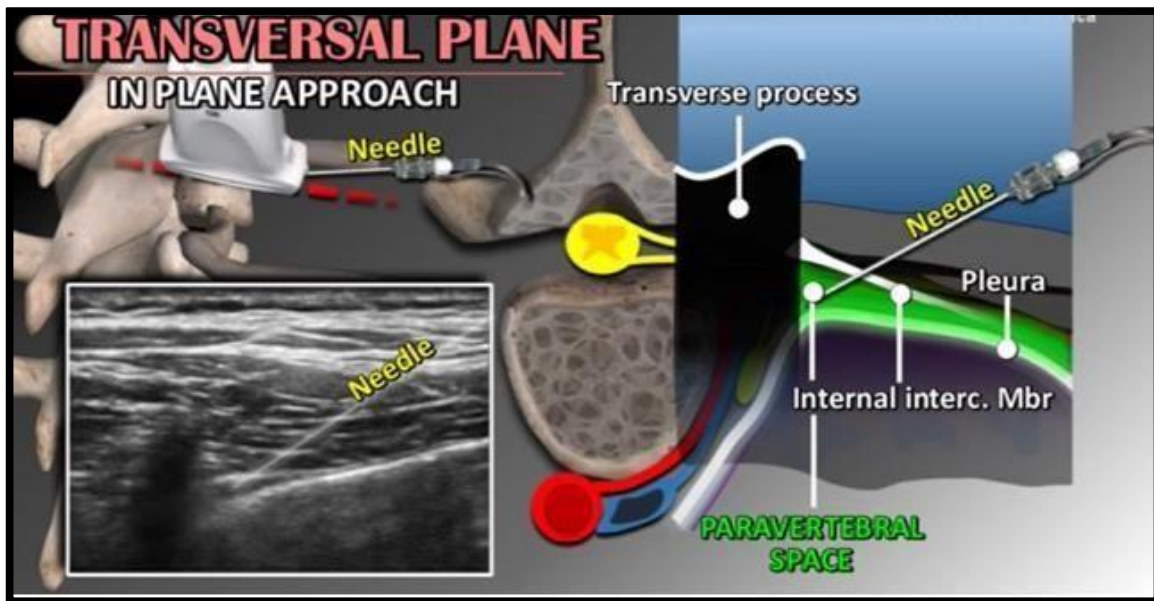


Figure 13: Image displaying the probe orientation, a transverse plane of the expected anatomy at vertebral level T5, as well as a transverse ultrasound image at vertebral level T5 during a paravertebral block. The image was taken from https://www.youtube.com/watch?v=f-gpZPjZ_Tc. Viewed on the 1st of May 2018.

The internal intercostal membrane is a medial extension of the internal intercostal muscle, continuous with the superior costotransverse ligament medially. Marginally inferior to the membrane, a slightly thicker hyperechoic line, the parietal pleura, can be found. The hypoechoic space found between these two structures is the paravertebral space. The needle should be advanced in a lateral- to- medial direction towards the transverse process until contact is made with the transverse process. Once contact is made, the needle is then redirected inferiorly to ‘walk-off’ the inferior edge of the transverse process (Figure 14). Usually, a ‘click’ can be felt as the needle advances through the superior costotransverse ligament (Loader and Ford, n.d.). After negative aspiration, the local anaesthetic can be injected. Introduction of the anaesthetic will cause the parietal pleura to be displaced inferiorly.

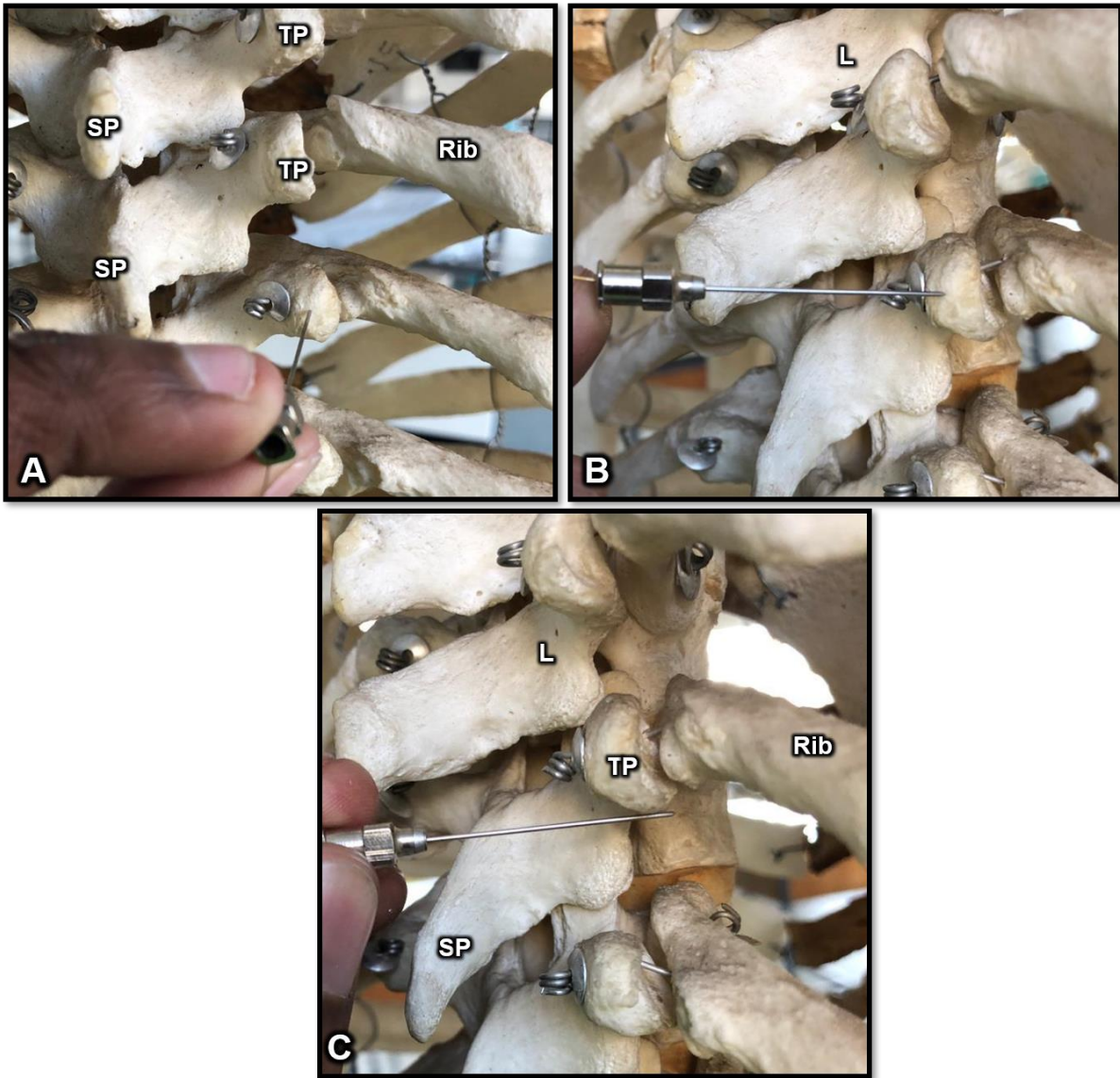


Figure 14: Images showing the needle course as it makes contact with the transverse process (A & B), before being ‘walked-off’ the inferior edge of the transverse process (C) into the paravertebral space. Key SP – spinous process, TP – transverse process, L – lamina.

b) *Paramedian plane/technique*

Orientation and structures appear as described under the paramedian approach in 2.2.b. The needle should be advanced in a caudal to cranial direction, through the superior costotransverse ligament into the paravertebral space (Nair *et al.*, 2020).

3.3 Aim

The aim of this chapter was to investigate the anatomy of the paravertebral block using ultrasound and CT scans.

3.4 Research objectives

- I. To evaluate the anatomy of the paravertebral space based on previously published literature, together with observations made from retrospectively examining existing ultrasound and CT scans by determining the average: distance from the spinous process to the hypothetical needle insertion site; distance from the spinous process to the tip of the transverse process; depth from the skin to the transverse process (lateral limit); depth from the skin to the paravertebral space; depth from the skin to the anterior border of the rib on the images in different paediatric age groups.
- II. To determine the relationship between the depth to the paravertebral space and the demographic features of the sample by using simple and multiple regression analysis.

3.5 Material and Methods

This study was approved by the PhD and Research Ethics Committee (94/2019), University of Pretoria, South Africa. Permission was obtained from the Head of the Department of Radiology and CEO of Steve Biko Academic Hospital to retrospectively source CT scans from patient archives. All records obtained were kept confidential as to keep patient identify anonymous.

a) ***Ultrasound component***

Using the eleven ultrasound scans obtained in section 2.5.a., the format of the scans was converted in order to be uploaded and interpreted onto RadiAnt, a Digital Imaging

and Communication in Medicine (DICOM) viewer, from which various measurements were taken at vertebral levels T5 and T8, bilaterally. Vertebral levels T5 and T8 were selected in order to track the thoracic and abdominal spread separately. These measurements include A – the distance from the spinous process to the lateral tip of the transverse process; B – the distance from the spinous process to the hypothetical needle insertion site; C – the depth from the skin to the transverse process; D – the depth from the skin to the paravertebral space; E – the depth from the skin to the anterior border of the rib on the ultrasound images (Figure 15).

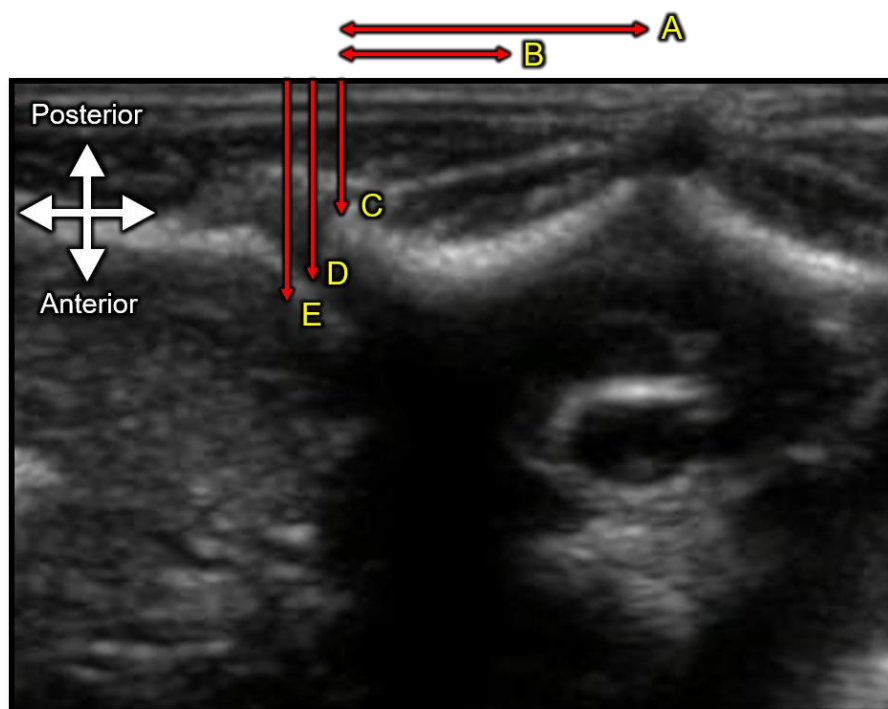


Figure 15: A transverse ultrasound image showing the various measurements taken. Measurements included: A – the distance from the spinous process to the lateral tip of the transverse process; B – the distance from the spinous process to the hypothetical needle insertion site; C – the depth from the skin to the transverse process; D – the depth from the skin to the paravertebral space; E – the depth from the skin to the anterior border of the rib.

b) ***Retrospective CT component***

One hundred and fifty CT images were retrospectively selected from the database of radiographic images at the Department of Radiology, Steve Biko Academic Hospital. Demographic information such as age and sex were recorded. Scans were grouped according to age groups: neonates (0 – 2 months), infants (>2 months – 2 years) and children (> 2 – 12 years). Scans with abnormal vertebral column development such as kyphosis and scoliosis, visceromegaly or space-occupying lesions, as diagnosed by the consulting radiologist, were excluded from this study. RadiAnt, DICOM viewer was then used to analyse the CT scans. Using the on-screen measuring function, calibrated for each image, various measurements were taken at vertebral levels T5 and T8 in a transverse section. Measurements included: A – the distance from the spinous process to the hypothetical needle insertion site; B – the distance from the spinous process to the tip of the transverse process; C – the depth from the skin to the transverse process; D – the depth from the skin to the paravertebral space; E – the depth from the skin to the anterior border of the rib on the CT image (Figure 16).

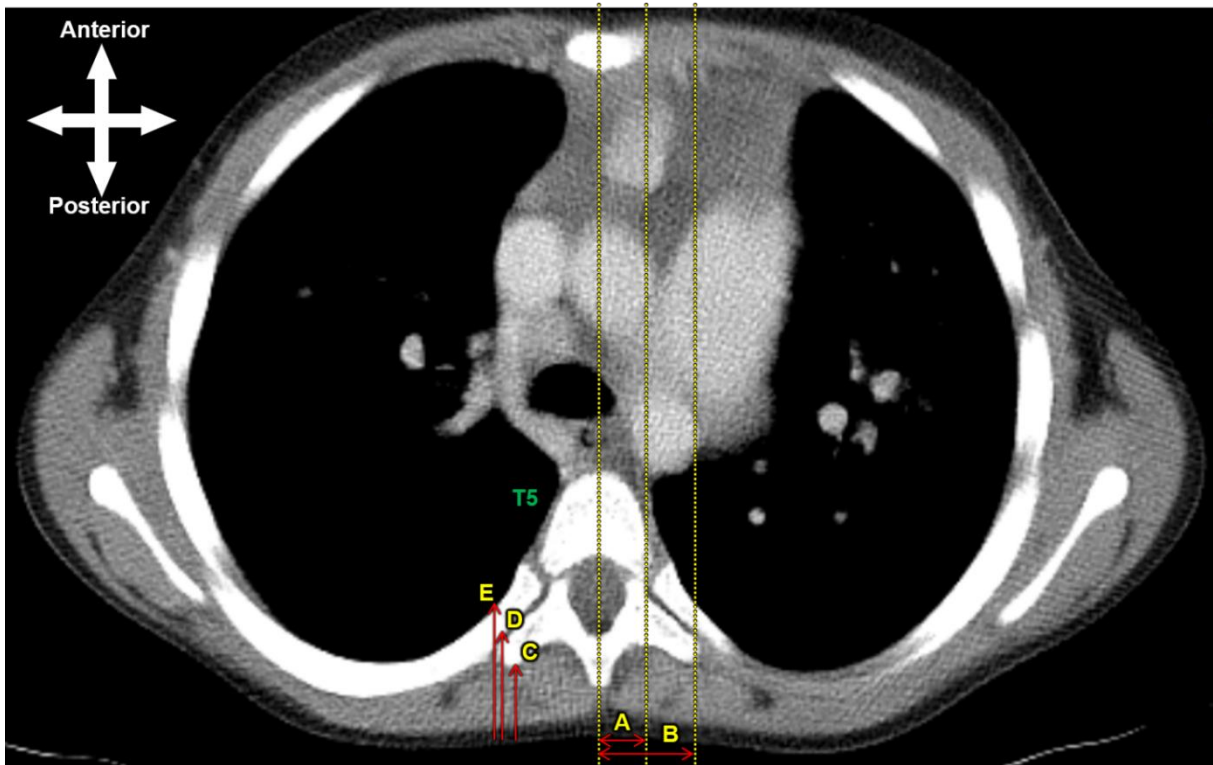


Figure 16: An axial thoracic CT image at vertebral level T5. Measurements included: A – the distance from the spinous process to the hypothetical needle insertion site; B – the distance from the spinous process to the lateral tip of the transverse process; C – the depth from the skin to the transverse process; D – the depth from the skin to the paravertebral space; E – the depth from the skin to the anterior border of the rib.

3.6 Statistical analysis

See section 2.6

3.7 Results

Upon intra- and inter-observer analysis, a student t-test was performed to compare the two sets of data in order to ensure that the measurements obtained were valid. The statistical results revealed a p-value greater than 0.05 for both the intra- and inter-reliability check indicating that there was no statistical significance between the data

sets. The initially obtained data measurements could, therefore, be considered as correct.

Additionally, the anatomy and sonographic anatomy corroborated with the previously described anatomy.

a) ***Ultrasound component***

From the data obtained, paired t-tests were performed to test for statistical significance between the right and left side measurements. Normality was further confirmed as the mean for each measurement was twice the standard deviation. Overall, there were a total of 9 comparisons, due to which the Bonferroni correction method was adopted. The Bonferroni method is used to adjust the p-value when numerous dependent or independent statistical tests are being performed simultaneously on a single data set (see 2.7a). Therefore, for this study, the new p-value was $0.05/9 = 0.0056$. A p-value of less than 0.0056 was considered significant. Table 16 summarises the results of the paired t-test.

Table 16. Results of the paired t-test of the paravertebral measurements taken from the neonate ultrasound scans.

Measurement on the right side	n	Mean (cm)	SD	Measurement on the left side	n	Mean (cm)	SD	p-value
T5SPtoNeedle	11	0.52	0.76	T5SPtoNeedle	11	0.51	0.08	0.89
T5SPtoTP	11	1.03	0.15	T5SPtoTP	11	1.01	0.14	0.12
T5SkintoTP	11	0.89	0.09	T5SkintoTP	11	0.94	0.10	0.02
T5SkintoPVS	11	1.12	0.19	T5SkintoPVS	11	1.14	0.21	0.22
T5SkintoRib	11	1.27	0.18	T5SkintoRib	11	1.33	0.20	0.43
T8SPtoNeedle	11	0.50	0.08	T8SPtoNeedle	11	0.52	0.08	0.17
T8SPtoTP	11	0.99	0.15	T8SPtoTP	11	0.96	0.12	0.18
T8SkintoTP	11	0.89	0.09	T8SkintoTP	11	0.91	0.11	0.28
T8SkintoPVS	11	1.08	0.19	T8SkintoPVS	11	1.07	0.18	0.79
T8SkintoRib	11	1.29	0.26	T8SkintoRib	11	1.27	0.05	0.28

KEY: **n** – sample size, **SD** – standard deviation, **T5** – vertebral level T5, **T8** – vertebral level T8, **SPtoNeedle** – Spinous process to Needle insertion site, **SPtoTP** – Spinous process to Transverse process, **SkintoTP** – Skin to Transverse process, **SkintoPVS** – Skin to Paravertebral space, **SkintoRib** – Skin to Rib.

From the total sample size, 5 scans belonged to females while the remaining 5 belonged to males. Based on these findings, there was no statistical significance between any of the measurements. Therefore, the data were pooled together to create averages for each measurement with a new standard deviation (Table 17).

Table 17. Descriptive statistics summary after pooling the right and left sides for the ultrasound component.

Measurement	n	Minimum (cm)	Maximum (cm)	Mean	SD
T5 Spinous process to Needle insertion site	11	0.22	0.31	0.25	0.08
T5 Spinous process to Transverse process	11	0.88	1.24	1.02	0.14
T5 Skin to Transverse process	11	0.79	1.11	0.92	0.09
T5 Skin to the Paravertebral space	11	0.91	1.51	1.13	0.19
T5 Skin to Rib.	11	1.06	1.66	1.31	0.15
T8 Spinous process to Needle insertion site	11	0.42	0.67	0.51	0.08
T8 Spinous process to Transverse process	11	0.81	1.19	0.98	0.12
T8 Skin to Transverse process	11	0.78	1.05	0.90	0.09
T8 Skin to the Paravertebral space	11	0.88	1.42	1.07	0.18
T8 Skin to Rib	11	0.99	1.72	1.28	0.20

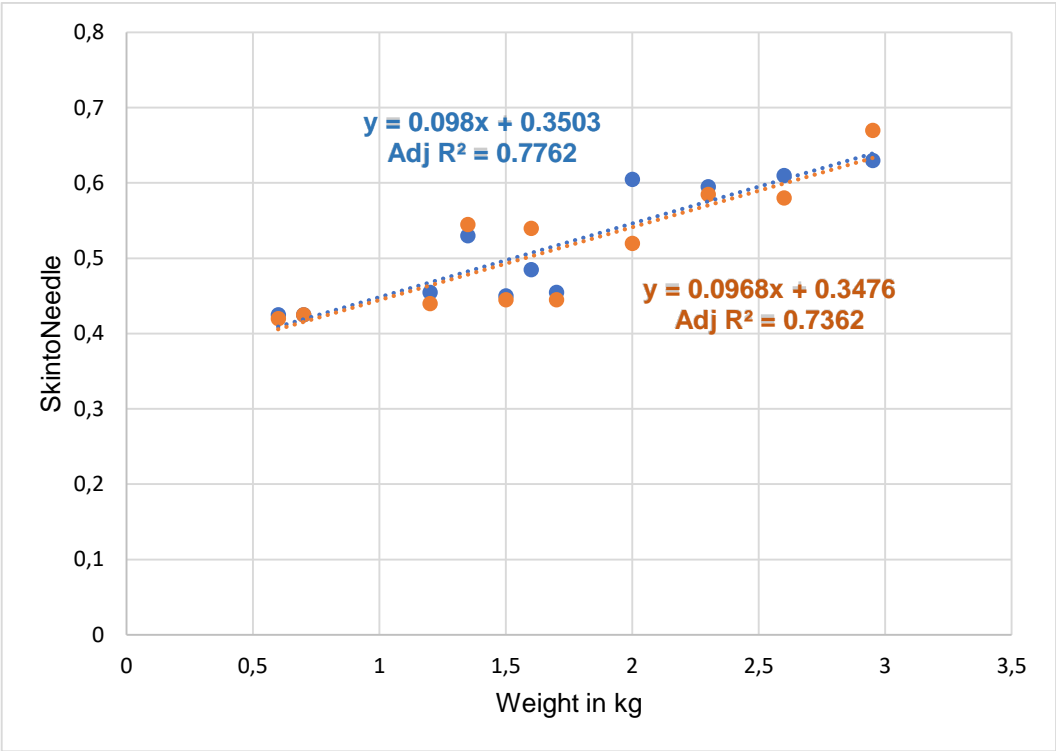
KEY: **n** – sample size, **SD** – standard deviation, **T5** – vertebral level T5, **T8** – vertebral level T8. The data obtained were taken from 11 individuals, however, the mean represents the average of the 22 measurements (right and left sides).

Using linear regression analysis, each measurement (the dependent variable) was further tested for correlation against fixed factors such as; sex, age, height and weight (the independent variables). Due to the nature of the data, the adjusted R^2 -value was used instead of the R^2 -value to predict the correlation. The adjusted R^2 -value is a modified version of the R^2 -value that has been adjusted for the number of predictors in the model. In other words, it can provide a more precise view of that correlation by taking into account how many independent variables are added to a particular model against which the data is measured. These additions usually increase the reliability of the model. Moreover, the adjusted R^2 -value quantifies how well a model fits the data.

From the results, there was no correlation between any of the measurements and sex. A weak correlation was found between T8 skin to transverse process (left side) and

weight (adjusted R²-value of 0.32). A strong correlation was found between the following measurements: T5 spinous process to needle insertion site, T5 spinous process to transverse process, T8 spinous process to needle insertion site, T8 spinous process to transverse process and weight, as all these measurements had an adjusted R²-value > 0.7.

Measurements with a strong correlation were then further plotted on a scatter plot to display the relationship of the correlation (Figure 17).



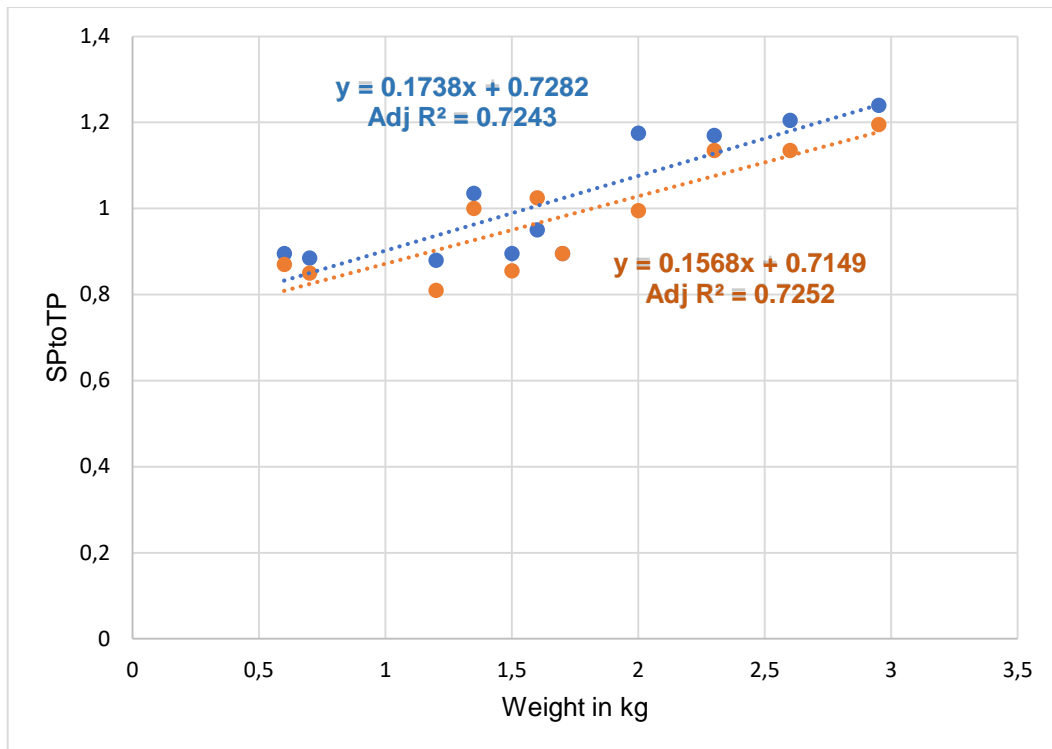


Figure 17: Scatter plot displaying the correlation between SPtoNeedle (top image - T8 in orange and T5 in blue) and SPtoTP (bottom image - T8 in orange and T5 in blue) in cm and weight in kg

As seen in figure 17, the adjusted R^2 -value indicate how much of the attribution is caused by weight. For the spinous process to the needle insertion site, the measurement at vertebral level T5 has a higher adjusted R^2 -value than vertebral level T8, meaning that for vertebral level T5, 78% of the variation in spinous process to the needle insertion site can be explained by weight, or is caused by age, while only 74% of the variation can be explained by age, or is caused by weight, at vertebral level T8. For spinous process to transverse process, adjusted R^2 -value was more or less the same for both vertebral levels. Therefore, 72% of the variation at both vertebral levels for spinous process to transverse process can be explained by weight or is caused by weight.

Likewise, a multivariate regression analysis was performed to assess the overall effect of the independent variables on the dependent variables as a whole. Subsequently, the multivariate regression models for the skin to paravertebral space measurement was then used to create a standard equation that can be utilised when performing the paravertebral block in a pre-term, neonatal paediatric sample (Table 18).

Table 18. Multivariate regression analysis for determining the depth to the paravertebral space in the ultrasound component.

Level	Parameter	Coefficient	SE	t	p-value	95% confidence interval	
						Lower	Upper
T5	Sex	-0.137	0.127	-1.08	0.318	-0.437	0.164
	Height (mm)	0.00008	0.001	0.08	0.938	-0.002	0.003
	Weight (kg)	0.107	0.094	1.14	0.294	-0.116	0.33
	-constant	0.986	0.504	1.96	0.01	-0.205	2.17
T8	Sex	-0.046	0.106	-0.44	0.673	-0.298	0.204
	Height (mm)	-0.002	0.0009	-2.08	0.076	-0.004	0.0002
	Weight (kg)	0.193	0.079	2.43	0.045	0.006	0.38
	-constant	1.68	0.422	3.96	0.005	0.676	2.67

Key: **SE** – standard error, **T5** – vertebral level T5, **T8** – vertebra level T8.

Sex was represented by numeric values. Males were assigned the number 0, while females were assigned the number 1 that could be inserted into the equations. As indicated in Table 18, none of the variables were statistically not significant ($p > 0.05$) and had a weak correlation (adjusted R^2 -value < 0.3). Nonetheless, formulae were created for vertebral level T5 and T8. Both formulae included the standard error of the estimate to indicate the accuracy of the predictions. The formulae were as follows:

- T5 skin to paravertebral space
 - Depth in cm = $0.00008(\text{height in mm}) + 0.107(\text{weight in kg}) - 0.137(\text{sex}) + 0.986 \pm \text{the standard error of estimate (0.180)}$
- T8 skin to paravertebral space
 - Depth in cm = $0.193(\text{weight in kg}) - 0.002(\text{height in mm}) - 0.046(\text{sex}) + 1.68 \pm \text{the standard error of estimate (0.151)}$

The adjusted R^2 -value for the formulae were 0.18 and 0.53 for vertebral level T5 and T8, respectively. The approximate distance from the spinous process to the insertion site at vertebral level T5 was 0.52 cm with a standard deviation of 0.08, while the distance at vertebral level T8 was 0.51 cm with a standard deviation of 0.08.

b) **CT component**

Again, paired t-tests were performed to test for statistical significance between the right and left side measurements. Normality was further confirmed as the mean for each measurement was twice the standard deviation. Overall, there were a total of 9 comparisons per group (group 1 – neonates, group 2 – infants, group 3 – children). After adopting the Bonferroni correction method, the new p-value was ≤ 0.0056 . Table 19 to 21 below summarises the results of the paired t-test for the various groups.

Table 19. Results of the paired t-test of the paravertebral measurements taken from the neonatal CT scans (group 1).

Measurement on the right side	n	Mean	SD	Measurement on the left side	n	Mean	SD	p-value
T5SPtoNeedle	43	1.04	0.16	T5SPtoNeedle	43	1.05	0.16	0.56
T5SPtoTP	43	1.29	0.21	T5SPtoTP	43	1.29	0.20	0.96
T5SkintoTP	43	1.41	0.38	T5SkintoTP	43	1.53	0.40	0.0045*
T5SkintoPVS	43	1.7	0.39	T5SkintoPVS	43	1.76	0.41	0.09
T5SkintoRib	43	2.12	0.41	T5SkintoRib	43	2.17	0.44	0.24
T8SPtoNeedle	42	1.00	0.16	T8SPtoNeedle	42	1.02	0.17	0.016
T8SPtoTP	42	1.25	0.19	T8SPtoTP	42	1.26	0.20	0.18
T8SkintoTP	42	1.04	0.28	T8SkintoTP	42	1.14	0.29	0.0018*
T8SkintoPVS	42	1.32	0.28	T8SkintoPVS	42	1.38	0.31	0.04
T8SkintoRib	42	1.75	0.33	T8SkintoRib	42	1.80	0.34	0.06

KEY: **n** – sample size, **SD** – standard deviation, **T5** – vertebral level T5, **T8** – vertebral level T8, **SPtoNeedle** – Spinous process to Needle insertion site, **SPtoTP** – Spinous process to Transverse process, **SkintoTP** – Skin to Transverse process, **SkintoPVS** – Skin to Paravertebral space, **SkintoRib** – Skin to Rib, * – represents statistically significant values as the p-value was less than 0.0056.

From the total sample size, 22 scans belonged to females while the remaining 21 belonged to males. A significant difference was seen between the right and left side of T5 skin to transverse process and T8 skin to transverse process in the neonatal group, while the rest of the measurements were not statistically significant. Statistically significant measurements were then plotted on a bar graph displaying its mean and standard error (Figure 18).

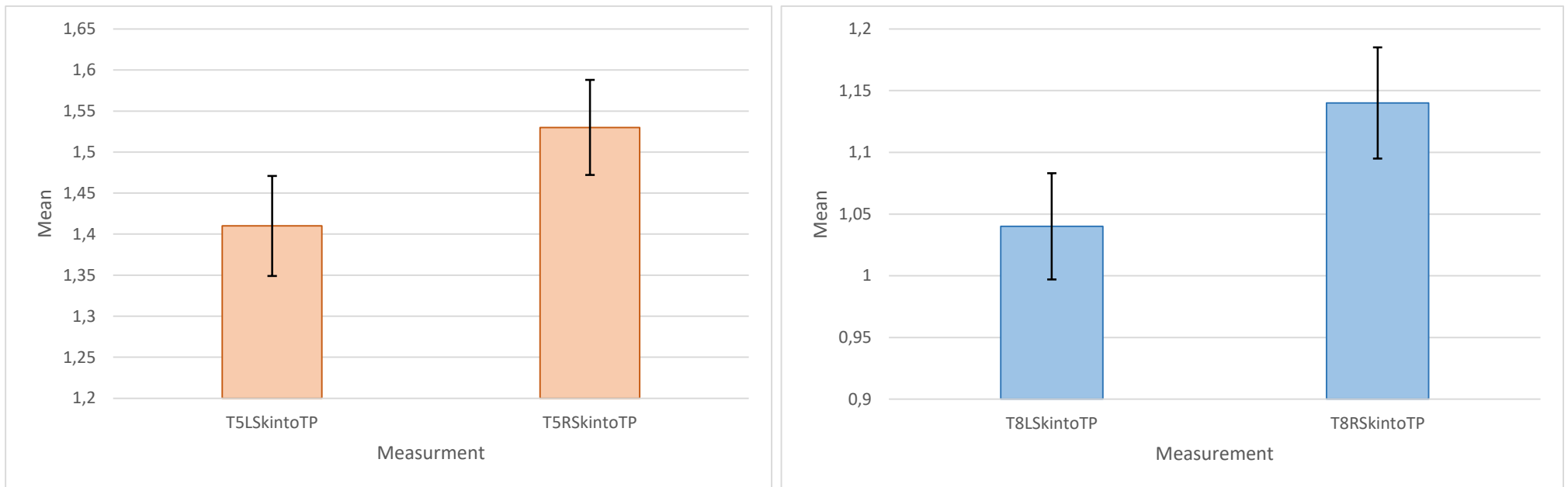


Figure 18: Bar graph showing the results from the paired t-test for the statistically significant measurements. The error bar represents the standard error in relation to the mean.

As seen in figure 18, the measurements from the skin to the transverse process at vertebral levels T5 and T8 were greater on the right side than on the left side. The error bar represents the standard error of the mean. The standard error is used to measure the accurateness with which a sample distribution represents a population by using the standard deviation. Error bars indicate the spread of data around the mean or how accurately the mean of the measurement represents the data set (i.e the variability). The error around the mean is similar for the left and right side for both measurements. Furthermore, standard error bars can use to estimate whether or not a difference is truly significant depending on the overlapping, or lack thereof. If standard error bars slightly overlap as indicated by both bar graphs, there is a probability that the difference is statistically significant, although it is not high. Overall, there is statistical significance between the measurements. The actual difference between the right and left side, however, is small.

Table 20. Results of the paired t-test of the paravertebral measurements taken from the infant CT scans (group 2).

Measurement on the right side	n	Mean	SD	Measurement on the left side	n	Mean	SD	p-value
T5SPtoNeedle	49	1.26	0.24	T5SPtoNeedle	49	1.27	0.22	0.74
T5SPtoTP	49	1.66	0.29	T5SPtoTP	49	1.63	0.28	0.47
T5SkintoTP	49	1.55	0.44	T5SkintoTP	49	1.60	0.51	0.07
T5SkintoPVS	49	1.98	0.53	T5SkintoPVS	49	1.99	0.59	0.61
T5SkintoRib	49	2.47	0.60	T5SkintoRib	49	2.49	0.66	0.44
T8SPtoNeedle	49	1.21	0.27	T8SPtoNeedle	49	1.25	0.31	0.02
T8SPtoTP	49	1.58	0.27	T8SPtoTP	49	1.62	0.33	0.15
T8SkintoTP	49	1.23	0.36	T8SkintoTP	49	1.26	0.36	0.43
T8SkintoPVS	49	1.67	0.48	T8SkintoPVS	49	1.66	0.48	0.84
T8SkintoRib	49	2.24	0.49	T8SkintoRib	49	2.22	0.48	0.53

KEY: **n** – sample size, **SD** – standard deviation, **T5** – vertebral level T5, **T8** – vertebral level T8, **SPtoNeedle** – Spinous process to Needle insertion site, **SPtoTP** – Spinous process to Transverse process, **SkintoTP** – Skin to Transverse process, **SkintoPVS** – Skin to Paravertebral space, **SkintoRib** – Skin to Rib.

For age group 2 (28 females and 21 males), no statistical significance was seen between any of the measurements on both the right and left sides.

Table 21. Results of the paired t-test of the paravertebral measurements taken from the children CT scans (group 3).

Measurement on the right side	n	Mean	SD	Measurement on the left side	n	Mean	SD	p-value
T5SPtoNeedle	59	1.45	0.21	T5SPtoNeedle	59	1.48	0.22	0.004*
T5SPtoTP	59	1.92	0.27	T5SPtoTP	59	1.93	0.27	0.28
T5SkintoTP	59	1.69	0.51	T5SkintoTP	59	1.72	0.48	0.42
T5SkintoPVS	59	2.11	0.55	T5SkintoPVS	59	2.09	0.54	0.46
T5SkintoRib	59	2.81	0.63	T5SkintoRib	59	2.74	0.61	0.05
T8SPtoNeedle	59	1.51	0.42	T8SPtoNeedle	59	1.55	0.42	0.14
T8SPtoTP	59	1.93	0.26	T8SPtoTP	59	1.94	0.25	0.11
T8SkintoTP	59	1.39	0.39	T8SkintoTP	59	1.41	0.41	0.31
T8SkintoPVS	59	1.85	0.44	T8SkintoPVS	59	1.81	0.44	0.086
T8SkintoRib	59	2.53	0.51	T8SkintoRib	59	2.48	0.54	0.121

KEY: **n** – sample size, **SD** – standard deviation, **T5** – vertebral level T5, **T8** – vertebral level T8, **SPtoNeedle** – Spinous process to Needle insertion site, **SPtoTP** – Spinous process to Transverse process, **SkintoTP** – Skin to Transverse process, **SkintoPVS** – Skin to Paravertebral space, **SkintoRib** – Skin to Rib, * – represents statistically significant values as the p-value was less than 0.0056.

In group 3 (children) (32 females and 27 males), a significant difference was seen between the right and left side of T5 spinous to needle insertion site. Statistically significant measurements were then plotted on a bar graph, displaying their mean and standard error (Figure 19).

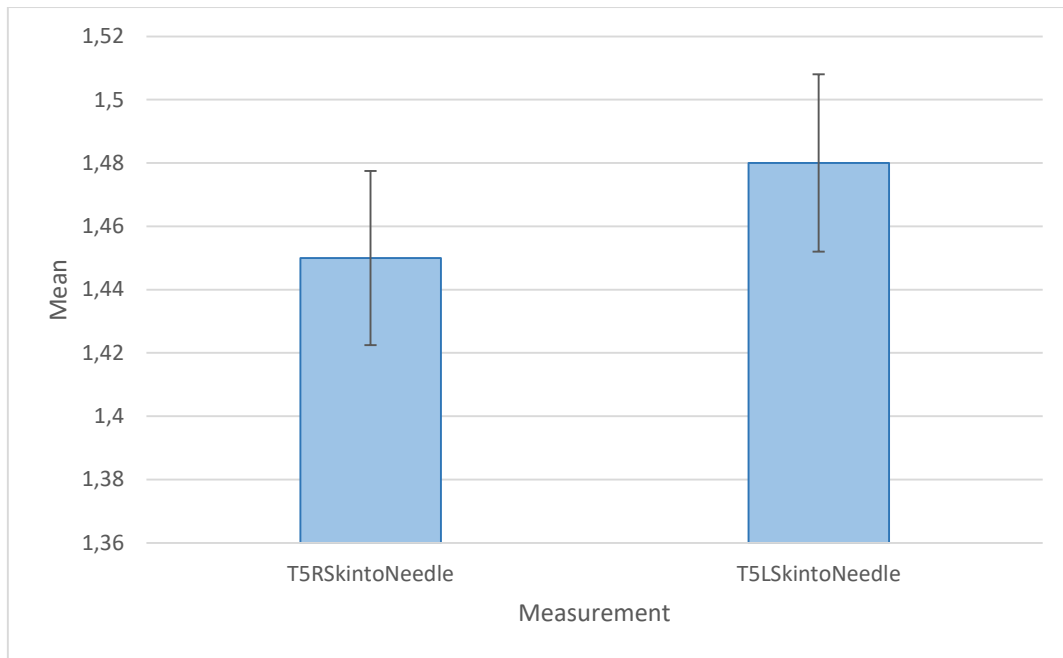


Figure 19: Bar graph showing the results from the paired t-test for the statistically significant measurements. The error bar represents the standard error in relation to the mean.

The measurements from the skin to the needle insertion site at vertebral level T5 was greater on the left side than on the right side. The error bar represents the standard error of the mean. The standard error is used to measure the accurateness with which a sample distribution represents a population by using the standard deviation. Error bars indicate the spread of data around the mean or how accurately the mean of the measurement represents the data set (i.e the variability). The error around the mean is similar for the right and left side for the measurements. As previously mentioned, standard error bars are used to estimate how significant a difference between two variables are. Due to the overlapping error bars as seen in Figure 19, there is a probability that the difference is statistically significant although it is not high. Overall, there is statistical significance between the measurements; however, the actual difference between the right and left sides is small.

Subsequently, comparative analysis was performed between groups to determine if there was a significant difference between individual measurements and groups before pooling the data. Results revealed a significant difference ($p\text{-value} > 0.05$) between

most measurements between groups, therefore the data was not pooled together. Further statistical testing was performed on the group individually.

Measurements from group 1 that was not statistically significant was pooled together to create averages for each measurement with a new standard deviation (Table 22). The T5 & T8 skin to transverse process was excluded from the pooled data.

Table 22. Descriptive statistics summary after pooling the right and left sides for the CT component (group 1).

Measurement	n	Minimum (cm)	Maximum (cm)	Mean (cm)	SD
T5SPtoNeedle	43	0.59	1.53	1.05	0.15
T5SPtoTP	43	0.44	0.55	0.50	0.02
T5SkintoPVS	43	0.30	0.62	0.49	0.06
T5SkintoRib	43	1.37	3.31	2.14	0.41
T8SPtoNeedle	42	0.65	1.51	1.01	0.16
T8SPtoTP	42	0.81	1.79	1.25	0.19
T8SkintoPVS	42	0.68	2.21	1.34	0.28
T8SkintoRib	42	1.08	2.65	1.77	0.32

KEY: **n** – sample size, **SD** – standard deviation, **T5** – vertebral level T5, **T8** – vertebral level T8. The data obtained were taken from 43/42 individuals, however, the mean represents the average of the 86/84 measurements (right and left sides).

Regression analysis was also performed to evaluate the correlation between the measurement (the dependent variable) and fixed factors such as sex and age (independent variables). From the results, no correlation was found between any of the measurements and sex or age. All regression models produced an adjusted R²-value of ≤ 0.1 .

Subsequently, a multivariate regression analysis was then performed to create a standard equation that can be utilised when performing the paravertebral block (Table 23). The equations/formulae highlight the depth at which the block needle can be inserted at different vertebral levels, should the block be performed using the 'blind' technique in age group 1 (0 – 2 months). For the analysis, factors such as sex and age were used, as these were the only demographic information available from the CT scans.

Table 23. Multivariate regression analysis for determining the depth to the paravertebral space (group 1).

Level	Parameter	Coefficient	SE	t	p-value	95% confidence interval	
						Lower	Upper
T5	Sex	0.012	0.022	0.552	0.584	-0.032	0.061
	Age	0.009	0.025	0.356	0.724	-0.042	0.061
	-cons	0.470	0.031	15.192	3.302	0.407	0.529
T8	Sex	0.038	0.094	0.408	0.685	-0.153	0.230
	Age	-0.054	0.111	-0.488	0.628	-0.278	0.170
	-cons	1.397	0.135	10.316	1.050	1.124	1.672

Key: **SE** – standard error, **T5** – vertebral level T5, **T8** – vertebra level T8.

Sex was represented by numeric values. Males were assigned the number 0, while females were assigned the number 1 that could be inserted into the equations. As indicated in Table 23, none of the variables were statistically significant ($p > 0.05$). Both formulae included the standard error of the estimate to indicate the accuracy of the predictions. The formulae were as follows:

- T5 skin to paravertebral space
 - o Depth in cm = $0.470 + 0.009(\text{age}) + 0.012(\text{sex})$ +/- the standard error of estimate (0.065)
- T8 skin to paravertebral space
 - o Depth in cm = $1.397 + 0.038(\text{age}) + 0.054(\text{sex})$ +/- the standard error of estimate (0.285)

The adjusted R²-value for the formulae were -0.33 and -0.43 for vertebral level T5 and T8, respectively. The approximate distance from the spinous process to the insertion site at vertebral level T5 was 1.53 cm with a standard deviation of 0.15, while the distance at vertebral level T8 was 1.01 cm with a standard deviation of 0.16.

The same tests were conducted for the remaining groups. Since there was no statically significance between right and left, the data was pooled together. (Table 24).

Table 24. Descriptive statistics summary after pooling the right and left sides for the CT component (group 2).

Measurement	n	Minimum (cm)	Maximum (cm)	Mean (cm)	SD
T5SPtoNeedle	49	0.56	1.94	1.26	0.22
T5SPtoTP	49	0.43	1.59	0.52	0.16
T5SkintoTP	49	0.38	0.72	0.49	0.66
T5SkintoPVS	49	0.40	0.68	0.50	0.05
T5SkintoRib	49	1.48	5.58	2.48	0.62
T8SPtoNeedle	49	0.61	2.44	1.23	0.29
T8SPtoTP	49	1.06	2.74	1.59	0.29
T8SkintoTP	49	0.62	2.39	1.24	0.35
T8SkintoPVS	49	1.03	3.71	1.67	0.47
T8SkintoRib	49	1.46	3.98	2.22	0.48

KEY: **n** – sample size, **SD** – standard deviation, **T5** – vertebral level T5, **T8** – vertebral level T8. The data obtained were taken from 49 individuals, however, the mean represents the average of the 98 measurements (right and left sides).

Regression analysis was performed to evaluate the correlation between the measurements – the dependent variable – and fixed factors such as sex and age – the independent variables. From the results, a weak correlation was found between the measurements and sex or age. All regression models produced an adjusted R²-value of ≤ 0.1 .

Subsequently, a multivariate regression analysis was performed to create a standard equation that can be utilised when performing the paravertebral block in age group 2. Since the data was pooled together, one formula was created for each vertebral level (Table 25). The equations/formulae highlight the depth at which the block needle can be inserted at different vertebral levels, in age group 2 (2 months – 2 years).

Table 25. Multivariate regression analysis for determining the depth from the skin to the erector spinae fascial plane space using the data from the CT component (group 2).

Level	Parameter	Coefficient	SE	t	p-value	95% confidence interval	
						Lower	Upper
T5	Sex	0.015	0.014	1.048	0.299	-0.013	0.043
	Age	0.0002	0.0008	0.252	0.802	-0.001	0.002
	-cons	0.491	0.017	28.783	4.597	0.456	0.525
T8	Sex	-0.184	0.132	-1.385	0.172	-0.451	0.083
	Age	0.011	0.008	1.401	0.167	-0.005	0.028
	-cons	1.598	0.158	10.073	3.227	1.279	1.918

Key: **SE** – standard error, **T5** – vertebral level T5, **T8** – vertebra level T8.

Sex was represented by numeric values. Males were assigned the number 0, while females were assigned the number 1 that could be inserted into the equations. As indicated in Table 25, none of the variables were statistically significant ($p > 0.05$). Both formulae included the standard error of the estimate to indicate the accuracy of the predictions. The formulae were as follows:

- T5 skin to paravertebral space
 - o Depth in cm = $0.491 + 0.0002(\text{age}) + 0.015(\text{sex})$ +/- the standard error of estimate (0.049)
- T8 skin to paravertebral space
 - o Depth in cm = $1.598 + 0.011(\text{age}) - 0.184(\text{sex})$ +/- the standard error of estimate (0.462)

The adjusted R²-value for the formulae were -0.02 and 0.40 for vertebral level T5 and T8, respectively. The approximate distance from the spinous process to the insertion site at vertebral level T5 was 1.26 cm with a standard deviation of 0.22, while the distance at vertebral level T8 was 1.23 cm with a standard deviation of 0.39.

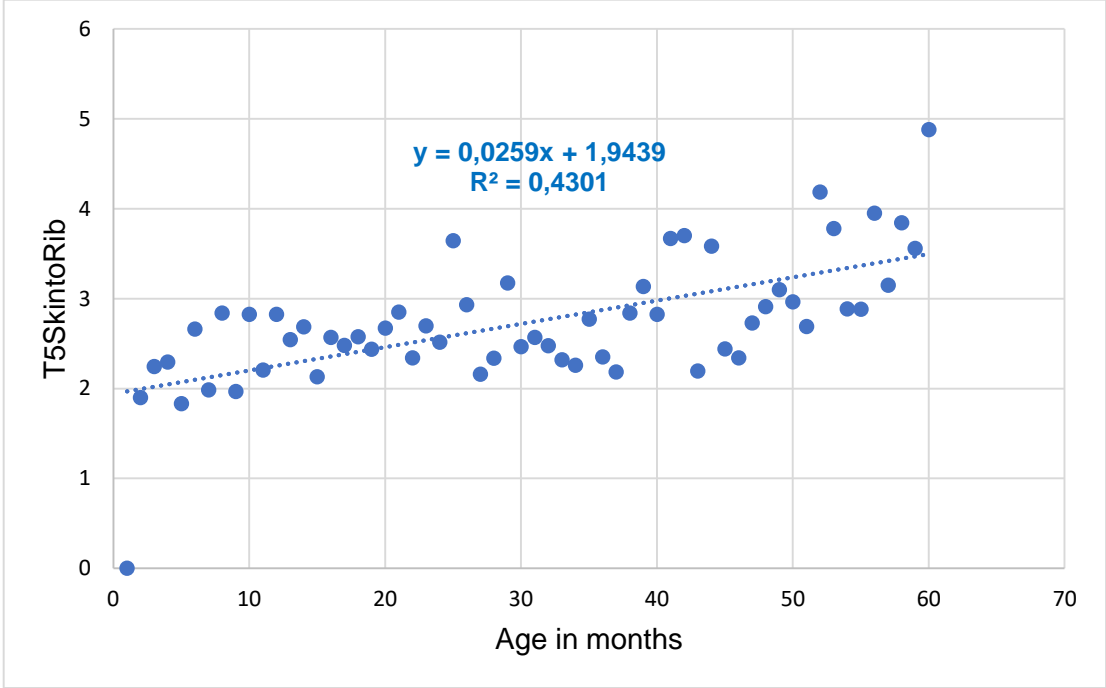
For age group 3, a statistical significance was found between right and left T5 spinous process to needle, therefore this measurement was excluded from the pooled data (Table 26).

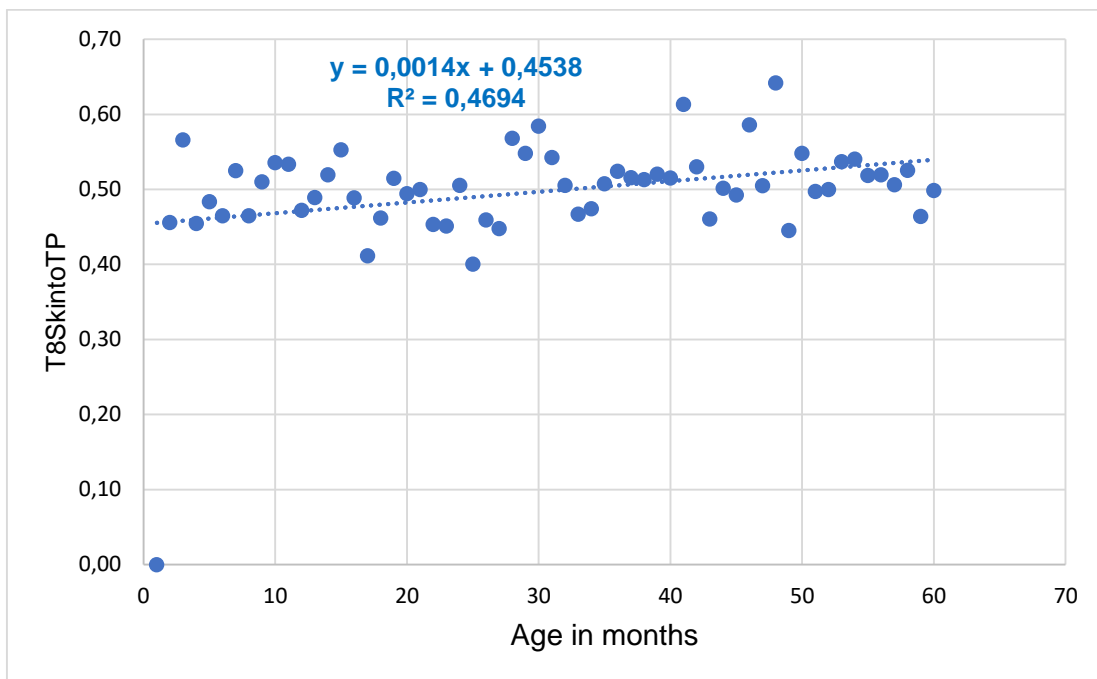
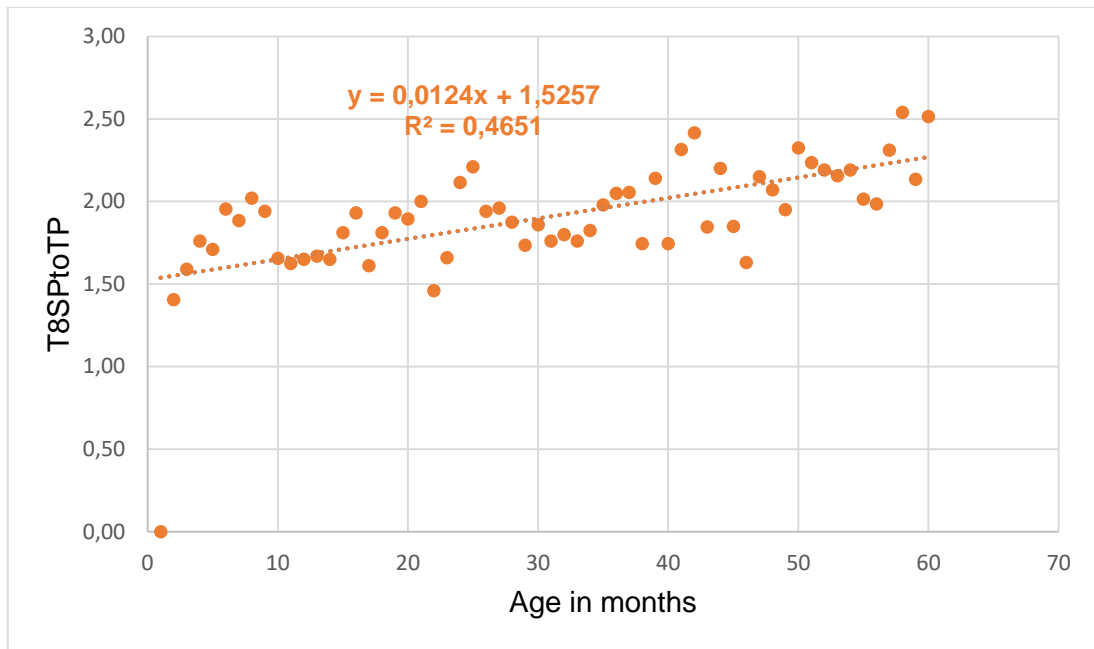
Table 26. Descriptive statistics summary after pooling the right and left sides for the CT component (group 3).

Measurement	n	Minimum (cm)	Maximum (cm)	Mean (cm)	SD
T5SPtoTP	59	0.44	0.55	0.49	0.02
T5SkintoTP	59	0.36	0.63	0.49	0.05
T5SkintoPVS	59	0.40	0.64	0.50	0.04
T5SkintoRib	59	1.83	4.88	2.77	0.61
T8SPtoNeedle	59	0.69	3.95	1.53	0.41
T8SPtoTP	59	1.40	2.54	1.93	0.25
T8SkintoTP	59	0.80	2.70	1.40	0.40
T8SkintoPVS	59	1.17	3.22	1.83	0.43
T8SkintoRib	59	1.82	4.42	2.50	0.52

KEY: **n** – sample size, **SD** – standard deviation, **T5** – vertebral level T5, **T8** – vertebral level T8. The data obtained were taken from 59 individuals, however, the mean represents the average of the 118 measurements (right and left sides).

Regression analysis was then performed to evaluate the correlation between the measurements – the dependent variable – and fixed factors such as sex and age – the independent variables. From the results, a weak correlation was found between the measurements and sex. A moderate correlation was found between: T5 right and left skin to needle insertion (adjusted R²-value of = 0.33 and 0.37, respectively), T8 skin to needle insertion (adjusted R²-value of = 0.30), T5 skin to rib (adjusted R²-value of = 0.43), T8 spinous process to transverse process (adjusted R²-value of = 0.46), T8 skin to transverse process (adjusted R²-value of = 0.46), T8 skin to paravertebral space (adjusted R²-value of = 0.41), T8 skin to rib (adjusted R²-value of = 0.37) and age. Measurements with a moderate correlation (greater than 0.4) were then further plotted on a scatter plot to display the relationship of the correlation (Figure 20).





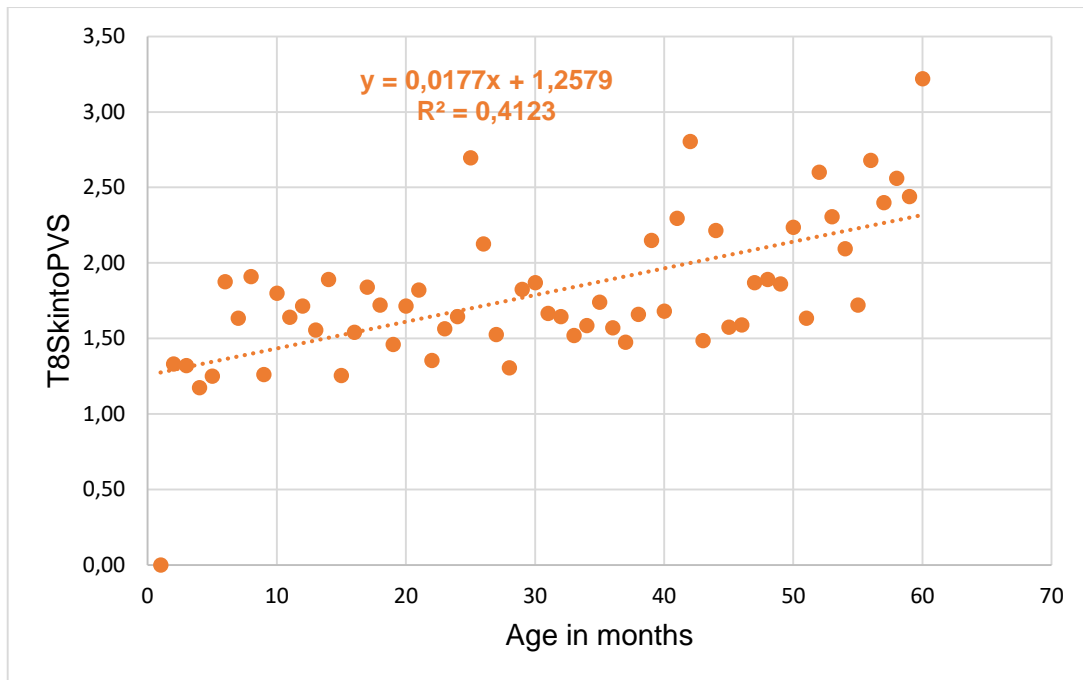


Figure 20: Scatter plot displaying the correlation between: T5SkintoRib in cm to age in months (top/first image), T8SPtoTP in cm to age in months (middle/second image), T8SkintoTP in cm to age in months (middle/third image), T8SkintoTP in cm to age in months (bottom/last image).

As seen in figure 20, the adjusted R^2 -values indicate how much of the attribution is caused by age. Therefore, 43% of the variation can be explained by age, or is caused by age for the skin to rib distance at vertebral level T5 can be explained. Whereas, for the spinous process to transverse process and skin to transverse process at vertebral level T8, 46% of the variation can be explained by age, or is caused by age. For the skin to paravertebral space at vertebral level T8, 41% of the variation can be explained by age or is caused by age

A multivariate regression analysis was then performed to create a standard equation that can be utilised when performing the paravertebral block in age group 3. Again, since the data was pooled together, one formula was created for each vertebral (Table 27). The equations/formulae highlight the depth at which the block needle can be inserted at different vertebral levels, in age group 3 (2 – 12 years).

Table 27. Multivariant regression analysis for determining the depth from the skin to the erector spinae fascial plane space using the data from the CT component (group 3).

Level	Parameter	Coefficient	SE	t	p-value	95% confidence interval	
						Lower	Upper
T5	Sex	-0.002	0.012	-0.153	0.878	-0.025	0.021
	Age	0.0003	0.0002	1.595	0.116	-0.025	0.022
	-cons	0.481	0.018	25.954	6.678	0.444	0.518
T8	Sex	-0.029	0.088	-0.335	0.738	-0.206	0.147
	Age	0.009	0.0014	6.332	4.352	0.006	0.011
	-cons	1.084	0.139	7.783	1.755	0.805	1.363

Key: **SE** – standard error, **T5** – vertebral level T5, **T8** – vertebra level T8.

Sex was represented by numeric values. Males were assigned the number 0, while females were assigned the number 1 that could be inserted into the equations. As indicated in Table 27, none of the variables were statistically significant ($p > 0.05$). Both formulae included the standard error of the estimate to indicate the accuracy of the predictions. The formulae were as follows:

- T5 skin to paravertebral space
 - Depth in cm = $0.481 + 0.0005(\text{age}) - 0.002(\text{sex})$ +/- the standard error of estimate (0.045)
- T8 skin to paravertebral space
 - Depth in cm = $1.084 + 0.009(\text{age}) - 0.029(\text{sex})$ +/- the standard error of estimate (0.337)

The adjusted R²-value for the formulae were 0.11 and 0.40 for vertebral level T5 and T8, respectively. The approximate distance from the spinous process to the insertion site at vertebral level T5 was 1.45 cm with a standard deviation of 0.21 on the right side and 1.48cm with a standard deviation of 0.22 on the left side, while the distance at vertebral level T8 was 1.53 cm with a standard deviation of 0.41.

3.8 Discussion

The paravertebral block (together with the epidural block) has been considered the gold standard for truncal surgeries. However, with recent developments in imaging techniques, together with the discovery of novel neuraxial blocks (interfascial blocks) the paravertebral block is no longer the 'front runner'. Currently, there are still questions regarding the anatomical differences between the paravertebral spaces in the thoracic and lumbar regions.

The discussion will be broken down into two sections, reporting on the measurements and spread separately.

a) ***Block measurements***

The measurements from the ultrasound component, in which pre-term neonates were evaluated, revealed no significant difference between the right and left sides. Moreover, no correlation was found between measurements and sex. A strong correlation was seen between T5 and T8 spinous process to needle insertion site and T5 and T8 spinous process to transverse process and weight. From the regression models, we were able to deduce that an increase in weight would cause an increase in the measurement. Overall, the approximate depth to perform the paravertebral block at T5 was 1.13 cm, with a standard deviation of 0.19, while the depth at vertebral level T8 was 1.07 cm, with a standard deviation of 0.18. The spinous process to needle insertion site distance at vertebral levels T5 and T8 are 0.25 cm and 0.51 cm (with a standard deviation of 0.08), respectively.

There was some statistical significance noted among the measurements in the CT component. The average depth to performing the block in age group 1 at vertebral levels T5 and T8 was 0.49cm (standard deviation of 0.06) and 1.34cm (standard deviation of 0.28). In age group 2, the average depth was 0.50cm with a standard deviation of 0.05 at vertebral level T5 and 1.67cm with a standard deviation of 0.47 at vertebral level T8. While in group 3 the average depth was 0.50cm with a standard deviation of 0.04 at vertebral level T5 and 1.83cm with a standard deviation of 0.43 at

vertebral level T8. Consistent results showed that as one progressed inferiorly from the mid-thoracic area, the depth from skin to paravertebral space increased in all age groups. Overall, the low standard deviations indicated little variation within the age groups.

From the multivariate regression models, estimation formulae were created to determine the depth at which the block can be performed in different paediatric age groups. Additionally, this study noted the skin to muscle distance in various age groups. Results revealed that changes in body habitus, which is directly related to age group, affects the overall size of muscular structures. This in turn directly relates to the depth at which the needle can be inserted in various age groups.

Lönnqvist (1992) created a standard set of formulae by also using measurements taken from CT scans to calculate the distance from the spinous process to the needle insertion site, and the depth to the paravertebral space in the thoracic region, with bodyweight (in kilograms) being the only parameter. Lönnqvist's formulae:

Distance from the spinous process to the insertion point

- Distance (mm) = $0.12 \times \text{body weight (kg)} + 10.2$

The depth to the paravertebral space

- Depth (mm) = $0.48 \times \text{body weight (kg)} + 18.7$

Contrary to Lönnqvist's formulae, our formulae produce values in centimetres and incorporated age, rather than weight. Different parameters, coupled with the larger sample size used by Lönnqvist, may explain for the discrepancies in the formulae constants, even though, as in this study, the formulae were restricted to the thoracic region. However, taking the results from this study into consideration, Lönnqvist's formulae may not apply to a younger South African paediatric group, as the constant values used in his formulae are higher than the mean for our skin-to- paravertebral space depth.

Taking Lönnqvist's formulae into consideration, Yoo *et al.* (2012) conducted a study to evaluate the depth of the needle insertion required to reach the paravertebral space, and the distance from the spinous process to the insertion point on the skin, using CT

scans of paediatric patients. Results from their study revealed a significant correlation between sex, age, height and weight. Upon further analysis, height was found to be multicollinearity and was, therefore, removed from the equations. The formulae were as follows:

- Distance from the spinous process to the insertion point:
 - $\text{Distance (mm)} = 13.56 - (0.33 \times \text{age in years}) + (0.06 \times \text{weight in kg}) + (0.47 \times \text{gender [female=0 and male=1]})$
- The depth to the paravertebral space:
 - $\text{Depth (mm)} = 17.49 - (0.35 \times \text{age in years}) + (0.55 \times \text{weight in kg})$

Contrary to the current study, Yoo *et al.* (2012) found sex to be significant in their study, which was not the case for our data. Furthermore, they used age in years (which was limited to 9 years) to calculate the constants, as opposed to months. The authors also conducted measurements at the level of all thoracic vertebrae, whereas we specifically concentrated on vertebral levels T5 and T8.

In the same year, Ponde and Desai (2012) derived a clinically useful formula for paravertebral blocks for the thoracic-, lumbar- and cervical levels, as per the ultrasound-guided measurements in neonates, infants and children up to 5 years of age. With a sample size of 75, they were able to derive two formulae for each region. The first formula calculates the distance (in centimetres) from the spinous process to the insertion point, and the second, the distance from the insertion point to the paravertebral space) (in centimetres). The formulae for the thoracic region were as follows:

- Distance from the spinous process to the insertion point:
 - $\text{Distance (cm)} = 0.02 \times \text{weight (kg)} + 0.003 \times \text{age (in months)} + 0.93$
- The depth to the paravertebral space:
 - $\text{Depth (cm)} = 0.03 \times \text{weight (kg)} + 0.03 \times \text{age (in months)} + 1.02$

When comparing these formulae to the formulae derived in this study, again we notice discrepancies in the constant values used. Apart from additional parameters used and the sample size, we can assume that external factors may contribute to variations between population groups, resulting in formulae inconsistencies.

We derived these formulae as a guideline to performing paravertebral blocks in different paediatrics age groups in a South African population for practitioners to whom ultrasound-guidance is not available. 'Blind' techniques rely solely on fascial 'clicks' or 'pops' (the loss of resistance method) and external measurements. Specific to paravertebral blocks, the needle should be advanced through the costotransverse ligament which offers quite a subtle loss of resistance as opposed to through the ligament flavum in the epidural area (Ponde and Desai, 2012). Therefore, this lack of resistance push-back may easily contribute to incorrect needle placement without measurement guidance. In a comparative study between landmark-based versus a predetermined distance approach for paravertebral blocks, the former displayed a higher failure rate of 5.2% while the latter only reported a rate of 2.3% (Nair *et al.*, 2020).

b) ***Injectate spread***

Multiple studies reporting on the spread and efficacy of the paravertebral block display encouraging results in a paediatric population. In a single case study done by Kendigelen and colleagues (2016), the paravertebral block was performed on a 3.5-year-old for a bronchoscopy. Using 0.5 ml/kg, the surgery was successful with no need for opioids until the 6th hour post-operative. The authors then stated that the paravertebral block can be used in the early post-operative period as it proves adequate analgesia. Yanovski and co-workers (2013) reported on a case study in which a continuous thoracic paravertebral block (at vertebral level T10) was performed on a 10-year-old child for post-operative pain management. During post-operative recovery, 10 ml of opaque contrast dye was injected, followed by anteroposterior chest radiographs. Results revealed an extensive longitudinal spread of contrast material within the paravertebral spaces from vertebral level T4/T5 (the intervertebral disc) to

vertebral level T10/T11 (the intervertebral disc). Distinct lateral extension of contrast material was also seen along the 5th to 10th intercostal nerves.

Albokrinov and Fesenko (2014) performed a cadaveric study to track the spread of dye after performing thoracic paravertebral blocks in infants. The age of the cadavers ranged from 1 to 13 months. The amount of contrast material varied between 0.1 – 0.5 ml/kg. Contrast material was present in the paravertebral space in all cadavers. Furthermore, cephalad and caudal spread was seen. The authors reported that the cephalad spread was associated with thoracic spinal nerve root and intercostal space staining, while the caudal spread was associated with lumbar plexus nerve root and dorsal surface of psoas muscle staining. They further concluded that 0.2 – 0.3 ml/kg of local anaesthetic was sufficient to cover five and six thoracolumbar segments, respectively.

Page and Taylor (2017) identified advantages of paravertebral blocks in paediatrics which include unilateral blockade, limited haemodynamic changes and stress response resulting from a bilateral sympathetic block. They also noted that the paravertebral block provided a complete somatosensory block as compared to the epidural block without the risk of epidural related spinal damage, allowing for higher doses of local anaesthetic to be used with less risk. In a separate study, after performing the block on a paediatric sample, the authors concluded that the paravertebral block has extremely low failure and complication rates in children (Naja and Lönnqvist, 2001). Similar findings were noted by ELdeen (2016).

The spread and efficacy of the block were also assessed in an adult population. Ruscio *et al.* (2020) used 27 cadavers to track the spread of dye, based on the type of technique used, landmark-based, or ultrasound-guided. Results revealed that a greater success rate in terms of correct needle placement was associated with the ultrasound-guided injections. However, the technique itself did not affect the overall spread of dye. The spread ranged from 1 to 5 vertebral levels. In addition, the authors stated that posterolateral truncal analgesia could still be achieved even if the spread did not directly reach the paravertebral space (Ruscio *et al.*, 2020). In another study, ultrasound guidance was used to track the spread of contrast material following

thoracic paravertebral blockade in 10 fresh cadavers. Results of the spread were summarised according to its end destination as either paravertebral-, intercostal- or epidural spread. For the paravertebral spread, contrast material was found surrounding the intercostal nerves, sympathetic ganglia, rami communicantes and the splanchnic nerves over an average of three vertebral segments. There was extensive intercostal contrast material spread in all cases. Additionally, contrast material spread over more segments (average of 4.5 vertebral levels) as compared to the paravertebral spread. With regard to the epidural spread, contrast material in the epidural space was continuous with the contrast spread from the paravertebral spread and was confined to 1 vertebral segment in each cadaver. The authors then concluded that the paravertebral space is not an isolated compartment and has communication with both the intercostal and epidural spaces (Cowie *et al.*, 2010).

Another author explained that the anaesthetic has to pass through the neural/intervertebral foramen to reach the epidural space (Piraccini *et al.*, 2019). In an imaging study, authors demonstrated that when contrast material was found in the paravertebral space, it was also found in the intercostal spaces spanning 2 to 6 intercostal spaces (Luyet *et al.*, 2009).

Another factor to consider regarding the efficacy of the spread, is the number of injections performed. Uppal *et al.*, (2017), compared the extent of spread, subsequent to performing an ultrasound-guided paravertebral block of equal volumes (25 ml) injected at 1 versus 5 vertebral segments. Results revealed similar dermatomal spread (5 vertebral segments) when comparing a single level block with multiple level blocks. These findings were contradictory to previously published literature by Cowie *et al.* (2010), who used 20 ml of contrast material and reported extensive spread across intercostal segments with 4.5 spaces and 6 spaces covered with a single level, versus multiple level injection, respectively.

Taketa and Fujitani (2017) performed a cadaveric trial to test the patterns of injectate spread when using the intercostal and para-laminar in-plane approach for paravertebral blocks. The paravertebral spread was confirmed in all procedures. For the intercostal approach, contrast material was found in the respective intercostal

spaces and its adjacent paravertebral space. However, the para-laminar approach had a more longitudinal and medial paravertebral spread rather than a lateral intercostal spread. The authors suggested that the ESP block had properties similar to a pectoral nerve block, unlike the paravertebral block.

In a different cadaver study, authors used methylene blue and plastic to model the dispersion of anaesthetic fluid in the thoracic paravertebral space. They explained that methylene blue dye is an aqueous solution, whereas plastic is a viscous solution, making it possible to compare the spread of both in the same cadaver. The aqueous spread displayed pre- and paravertebral spread, as well as intercostal spread over multiple segments. The viscous solution spread was limited, but was able to give a detailed picture of the anatomy. The methylene blue dye was also found around the azygos system and neurovascular bundle. The overall distribution of spread was found along the sympathetic chain, intercostal and paravertebral spaces (Bouman *et al.*, 2017).

To test the continuity of the intercostal space with the paravertebral space, Paraskeuopoulos and colleagues (2010) conducted a cadaveric study to compare two techniques, the transverse and longitudinal approach of the intercostal technique. Results showed a successful spread of methylene blue dye along the intercostal space into the paravertebral space in 89.5% of cases for the transverse approach, and 92.8% of cases for the longitudinal approach. In three cases, the bulk of the dye was injected into the intercostal muscle, therefore, no spread was seen in both the intercostal and paravertebral spaces. On average, the transverse approach required two-needle insertion attempts, while the longitudinal approach required four.

These techniques were performed based on the observation that methylene blue dye injected into the triangular space bounded by the subcostal groove, the posterior intercostal membrane and the innermost intercostal muscle, spread medially into the paravertebral space. Additionally, by placing the needle into the intercostal space, which is lateral to the paravertebral space, the chances of inadvertent neuraxial needle placement could be decreased. The authors concluded that, although the techniques require accurate, guided manoeuvring of the needle, it still leads to the direct spread

of injectate into the paravertebral space, which can further spread to the sympathetic chain and the adjacent paravertebral spaces.

Studies by Davies *et al.* (2006) and Fahy *et al.* (2014) concluded that paravertebral blocks result in a decreased need for post-operative antiemetic medication in patients undergoing a mastectomy. Similar results were reported by Ilić *et al.* (n.d.), who conducted a literature review for paravertebral blocks. The authors concluded that, based on current evidence, performing the paravertebral blocks at the level of the thoracic and lumbar vertebrae, is associated with less pain during the post-operative period. Furthermore, results revealed less post-operative nausea and vomiting, as well as greater patient satisfaction.

In a more recent study, the different paravertebral techniques such as surface anatomy (or landmark guided), ultrasound-guided, neurostimulation-guided and direct visualization by the surgeon, were analysed and described in terms of their analgesic effects for thoracic surgery. Authors concluded that the ultrasound-guided techniques and surface-based techniques showed better consistency to manage post-operative acute pain in thoracic surgery (Cadavid-Puentes *et al.*, 2020). A possible explanation for the efficacy of the surface-based technique as stated by Costache *et al.* (2018), is the probability of blocking the spinal nerve roots in the paravertebral space without actually penetrating the space, remaining in the “paraspinal” location and in the proximity of the transverse costal ligament.

When, compared to alternative techniques, the paravertebral block produced diverse results. Loftus and colleagues (2016) compared the efficacy of epidural and paravertebral blocks for pectus excavatum repair in children. They concluded that using paravertebral and even intercostal blocks for pectus excavatum repair was a safer and more effective alternative to epidural analgesia. Furthermore, results showed that after the paravertebral block, the hospitalisation of the patient was shorter. Additionally, equal pain scores for the paravertebral and epidural block by day three post-operative and no significant increase in daily emesis we noticed. Sondokoppam *et al.* (2019) though, noted no differences in efficacy or results when comparing

bilateral thoracic paravertebral to bilateral thoracic epidural blocks for a variety of abdominal surgeries.

3.9 Paravertebral blocks versus ESP blocks

Diwan *et al.* (2019) conducted a thorough study comparing the paravertebral block to the ESP block using five formalin-fixed cadavers. Bilateral blocks were performed in all cadavers by administering an ultrasound-guided, left sided thoracic ESP- and a right sided paravertebral block. Results revealed bilateral medial retrolaminar spread, bilateral paravertebral spread and bilateral epidural spread. Upon closer inspection, dye spread was seen medially over the retrolaminar area, spreading laterally along the laminae and superiorly towards the spinous process, but not crossing the midline. Furthermore, the dye spread laterally on both sides across the costotransverse foramen, deep towards the paravertebral spread and further lateral into the intercostal spaces, engulfing the intercostal nerves. Dye was seen surrounding the thoracic nerve roots near the intervertebral foramen and across the lateral-, dorsal- and ventral aspects of the epidural space. Retrograde spread of dye was also noted from the thoracic paravertebral space to the erector spinae fascial plane, intervertebral foramen and epidural space, medially. In two cadavers, the dye encroached as far as the prevertebral area, bilaterally. Due to the endothoracic fascia, there was no dye spread or spillage into the thoracic cavity (posterior mediastinum). Although the results for both blocks were the same, the authors were not sure as to how much volume of the injection encroached upon the contralateral intervertebral foramina and epidural spaces.

In a randomized, blind study by Zhao and colleagues (2020), the analgesic efficacy between paravertebral and ESP blocks for video-assisted thoracic surgery were compared. Single-shot injections were performed at vertebral levels T4 and T6 in a total of 66 patients. Although the spread was not documented, results revealed that a single shot bi-level ESP block produced similar analgesic effects as compared to a paravertebral block in terms of pain scores, analgesic rescue requirement and quality of recovery.

Other studies also reported on the analgesic effects of the ESP block and the paravertebral block. El Ghamry and Amer (2019) conducted a prospective, randomised trial on the role of ESP blocks versus paravertebral blocks for pain control. They concluded that both regional blocks reduced intra-operative and post-operative opioid requirement. However, the incidence of complications was lower for ESP blocks. The authors noted that the overall performance of the ESP block was easier as compared to the paravertebral block. Gürkan and co-workers (2020) compared the ESP block to the paravertebral block for breast surgery. They found that both blocks provided good post-operative analgesia and recommended that clinicians choose a block based on their clinical experience and personal preference.

Ultrasound-guided ESP blocks were compared to thoracic paravertebral blocks for patients undergoing lobectomy. The prospective, randomized study revealed that the ESP block had superior post-operative analgesic effects as compared to the thoracic paravertebral block, without causing any adverse effects. Upon assessment, the ESP group pain control was better during the 6-8-hour period, but not at the 1-hour period. The authors stated that this implied that the effects of the ESP block were more persistent. They also hypothesised that, because the local anaesthetic was injected into the erector spinae fascial plane space, there was gradual penetration anteriorly thorough the intertransverse connective tissue complex into the paravertebral space. This gradual effect was observed even though a higher dose was given to the ESP group. The authors also commented on the significant lack of complications in the study, suggesting that both the ESP and paravertebral block are superior to the epidural block (Ma *et al.*, 2020).

Fandino (2019) conducted a comparative study between ESP blocks and paravertebral blocks for thoracic surgery. Based on the results, the author concluded his study by commenting on the lack of popularity gained by the paravertebral block. This was due to the technical difficulties associated with performing the block. Even in expert hands, there are still concerns regarding the occurrence of potential complications. He further went on to say that, with the discovery of the ESP block, a new path to optimize pain management in patients undergoing a wide range of procedures, has been opened.

In a more recent study, the ESP block was combined with a simplified paravertebral block for 8 cases of oncological breast surgery. After performing the classical approach for the ESP block at vertebral level T4, the needle tip was then directed towards the superior costotransverse ligament cranially. The ligament was perforated at the most superior point where it attaches onto the transverse process of T4. Once the ligament was perforated, no injectate was administered, nor was the area aspirated. The needle was then withdrawn completely. Using this combination led to more effective spread with lower doses of local anaesthetic. No complications or side effects were observed with this combination method (Sahin *et al.*, 2020).

From the few reported comparative studies, most authors acknowledged the ESP block to be superior to the paravertebral block. While the results from other studies were uniform, the authors stated that the choice of the block should be based on the operators' preference. Overall, most authors commented on the lower risk profile and ease of application for the ESP block and recommended it as an appropriate alternative.

3.10 Advantages and disadvantages

Compared to epidural blocks, the paravertebral block is safer to perform, with fewer side effects (Luyet *et al.*, 2009). Advantages of the block include reduced post-operative pain, lower post-operative analgesic requirements and reduced post-operative nausea (Loader and Ford, n.d.). However, it is also associated with hypotension, respiratory depression, urinary retention, permanent neurological injury, or even incomplete blocks (D'Ercole *et al.*, 2018). Conversely, despite being able to visualise the paravertebral space, it may prove challenging in inexperienced hands to identify and access the space, due to the crowding of bony structures (Teeter and Kumar, 2015).

3.11 Limitations

See section 2.11 b), CT paragraph for limitations.

3.12 Conclusion

Based on the anatomy, the paravertebral space is a continuous potential space that communicates with the intercostal space laterally, and the epidural space medially. Paravertebral blocks produce unilateral multi-dermatomal anaesthesia and analgesia for thoracic and abdominal procedures. In experienced hands, the block can be relatively easy to perform. Additionally, ultrasound guidance increases the safety and reliability of the block. However, more recent paraspinal blocks may rival the paravertebral block, as they can be performed distant from neuraxial structures and have fewer associated complications.

Results from this study revealed that the average depth to performing the block in age group 1 at vertebral levels T5 and T8 was 0.49cm (standard deviation of 0.06) and 1.34cm (standard deviation of 0.28). In age group 2, the average depth was 0.50cm with a standard deviation of 0.05 at vertebral level T5 and 1.67cm with a standard deviation of 0.47 at vertebral level T8. While in group 3 the average depth was 0.50cm with a standard deviation of 0.04 at vertebral level T5 and 1.83cm with a standard deviation of 0.43 at vertebral level T8.

Chapter 4 – Epidural block

Epidural blocks are an alternative to general anaesthesia for providing effective thoracic and abdominal analgesia (Nair *et al.*, 2019). Together with paravertebral blocks, they have been considered the golden standard for post-thoracotomy pain relief (Elsayed *et al.*, 2012; Teeter and Kumar, 2015; Abdl Fatah and Abdl Aleem, 2016; Singh *et al.*, 2017). The epidural block procedure entails injecting anaesthetic into the epidural space at various vertebral levels, targeting the spinal cord and its nerve roots, to attain successful anaesthesia and analgesia.

This can be achieved using a single-shot injection, or by inserting an epidural catheter for continuous anaesthetic spread. Previously, anaesthetists mainly relied on anatomical landmarks or the loss of resistance technique to identify the epidural space. Even though anatomical landmarks are useful, they are surrogate markers, making it difficult to palpate in obese patients. Furthermore, it does not take into account anatomical variations or abnormalities (Karmakar *et al.*, 2009). However, with the advancements in technology, ultrasound guidance has bridged the gap in the downfalls of the previously employed techniques. Pre-procedure scanning may help with appropriate localization of the block level, especially in infants and younger children. Epidural analgesia is effective and has been reported to be part of a multimodal approach for acute and chronic pain management in children (Patel, 2006).

One of the earliest reported cases was in 1983 by Meigner and co-workers. They demonstrated the safety and efficacy of the thoracic epidural technique in eight children. A few years later, Tozbikian (1992) performed this technique on a larger sample size consisting of 30 neonates, infants and children. In 1993, Tobias and co-workers (1993) conducted a review of thoracic epidural procedures with the use of catheter placement for pain management in 60 paediatric patients. The patients' ages ranged from 3 months to 18 years. In all cases, Tobias reported no difficulty in placing the catheter and achieving full analgesic spread between 48 to 72 hours post-surgery. With the majority of the cases a success, he expressed his concern as to why this technique was not used more extensively in children (Tobias *et al.*, 1993). Bosenberg,

(1998) reported on his experience of epidural analgesia in 240 infants, of which 29 cases were thoracic epidurals and 211 were lumbar epidurals. He stated that loss of resistance occurred at a depth of 8 to 12 millimetres. Furthermore, these measurements did not correlate with the patient's weight. Keech (2015) suggested that the average depth from the skin to the epidural space linearly increases with age in the lumbar region, ranging from 10 to 30 millimetres and that the expected distance in children aged 6 months to 10 years is approximately 1 mm/body weight in kg (Keech, 2015).

In 1980, Cork and colleagues were the first to describe the possibility of direct visualisation of the epidural space. Although ultrasound guidance was in its preliminary stages, it wasn't until later that the technique was properly introduced. Rapp and co-workers (2005) carried out an investigation to determine whether ultrasound imaging can be used to detect neuraxial structures before and during catheter placement into the epidural space in paediatric patients. Twenty-five patients underwent catheter insertions between vertebral levels T6-T7 interspace to the L4-L5 interspace. They reported the average depth to the epidural space as between 10 – 28 millimetres. They further concluded that ultrasound is a valuable tool to use when dealing with paediatric patients, as relevant anatomical structures and their corresponding locations can be identified.

In 1993, Bosenberg reported that ultrasound guidance had paved a way for new medical techniques: pre-procedure scanning that may be beneficial, especially in smaller children, to localize the block level; assess the ligamentum flavum depth and estimate the distance to the epidural space (Sawardekar *et al.*, 2013). Ultrasound guidance is particularly useful in infants and small children, especially since incomplete vertebrae ossification facilitates the penetration of ultrasound waves into the vertebral column, making spinal structures easier to identify (Kil, 2018). Additionally, real-time visualization is not affected by changes in patient positioning (Elsharkawy *et al.*, 2017). However, even with ultrasound guidance, the entry route is heavily shielded by bone, still making it difficult to envisage, even with real-time visualization (McClymont and Celnick, 2018).

In paediatric patients, epidural analgesia can be associated with neurological injuries and permanent long-term effects. Thus, a thorough understanding of the anatomy of the paediatric vertebral column may provide valuable information that could be used to avoid incorrect needle placement and spinal injuries (Wani *et al.*, 2018). Bhattay, (2018) summarized the anatomical considerations when performing epidural blocks in children in comparison to adults in a South African context. Due to the short skin- to-epidural space distance, the author suggested using the formula: 1 mm/kg to calculate the epidural depth in children aged 6 months to 10 years. However, the epidural space can be limited in infants and children, since changes in the body habitus with ageing are diverse, making it difficult to truly predict the skin-to-epidural space distance (Kil, 2018).

The intercrystal line (or supracrystal plane), which is a horizontal line drawn across the superior aspect of the highest points of the iliac crests, bisects the 5th lumbar vertebra in adults, whereas it bisects the 3rd/4th lumbar vertebral in children (Bhattay, 2018). In younger children, the ligamentum flavum is softer and less fibrous, therefore, limiting the tactile feedback of loss of resistance when inserting the needle into the epidural space. A narrow epidural space in children may hinder dural puncture more and will most likely contribute to difficulties in catheter threading. The conus medullaris is more caudal in children, at vertebral level L3, as opposed to adults – vertebral level L1. Moreover, the vertebrae are mainly cartilaginous at birth due to incomplete ossification. The lamina between vertebral levels L1 to L4 progressively fuse during the first year, while the 5th lumbar lamina only ossifies during the 5th year of age (Bhattay, 2018).

Additionally, anatomical differences exist between the regions of the vertebral column. In the thoracic area, the vertebral bodies are less angulated, requiring a perpendicular approach to the skin (Bhattay, 2018). In children, the fascia and sheaths are loosely attached to the surrounding structures. Furthermore, up to the age of 6 to 8 years, the epidural fat has a more fluid consistency (Kil, 2018). This allows for easier spread of local anaesthetic within the space. Regarding the pharmacokinetics consideration in neonates/infants versus adults the local anaesthetic in neonates/infants has a lower clearance due to the immature/developing liver. Based on pharmacodynamic considerations, neonates/infants have thinner nerve fibres with incomplete myelin

sheaths and closer nodes of Ranvier. These contribute to the lower concentrations needed to achieve the same effect as in adults (Bhettay, 2018).

The epidural space can be accessed via various entry points, namely the interlaminar space using the loss-of-resistance- or hanging drop method, transforaminal, trans-sacral, paravertebral, or under direct visualisation (Richardson and Groen, 2005). In paediatrics, the epidural block has been indicated for rib fractures. However, paediatric ribs are less mineralised and tend to be more pliable. As a result, the block offers less protection to the underlying lungs making them prone to further injuries such as pulmonary contusion, traumatic wet lung and haemothorax. Alternatively, this block is indicative for surgical procedures below the waist or for patients who prefer to avoid general anaesthesia for various reasons (Keech, 2015; McClymont and Celnick, 2018).

Relative and absolute contraindication must be considered prior to performing any block. As it stands, relative and absolute contraindications are the same for both paediatric and adult patients (Tobias *et al.*, 1993; Patel, 2006). Relative contraindications include intrinsic coagulopathy or the use of anticoagulants, abnormalities of the vertebral column or adjacent soft tissue, neurologic diseases, sepsis, elevated intracranial pressure and the administering of large quantities of anaesthetic prior to the procedure. Absolute contraindications include parent refusal, sepsis or bacteraemia, cardiac disease with fixed output state, infection at the needle insertion area, haemodynamic instability and allergy to local anaesthetics (Patel, 2006; Keech, 2015; Bhettay, 2018).

4.1 Anatomy

The epidural space lies within the vertebral canal and is defined as that part of the vertebral canal that is not occupied by the dura and its contents. It extends from the foramen magnum at the base of the skull to the sacral hiatus (Ellis, 2009). The space is bordered superiorly by the continuation of the spinal and periosteal layers of the dura mater, inferiorly by the posterior sacrococcygeal ligament, anteriorly by the posterior longitudinal ligament, vertebral bodies and the intervertebral discs, posteriorly by the

ligamentum flavum, vertebral laminae and the zygapophyseal joint capsule and laterally, by the pedicles and intervertebral foramen (Figure 21) (Richardson and Groen, 2005).

The space can further be divided into anterior and posterior compartments. The space is more extensive and easily distensible posteriorly, while anteriorly, the dura mater adheres close the periosteum of the vertebral bodies. The anterior epidural space can be found between the posterior longitudinal ligament and the anterior part of the dura mater, while the posterior epidural space can be found between the posterior part of the dura mater and the ligamentum flavum (Figure 21) (Tardieu *et al.*, 2016).

The epidural space is divided into regions according to the curvatures of the vertebral column. The thoracic epidural space extends from the inferior border of the 7th cervical vertebra to the superior border of the 1st lumbar vertebra. The lumbar epidural space extends the inferior border of the 1st lumbar vertebra to the superior border of the 1st sacral vertebra. The sacral epidural space lies between the superior border of the 1st sacral vertebra and the posterior sacrococcygeal ligament.

The content of the epidural space is contained in a series of circumferentially discontinuous compartments separated by zones where the periosteal layer of the dura mater contacts the internal wall of the vertebral canal. The contents include fat (more in the lumbar region), the dural sac, lymphatics, roots of the spinal nerves, loose areolar connective tissue and the internal venous plexus (anterior and posterior), as well as epidural arteries (Fyनेface-Ogan, 2012).

The epidural fat is loose and allows for easy diffusion of local anaesthetic through the epidural space. The lymphatics can be found in a concentrated manner around the dural roots. The spinal nerves can be found passing through the intervertebral foramen into the paravertebral space. As the nerves travel, they carry extradural fat pockets that further assist the spread of local anaesthetic and act as reservoirs (Ellis, 2009; Fyनेface-Ogan, 2012). The anterior internal vertebral venous plexus can be found in the anterior epidural space. These are valveless veins, which connect to the basilar-vertebral venous system in the skull, as well as the azygos venous system in the thorax

(McLeod and Cumming, 2004). Epidural arteries can be found in the lateral regions of the space, and thus are not in danger when advancing an epidural needle into the space (Fyneface-Ogan, 2012).

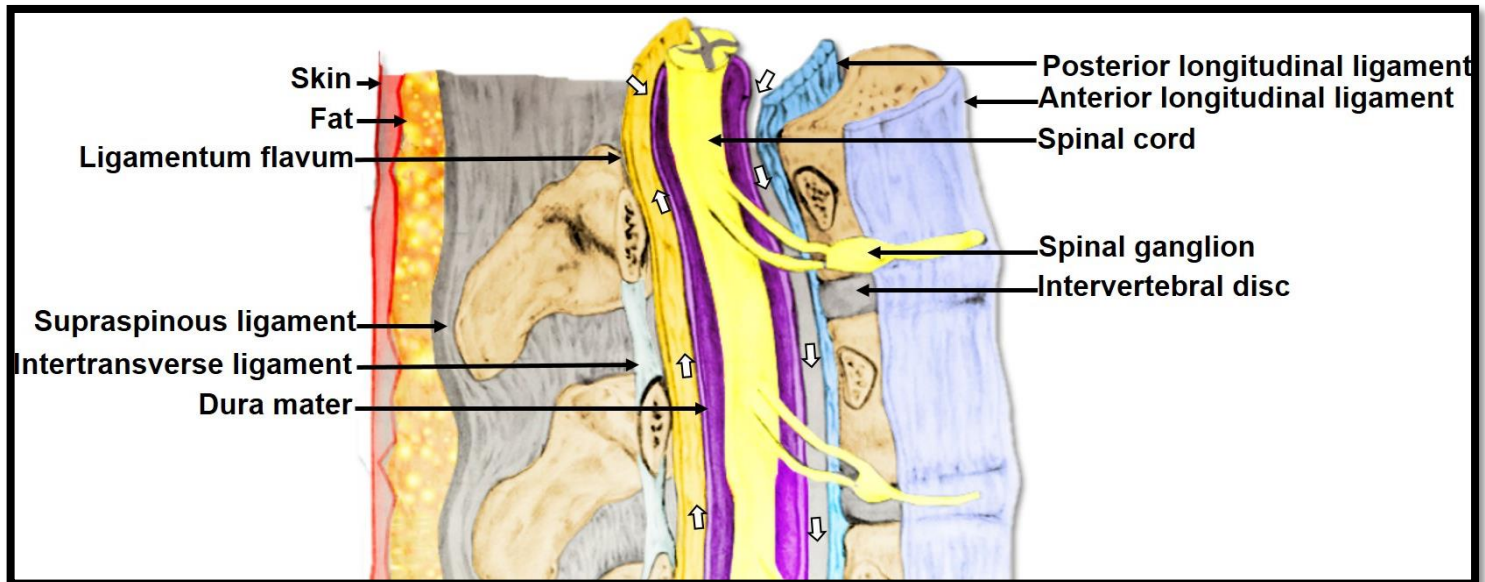


Figure 21: A right lateral view of the epidural space, with the right side of the vertebral arch removed. Anterior, posterior parts and its related borders. Key: white arrow represents the epidural space.

4.2 Ultrasound anatomy

There are two main longitudinal approaches for epidural blocks, namely the midline approach and the paramedian approach. The patient should be placed in a lateral decubitus position, keeping aseptic precautions in mind, with his/her hips and knees flexed and vertebral column arched anteriorly to open the interlaminar space (Bosenberg, 1998). The anaesthesiologist should be on the side of the patient's back, facing the ultrasound screen, both in a straight line.

Depending on the area of interest, the probe should be placed on the skin overlying the adjacent spinous processes. The size and incomplete ossification of the vertebrae in paediatric patients allow for easier visualisation and localisation of the depth of the

epidural space (Rapp *et al.*, 2005; Marcelino *et al.*, 2019). In paediatric patients, the spinous processes of the thoracic vertebra are almost horizontal and the ligamentum flavum is narrower, which favours a midline approach to the epidural space (Keech, 2015; Patel *et al.*, 2019).

a) **Midline approach**

The midline approach involves inserting the needle between the spinous processes of adjacent vertebrae through the supraspinous and interspinous ligaments, as well as the ligamentum flavum, into the epidural space. The midline approach is most commonly used as the ligamentum flavum is widest in the midline and is easily identifiable (Leeda *et al.*, 2005; McClymont and Celnick, 2018).

b) **Paramedian approach**

The paramedian approach, which offers a larger 'ultrasound window', is performed in the interlaminar space (Tsui and Suresh, 2010). In this approach, the needle is inserted marginally lateral to the spinous process, avoiding the supraspinous and interspinous ligaments before reaching the epidural space (Boon *et al.*, 2003; Keech, 2015; Singh *et al.*, 2017) (Figure 21). Thus, there is minimal need for medial or lateral needle angulation (Le-Wendling *et al.*, 2014). The needle will pierce the skin, subcutaneous fat, fascia, muscles (depending on the vertebral level, it will pierce the trapezius-, rhomboid- and erector spinae muscles) and the ligamentum flavum.

This procedure is initiated by identifying the spinous process of the desired vertebra by palpating and outlining the superior and inferior borders of the spinous process. The interspinous space should lie just below the inferior border of the upper spinous process. This can be further confirmed using ultrasound guidance. The needle should be inserted perpendicular to the skin, using the in-plane approach and directed towards the lamina. It should then be advanced in a cephalad orientation, towards the lamina. Once the needle hits the lamina, thereby confirming the correct position the needle tip

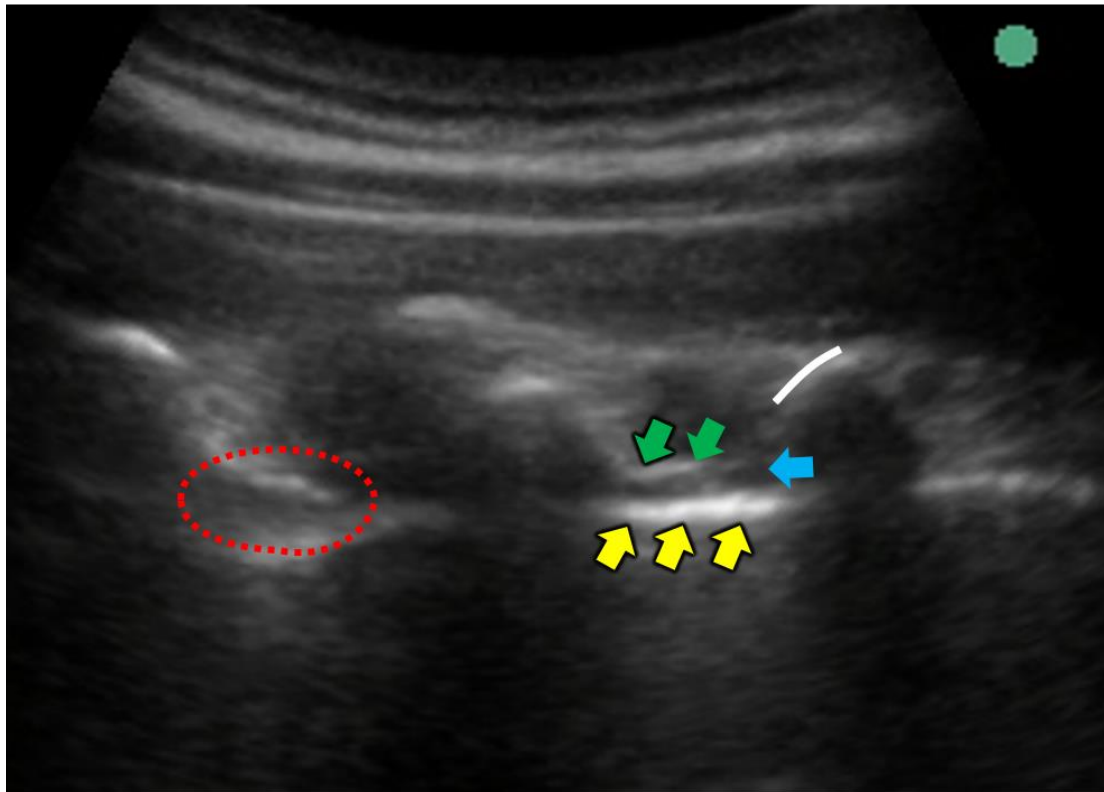
should then be “walked” superomedially off the lamina and through the interlaminar space (McClymont and Celnick, 2018).

The most evident structure on the ultrasound screen is the lamina of the vertebral arch which appears as a hyperechoic structure. In the thoracic area, the lamina appears as a flat, plate-like structure, unlike the sloping saw-tooth like structure in the lumbar area. Since bone impedes ultrasound sound wave penetration, there is an acoustic shadow anterior to each lamina. The interlaminar space (gap) can be found between the adjoining laminae and is the “acoustic window” through which the neuraxial structures are visualized (Figure 22).

The ligamentum flavum appears as a hyperechoic band, anteriorly across the adjacent lamina. Deep or anterior to that, the posterior part of the dura mater can be seen as another hyperechoic line (Figure 22). The posterior epidural space can be seen as a hypoechoic space between the ligamentum flavum and the posterior part of the dura (posterior complex). The intrathecal space, which is filled with cerebral spinal fluid, can be seen as an anechoic space anterior to the posterior part of the dura. Depending on the vertebral level, the cauda equina, also found in the intrathecal space, appears as multiple horizontal, hyperechoic shadows. The anterior epidural space can be seen as a hypoechoic area between the hyperechoic anterior part of the dura mater and the posterior longitudinal ligament (anterior complex) (Karmakar *et al.*, 2009).

Linear probes, which are preferred for this approach, are recommended for the visualization of the neuraxial anatomy in infants (up to three months, after which the visualization decreases in an age-dependent manner) and young children (Bhettay, 2018). The practitioner should always aspirate to confirm needle position and avoid intravascular injections. Saline solution should slowly be introduced to enlarge the epidural space before the anaesthetic is injected.

Superficial/posterior



Deep/anterior

Figure 22: Ultrasound image displaying the paramedian plane of the thoracic epidural block. Key: green arrows – ligamentum flavum, yellow arrows – dura mater, blue arrow – epidural space, red dotted circle – posterior complex, white solid line – lamina.

4.3 Aim

The aim of this chapter was to investigate the anatomy of the epidural block using ultrasound and CT scans.

4.4 Research objectives

- I. To evaluate the anatomy of the epidural space based on previously published literature together with observations made from retrospectively examining existing ultrasound and CT scans by determining the average: depth from the skin to the epidural space; depth from the skin to the epidural space, at an incline, in different paediatric age groups; distance between the adjacent spinous processes in different paediatric age groups.
- II. To determine the relationship between the depth to the epidural space and the demographic features of the sample by using simple and multiple regression analysis.

4.5 Materials and Methods

This study was approved by the PhD and Research Ethics Committee (94/2019), University of Pretoria, South Africa. Permission was also obtained from the Head of the Department of Radiology and CEO of Steve Biko Academic Hospital, to retrospectively source CT scans from patient archives. All records obtained were kept confidential as to keep patient identify anonymous.

a) ***Ultrasound component***

Using the ultrasound scans obtained in 2.3.a, the format of the scans was converted and then uploaded onto RadiAnt, a Digital Imaging and Communication in Medicine (DICOM) viewer, from which various measurements were taken. These measurements include: A – the distance from the skin to the anterior border of the ligamentum flavum; B – the distance from the skin to the anterior border of the ligamentum flavum at an incline; C – the distance from the inferior border of the spinous process (superiorly) to the superior border of the subjacent spinous process (inferiorly) (Figure 23). The reason for repeating measurement A, at an incline (B), is to accommodate all circumstances. In other words, the straight measurement from the skin to ligament flavum applies to ultrasound guidance as the needle or catheter can be guided, when

in reality, the angle at the thoracic region is more acute and needs to be considered, should the block be performed using the 'blind' technique.

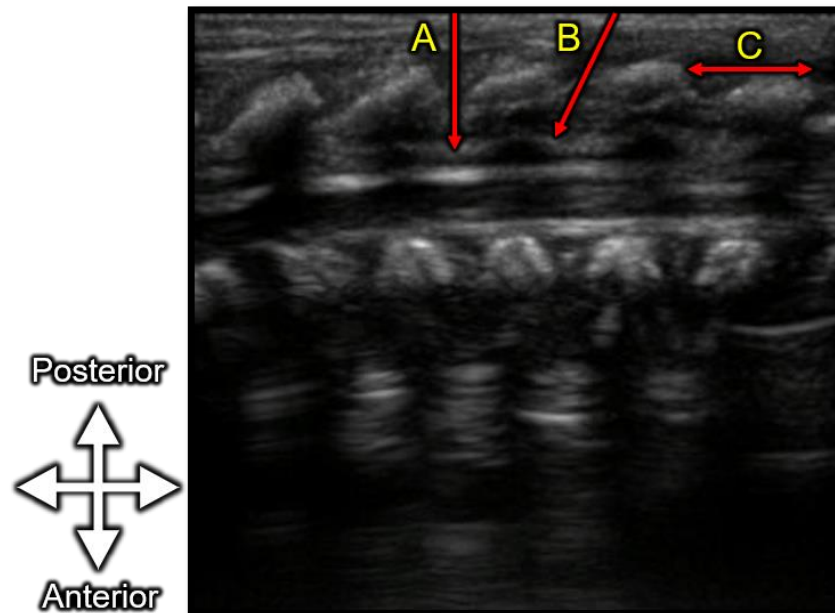


Figure 23: A median sagittal ultrasound image of the vertebral column showing the various measurements taken. Measurements taken: A – the distance from the skin to the anterior border of the ligamentum flavum; B – the distance from the skin to the anterior border of the ligamentum flavum at an incline; C – the distance from the inferior borders of the adjacent spinous process.

b) ***Retrospective CT component***

One hundred and fifty CT images were retrospectively selected from the database of radiographic images at the Department of Radiology, Steve Biko Academic Hospital. Demographic information such as age and sex were recorded. Scans were grouped according to age groups: neonates (0 – 2 months), infants (>2 months – 2 years) and children (> 2 – 12 years). Scans with abnormal vertebral column development such as kyphosis and scoliosis, visceromegaly or space-occupying lesions, as diagnosed by the consulting radiologist, were excluded from this study. RadiAnt, DICOM viewer was then used to analyse the CT scans. Using the on-screen measuring function, calibrated for each image, various measurements were taken at vertebral levels T5 and T8 from a parasagittal section. Measurements included: A – the distance from the skin to the

anterior border of the ligamentum flavum; B – the distance from the skin to the anterior border of the ligamentum flavum at an incline; C – the distance from the inferior border of the upper spinous process of the interspinous space and the superior border of the lower spinous process (Figure 24).

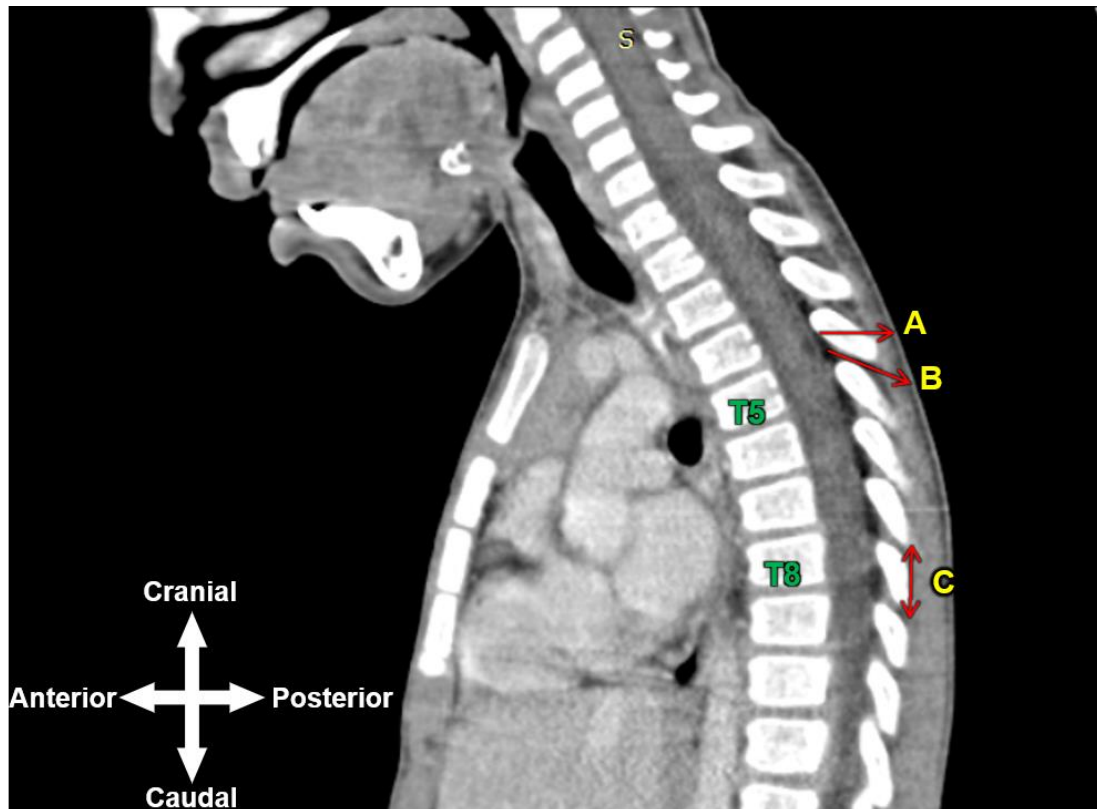


Figure 24: A CT scan of a sagittal section through the vertebral column. From this view, the 5th and 8th vertebral levels can be identified. Measurements taken: A – the distance from the skin to the anterior border of the ligamentum flavum; B – the distance from the skin to the anterior border of the ligamentum flavum at an incline; C – the distance from the inferior border of the upper spinous process of the interspinous space and the superior border of the lower spinous process.

4.6 Statistical analysis

See section 2.6.

4.7 Results

Upon intra- and inter-observer analysis, a student t-test was performed to compare the two sets of data in order to ensure that the measurements obtained were valid. The statistical results revealed a p-value greater than 0.05 for both the intra- and inter-reliability check. Therefore, there was no statistical significance between the data sets, meaning that the initially obtained data measurements were considered to be correct.

Additionally, the anatomy and sonographic anatomy corroborated with the previously described anatomy.

a) *Ultrasound component*

Normal descriptive statistics were applied to the data to obtain means and standard deviation for each measurement. Table 28 below summarizes the results from the ultrasound component.

Table 28. Descriptive statistics summary of the epidural measurements taken from the neonate ultrasound scans.

Measurement	n	Minimum (cm)	Maximum (cm)	Mean (cm)	SD
T5SkintoLig	11	0.85	1.22	1.03	0.10
T5SkintoLig(inc)	11	0.95	1.23	1.08	0.11
T5SPtoSP	11	0.87	0.75	0.75	0.82
T8SkintoLig	11	0.97	0.86	0.86	0.11
T8SkintoLig(inc)	11	0.85	1.23	0.98	0.11
T8SPtoSP	11	0.78	1.40	0.97	0.19

KEY: **n** – sample size, **SD** – standard deviation, **T5** – vertebral level T5, **T8** – vertebral level T8, **SkintoLig** – Skin to Ligamentum flavum, **SkintoLig(inc)** – Skin to Ligamentum flavum (incline), **SPtoSP** - Spinous process to Spinous process.

From the total sample size, 6 scans belonged to females, while the remaining 5 scans belonged to males. Using regression analysis, each measurement (the dependent variable) was further tested for correlation against fixed factors such as sex, age, height and weight (the independent variables). Due to the nature of the data, the adjusted R²-value was used instead of the R²-value to predict the correlation (see 2.7b). From the results, no correlation was seen between any of the measurements for both sex and height, while a weak correlation (adjusted R²-value < 0.5) was found between vertebral levels T5 and T8 skin to ligamentum flavum(incline), and weight.

Likewise, a multivariant regression analysis was performed to assess the overall effect of the independent variables on the dependent variables as a whole. Subsequently, the multivariant regression models for T5 skin to ligamentum flavum-, T5 skin to ligamentum flavum(incline)-, T8 skin to ligamentum flavum -and T8 skin to ligamentum flavum(incline) measurements were then used to create a standard equation that can be utilised when performing the epidural block in a preterm, neonatal paediatric sample (Table 29).

Table 29. Multivariant regression analysis for determining the depth to the epidural space in a preterm neonatal sample.

Level	Parameter	Coefficient	SE	t	p-value	95% confidence interval	
						Lower	Upper
T5 SkintoL ig	Sex	0.081	0.074	1.094	0.310	-0.093	0.255
	Weight (kg)	0.0004	0.001	0.693	0.511	-0.001	0.002
	Height (mm)	0.031	0.056	0.551	0.599	-0.101	0.162
	-constant	0.798	0.310	2.283	0.560	-0.025	1.444
T5 SkintoL ig(inc)	Sex	0.087	0.053	1.638	0.145	-0.038	0.211
	Weight (kg)	0.098	0.040	0.682	2.451	0.044	0.003
	Height (mm)	1.434	0.001	0.028	0.978	0.978	-0.001
	-constant	0.870	0.223	3.900	0.006	0.003	0.193
T8 SkintoL ig	Sex	0.155	0.060	2.600	0.035	0.014	0.295
	Weight (kg)	0.034	0.045	0.744	0.481	-0.001	0.001
	Height (mm)	0.0001	0.001	0.181	0.861	-0.073	0.140
	-constant	0.672	0.251	2.677	0.032	1.264	0.078
T8 SkintoL ig(inc)	Sex	0.017	0.072	0.239	0.818	-0.152	0.186
	Weight (kg)	0.088	0.054	1.628	0.147	-0.039	0.216
	Height (mm)	9.325	0.001	0.137	0.895	-0.001	0.001
	-constant	0.777	0.302	2.570	0.037	0.062	1.491

Key: **SE** – standard error, **T5** – vertebral level T5, **T8** – vertebra level T8, **SkintoLig** – Skin to Ligamentum flavum, **SkintoLig(inc)** – Skin to Ligamentum flavum at an incline.

Sex was determined with numeric values. Males were assigned the number 0, while females were assigned the number 1 that could be inserted into the equations. Although none of the variables were statistically significant ($p > 0.05$), formulae were still created for this component. These formulae included the standard error of the

estimate to indicate the accuracy of the predictions. Therefore, the formulae were as follows:

- T5 skin to ligamentum flavum:
 - Depth in cm = $0.789 + 0.081(\text{sex}) + 0.004 (\text{weight in kg}) + 0.031 (\text{height in mm}) \pm \text{SEE} (0.107)$
- T5 skin to ligamentum flavum (incline):
 - Depth in cm = $0.870 + 0.087(\text{sex}) + 0.098 (\text{weight in kg}) + 1.434 (\text{height in mm}) \pm \text{SEE} (0.077)$
- T8 skin to ligamentum flavum:
 - Depth in cm = $0.789 + 0.081(\text{sex}) + 0.004 (\text{weight in kg}) + 0.031 (\text{height in mm}) \pm \text{SEE} (0.086)$
- T8 skin to ligamentum flavum (incline):
 - Depth in cm = $0.777 + 0.017(\text{sex}) + 0.088 (\text{weight in kg}) + 9.325 (\text{height in mm}) \pm \text{SEE} (0.104)$

The adjusted R²-values for the formulae were as follows for T5 skin to ligament and skin to ligament (incline), -0.05 and 0.48. While the adjusted R²-values for the formulae at T8 skin to ligament and skin to ligament (incline) was 0.56 and 0.39. The approximate distance from the skin to the epidural space at vertebral level T5 was 1.03 cm and 1.08 cm (at an incline), with a standard deviation of 0.10 (0.11 at an incline). The distance at vertebral level T8 was 0.86 cm and 0.98 cm (at an incline), with a standard deviation of 0.11.

b) **CT component**

Descriptive statistics were also applied to the CT data to obtain means and standard deviations. Tables 30 to 32 below summarise the results for the different age groups.

Table 30. Descriptive statistics summary of the epidural measurements taken from the neonatal CT scans (group 1, 22 females and 22 males).

Measurement	n	Minimum (cm)	Maximum (cm)	Mean (cm)	SD
T5SkintoLig	44	0.74	2.90	1.42	0.47
T5SkintoLig(inc)	44	0.94	2.91	1.57	0.43
T5SPtoSP	44	0.50	1.28	0.77	0.18
T8SkintoLig	44	0.69	2.12	1.25	0.41
T8SkintoLig(inc)	44	0.76	2.98	1.41	0.47
T8SPtoSP	44	0.51	1.35	0.79	0.17

KEY: **n** – sample size, **SD** – standard deviation, **T5** – vertebral level T5, **T8** – vertebral level T8, **SkintoLig** – Skin to Ligamentum flavum, **SkintoLig(inc)** – Skin to Ligamentum flavum (incline), **SPtoSP** – Spinous process to Spinous process.

Table 31. Descriptive statistics summary of the epidural measurements taken from the infant CT scans (group 2, 27 females and 21 males).

Measurement	n	Minimum (cm)	Maximum (cm)	Mean (cm)	SD
T5SkintoLig	48	1.00	3.30	1.76	0.43
T5SkintoLig(inc)	48	1.02	4.34	1.96	0.55
T5SPtoSP	48	0.67	2.01	1.15	0.29
T8SkintoLig	48	0.96	2.82	1.53	0.39
T8SkintoLig(inc)	48	1.09	3.36	1.73	0.47
T8SPtoSP	48	0.65	1.89	1.14	0.27

KEY: **n** – sample size, **SD** – standard deviation, **T5** – vertebral level T5, **T8** – vertebral level T8, **SkintoLig** – Skin to Ligamentum flavum, **SkintoLig(inc)** – Skin to Ligamentum flavum (incline), **SPtoSP** – Spinous process to Spinous process.

Table 32. Descriptive statistics summary of the epidural measurements taken from the children CT scans (group 3, 32 females and 24 males).

Measurement	n	Minimum (cm)	Maximum (cm)	Mean (cm)	SD
T5SkintoLig	56	1.17	3.75	2.22	0.51
T5SkintoLig(inc)	56	1.32	4.16	2.56	0.59
T5SPtoSP	56	0.70	2.29	1.52	0.27
T8SkintoLig	56	0.98	3.16	1.99	0.44
T8SkintoLig(inc)	56	1.06	3.86	2.45	0.57
T8SPtoSP	56	0.82	2.15	1.48	0.28

KEY: **n** – sample size, **SD** – standard deviation, **T5** – vertebral level T5, **T8** – vertebral level T8, **SkintoLig** – Skin to Ligamentum flavum, **SkintoLig(inc)** – Skin to Ligamentum flavum (incline), **SPtoSP** – Spinous process to Spinous process.

Subsequently, comparative analysis was performed between groups to determine if there was a significant difference between individual measurements and groups before pooling the data. Results revealed a significant difference (p -value > 0.05) between;

most measurements. Due to the statistical difference between groups, the data was not pooled, and further statistical testing was performed on the group individually.

Regression analysis was then performed to evaluate the correlation between the measurement (the dependent variable) and fixed factors such as sex and age (the independent variable) for each group. In group 1, a weak correlation was found between the measurement and sex or age (adjusted R^2 -value ≤ 0.1). In group 2, no correlation was found between any of the measurements and sex. While a moderate correlation, with an adjusted R^2 -value < 0.3 was found between T5 spinous process to spinous process. In group 3, a moderate to strong correlation was found between; T5 skin to ligamentum flavum) (adjusted R^2 -value = 0.38), T5 skin to ligamentum flavum(incline) (adjusted R^2 -value = 0.38), T8 skin to ligamentum flavum) (adjusted R^2 -value = 0.46), T8 skin to ligamentum flavum(incline)) (adjusted R^2 -value = 0.39), T8 spinous process to spinous process and age) (adjusted R^2 -value = 0.30). Measurements with a strong correlation were then further plotted on a scatter plot to display the relationship of the correlation (Figure 25).

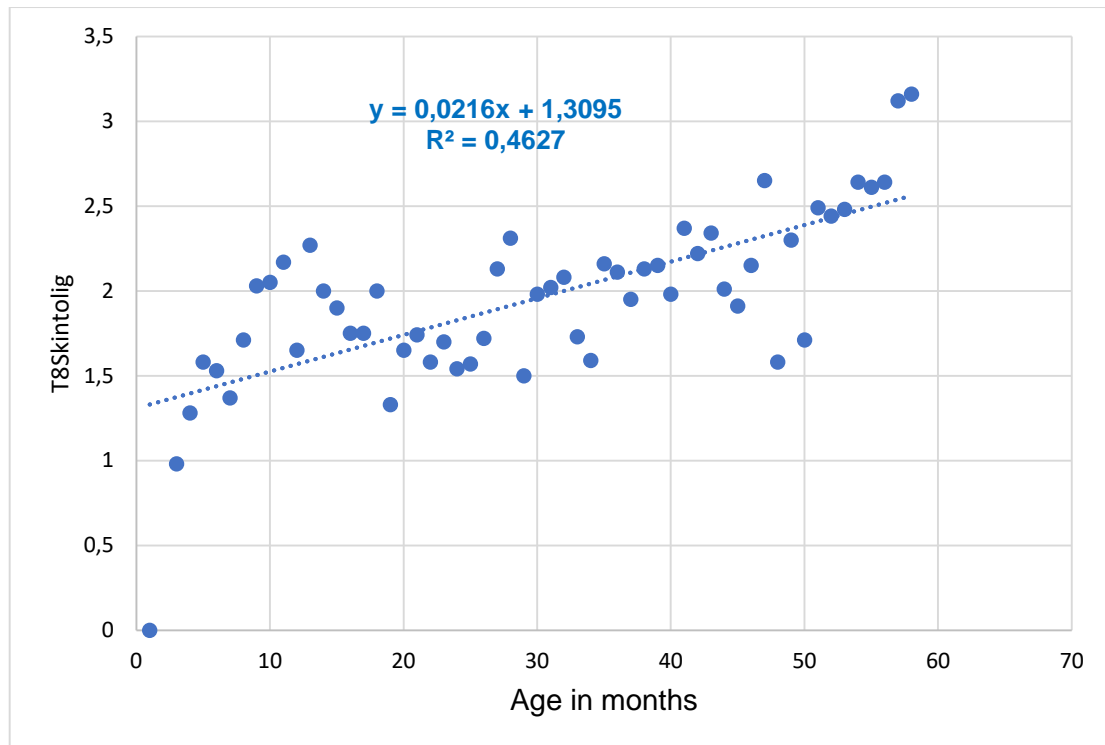


Figure 25: Scatter plot displaying the correlation between T8Skintolig in cm to age in months.

As shown in figure 25, the adjusted R^2 -value indicate how much of the attribution is caused by age. For T8 skin to ligament flavum, 46% of the variation can be explained by age or is caused by age.

Also, from the CT data, multivariate regression analysis was performed to create a standard equation that can be utilised when performing the epidural block in different paediatric groups (Table 33 to 35). For the analysis, factors such as sex and age were used, as these were the only demographic information available from the CT scans. The equation/formula indicates the depth at which the block needle can be inserted at different vertebral levels, should the block be performed using the 'blind' technique in each age group.

Table 33. Multivariant regression analysis for determining the depth to the epidural space (group 1).

Level	Parameter	Coefficient	SE	t	p-value	95% confidence interval	
						Lower	Upper
T5 SkintoLig	Sex	0.022	0.154	0.143	0.886	-0.289	0.333
	Age	-0.019	0.184	-0.105	0.917	-0.391	0.352
	-cons	1.432	0.225	6.347	1.390	0.976	1.888
T5 SkintoLig (inc)	Sex	0.026	0.142	0.186	0.854	-0.259	0.312
	Age	-0.065	0.169	-0.383	0.703	-0.406	0.277
	-cons	1.632	0.207	7.873	9.920	1.213	2.051
T8 SkintoLig	Sex	0.046	0.133	0.347	0.729	-0.223	0.315
	Age	-0.053	0.159	-0.335	0.739	-0.374	0.268
	-cons	1.289	0.195	6.608	5.900	0.895	1.683
T8SkintoLig (inc)	Sex	0.148	0.151	0.977	0.334	-0.158	0.453
	Age	-0.177	0.180	-0.980	0.333	-0.541	0.187
	-cons	1.552	0.221	7.015	1.570	1.105	1.999

Key: **SE** – standard error, **T5** – vertebral level T5, **T8** – vertebra level T8, **SkintoLig** – Skin to Ligamentum flavum, **SkintoLig(inc)** – Skin to Ligamentum flavum at an incline.

Sex was determined with numeric values. Males were assigned the number 0, while females were assigned the number 1 that could be inserted into the equations. However, since sex was not statistically significant, it was not included in the formulas. As indicated in Table 33, none of the variables were statistically significant ($p > 0.05$). All formulae included the standard error of the estimate to indicate the accuracy of the predictions. The formulae are as follows:

- T5 skin to ligamentum flavum:
 - Depth in cm = $1.432 - 0.019(\text{age in months}) + 0.022(\text{sex}) \pm$ standard error of estimate (0.483) (adjusted R^2 -value = -0.048),
- T5 skin to ligamentum flavum at an incline:

- Depth in cm = $1.632 - 0.065(\text{age in months}) + 0.026(\text{sex})$ +/- standard error of estimate (0.444) (adjusted R²-value = -0.045),
- T8 skin to ligamentum flavum:
 - Depth in cm = $1.289 - 0.053(\text{age in months}) + 0.046(\text{sex})$ +/- standard error of estimate (0.418) (adjusted R²-value = -0.044),
- T8 skin to ligamentum flavum at an incline:
 - Depth in cm = $1.552 - 0.177(\text{age in months}) + 0.148(\text{sex})$ +/- standard error of estimate (0.474) (adjusted R²-value = -0.013),

The mean distance between the adjacent spinous processes for the different age groups should be taken into account when inserting the block needle. Results from this study showed the mean distance between the adjacent spinous processes at vertebral levels T5 and T8 is 0.77cm and 0.79cm (standard deviation of 0.18 and 0.17, respectively) for age group 1.

A multivariate regression analysis was also performed for age group 2, to create a standard equation that can be utilised when performing the epidural block (Table 34).

Table 34. Multivariant regression analysis for determining the depth to the epidural space (group 2).

Level	Parameter	Coefficient	SE	t	p-value	95% confidence interval	
						Lower	Upper
T5 SkintoLig	Sex	-0.199	0.115	-1.727	0.091	-0.431	0.033
	Age	0.019	0.007	2.743	0.009	0.005	0.034
	-cons	1.578	0.137	11.550	4.710	1.303	1.853
T5 SkintoLig (inc)	Sex	-0.240	0.152	-1.576	0.122	-0.547	0.067
	Age	0.021	0.009	2.253	0.029	0.002	0.040
	-cons	1.776	0.180	9.833	8.770	1.412	2.139
T8 SkintoLig	Sex	-0.158	0.104	-1.517	0.136	-0.367	0.052
	Age	0.019	0.006	2.928	0.005	0.006	0.032
	-cons	1.341	0.123	10.878	3.480	1.093	1.589
T8SkintoLig (inc)	Sex	-0.190	0.126	-1.513	0.137	-0.444	0.063
	Age	0.021	0.008	2.741	0.009	0.005	0.037
	-cons	1.521	0.149	10.204	2.740	1.221	1.822

Key: **SE** – standard error, **T5** – vertebral level T5, **T8** – vertebra level T8, **SkintoLig** – Skin to Ligamentum flavum, **SkintoLig(inc)** – Skin to Ligamentum flavum at an incline.

Sex was determined with numeric values. Males were assigned the number 0, while females were assigned the number 1 that could be inserted into the equations. Again, none of the variables were statistically significant ($p > 0.05$). The formulae are as follows:

- T5 skin to ligamentum flavum:
 - Depth in cm = $1.578 + 0.019(\text{age in months}) - 0.019(\text{sex}) \pm$ standard error of estimate (0.396) (adjusted R^2 -value = 0.153),
- T5 skin to ligamentum flavum at an incline:
 - Depth in cm = $1.776 + 0.021(\text{age in months}) - 0.240(\text{sex}) \pm$ standard error of estimate (0.523) (adjusted R^2 -value = 0.105),
- T8 skin to ligamentum flavum:

- Depth in cm = 1.341 + 0.019(age in months) - 0.158(sex) +/- standard error of estimate (0.357) (adjusted R²-value = 0.158),
- T8 skin to ligamentum flavum at an incline:
 - Depth in cm = 1.521 + 0.021(age in months) - 0.190(sex) +/- standard error of estimate (0.432) (adjusted R²-value = 0.142),

Results from this study showed the mean distance between the adjacent spinous processes at vertebral levels T5 and T8 is 1.15cm and 1.14cm (standard deviation of 0.29 and 0.27, respectively) for age group 2.

Likewise, a multivariant regression analysis was performed for group 3 (Table 35).

Table 35. Multivariant regression analysis for determining the depth to the epidural space (group 3).

Level	Parameter	Coefficient	SE	t	p-value	95% confidence interval	
						Lower	Upper
T5 SkintoLig	Sex	0.044	0.108	0.410	0.683	-0.173	0.262
	Age	0.011	0.002	5.910	2.510	0.007	0.014
	-cons	1.287	0.179	7.182	2.290	0.927	1.647
T5 SkintoLig (inc)	Sex	0.034	0.128	0.271	0.787	-0.222	0.292
	Age	0.013	0.002	5.830	3.370	0.008	0.017
	-cons	1.478	0.212	6.973	4.990	1.053	1.903
T8 SkintoLig	Sex	0.046	0.086	0.537	0.593	-0.127	0.220
	Age	0.010	0.001	6.983	4.810	0.007	0.013
	-cons	1.101	0.143	7.681	3.620	0.813	1.389
T8SkintoLig (inc)	Sex	0.034	0.120	0.283	0.777	-0.207	0.275
	Age	0.012	0.002	6.058	1.460	0.008	0.017
	-cons	1.388	0.198	6.980	4.850	0.989	1.786

Key: **SE** – standard error, **T5** – vertebral level T5, **T8** – vertebra level T8, **SkintoLig** – Skin to Ligamentum flavum, **SkintoLig(inc)** – Skin to Ligamentum flavum at an incline.

Sex was determined with numeric values. Males were assigned the number 0, while females were assigned the number 1 that could be inserted into the equations. Since none of the variables were statistically significant ($p > 0.05$) it was included in the formulae. The formulae are as follows:

- T5 skin to ligamentum flavum:
 - Depth in cm = $1.287 + 0.011(\text{age in months}) + 0.044(\text{sex}) \pm$ standard error of estimate (0.400) (adjusted R^2 -value = 0.375),
- T5 skin to ligamentum flavum at an incline:
 - Depth in cm = $1.478 + 0.013(\text{age in months}) + 0.034(\text{sex}) \pm$ standard error of estimate (0.473) (adjusted R^2 -value = 0.368),
- T8 skin to ligamentum flavum:
 - Depth in cm = $1.101 + 0.010(\text{age in months}) + 0.046(\text{sex}) \pm$ standard error of estimate (0.320) (adjusted R^2 -value = 0.460),
- T8 skin to ligamentum flavum at an incline:
 - Depth in cm = $1.388 + 0.012(\text{age in months}) + 0.034(\text{sex}) \pm$ standard error of estimate (0.444) (adjusted R^2 -value = 0.387),

The mean distance between the adjacent spinous processes at vertebral levels T5 and T8 is 1.52cm and 1.48cm (standard deviation of 0.27 and 0.28, respectively) for age group 3.

4.8 Discussion

The epidural block is an effective technique for providing analgesia following major thoracic and abdominal procedures. Over the years, there have been various ongoing debates as to which approach, the paravertebral- or epidural block, is more superior. Both blocks can be used to provide peri- and post-operative pain relief for similar procedures, each having their pros and cons. One author, in particular, stated that there is no difference between the two blocks (Elsayed *et al.*, 2012).

Since its recent discovery, however, the ESP block proved to be more effective and superior to both the paravertebral and epidural blocks. When performing epidural blocks, the skin-to-epidural space distance is important and can differ considerably amongst individuals. Anatomical factors and body habitus can significantly influence the depth of the epidural space in different age groups.

The discussion will be broken down into two sections, reporting on the measurements and spread separately.

a) ***Block measurements***

The measurements from the ultrasound component revealed no correlation between measurements and sex, or between measurements and height, while a weak correlation was seen between T5 and T8 skin to ligamentum flavum (incline) and weight. From the regression models, we were able to deduce that an increase in weight would cause an increase in the measurement. Overall, the approximate depth to perform the epidural block at vertebral levels T5 and T8 for skin to ligamentum flavum was 1.03 cm and 0.86 cm, respectively. The standard deviation was 0.10 and 0.11 for, while the depth at vertebral levels T5 and T8 for skin to ligamentum flavum (incline) was 1.08 cm and 0.98 cm, respectively. The standard deviation for both values was of 0.11.

Measurements from the CT component revealed a significant difference between groups, therefore each group was assessed individually. In age group 1, the approximate depth to perform the epidural block at vertebral levels T5 and T8 for skin to ligamentum flavum(incline) was 1.57 cm and 1.41 cm, respectively, with a standard deviation of 0.43 and 0.47. For age group 2, the distance at vertebral levels T5 and T8 for skin to ligamentum flavum(incline) was 1.96 cm and 1.73 cm, respectively, with a standard deviation of 0.55 and 0.47, while for age group 3, the distance at vertebral levels T5 and T8 for skin to ligamentum flavum(incline) was 2.56 cm and 2.45 cm, respectively, with a standard deviation of 0.59 and 0.57. Consistent results showed that the-skin-to ligament distance progressively decreases as one moves inferiorly

from the mid-thoracic region in all age groups. Moreover, the low standard deviations indicated little variation within the age groups.

Regression models indicated that as age in months increases, so does the measurement in cm. Estimation formulae were created to determine the depth at which the block can be performed at vertebral levels T5 and T8 in different paediatric age groups. These formulae can help provide information of the thoracic depth that may be a useful adjunct for the practitioner, especially if the block is being performed using the 'blind' technique', as it may help reduce the risk of complications.

Wong and Lim (2019) investigated the skin-to-epidural distance in a Singapore paediatric population in the thoracic and lumbar regions. They further evaluated the relationship between age, weight, ethnicity and gender, to the depth of the epidural space. The mean depth for thoracic epidurals in paediatrics aged 0 – 13 years was 22.7mm (range 8.0-65mm), while the mean depth for lumbar epidurals in paediatrics aged 0 – 14 years was 21.5mm (range 3.0-70.0mm). The study revealed a distinct correlation between weight and skin-to-epidural distance. This correlated with several other studies (Bösenberg and Gouws, 1995; Masir *et al.*, 2006). Furthermore, the skin-to-epidural distance was similar to that in the Japanese population, suggesting that ethnicity might play a role. Overall, a weak correlation was found between age, ethnicity and gender to the skin-to-epidural distance (Wong and Lim, 2019).

In a magnetic resonance imaging study, one hundred and nine scans of the paediatric spine were taken in a group of patients aged 1 month to 8 years. The authors aimed to derive a skin-to-epidural space formulae in infants and children. Measurements were taken from the surface of the skin to the internal aspect of the ligamentum flavum at vertebral levels T6-T7 and T9-T10 interspinous spaces. Two measurements were taken, the first perpendicular to the long axis of the body, while the second was taken between the spinous processes, parallel to the process (at an incline). The univariate analysis showed that all variables (age, height and weight) had a significant positive relationship to the skin-to-epidural space distance at both vertebral levels. Weight showed the strongest association with the inclined skin-to-epidural space distance. The mean distance at T4-T5 interspinous space was 19.3 mm +/- 3.1(straight) and

22.1 mm +/- 4.1(incline). The mean distance at T7-T8 interspinous space was 22.8 mm +/- 5(straight) and 28.3 mm +/- 18.7(incline) (Wani *et al.*, 2017). Although these mean distances do not specify an age group, their measurements do fall within the upper measurement range of this study.

A challenge confronted when attempting to measure the skin-to-epidural space distance is that the distance will be affected by the needle angle. Wani *et al.* (2017) noticed that the distance increased when the angles decreased to less than 90° to the skin. Taking this into account the current study performed two measurements – straight and inclined, noting that the thoracic epidural space is more inclined than the lumbar epidural space. Discrepancies between the formulae can be explained by the differences in the cohorts used in the studies. Furthermore, the current study used age as a parameter, as compared to Wani *et al.* (2017) who used weight.

The same authors recently published a magnetic resonance imaging-based study, in which thoracic- and lumbar spinal images were taken in paediatric patients up to the age of 8 years, to measure the dura-to-spinal cord distance at different vertebral levels, to better understand the vertebral canal anatomy. The mean dura-to-spinal cord distance was 5.9 +/- 1.6 mm at vertebral level T6 – T7, 5.0 +/- 1.6 mm at vertebral level T9 – T10 and 3.6 +/- 1.2 mm at vertebral level L1 – L2. Results showed that the distance progressively decreases from the mid-thoracic to upper lumbar region. Moreover, compared to the mid-thoracic area, the spinal cord at the lower thoracic- and upper lumbar levels appears more dorsal, as it occupies more space due to the lumbar enlargement. Therefore, the risk of spinal cord injury may be greater in the lumbar region. Overall, the authors concluded the study by suggesting that epidurals performed in the lumbar region are safer compared to the thoracic region, challenging the results of alternative studies (Wani *et al.*, 2018). Based on the findings, the midline approaches posed more risk when performed at the lower thoracic and upper lumbar levels. Table 36 summaries the existing formulae created by various authors to calculate the skin-to-epidural space distance.

Table 36. Skin-to-epidural space distance formulae as described in the literature from previous authors.

Author	Formula
<i>Thoracic epidural depth</i>	
Masir <i>et al.</i> (2006)	Depth (cm) = (0.01 x age (months)) + 2.15 Depth (cm) = (0.45 x weight (kg)) + 1.95
Wong and Lim (2019)	Depth (mm) = (0.67 x weight (kg)) + 10.6
Wani <i>et al.</i> (2018)	T6-7 incline (mm) = 7 + (0.9 x weight (kg)) T9-10 incline (mm) = 7 + (0.8 x weight (kg))
<i>Lumbar epidural depth</i>	
Wong and Lim (2019)	Depth (mm) = (0.63 x weight (kg)) + 9.2
Hasan <i>et al.</i> (1994)	Depth (cm) = 1 x 0.15 (age in years) Depth (cm) = 0.8 + 0.05 (weight in kg)
Bosenberg and Gouws (1995)	Depth (mm) = 0.8 (weight in kg) + 3.93
Uemura and Yamashita (1992)	Depth (mm) = 7.719 + 0.789 (weight in kg)
Choi <i>et al.</i> (2009)	Depth (mm) = 9 + 0.5 (weight in kg) – 0.2 (age in months)

The formulae described by Masir *et al.* (2006) are based on a Belgian population and are notably different from the equations derived from Wong and Lim (2019). The difference between these studies can be accounted for based on the needle approach. Masir *et al.* (2006) adopted a cephalad angulation approach, whereas Wong and Lim (2019) adopted a perpendicular approach. Based on our formulae, those of Masir *et al.* (2006) would not be applicable to a younger South African paediatric group, as the constant used in their formulae is higher than the mean for our skin-to-ligament (epidural depth) distance. The formulae of Hasan *et al.* (1992) are comparable to the formulae in this study, as the constants closely resemble the constants calculated in the current study.

Fideler and Grasshoff (2019) investigated the paediatric thoracic spine and evaluated whether a combination of ultrasound-guided measurement of the perpendicular depth to the epidural space, corrected by a trigonometric ration equation, is superior in

predicting the skin-to-epidural space distance compared with estimation of the perpendicular depth. Twenty-four children, aged 5 – 12 years, were used in this study. Once the needle was inserted under ultrasound guidance, the angle between the needle and the skin surface above the spinous process was defined by using a sterile protractor. The skin-to-epidural space distance was calculated using Pythagorean triangle geometry.

After the epidural needle was advanced using the midline approach, the needle tip to skin level was read according to the 5 mm graduation on it, compared with the mm graduation of the protractor. Statistical analysis implied that the combination method is a useful tool to estimate the depth of loss of resistance prior to insertion of the epidural needle. The authors further added that by using the correction of the ultrasound-guided perpendicular measurement, it allowed for better estimation of the distance before the loss of resistance occurred. They also stated that it was an invaluable tool when the peridural needle is inserted at a steep angle.

A study by Kil (2018) found that the length of the epidural space in infants is less than 2 millimetres wide, whereas the bevel length of a paediatric epidural needle is about 1.5 – 2 millimetres. Therefore, when performing the block in infants and younger children, the approach of the needle should be at an angle (pointed cephalad) from the midline in order to view the tip of the needle. He further suggested alternative needle tactics and probe placement for different age groups in paediatric patients. At the thoracic levels in patients up to 9 months, the needle should be inserted perpendicular to the skin. As the vertebral column develops with age, the needle should be inserted in an ascending/upwards orientation. In older children, due to the sharper angle between the spinous process and the vertebral arch, a low-frequency convex probe should be used, rather than a high-frequency linear one.

b) ***Injectate spread***

Patel (2006) wrote a paper comparing thoracic-, lumbar- and caudal blocks in paediatric patients. It was concluded that the block chosen should be tailored to the anticipated post-operative pain, surgical procedure and the patient's underlying

condition. He further stated that experienced operators should perform continuous epidural blocks only in institutions where appropriate equipment, staff and monitoring are available. He also expressed his opinion on the lumbar approach being safer for infants as opposed to the thoracic approach.

This corresponded to a study by Keech (2015), who summarised three potential factors that may be encountered during a thoracic epidural block: firstly, the uncertainty regarding safety and efficacy; secondly, the technical challenges of paediatric thoracic epidural placement, including technique and equipment concerns and lastly, the drug selection, dosage and toxicity.

Several studies have reported on the epidural spread within both the paediatric and adult populations. The spread of radiopaque dye was assessed in 10 infants to test the hypothesis that the extent of spread of dye would vary in proportion to the amount of volume used (0.5 or 1 ml/kg). Uniformly circumferential spread along the vertebral column was only seen in one patient. The remaining patients exhibited circumferential- and cylindrical spread, limited to a few vertebral levels. The rest of the spread was compartmentalized into anterior and posterior spread. The posterior spread was uniform and denser in all patients, while the anterior spread was thin and patchy with a few skipped vertebral segments. The spread ranged from 5 – 18 vertebral and 7 – 18 vertebral segments when 0.5 ml/kg and 1 ml/kg was used respectively. The extent of the spread either increased or became denser and less patchy with the larger dose.

Factors that influenced the spread of dye included volume used, the speed of the injection, the back leak of the solution in the needle track (seen in the majority of cases), and the pressures achieved in the space and inherent divisions of the epidural space. Even though the volume used doubled, (1 ml/kg) the number of vertebral segments covered, did not. The authors concluded the study by stating that there is considerable individual variation in the extent, quality and uniformity of spread. Doubling the dose does not necessarily increase the number of vertebral segments covered, but it does improve the density and extent of the craniocaudal spread (Vas *et al.*, 2003).

Similar results were reported by Hong (2016), who conducted fluoroscopically guided thoracic interlaminar epidural injections in adults, using 2.5 ml and 5 ml of contrast material. The author noted that the level of sensory blockade after an epidural injection differs considerably amongst individuals, and factors that might affect this distribution remain controversial. The extent of spread was assessed by evaluating the upper and lower endplates of the vertebra from a lateral view. All patients in both groups – 2.5 ml (Group A) and 5 ml (Group B) – showed bilateral contrast spread evenly distributed. Group B showed higher contrast distribution in the cephalad direction compared to group A. Results showed no significant difference in the number of vertebral segments covered between the two groups. The total number of vertebral segments was 7.5 ± 2.0 and 8.4 ± 2.6 in group A and B, respectively. Results from this study supported the conclusion of Vas *et al.* (2003) who stated that doubling the dose does not double the number of vertebral segments covered.

Authors of another study investigated whether the lateral decubitus position would result in a more extensive distribution of contrast material, compared to the neutral position. Patients were divided into groups – lateral decubitus(L) and prone(P) – before receiving thoracic epidural catheterization. Results revealed the craniocaudal spread of contrast material to be over 7.4 ± 2.2 vertebral segments for the P-group and 9.2 ± 1.8 vertebral segments for the L-group. The distribution of spread was higher towards the cranial direction in the L-group than towards the caudal direction. The authors hypothesized that the reduced epidural pressure due to the posture of the neck and hip flexion in the L-group, may have contributed to the more extensive distribution of contrast material. Furthermore, they found that the distance between the spinal cord and the posterior arch of the cervical canal was widened by/up to 89% during flexion, and narrowed by/up to 17% during extension (Hong *et al.*, 2017).

Based on common anatomical knowledge, the volume of the epidural space per vertebral segment differs between the vertebral divisions and can potentially play a role in determining the volume doses. In a magnetic resonance imaging study, 20 patients aged 0 – 3 years were assessed to determine the epidural volume per vertebral segment. The vertebral column was divided into three regions: T6 – T12 (thoracic), L1 – L5 (lumbar) and S1 – S5 (caudal). After obtaining the volume from the

magnetic resonance images, the respective volumes of the epidural space were then divided by the related number of vertebrae in each region. Results revealed the mean volume to be 0.60 ml in the thoracic region, 1.18 ml in the lumbar region and 0.85 ml in the caudal region. These volumes are important, as they can be used as an indication for volume dosing in paediatric patients for epidurals. Linear correlation showed a good relationship between the volume and height and weight, height being the strongest, while a curvilinear correlation was found for age (Forestier *et al.*, 2017).

The efficacy of the block has also been investigated. Martin *et al.* (2019) reported on their experience with using epidurals for major abdominal surgery in patients younger than 11 months. Results revealed that epidural analgesia is associated with decreased long-acting opioid requirements, intra-operatively. Furthermore, epidural placement did not impede post-operative opioid exposure. Findings from the study supported the use of epidural analgesia for infants who are at risk of opioid-induced respiratory depression, sedation and apnoea in the immediate post-operative period. Minor complications such as epidural leaking and inadequate blockade were noted.

In a recent study, Akhil Gupta *et al.* (2020) conducted a retrospective observational cohort study to analyse the use of perioperative, paediatric epidural analgesia at a tertiary paediatric hospital over a period of twenty years. Results revealed a gradual decrease in the trend over the study period. The incidence of paediatric analgesia declined from 4.8% (1996) to 0.45% (2016), while the number of surgical procedures performed over the same period increased. Regarding surgical specialities, the use of paediatric epidural analgesia for general surgery declined the most from 64% (1996) to 29% (2003), whereas its use for orthopaedic surgery increased from 0.4% to 23% within the same period. Adverse events included cardiac arrest, respiratory arrest, epidural site collection, permanent nerve injury and death. These complications were more prevalent in the 1 – 8-year-old age group (Akhil Gupta *et al.*, 2020). One of the main reasons for the decreased use of epidurals in paediatric surgery, is the introduction of alternative regional anaesthetic techniques which offer a higher safety profile. Wong and Lim (2019) also commented on the diminishing trend in the popularity of paediatric epidurals. However, the authors acknowledged that paediatric epidurals remain as an invaluable tool for optimising perioperative pain relief.

When compared to alternative neuraxial techniques, the epidural block produced diverse results. Beard *et al.* (2020) compared the quality of analgesia between a plane (serratus anterior)-, paravertebral- and epidural block. Where one block fell short, the other proved to be superior. Pre- and post-operative pain scores showed that the thoracic epidural group had the highest percentage of post-operative pain relief. High mortality rates were seen in the thoracic epidural group, followed by the paravertebral group and then the plane group. The length of hospital stay was highest in the plane group, followed by the thoracic epidural group. The shortest length of stay was in the paravertebral group. The authors concluded by saying, given the inherent limitations of thoracic epidural and paravertebral blocks, plane blocks (serratus anterior) offer a more attractive analgesic option for patients.

4.9 Epidural blocks versus ESP blocks

ESP blocks have been used as a rescue strategy after epidural failure in the past (Forero *et al.*, 2017). Studies also reported on results of ESP blocks as part of a regimen to avoid thoracic epidural, due to its side effects and complications (Warusawitharana *et al.*, 2019). Adler *et al.* (2019) reported on a case study in which a three-week-old neonate (4kg) necessitated a thoracotomy. The traditional regional anaesthetic approach for post-thoracotomy relied on thoracic epidurals, however, due to the shorter distance from the skin to the dura, the risk of complication is higher. The alternative approach was a caudally threaded epidural, but recent studies reported high rates of catheter migration in paediatrics (Simpao *et al.*, 2019). Therefore, due to its safety profile, the ESP block (0.1 ml/kg) was used for the procedure. Positive results lead the authors to conclude that the ESP block is potentially reliable and a safe alternative to epidural and paravertebral catheters, especially in neonates (Adler *et al.*, 2019).

ESP blocks have also been used when epidural analgesia is relatively contraindicated. Lima and colleagues (2020) considered using an epidural block for ankle/foot surgery in three paediatric patients. However, due to the concern regarding the potential side effects of morphine on the central nervous system, the authors decided against the

block. They commented that the duration of analgesia would be shorter when compared to the ESP block. They further concluded their study by stating that the ESP block appears as a potential alternative for analgesia for paediatric surgery when combined with general surgery and multimodal analgesia. These case studies contributed to the literature favouring the use of ESP block for lower limb surgery.

Arun and Singh (2020) relayed positive results after performing a bilateral ESP block in a patient with moderate scoliosis. This comorbidity made it difficult to locate the epidural space. The authors concluded that the ESP block may be an effective technique for post-operative analgesia in patients where epidurals are not an option. They also stated that the ESP block provides extensive analgesia, as the ESP plane is larger than the confined epidural space. Similarly, a landmark guided continuous ESP was performed as an alternative to an epidural block, due to scoliosis (Dey *et al.*, 2020). In a more recent case report, the ESP block was performed in a patient posted for nephrectomy, for which the epidural block was deferred due to previous spinal surgery and neurological deficits. After an uneventful block, they concluded that the ESP block is comparatively safer, as there is no risk of hypotension usually associated with epidural blocks, nor epidural spread or vascular complication which can be associated with paravertebral blocks (Pathak and Krishna, 2020).

Sakae *et al.*, (2020) performed a randomized clinical trial to compare ESP and epidural block techniques for post-operative analgesia after open cholecystectomies. Results revealed a statistically significant difference between the two groups after a 24-hour assessment period on the numeric pain scale. The intervention group – the ESP block – had a higher mean pain score within the 24-hour assessment period. Furthermore, the intervention group required more opioid use in the post-anaesthetic care and had an overall higher need for the use of rescue opioids than the epidural group. The authors concluded that the ESP block was less effective when compared to epidural anaesthesia. In a different study comparing thoracic epidural analgesia and a bilateral continuous ESP block for cardiac surgery, results revealed comparable pain scores, incentive spirometry, intensive care unit duration and the number of ventilator days (Nagaraja *et al.*, 2018).

Contrary to results obtained from the previous studies, Shokri and Kasem (2020) conducted a comparative study which generated favourable results. Bilateral ESP blocks were compared to thoracic epidurals for patients undergoing transthoracic oesophageal surgical procedures. Results from this prospective study indicated that the patients in the non-invasive ESP group had a shorter hospital stay, lower visual analogue scale scores, required less post-operative opioids, experienced a lower incidence of complication and overall higher patient satisfaction. The authors concluded the study by stating that the ESP block had a brilliant beneficial effect in reducing pain and providing higher satisfaction scores with a lower risk profile as compared to thoracic epidural anaesthesia. Likewise, Nagaraja *et al.* (2018) conducted a comparative study on the same two techniques. Although the results were similar, the authors noted that the length of hospital stay and post-operative complications were comparable in both groups. Other comparative studies reported the ESP to be easier to perform, as the needle is limited by the bone structure (Altinpulluk *et al.*, 2019).

ESP blocks have also been compared to thoracic epidural blocks for post-mastectomy pain control. Results revealed a shorter administration time for the ESP group as compared to the thoracic epidural group. Moreover, the need for post-operative morphine, visual analogue scale and patient satisfaction scores were better in the ESP group. The authors stated that, even though thoracic epidurals have been considered the golden standard, ESP blocks are now emerging as a better alternative technique with better efficiency, satisfaction and fewer complications (Ahmed and Abdelraouf, 2020). Given the epidural-like effects of bilateral ESP blocks, however, consideration needs to be taken regarding the potential effect of higher infusion- or injection volumes. Higher volumes may result in greater epidural involvement, as well as the side effects such as hypotension or lower extremity motor blockade (Pak and Singh, 2020).

4.10 Advantages and disadvantages

Compared to a paravertebral block, the volume of anaesthetic required to complete an epidural block is less. Additionally, epidural blocks offer physiological advantages over systemic opioid analgesia in both infants and children, including a reduced need for

post-operative ventilatory support, improved analgesia without the risk of opioid-induced respiratory depression and improved control of the surgical stress response (“Effects of Perioperative Central Neuraxial Analgesia on Outcome after Coronary Artery Bypass Surgery,” n.d.; Wani *et al.*, 2017). It is also associated with fewer neurological complications (Reich and Strümper, 2000; Teeter and Kumar, 2015).

Other epidural benefits include less surgical stress and prompt gastrointestinal motility (Martin *et al.*, 2019). Difficulties that are associated with epidural blocks include dural puncture, epidural venous placement (Elsharkawy *et al.*, 2017), intrapleural puncture, spinal cord injury, nerve injury, difficulty to access the epidural and subarachnoid space, difficulty with intravascular catheter placement (Belani *et al.*, 2016), delayed micturition or urinary retention, and local anaesthetic systemic toxicity (Marcelino *et al.*, 2019). Due to the intricacy of the technique, thoracic epidural placement in infants and young children should be restricted to those practitioners who are experienced in the technique (Patel, 2006).

4.11 Limitations

In a live subject, the skin-to epidural space depth can be underestimated due to compression of the soft tissue at the intervertebral space by the probe. Therefore, measurements taken from the ultrasound scans maybe be diminished by a few millimetres.

More limitations see section 2.11.

4.12 Conclusion

Epidural analgesia continues to play a role in major paediatric surgery, particularly for perioperative and post-operative pain management. A vast knowledge of the anatomy of the epidural space is imperative in the exploration of this space. The identification of this space demands some skill due to its complexity. Thus, inadequate knowledge

of the anatomy of the space and lack of skill to identify it, can expose the patient to avoidable hazards. Nonetheless, its importance in post-operative pain management cannot be under-emphasized (Fyनेface-Ogan, 2012). Although epidural blocks are effective, new emerging techniques may prove to be better alternatives. Depending on the age group and vertebral level, the block can be performed at a depth ranging from 1.41 cm to 2.56 cm.

Chapter 5 – Conclusion of the thesis

Over the past two decades, there have been significant changes in the management of pain for a paediatric population. These changes were brought about due to the misconceptions that neonates, infants and children do not feel or experience pain in the same way as adults do. This thesis aimed to evaluate the anatomical differences between existing neuraxial techniques, the paravertebral and epidural block, as well as the novel interfascial ESP block, for the management of pain in paediatric patients. Although the route of access or spread is similar in the paravertebral and ESP block, the ESP block offers a better safety profile, as the block is performed distant to neuraxial structures. Similarly, paediatric epidural analgesia is gradually being superseded by alternative techniques such as the ESP block, due to the simplicity and lower risk profile of the latter.

Imaging modalities such as ultrasound guidance and CT scanning also play an important role in the understanding and interpretation of the anatomy. Based on the results from this study, the ESP block demonstrates extensive craniocaudal spread covering multiple dermatomal segments, while targeting nerves that are involved in both the paravertebral and epidural blocks. Furthermore, when combined with ultrasound guidance, the anatomical landmarks and borders are easier to identify, making the block more appealing than paravertebral-, epidural- and other neuraxial blocks.

Essential training of anaesthesiologists in paediatric regional anaesthesia and a thorough knowledge of the three-dimensional paediatric anatomy is needed for the safe and successful administration of any neuraxial block. The anatomical and physiological differences between an adult and paediatric population make it inaccurate to extrapolate data from an adult sample to a paediatric population. Moreover, due to the inconsistent growth development from a neonate to an adult, neuraxial techniques and regional blocks will have to be adapted appropriately for the population group. Poorly controlled pain in neonates and infants could lead to morbidity in the vulnerable population.

Data obtained from this study is invaluable, as there is limited paediatric text available surrounding the topic. Furthermore, the results from this study, together with the derived formulae, can assist anaesthesiologists and clinicians when performing either of these truncal blocks by taking into consideration the anatomical and clinical aspects of each block.

References

- Abdelhamid, K., ElHawary, H., Turner, J.P. (2020) The Use of the Erector Spinae Plane Block to Decrease Pain and Opioid Consumption in the Emergency Department: A Literature Review. *J Emerg Med.* 58, 603–609.
- Abdl Fatah, M.M., Abdl Aleem, M.I. (2016) Case report and review of literatures: Thoracic epidural as a sole anaesthetic technique in laparoscopic myomectomy. *Egypt J Anaesth.* 32, 435–437.
- Adhikary, S.D., Bernard, S., Lopez, H., Chin, K.J. (2018) Erector Spinae Plane Block Versus Retrolaminar Block: A Magnetic Resonance Imaging and Anatomical Study. *Reg Anesth Pain Med.* 43, 756–762.
- Adler, A.C., Yim, M.M., Chandrakantan, A. (2019) Erector spinae plane catheter for neonatal thoracotomy: a potentially safer alternative to a thoracic epidural. *Can J Anaesth.* 66, 607–608.
- Adstrum, S., Hedley, G., Schleip, R., Stecco, C., Yucesoy, C.A. (2017) Defining the fascial system. *J Bodyw Mov Ther.* 21, 173–177.
- Ahiskalioglu, A., Tulgar, S., Celik, M., Ozer, Z., Alici, H.A., Aydin, M.E. (2020) Lumbar Erector Spinae Plane Block as a Main Anesthetic Method for Hip Surgery in High Risk Elderly Patients: Initial Experience with a Magnetic Resonance Imaging. *Eurasian J Med.* 52, 16–20.
- Ahmed, I., Abdelraouf, H. (2020) Ultrasound guided Erector Spinae Plane block versus thoracic epidural for post-mastectomy analgesia. *Al Azhar Med J.* 1(2),120-124.
- Aksu, C., Gürkan, Y. (2020) Sacral Erector Spinae Plane Block with longitudinal midline approach: Could it be the new era for pediatric postoperative analgesia? *J Clin Anesth.* 59, 38–39.
- Aksu, C., Gürkan, Y. (2019a) Aksu approach for lumbar erector spinae plane block for pediatric surgeries. *J Clin Anesth.* 54, 74–75.
- Aksu, C., Gurkan, Y. (2019b) Defining the Indications and Levels of Erector Spinae Plane Block in Pediatric Patients: A Retrospective Study of Our Current Experience. *Cureus.* 11(8):e5348.

- Aksu, C., Gürkan, Y. (2019c) Do we still need central blocks while we have erector spinae plane block? Case of 2.5 month old infant. *Braz J Anesthesiol* (English Edition). 69, 417–419.
- Aksu, C., Gürkan, Y. (2019d) Ultrasound-guided bilateral erector spinae plane block could provide effective postoperative analgesia in laparoscopic cholecystectomy in paediatric patients. *Anaesth Crit Care PA*. 38, 87–88.
- Aksu, C., Gürkan, Y. (2019e) Erector spinae plane block: A new indication with a new approach and a recommendation to reduce the risk of pneumothorax. *J Clin Anesth*. 54, 130–131.
- Aksu, C., Gürkan, Y. (2019f) Erector spinae plane block: Safety in altered anatomy. *Saudi J Anaesth*. 13, 177.
- Aksu, C., Gürkan, Y. (2018a) Ultrasound guided erector spinae block for postoperative analgesia in pediatric nephrectomy surgeries. *J Clin Anesth*. 45, 35–36.
- Aksu, C., Gürkan, Y. (2018b) Opioid sparing effect of Erector Spinae Plane block for pediatric bilateral inguinal hernia surgeries. *J Clin Anesth*. 50, 62–63.
- Aksu, C., Şen, M.C., Akay, M.A., Baydemir, C., Gürkan, Y. (2019) Erector Spinae Plane Block vs Quadratus Lumborum Block for pediatric lower abdominal surgery: A double blinded, prospective, and randomized trial. *J Clin Anesth*. 57, 24–28.
- Albokrinov, A.A., Fesenko, U.A. (2014) Spread of dye after single thoracolumbar paravertebral injection in infants: A cadaveric study. *Euro J Anaesthesiol*. 31, 305–309.
- Altinpulluk, E.Y., Ozdilek, A., Colakoglu, N., Beyoglu, C.A., Ertas, A., Uzel, M., Yildirim, F.G., Altindas, F. (2019) Bilateral postoperative ultrasound-guided erector spinae plane block in open abdominal hysterectomy: a case series and cadaveric investigation. *Rom J Anaesth Intensive Care*. 26, 83–88.
- Altıparmak, B., Korkmaz Toker, M., Uysal, A.İ., Özcan, M., Gümüş Demirbilek, S. (2019) Erector spinae plane block for pain management of esophageal atresia in a preterm neonate. *J Clin Anesth*. 56, 115–116.
- Aponte, A., Sala-Blanch, X., Prats-Galino, A., Masdeu, J., Moreno, L.A., Sermeus, L.A. (2019) Anatomical evaluation of the extent of spread in the erector spinae plane block: a cadaveric study. *J Clin Anesth*. 66, 886–893.

- Arun, N., Singh, S. (2020) Is ESP block an answer for upper abdominal surgeries where epidural analgesia can't be used? *J Anaesthesiol Clin Pharmacol.* 36, 117–118.
- Aydin, T., Turgut, M., BalaFban, O. (2019) Ultrasound guided bi-level thoracic and lumbar erector spinae plane block as surgical anaesthesia method for inguinal hernia repair in a high-risk patient: Case report. *Indian J Anaesth.* 63, 957.
- Aygun, H., Thomas, D.T., Tulgar, S. (2020a) The “dry leaf” technique for erector spinae plane block in supine position: An alternative to lateral decubitus or prone position. *J Clin Anesth.* 59, 34–35.
- Aygun, H., Kavrut Ozturk, N., Pamukcu, A., Inal, A., Kiziloglu, I., Thomas, D., Tulgar, S. and Nart, A. (2020b) Comparison of ultrasound guided Erector Spinae Plane Block and quadratus lumborum block for postoperative analgesia in laparoscopic cholecystectomy patients; a prospective randomized study. *J Clin Anesth.* 62,109696.
- Barker, P.J., Briggs, C.A. (1999) Attachments of the Posterior Layer of Lumbar Fascia. *Spine.* 24, 1757.
- Baca, Q., Lin, C., O'Hare, K., Golianu, B., Tsui, B. (2019) Erector spinae plane block for pediatric palliative care. *Paediatr Anesth.* 29, 386–387.
- Balaban, O., Koçulu, R., Aydın, T. (2019) Ultrasound-guided Lumbar Erector Spinae Plane Block For Postoperative Analgesia in Femur Fracture: A Pediatric Case Report. *Cureus.* 11(7): e5148.
- Bang, S. (2019) Erector spinae plane block: an innovation or a delusion? *Korean J Anesthesiol.* 72, 1–3.
- Barrios, A., Camelo, J., Gómez, J., Forero, M. (2020) Evaluation of Sensory Mapping of Erector Spinae Plane Block. *Pain Physician.* 23(3):E289-E296.
- Basaran, B., Akkoyun, I. (2020) Erector spinae plane block for management of major abdominal surgery in a low birth weight preterm neonate. *J Clin Anesth.* 61, 109641.
- Basu, S. (2012) Spinal Injuries in Children. *J Clin Anesth.* 61:109641.
- Beard, L., Hillermann, C., Beard, E., Millerchip, S., Sachdeva, R., Smith, F.G., Veenith, T. (2020) Multicenter longitudinal cross-sectional study comparing effectiveness of serratus anterior plane, paravertebral and thoracic epidural for the analgesia of multiple rib fractures. *Reg Anesth Pain Med.* 45, 351–356.

- Belani, K., Montealegre-Gallegos, M., Ferla, B., Matyal, R. (2016) Intrapleural placement of a thoracic epidural catheter in a patient with spinal stenosis. *J Minim Access Surg.* 35, 195–197.
- Bhettay, A.Z. (2018) Neuraxial anaesthetic techniques in children: Using the evidence to make it safer. *South African J Anaesth Analg.* 24(3), 81-85.
- Bhoi, D., Acharya, P., Talawar, P., Malviya, A. (2018) Continuous erector spinae plane local anesthetic infusion for perioperative analgesia in pediatric thoracic surgery. *Saudi J Anaesth.* 12, 502–503.
- Boon, J.M., Prinsloo, E., Raath, R.P. (2003) A paramedian approach for epidural block: An anatomic and radiologic description. *Reg Anesth Pain Med.* 28, 221–227.
- Bosenberg, A.T. (1998) Epidural analgesia for major neonatal surgery. *Pediatr Anesth.* 8, 479–483.
- Bösenberg, A.T., Gouws, E. (1995) Skin-epidural distance in children. *Anaesthesia.* 50, 895–897.
- Boules, M.L., Goda, A.S., Abdelhady, M.A., Abu El-Nour Abd El-Azeem, S.A., Hamed, M.A. (2020) Comparison of Analgesic Effect Between Erector Spinae Plane Block and Transversus Abdominis Plane Block After Elective Cesarean Section: A Prospective Randomized Single-Blind Controlled Study. *J Pain Res.* 13, 1073–1080.
- Bouman, E.A.C., Sieben, J.M., Balthasar, A.J.R., Joosten, E.A., Gramke, H.-F., van Kleef, M., Lataster, A. (2017) Boundaries of the thoracic paravertebral space: potential risks and benefits of the thoracic paravertebral block from an anatomical perspective. *Surg Radiol Anat.* 39, 1117–1125.
- Cadavid-Puentes, A.M., Casas-Aroyave, F.D., Palacio-Montoya, L.M., Valencia-Gallón, E. (2020) Efficacy of paravertebral block techniques in thoracic surgery: systematic literature review. *Colombian J Anesthesiol.* 48, 20–29.
- Celik, M., Tulgar, S., Ahiskalioglu, A., Alper, F. (2019) Is high volume lumbar erector spinae plane block an alternative to transforaminal epidural injection? Evaluation with MRI. *Reg Anesth Pain Med.* 44, 906–907.
- Cesur, S., Ay, A.N., Yayık, A.M., Naldan, M.E., Gürkan, Y. (2018) Ultrasound-guided erector spinae plane block provides effective perioperative analgesia and anaesthesia for thoracic mass excision: A report of two cases. *Anaesth Crit Car PA.*

- Chaudhary, N., Singh, S. (2018) The right plane for drug injection in ultrasound-guided erector spinae plane block. *Indian J Anaesth.* 62(5), 405.
- Chaudhary, O., Baribeau, Y., Urits, I., Sharkey, A., Rashid, R., Hess, P., Krumm, S., Fatima, H., Zhang, Q., Gangadharan, S., Mahmood, F., Matyal, R. (2020) Use of Erector Spinae Plane Block in Thoracic Surgery Leads to Rapid Recovery from Anesthesia. *Ann Thoracic Surg.* 110(4), 1153 - 1159.
- Chin, K.J. (2019) Thoracic wall blocks: From paravertebral to retrolaminar to serratus to erector spinae and back again – A review of evidence. *Best Practice & Research Clinical Anaesthesiology, Future directions in regional anesthesia.* 33, 67–77.
- Chin, K.J., Adhikary, S., Sarwani, N., Forero, M. (2017) The analgesic efficacy of pre-operative bilateral erector spinae plane (ESP) blocks in patients having ventral hernia repair. *Anaesthesia.* 72, 452–460.
- Choi, J., Hong, J., Kim, J. and Kil, H. (2009) Estimating lumbar epidural space depth in infants and children of Korea. *Korean J Anesthesiol.* 56(5),531.
- Choi, Y.-J., Kwon, H.-J., O, J., Cho, T.-H., Won, J.Y., Yang, H.-M., Kim, S.H. (2019) Influence of injectate volume on paravertebral spread in erector spinae plane block: An endoscopic and anatomical evaluation. *Plos ONE.* 14, e0224487.
- Ciftci, B., Ekinci, M. (2019a) Bilateral erector spinae plane block provides postoperative analgesia for laparoscopic distal esophagectomy surgery. *Ain-Shams J Anesthesiol.* 11, 15.
- Ciftci, B., Ekinci, M., Demiraran, Y. (2019b) Ultrasound-Guided Single-Shot Preemptive Erector Spinae Plane Block for Postoperative Pain Management. *J Cardiothorac Vasc Anesth.* 33, 1175–1176.
- Committee on Psychosocial Aspects of Child and Family Health, Task Force on Pain in Infants, Children, and Adolescents, 2001. The Assessment and Management of Acute Pain in Infants, Children, and Adolescents. *Pediatrics.* 108, 793–797.
- Continuous Erector Spinae Block Versus Continuous Paravertebral Block [WWW Document], n.d. URL <https://www.smartpatients.com/trials/NCT03768440> (accessed 6.2.20).
- Cork, R.C., Kryc, J.J., Vaughan, R.W. (1980) Ultrasonic localization of the lumbar epidural space. *Anesthesiology.* 52, 513–516.
- Cornish, P. (2019) Erector spinae plane block and ‘A Cadaveric Conundrum.’ *Reg Anesth Pain Med.*44, 269–270.

- Coşarcan, S.K., Gürkan, Y., Doğan, A.T., Erçelen, Ö. (2020) Targeted modification of erector spinae plane block. *Acta Anaesthesiol Scand.* 64, 276–276.
- Costache, I., Pawa, A., Abdallah, F.W. (2018) Paravertebral by proxy – time to redefine the paravertebral block. *Anaesthesia.* 73, 1185–1188.
- Cowie, B., McGlade, D., Ivanusic, J., Barrington, M.J. (2010) Ultrasound-Guided Thoracic Paravertebral Blockade: A Cadaveric Study. *Anesth Analg.* 110, 1735–1739.
- Darling, C.E., Pun, S.Y., Caruso, T.J., Tsui, B.C.H. (2018) Successful directional thoracic erector spinae plane block after failed lumbar plexus block in hip joint and proximal femur surgery. *J Clin Anesth.* 49, 1–2.
- Davies, R.G., Myles, P.S., Graham, J.M. (2006) A comparison of the analgesic efficacy and side-effects of paravertebral vs epidural blockade for thoracotomy--a systematic review and meta-analysis of randomized trials. *Br J Anaesth.* 96, 418–426.
- De Cassai, A., Andreatta, G., Bonvicini, D., Boscolo, A., Munari, M., Navalesi, P. (2020) Injectate spread in ESP block: A review of anatomical investigations. *J Clin Anesth.* 61, 109669.
- De Cassai, A., Bonvicini, D., Correale, C., Sandei, L., Tulgar, S., Tonetti, T. (2019) Erector spinae plane block: a systematic qualitative review. *Minerva Anesthesiol.* 85.
- De Cassai, A., Stefani, G., Ori, C. (2018) Erector spinae plane block and brachial plexus. *J Clin Anesth.* 45, 32.
- de Haan, J.B., Hernandez, N., Sen, S. (2018) Erector spinae block for postoperative analgesia following axillary hidradenitis suppurativa resection: a case report. *Local Reg Anesth.* 11, 87–90.
- De la Cuadra-Fontaine, J.C., Concha, M., Vuletin, F., Arancibia, H. (2018) Continuous Erector Spinae Plane block for thoracic surgery in a pediatric patient. *Pediatric Anesth.* 28, 74–75.
- D’Ercole, F., Arora, H., Kumar, P.A. (2018) Paravertebral Block for Thoracic Surgery. *J Cardiothorac Vasc Anesthesia.* 32, 915–927.
- Dey, S., Mistry, T., Mittapalli, J., Neema, P.K. (2020) Landmark guided continuous erector spinae plane block: An adjunct for perioperative analgesia in a patient with difficult back operated for total hip arthroplasty. *Saudi J Anaesth.* 14, 276–277.
- Diedericks, J. (2006) Postoperative pain management in the paediatric patient. *S Afr J Psychol.* 48, 37–42.

- Diwan, S., Garud, R., Nair, A. (2019) Thoracic paravertebral and erector spinae plane block: A cadaveric study demonstrating different site of injections and similar destinations. *Saudi J Anaesth.* 13, 399–401.
- Diwan, S., Nair, A. (2020) Is Paravertebral-Epidural Spread the Underlying Mechanism of Action of Erector Spinae Plane Block? *Turk J Anaesthesiol Reanim.* 48, 86–87.
- Ekinci, M., Ciftci, B., Güven, S., Thomas, D.T. (2020) An alternative and novel usage for ultrasound-guided erector spinae plane block: Extracorporeal shock wave lithotripsy in a paediatric patient. *Indian J Anaesth.* 64, 247–248.
- El Ghamry, M.R., Amer, A.F. (2019) Role of erector spinae plane block versus paravertebral block in pain control after modified radical mastectomy. A prospective randomised trial. *Indian J Anaesth.* 63, 1008–1014.
- ELdeen, H.M.S. (2016) Ultrasound-guided thoracic epidural and paravertebral blocks for cholecystectomy in pediatric patients with a cyanotic heart disease: A randomized controlled study. *Egypt J Anaesth.* 32, 89–96.
- El-Emam, E.-S., El motlb, Enas. A.A. (2019) Ultrasound-guided erector spinae versus ilioinguinal/iliohypogastric block for postoperative analgesia in children undergoing inguinal surgeries. *Anesth Essays Res.* 13, 274.
- Elkoundi, A., Bentalha, A., Kettani, S.E.-C.E., Mosadik, A., Koraichi, A.E. (2019) Erector spinae plane block for pediatric hip surgery -a case report-. *Korean J Anesthesiol.* 72, 68–71.
- Elkoundi, A., Eloukkal, Z., Bensghir, M., Belyamani, L. (2019b) Priapism following erector spinae plane block for the treatment of a complex regional pain syndrome. *Am J Emerg Med.* 37, 796.e3-796.e4.
- Ellis, H. (2009) The anatomy of the epidural space. *Anesth Int Care Med.* 7(11), 402 - 404.
- Elsayed, H., McKeivith, J., McShane, J., Scawn, N. (2012) Thoracic Epidural or Paravertebral Catheter for Analgesia After Lung Resection: Is the Outcome Different? *J Cardiothorac Vasc Anesth.* 26, 78–82.
- Elsharkawy, H., Bajracharya, G.R., El-Boghdadly, K., Drake, R.L., Mariano, E.R. (2019) Comparing two posterior quadratus lumborum block approaches with low thoracic erector spinae plane block: an anatomic study. *Reg Anesth Pain Med.* 44, 549–555.

- Elsharkawy, H., Pawa, A., Mariano, E.R. (2018) Interfascial Plane Blocks: Back to Basics. *Reg Anesth Pain Med.* 43, 341–346.
- Elsharkawy, H., Sonny, A., Chin, K.J. (2017) Localization of epidural space: A review of available technologies. *J Anaesthesiol Clin Pharmacol.* 33, 16–27.
- Fahy, A.S., Jakub, J.W., Dy, B.M., Eldin, N.S., Harmsen, S., Sviggum, H., Boughey, J.C. (2014) Paravertebral blocks in patients undergoing mastectomy with or without immediate reconstruction provides improved pain control and decreased postoperative nausea and vomiting. *Ann. Surg. Oncol.* 21, 3284–3289.
- Fideler, F., Grasshoff, C. (2019) Calculation improves the estimation of needle depth from skin to thoracic epidural space in infants. *Eur J Anaesthesiol.* 36, 235–237.
- Fandino, W. (2019) Erector Spinae Plane Block compared to Paravertebral Block in the post-operative pain management of patients undergoing elective Video-Assisted Thoracic Surgical lobectomy for lung cancer: a randomized, non-inferiority clinical trial protocol. *Princ Pract Clin Res.* 5(2), 36-43.
- Forero, M., Adhikary, S.D., Lopez, H., Tsui, C., Chin, K.J. (2016) The Erector Spinae Plane Block: A Novel Analgesic Technique in Thoracic Neuropathic Pain. *Reg Anesth Pain Med.* 41, 621–627.
- Forero, M., Rajarathinam, M., Adhikary, S., Chin, K.J. (2017) Continuous Erector Spinae Plane Block for Rescue Analgesia in Thoracotomy After Epidural Failure: A Case Report. *A&A Case Reports.* 8, 254–256.
- Forestier, J., Castillo, P., Finnbogason, T., Lundblad, M., Eksborg, S., Lönnqvist, P.A. (2017) Volumes of the spinal canal and caudal space in children zero to three years of age assessed by magnetic resonance imaging: implications for volume dosage of caudal blockade. *Br J Anaesth.* 119, 972–978.
- Fyनेface-Ogan, S. (2012) Anatomy and Clinical Importance of the Epidural Space, in: Fyनेface-Ogan, S. (Ed.), *Epidural Analgesia - Current Views and Approaches. InTech.*
- Gad, M., Abdelwahab, K., Abdallah, A., Abdelkhalek, M., Abdelaziz, M. (2019) Ultrasound-guided erector spinae plane block compared to modified pectoral plane block for modified radical mastectomy operations. *Anesth Essays Res.* 13, 334.
- Gaio-Lima, C., Costa, C.C., Moreira, J.B., Lemos, T.S., Trindade, H.L. (2018) Continuous erector spinae plane block for analgesia in pediatric thoracic surgery: A case report. *Rev Esp Anesthesiol (English Edition).* 65, 287–290.

- Garcia, J.B.S., Bonilla, P., Kraychete, D.C., Flores, F.C., de Valtolina, E.D.P., Guerrero, C. (2017) Optimizing post-operative pain management in Latin America. *Braz J Anesthesiol* (English Edition). 67, 395–403.
- Gawęda, B., Borys, M., Belina, B., Bąk, J., Czuczwar, M., Wołoszczuk-Gębicka, B., Kolowca, M., Widenka, K. (2020) Postoperative pain treatment with erector spinae plane block and pectoralis nerve blocks in patients undergoing mitral/tricuspid valve repair — a randomized controlled trial. *BMC Anesthesiol.* 20, 51.
- Gerrard, C., Roberts, S. (2012) Ultrasound-Guided Regional Anaesthesia in the Paediatric Population. *ISRN Anesthesiol.* 2012, 1–7.
- Glazov, Y., Mirgorodskaya, D. (2020) Application of erector spinae plane block in a child with pyothorax: a description of a clinical case. *Pain Med.* 5, 57–59.
- Godlewski, C. (2019) Erector spinae plane block provides complete perioperative analgesia for chronic scapulothoracic pain. *J Anaesthesiol Clin Pharmacol.* 35, 424.
- Govender, S., Mohr, D., Bosenberg, A., Van Schoor, A.N. (2020a) A cadaveric study of the erector spinae plane block in a neonatal sample. *Reg Anesth Pain Med.* 45(5),386-388.
- Govender, S., Mohr, D., Neels Van Schoor, A., Bosenberg, A. (2020b) The extent of cranio-caudal spread within the erector spinae fascial plane space using computed tomography scanning in a neonatal cadaver. *Pediatr Anaesth.* 30(6),667-670
- Govender, S., Mohr, D., Bosenberg, A., Neels Van Schoor, A. (2020c) The anatomical features of an ultrasound-guided Erector Spinae Fascial Plane block in a cadaveric neonatal sample. *Pediatr Anaesth.* 45(5).
- Greenhalgh, K., Womack, J., Marcangelo, S. (2019) Injectate spread in erector spinae plane block. *Anaesthesia.* 74, 126–127.
- Gupta, Anju, Gupta, N., Choudhury, A., Agrawal, N. (2020) Erector spinae plane block using clonidine as an adjuvant for excision of chest wall tumor in a pediatric patient. *Ann Cord Anesth.* 23, 221.
- Gupta, Akhil, Jay, M.A., Williams, G. (2020) Evolving pediatric epidural practice: An institution’s clinical experience over 20 years—A retrospective observational cohort study. *Pediatric Anesth.* 30, 25–33.
- Gupta, A., Usha, U. (2014) Spinal anesthesia in children: A review. *J Anaesthesiol Clin Pharmacol.* 30, 10.

- Gürkan, Y., Aksu, C., Kuş, A., Yörükoğlu, U.H. (2020) Erector spinae plane block and thoracic paravertebral block for breast surgery compared to IV-morphine: A randomized controlled trial. *J Clin Anesth.* 59, 84–88.
- Gürkan, Y., Aksu, C., Kuş, A., Yörükoğlu, U.H., Kılıç, C.T. (2018) Ultrasound guided erector spinae plane block reduces postoperative opioid consumption following breast surgery: A randomized controlled study. *J Clin Anesth.* 50, 65–68.
- Guy's and St Thomas' NHS Foundation Trust. London, United Kingdom, Fandino, W. (2019) Erector Spinae Plane Block compared to Paravertebral Block in the post-operative pain management of patients undergoing elective Video-Assisted Thoracic Surgical lobectomy for lung cancer: a randomized, non-inferiority clinical trial protocol. *ppcrj.* 5.
- Hagen, J., Devlin, C., Barnett, N., Padover, A., Kars, M., Bebic, Z. (2019) Erector spinae plane blocks for pediatric cardiothoracic surgeries. *J Clinl Anesth.* 57, 53–54.
- Hamadnalla, H., Elsharkawy, H., Shimada, T., Maheshwari, K., Esa, W.A.S., Tsui, B.C.H. (2019) Cervical erector spinae plane block catheter for shoulder disarticulation surgery. *J Clinl Anesth.* 66, 1129–1131.
- Hamilton, D.L. (2019a) Does Thoracolumbar Intermuscular Plane Block Provide More Focused Analgesia Than Erector Spinae Plane Block in Lumbar Spine Surgery?: *J Neurosurg Anesthesiol.* 1.
- Hamilton, D.L. (2019b) Pneumothorax following erector spinae plane block. *J Clin Anesth.* 52, 17.
- Hamilton, D.L., Manickam, B.P. (2017) Is the erector spinae plane (ESP) block a sheath block? *Anaesthesia.* 72, 915–916.
- Hasan, M.A., Howard, R.F., Lloyd-Thomas, A.R. (1994) Depth of epidural space in children. *Anaesthesia.* 49, 1085–1087.
- Hernandez, M.A., Palazzi, L., Lapalma, J., Cravero, J. (2018) Erector spinae plane block for inguinal hernia repair in preterm infants. *Pediatric Anesth.* 28, 298–299.
- Hernandez, M.A., Palazzi, L., Lapalma, J., Forero, M., Chin, K.J. (2017) Erector Spinae Plane Block for Surgery of the Posterior Thoracic Wall in a Pediatric Patient: *Reg Anesth Pain Med.* 43(2):217-219
- Holland, E.L., Bosenberg, A.T. (2020) Early experience with erector spinae plane blocks in children. *Pediatr Anaesth.* 30, 96–107.

- Hong, J., Jung, S.W. (2016) Fluoroscopically Guided Thoracic Interlaminar Epidural Injection: A Comparative Epidurography Study Using 2.5 mL and 5 mL of Contrast Dye. *Pain Phys.* 19(7),E1013-E1018.
- Hong, J.H., Jung, S.W., Park, J.H. (2017) Posture Influences the Extent of Spread of Contrast Medium During Thoracic Epidurography: A Prospective Randomized Trial. *Pain Phys.* 20(6), 501–588.
- Ibbotson, W.J., Greenberg, R., Brendt, P. (2020) Erector Spinae Block for Chest Trauma in Aeromedical Prehospital and Retrieval Medicine. *Prehosp. Disaster med.* 1–3.
- Ilić, M.K., Matolić, M., Butković, D. n.d. Paravertebral block: review of the literature 3.
- Ince, I., Aksoy, M., Ozmen, O. (2019) Ultrasound guided erector spinae plane block for postoperative analgesia in a 13 year-old child undergoing abdominal surgery: A new approach. *J Clin Anesth.* 55, 77–78.
- Ip, V.H.Y., Sondekoppam, R.V., Özelsel, T.J.P. (2019) Evaluating the success of Erector Spinae Plane block: Believing is seeing? *J Clin Anesth.* 57, 5–6.
- Ivanusic, J., Konishi, Y., Barrington, M.J. (2018) A Cadaveric Study Investigating the Mechanism of Action of Erector Spinae Blockade: *Reg Anesth Pain Med.* 43, 567–571.
- Jadon, A., Swarupa, C., Amir, M. (2018) Fluoroscopic-guided erector spinae plane block: A feasible option. *Indian J Anaesth.* 62, 806.
- Jain, K., Jaiswal, V., Puri, A. (2018) Erector spinae plane block: Relatively new block on horizon with a wide spectrum of application – A case series. *Indian J Anaesth.* 62, 809.
- Kaplan, I., Jiao, Y., AuBuchon, J.D., Moore, R.P. (2018) Continuous Erector Spinae Plane Catheter for Analgesia After Infant Thoracotomy: A Case Report. *A&A Practice* 11, 250–252.
- Karaca, Ömer. (2019) Efficacy of Ultrasound-Guided Bilateral Erector Spinae Plane Block for Pediatric Laparoscopic Cholecystectomy: Case Series. *Agri.*
- Karaca, O., Pinar, H.U. (2020) Is high dose lumbar erector spinae plane block safe? *Clin J Anaesth.* 62, 109721.
- Karmakar, M.K., Booker, P.D., Franks, R., Pozzi, M. (1996) Continuous extrapleural paravertebral infusion of bupivacaine for post-thoracotomy analgesia in young infants. *Br J Anaesth.* 76, 811–815.

- Karmakar, M.K., Li, X., Ho, A.M.-H., Kwok, W.H., Chui, P.T. (2009) Real-time ultrasound-guided paramedian epidural access: evaluation of a novel in-plane technique. *Br J Anaesth.* 102, 845–854.
- Karmakar, M.K., Li, X., Li, J., Hadzic, A. (2012) Volumetric Three-Dimensional Ultrasound Imaging of the Anatomy Relevant for Thoracic Paravertebral Block: *Anesth Analg.* 115, 1246–1250.
- Kaushal, B., Chauhan, S., Magoon, R., Krishna, N.S., Saini, K., Bhoi, D., Bisoi, A.K. (2020) Efficacy of Bilateral Erector Spinae Plane Block in Management of Acute Postoperative Surgical Pain After Pediatric Cardiac Surgeries Through a Midline Sternotomy. *J Cardiothorac Vasc Anesth.* 34, 981–986.
- Keech, B.M. (2015) Thoracic epidural analgesia in a child with multiple traumatic rib fractures. *Clin J Anaesth.* 27, 685–691.
- Kendigelen, P., Özcan, R., Emre, Ş. (2016) Ultrasound-Guided Thoracic Paravertebral Block Experience in a Child. *Turk J Anaesthesiol Reanim.* 44, 57–58.
- Khorasanizadeh, S., Arabzadeh, B., Teymourian, H., Mohseni, G.R. (2020) Pectoral Nerve Block and Erector Spinae Plane Block and Post-Breast Surgery Complications. *Int J Cancer Manag.* 13.
- Kil, H.K. (2018) Caudal and epidural blocks in infants and small children: historical perspective and ultrasound-guided approaches. *Korean J Anesthesiol.* 71, 430–439.
- Krishna, S.N., Chauhan, S., Bhoi, D., Kaushal, B., Hasija, S., Sangdup, T., Bisoi, A.K. (2019) Bilateral Erector Spinae Plane Block for Acute Post-Surgical Pain in Adult Cardiac Surgical Patients: A Randomized Controlled Trial. *J. Cardiothorac. Vasc. Anesth.* 33, 368–375.
- Krishnan, S., Cascella, M. (2020) Erector Spinae Plane Block, in: StatPearls. StatPearls Publishing, Treasure Island (FL).
- Leeda, M., Stienstra, R., Arbous, M.S., Dahan, A., Th. Veering, B., Burm, A.G.L., Van Kleef, J.W. (2005) Lumbar epidural catheter insertion: the midline vs. the paramedian approach. *Eur J Anaesthesiol.* 22, 839–842.
- Le-Wendling, L., DeLoach, J., Haller, A., Ihnatsenka, B. (2014) Analgesia for the Trunk: A Comparison of Epidural, Thoracic Paravertebral and Transversus Abdominis Plane. DOI:10.5772/57403.

- Leyva, F.M., Mendiola, W.E., Bonilla, A.J., Cubillos, J., Moreno, D.A., Chin, K.J. (2017) Continuous Erector Spinae Plane (ESP) Block for Postoperative Analgesia after Minimally Invasive Mitral Valve Surgery. *J Cardiothorac Vas.* 108(1), E19-E20.
- Lima, F.V. de, Zandomenico, J.G., Prado, M.N.B. do, Favreto, D. (2020) Erector spinae plane block in pediatric orthopedic surgery: two case reports. *Braz J Anesthesio* (English Edition).
- Loader, J., Ford, P., n.d. Thoracic Paravertebral Block 4.
- Loftus, P.D., Elder, C.T., Russell, K.W., Spanos, S.P., Barnhart, D.C., Scaife, E.R., Skarda, D.E., Rollins, M.D., Meyers, R.L. (2016) Paravertebral regional blocks decrease length of stay following surgery for pectus excavatum in children. *J. Pediatr. Surg.* 51, 149–153.
- Lönnqvist, P.-A. (1992a) A formula for determining the distance from the skin to the lumbar epidural space in infants and children, *Pediatric Anesth.* 2, 305–307.
- Lönnqvist, P.-A. (1992b) Continuous paravertebral block in children.: Initial experience. *Anaesthesia.* 47, 607–609.
- Lönnqvist, P.A., MacKenzie, J., Soni, A.K., Conacher, I.D. (1995) Paravertebral blockade.: Failure rate and complications. *Anaesthesia.* 50, 813–815.
- López, M.B., Cadórniga, Á.G., González, J.M.L., Suárez, E.D., Carballo, C.L., Sobrino, F.P. (2018) Erector Spinae Block. A Narrative Review. *Central Eur J Clin Res.* 1, 28–39.
- Luftig, J., Mantuani, D., Herring, A.A., Dixon, B., Clattenburg, E., Nagdev, A. (2017) Successful emergency pain control for posterior rib fractures with ultrasound-guided erector spinae plane block. *Am J Emerg Med.* 36(8), 1391–1396.
- Luis-Navarro, J.C., Seda-Guzmán, M., Luis-Moreno, C., López-Romero, J.L. (2018) The erector spinae plane block in 4 cases of video-assisted thoracic surgery. *Res Esp Anesthesiol* (English Edition). 65(4), 204 - 208.
- Luyet, C., Eichenberger, U., Greif, R., Vogt, A., Szücs Farkas, Z., Moriggl, B. (2009) Ultrasound-guided paravertebral puncture and placement of catheters in human cadavers: an imaging study. *Br J Anaesth.* 102, 534–539.
- Ma, D., Ren, H., Li, X., Li, H., Jiang, J., Wu, A., Wang, Y. (2020) Ultrasound-guided single erector spinae plane block versus thoracic paravertebral block for patients undergoing video-assisted thoracoscopic lobectomy: a single center randomized controlled trial (preprint). In Review. DOI:10.21203/rs.2.14933/v2

- Macaire, P., Ho, N., Nguyen, T., Nguyen, B., Vu, V., Quach, C., Roques, V., Capdevila, X. (2019) Ultrasound-Guided Continuous Thoracic Erector Spinae Plane Block Within an Enhanced Recovery Program Is Associated with Decreased Opioid Consumption and Improved Patient Postoperative Rehabilitation After Open Cardiac Surgery—A Patient-Matched, Controlled Before-and-After Study. *J Cardiothorac Vasc Anesth.* 33, 1659–1667.
- Marcelino, R., Sawardekar, A., Suresh, S. (2019) Neuraxial anaesthesia in paediatrics. *Anaesth intens care.* 20, 338–343.
- Martin, L.D., Adams, T.L., Duling, L.C., Grigg, E.B., Bosenberg, A., Onchiri, F., Jimenez, N. (2019a) Comparison between epidural and opioid analgesia for infants undergoing major abdominal surgery. *Paediatr Anaesth.* 29, 835–842.
- Masir, F., Driessen, J.J., Thies, K.C., Wijnen, M.H., Egmond, J.V. (2006) Depth of the thoracic epidural space in children. 5.
- McClymont, W., Celnick, D. (2018) Techniques of epidural block. *Anaesth Inten Care Med.* 19, 600–606.
- McLeod, G., Cumming, C. (2004) Thoracic epidural anaesthesia and analgesia. Continuing Education in Anaesthesia. *Anesth Crit Care PA.* 4, 16–19.
- Meignier, M., Souron, R., Le Neel, J.C. (1983) Postoperative dorsal epidural analgesia in the child with respiratory disabilities. *Anesthesiology.* 59, 473–475.
- Missair, A., Flavin, K., Paula, F., Marrero, E.B. de, Lopez, J.B., Matadial, C. (2019) Leaning Tower of Pisa? Avoiding a major neurologic complication with the erector spinae plane block. *Reg Anesth Pain Med.* 44, 713–714.
- Moore, R., Kaplan, I., Jiao, Y., Oster, A. (2018) The use of continuous Erector Spinae Plane blockade for analgesia following major abdominal surgery in a one-day old neonate. *J Clin Anesth.* 49, 17–18.
- Moore, R.P., Liu, C.-J.J., George, P., Welch, T.P., AuBuchon, J.D., Jiao, Y., Drobish, J.K. (2019) Early experiences with the use of continuous erector spinae plane blockade for the provision of perioperative analgesia for pediatric liver transplant recipients. *Reg Anesth Pain Med.* 44(6), 679–682.
- Mostafa, S.F., Abdelghany, M.S., Abdelraheem, T.M., Abu Elyazed, M.M. (2019) Ultrasound-guided erector spinae plane block for postoperative analgesia in pediatric patients undergoing splenectomy: A prospective randomized controlled trial. *Pediatr Anaesth.* 13758.

- Muñoz, F., Cubillos, J., Bonilla, A.J., Chin, K.J. (2017) Erector spinae plane block for postoperative analgesia in pediatric oncological thoracic surgery. *Can J Anesth.* 64, 880–882.
- Munshey, F., Caruso, T.J., Wang, E.Y., Tsui, B.C.H. (2018a) Programmed Intermittent Bolus Regimen for Erector Spinae Plane Blocks in Children: A Retrospective Review of a Single-Institution Experience. *Anesth Analg.* 1.
- Munshey, F., Rodriguez, S., Diaz, E., Tsui, B. (2018b) Continuous erector spinae plane block for an open pyeloplasty in an infant. *J Clin Anesth.* 47, 47–49.
- Nagaraja, P.S., Ragavendran, S., Singh, N.G., Asai, O., Bhavya, G., Manjunath, N., Rajesh, K. (2018) Comparison of continuous thoracic epidural analgesia with bilateral erector spinae plane block for perioperative pain management in cardiac surgery. *Ann Card Anaesth.* 21, 323–327.
- Nair, A., Seelam, S., Naik, V., Rayani, B. (2018) Opioid-free mastectomy in combination with ultrasound-guided erector spinae block: A series of five cases. *Indian J Anaesth.* 62, 632.
- Nair, A.S., See
lam, S. (2019) The risks associated with erector spinae plane block in patients with abnormalities of coagulation. *Korean J Anesthesiol.* 72, 275–276.
- Nair, S., Gallagher, H., Conlon, N. (2020) Paravertebral blocks and novel alternatives. *Br J Anaesth. Education.* 20, 158–165.
- Nair, S., McGuinness, S., Masood, F., Boylan, J.F., Conlon, N.P. (2019) Erector Spinae Plane Blocks in Major Hepatopancreaticobiliary Surgery: A Case Series. *A&A Practice.* 13, 332–334.
- Naja, Z., Lönnqvist, P.-A. (2001) Somatic paravertebral nerve blockade Incidence of failed block and complications. *Anaesthesia.* 56, 1181–1201.
- Narayanan, M., Venkataraju, A. (2019) Transverse approach to the erector spinae block: is there more? *Reg Anesth Pain Med.* 44, 529–530.
- Nardiello, M.A., Herlitz, M. (2018) Bloqueo bilateral del plano del músculo erector de la columna espinal para cirugía de pectus excavatum y pectus carinatum en pacientes pediátricos. *Res Esp Anesthesiol (English Edition).* 65, 530–533.
- Ng, D.S.C., Chazapis, D.M., West, D.S. (2018) Ultrasound-Guided Paravertebral Block.

- Ohgoshi, Y., Ando, A., Kubo, E.N. (2020a) Paravertebral spread after different nerve blocks in the peri-paravertebral area. *J Clin Anesth.* 62, 109747.
- Ohgoshi, Y., Ohtsuka, A., Takeda, Y. (2020b) Membrane-mediated paravertebral spread after modified erector spinae plane blocks: A cadaveric study. *J Clin Anesth.* 65, 109880.
- Ohgoshi, Y., Usui, Y., Ando, A., Takeda, Y., Ohtsuka, A. (2019) Injection at the costotransverse notch facilitates paravertebral spread of the erector spinae plane block: A cadaveric study. *J Clin Anesth.* 109630.
- Öksüz, G., Arslan, M., Bilal, B., Gişi, G., Yavuz, C. (2020) Ultrasound guided sacral erector spinae block for postoperative analgesia in pediatric anoplasty surgeries. *J Clin Anesth.* 60, 88.
- Onishi, E., Toda, N., Kameyama, Y., Yamauchi, M. (2019) . *BioMed Res Int.* 2019, 1–8.
- Özkalaycı, Ö., Çetin, S., Yenigün, Y., Karakaya, M.A., Gürkan, Y., Erçelen, Ö. (2020) Erector spinae plane block for peroral endoscopic myotomy analgesia in pediatric patients. *Reg Anesth Pain Med.* 45, 482–482.
- Page, E.A., Taylor, K.L. (2017) Paravertebral block in paediatric abdominal surgery'a systematic review and meta-analysis of randomized trials. *Br J Anaesth.* 118, 159–166.
- Pak, A., Singh, P. (2020) Epidural-Like Effects With Bilateral Erector Spinae Plane Catheters After Abdominal Surgery: A Case Report. *A&A Practice.* 14, 137–139.
- Paraskeuopoulos, T., Saranteas, T., Kouladouros, K., Krepi, H., Nakou, M., Kostopanagiotou, G., Anagnostopoulou, S. (2010) Thoracic paravertebral spread using two different ultrasound-guided intercostal injection techniques in human cadavers. *Clin Anat.* 23, 840–847.
- Patel, D. (2006) Epidural analgesia for children. *Anaesth Crit Care PA.* 6, 63–66.
- Patel, N.V., Glover, C., Adler, A.C. (2019) Erector Spinae Plane Catheter for Postoperative Analgesia After Thoracotomy in a Pediatric Patient: A Case Report. *A&A Pract.* 12, 299–301.
- Pathak, N., Krishna, B. (2020) Erector Spinae Block in a Patient Posted for Nephrectomy with History of Spine Surgery. *J Evid Based Med Health.* 7, 887–889.
- Pawa, A., Wojcikiewicz, T., Barron, A., El-Boghdadly, K. (2019) Paravertebral Blocks: Anatomical, Practical, and Future Concepts. *Curr Anesthesiol Rep.* 9, 263–270.

- Petsas, D., Pogiati, V., Galatidis, T., Drogouti, M., Sofianou, I., Michail, A., Chatzis, I., Donas, G. (2018) Erector spinae plane block for postoperative analgesia in laparoscopic cholecystectomy: a case report. *J Pain Res.* 11, 1983–1990.
- Piliego, C., Longo, F., Agrò, F. (2020) Erector spinae plane block growing potential: Pain management in laparoscopy nephrectomy. *Saudi J Anaesth.* 14, 275.
- Piraccini, E., Biondi, G., Corso, R.M., Maitan, S. (2019) Should we assess the epidural anaesthetic spread during ultrasound-guided thoracic paravertebral block? *Tumori.* 105, 533–534.
- Piraccini, E., Byrne, H., Taddei, S. (2020a) Superior costotransverse ligament: a new target for fascial plane blocks. *Reg Anesth Pain Med.* 2020-101315
- Piraccini, E. (2020b) Rhomboid Intercostal Block for Breast Surgery: An Alternative to the Erector Spinae Plane Block? *Turk J Anaesthesiol Reanim.* 48,346-347.
- Piraharkhiz, N., Comolli, K., Fujiwara, W., Stasiewicz, S., Boyer, J.M., Begin, E.V., Rubinstein, A.J., Henderson, H.R., Lazar, J.F., Watson, T.J., Eger, C.M., Trankiem, C.T., Phillips, D.G., Khaitan, P.G. (2020) Utility of erector spinae plane block in thoracic surgery. *J Cardiothorac Surg.* 15, 91.
- Ponde, V. (2019) Recent trends in paediatric regional anaesthesia. *Indian J Anaesth.* 63, 746.
- Ponde, V., Desai, A. (2012) Echo-guided estimation of formula for paravertebral block in neonates, infants and children till 5 years. *Indian J Anaesth.* 56, 382.
- Pourkashanian, A., Narayanan, M., Venkataraju, A. (2019) The Erector Spinae Plane Block: A Review of Current Evidence. 11.
- Rapp, H.-J., Folger, A., Grau, T. (2005) Ultrasound-Guided Epidural Catheter Insertion in Children: *Anesth Analg.* 101, 333–339.
- Reich, A., Strümper, D. (2000) Lumbar and thoracic epidural anaesthesia in children. *Best Pract Res Clin Anaesthesiol.* 14, 731–743.
- Reina, M., Sala-Blanch, X. (2015) Ultrastructure of the Epineurium. Atlas of Functional Anatomy for Regional Anesthesia and Pain Medicine. Springer, Cham.
- Richardson, J., Groen, G.J. (2005) Applied epidural anatomy. *Anaesth Crit Care PA.* 5, 98–100.
- Rincón, C., Moreno, D.A., Moore, A. (2020) Erector spinae plane block for post-caesarean delivery analgesia. *Int J Obstet Anesth.* 41, 120–122

- Roy, R., Agarwal, G., Pradhan, C., Kuanar, D. (2020) RACK approach to erector spinae plane block. *J Anaesthesiol Clin Pharmacol.* 36, 120–121.
- Ruscio, L., Renard, R., Lebacle, C., Zetlaoui, P., Benhamou, D., Bessede, T. (2020) Thoracic paravertebral block: comparison of different approaches and techniques. A study on 27 human cadavers. *Anaesth Critl Care PA.* 39, 53–58.
- Sahin, A., Gültekin, A., Yildirim, I., Baran, O., Arar, C. (2020) Ultrasound Guided Erector Spinae Block with Costotransverse Ligament Puncture Is More Effective than Erector Spinae Block Alone; Eight Cases for Oncologic Breast Surgery; A Brief Technical Report. *Open J Anesthesiology.* 10, 179–189.
- Saito, T., Den, S., Tanuma, K., Tanuma, Y., Carney, E., Carlsson, C. n.d. Anatomical bases for paravertebral anesthetic block: fluid communication between the thoracic and lumbar paravertebral regions. *Region Anesth Pain M.* 21(6). 359–363.
- Sakae, T.M., Yamauchi, L.H.I., Takaschima, A.K.K., Brandão, J.C., Benedetti, R.H. (2020) Comparison between erector spinal plane block and epidural block techniques for postoperative analgesia in open cholecystectomies: a randomized clinical trial. *Braz J Anaesth (English Edition).* 70, 22–27.
- Saranteas, T., Paraskeuopoulos, T., Anagnostopoulou, S., Kanellopoulos, I., Mastoris, M., Kostopanagiotou, G. (2010) Ultrasound anatomy of the cervical paravertebral space: a preliminary study. *Surg Radiol Anat.* 32, 617–622.
- Sawardekar, A., Szczodry, D., Suresh, S. (2013) Neuraxial anaesthesia in paediatrics. *Anaesth Intens Care Med.* 14, 251–254.
- Schwartzmann, A., Peng, P., Maciel, M.A., Alcarraz, P., Gonzalez, X., Forero, M. (2020) A magnetic resonance imaging study of local anesthetic spread in patients receiving an erector spinae plane block. *Can J Anesth.* 67(8):942-948
- Schwartzmann, A., Peng, P., Maciel, M.A., Forero, M. (2018) Mechanism of the erector spinae plane block: insights from a magnetic resonance imaging study. *Can J Anesth.* 65, 1165–1166.
- Selvi, O., Tulgar, S. (2018) Ultrasound guided erector spinae plane block as a cause of unintended motor block. *Rev Esp Anesthesiol (English Edition).* 65, 589–592.
- Shan, Z., Chu, H., Wang, S., Liang, Y. (2020) Should erector spinae plane block be routinely used for postoperative analgesia? *J Clin Anesth.* 60, 16.

- Shibata, Y., Kampitak, W., Tansatit, T. (2020) The Novel Costotransverse Foramen Block Technique: Distribution Characteristics of Injectate Compared with Erector Spinae Plane Block. *Pain Physician*. 10.
- Shokri, H., Kasem, A. (2020) Analgesic efficacy of erector spinae block in comparison to thoracic epidural anesthesia in patients undergoing transthoracic esophageal surgical procedure. *Res Opin Anesth Intensive Care*. 7, 124.
- Simpao, A.F., Gálvez, J.A., Wartman, E.C., England, W.R., Wu, L., Rehman, M.A., Ngo, T.V. (2019) The Migration of Caudally Threaded Thoracic Epidural Catheters in Neonates and Infants. *Anesth Analg*. 129, 477–481.
- Singh, S., Jacob, M., Hasnain, S., Krishnakumar, M. (2017) Comparison between continuous thoracic epidural block and continuous thoracic paravertebral block in the management of thoracic trauma. *Med J Armed Forces India*. 73, 146–151.
- Sondekoppam, R.V., Uppal, V., Brookes, J., Ganapathy, S. (2019) Bilateral Thoracic Paravertebral Blocks Compared to Thoracic Epidural Analgesia After Midline Laparotomy: A Pragmatic Noninferiority Clinical Trial. *Anesth Analg*. 129, 855–863.
- Spencer, S. Liu., Brian, M. Block., Christopher, L. Wu. (2004) Effects of Perioperative Central Neuraxial Analgesia on Outcome after Coronary Artery Bypass Surgery: A Meta-analysis. *Anesthesiology*. 101:153–161
- Sullivan, T.R., Kanda, P., Gagne, S., Costache, I. (2019) Harlequin Syndrome Associated with Erector Spinae Plane Block: *Anesthesiology*. 131, 665.
- Taketa, Y., Fujitani, T. (2017) Approach affects injectate spread in ultrasound-guided thoracic paravertebral block: a cadaveric trial. *Br J Anaesth*. 119, 339–340.
- Tardieu, G.G., Fisahn, C., Loukas, M., Moisi, M., Chapman, J., Oskouian, R.J., Tubbs, R.S. (2016) The Epidural Ligaments (of Hofmann): A Comprehensive Review of the Literature. *Cureus*. 8.
- Teeter, E.G., Kumar, P.A. (2015) Pro: Thoracic Epidural Block Is Superior to Paravertebral Blocks for Open Thoracic Surgery. *J Cardiothorac Vasc Anesth*. 29, 1717–1719.
- Thomas, D.T., Tulgar, S. (2018) Ultrasound-guided Erector Spinae Plane Block in a Child Undergoing Laparoscopic Cholecystectomy. *Cureus*. 10(2):e2241.
- Tighe, S.Q.M., Greene, M.D., Rajadurai, N. (2010) Paravertebral block. *Contin Educ Anaesth Crit Care Pain*. 10, 133–137.

- Tobias, J.D., Lowe, S., O'Dell, N., Holcomb, G.W. (1993) Thoracic epidural anaesthesia in infants and children. *Can J Anaesth.* 40, 879–882.
- Tsui, B.C.H., Fonseca, A., Munshey, F., McFadyen, G., Caruso, T.J. (2019) The erector spinae plane (ESP) block: A pooled review of 242 cases. *J Clin Anesth.* 53, 29–34.
- Tsui, B.C.H., Navaratnam, M., Boltz, G., Maeda, K., Caruso, T.J. (2018) Bilateral automatized intermittent bolus erector spinae plane analgesic blocks for sternotomy in a cardiac patient who underwent cardiopulmonary bypass: A new era of Cardiac Regional Anesthesia. *J Clin Anesth.* 48, 9–10.
- Tsui, B.C.H., Suresh, S. (2010) Ultrasound Imaging for Regional Anesthesia in Infants, Children, and Adolescents A Review of Current Literature and Its Application in the Practice of Extremity and Trunk Blocks. *Anesthesiology.* 112, 473–492.
- Tukaç, ismail cem. (2019) Erector spinae plane block as rescue analgesia in gestational week 16. *Agri.* 31(4):214-215.
- Tulgar, S., Ahiskalioglu, A., De Cassai, A., Gurkan, Y. (2019a) Efficacy of bilateral erector spinae plane block in the management of pain: current insights. *J Pain Res.* 12, 2597–2613.
- Tulgar, S., Kapakli, M.S., Kose, H.C., Senturk, O., Selvi, O., Serifsoy, T.E., Thomas, D.T., Ozer, Z. (2019b) Evaluation of Ultrasound-Guided Erector Spinae Plane Block and Oblique Subcostal Transversus Abdominis Plane Block in Laparoscopic Cholecystectomy: Randomized, Controlled, Prospective Study. *Anesth Essays Res.* 13, 50–56.
- Tulgar, S., Selvi, O., Senturk, O., Serifsoy, T.E., Thomas, D.T. (2019c) Ultrasound-guided Erector Spinae Plane Block: Indications, Complications, and Effects on Acute and Chronic Pain Based on a Single-center Experience. *Cureus.* 11(1):e3815.
- Ueshima, H., Hiroshi, O. (2018) Spread of local anesthetic solution in the erector spinae plane block. *J Clin Anesth.* 45, 23.
- Ueshima, H., Inagaki, M., Toyone, T., Otake, H. (2019) Efficacy of the Erector Spinae Plane Block for Lumbar Spinal Surgery: A Retrospective Study. *Asian Spine J.* 13, 254–257.
- Ueshima, H., Otake, H. (2018) Clinical experiences of erector spinae plane block for children. *J Clinical Anesth.* 44, 41.

- Uppal, V., Sondekoppam, R.V., Sodhi, P., Johnston, D.F., Ganapathy, S. (2017) Single-Injection Versus Multiple-Injection Technique of Ultrasound-Guided Paravertebral Blocks: A Randomized Controlled Study Comparing Dermatomal Spread. *Reg Anesth Pain Med.* 42(5), 575–581.
- Vadera, H., Mistry, T. (2019) Erector spinae plane block: Anatomical landmark-guided technique. *Saudi J Anaesth.* 13, 268.
- Vas, L., Kulkarni, V., Mali, M., Bagry, H. (2003) Spread of radioopaque dye in the epidural space in infants. *Paediatr Anaesth.* 13, 233–243.
- Verduzco, L.A. (2020) Erector spinae plane block as primary anesthetic for kyphoplasty. *J Clin Anesth.* 61, 109670.
- Vidal, E., Giménez, H., Forero, M., Fajardo, M. (2018) Erector spinae plane block: A cadaver study to determine its mechanism of action. *Rev Esp Anesthesiol (English Edition)* .65, 514–519.
- Visoiu, M., Scholz, S. (2019) Thoracoscopic visualization of medication during erector spinae plane blockade. *J Clin Anesth.* 57, 113–114.
- Wani, T., Beltran, R., Veneziano, G., AlGhamdi, F., Azzam, H., Akhtar, N., Tumin, D., Majid, Y., Tobias, J.D. (2018) Dura to Spinal Cord Distance at Different Vertebral Levels in Children and Its Implications on Epidural Analgesia: A Retrospective Mri-Based Study. *Pediatr Anesth.* 28, 338–341.
- Wani, T.M., Rafiq, M., Nazir, A., Azzam, H.A., Al Zuraigi, U., Tobias, J.D. (2017) Estimation of the depth of the thoracic epidural space in children using magnetic resonance imaging. *J Pain Res.* 10, 757–762.
- Warusawitharana, C., Tariq, Z., Jackson, B., Niraj, G. (2019) Continuous Erector Spinae Plane and Intrathecal Opioid Analgesia: Novel Regimen Avoiding Thoracic Epidural Analgesia and Systemic Morphine in Open Radical Cystectomy. *A&A Pract.* 12, 212–214.
- Wellbeloved, M.A., Kemp, E. (2020) Bilateral erector spinae catheter placement for bilateral nephrectomy in a paediatric patient. *Indian J Anesth.* 64, 81.
- Willard, F.H., Vleeming, A., Schuenke, M.D., Danneels, L., Schleip, R. (2012) The thoracolumbar fascia: anatomy, function and clinical considerations: The thoracolumbar fascia. *J Anat.* 221, 507–536.

- Wong, J., Lim, S.S.T. (2019) Skin-to-epidural distance in the Southeast Asian paediatric population: multiethnic morphometrics and international comparisons. *Singap Med J.* 60, 136–139.
- Wong, J., Navaratnam, M., Boltz, G., Maeda, K., Ramamurthi, R.J., Tsui, B.C.H. (2018) Bilateral continuous erector spinae plane blocks for sternotomy in a pediatric cardiac patient. *J Clin Anesth.* 47, 82–83.
- Wyatt, K., Elattary, T. (2019) The erector spinae plane block in a high-risk Ehlers-Danlos syndrome pediatric patient for vascular ring repair. *J Clin Anesth.* 54, 39–40.
- Yang, H.-M., Choi, Y.J., Kwon, H.-J., O, J., Cho, T.H., Kim, S.H. (2018) Comparison of injectate spread and nerve involvement between retrolaminar and erector spinae plane blocks in the thoracic region: a cadaveric study. *Anaesthesia.* 73, 1244–1250.
- Yanovski, B., Gat, M., Gaitini, L., Ben-David, B. (2013) Pediatric thoracic paravertebral block: roentgenologic evidence for extensive dermatomal coverage. *J Clin Anesth.* 25, 214–216.
- Yoo, S., Lee, D., Moon, D., Song, H., Jang, Y., Kim, J. (2012) Anatomical Investigations for Appropriate Needle Positioning for Thoracic Paravertebral Blockade in Children. *J Int Med Res.* 40, 2370–2380.
- Yörükoğlu, H.U., Aksu, C., Tor Kılıç, C., Gürkan, Y. (2019) Bilateral erector spinae plane block with single injection. *J Clin Monit Comput.* 33(6), 1145-1146.
- Zhang, J., He, Y., Wang, S., Chen, Z., Zhang, Y., Gao, Y., Wang, Q., Xia, Y., Papadimos, T.J., Zhou, R. (2020) The erector spinae plane block causes only cutaneous sensory loss on ipsilateral posterior thorax: a prospective observational volunteer study. *BMC Anesthesiol.* 20.
- Zhao, H., Xin, L., Feng, Y. (2020) The effect of preoperative erector spinae plane vs. paravertebral blocks on patient-controlled oxycodone consumption after video-assisted thoracic surgery: A prospective randomized, blinded, non-inferiority study. *J Clin Anesth.* 62, 109737.

A cadaveric study of the erector spinae plane block in a neonatal sample

Sabashnee Govender ^{1,2}, Dwayne Mohr,² Adrian Bosenberg,³
Albert Neels Van Schoor ²

¹Department of Anatomy, Sefako Makgatho Health Sciences University, Pretoria, Gauteng, South Africa

²Department of Anatomy, University of Pretoria, Pretoria, Gauteng, South Africa

³Department of Anaesthesiology and Pain Management, University Washington, Seattle Children's Hospital, Seattle, Washington, USA

Correspondence to

Sabashnee Govender, Anatomy, Sefako Makgatho Health Sciences University, Pretoria, Gauteng, South Africa; g.sabashnee@yahoo.com

Received 10 September 2019
Revised 20 January 2020
Accepted 22 January 2020
Published Online First
10 February 2020

ABSTRACT

Background The aim of this article was to provide a detailed description of the neonatal anatomy related to the erector spinae plane block and to report the spread of the dye within the fascial planes and potential dermatomal coverage.

Methods Using ultrasound guidance, the bony landmarks and anatomy of the erector spinae fascial plane space were identified. The erector spinae plane block was then replicated unilaterally in two fresh unembalmed neonatal cadavers. Using methylene blue dye, the block was performed at vertebral levels T5—using 0.5 mL in cadaver 1—and T8—using 0.2 mL in cadaver 2. The craniocaudal spread of dye was tracked within the space on the ultrasound screen and further confirmed on dissection.

Results Craniocaudal spread was noted from vertebral levels T3 to T6 when the dye was introduced at vertebral level T5 and from vertebral levels T7 to T11 when the dye was introduced at vertebral level T8. Furthermore, the methylene blue spread was found anteriorly in the paravertebral and epidural spaces, staining both the dorsal and ventral rami of the spinal nerves T2 to T12. Small amounts of dye were also found in the intercostal spaces.

Conclusion In two neonatal fresh cadavers, the dye was found to spread to multiple levels and key anatomic locations.

INTRODUCTION

The erector spinae plane (ESP) block is a novel ultrasound-guided interfascial technique serendipitously discovered while treating thoracic neuropathic pain in an adult.^{1,2} ESP has further been reported to successfully manage acute and chronic pain for truncal procedures.^{3,4} This 'happily accidental' block has been compared with other neuraxial techniques such as the epidural and paravertebral block and may prove to be a safer alternative.⁴ Although the ESP block has been successful in the adult population, there are only 42 documented cases (as of December 2019) in neonates, infant, and children.^{5–14} Despite the increasing number of indications for the ESP block, the anatomy, mechanism of action, concentration, and volume of anesthetic is yet to be determined especially in neonates and children.^{3,5}

OBJECTIVES

The aim of this study was to provide a detailed description of the anatomy related to the ESP block

in a small neonatal sample. The extent of the spread of a fluid—in this case, methylene blue dye—was also determined.

MATERIALS AND METHODS

This study was approved by the PhD and Research Ethics Committee, University of Pretoria, South Africa. Two fresh unembalmed neonatal cadavers subject to cryopreservation were obtained through the National Tissue Bank, University of Pretoria. We performed a unilateral ESP block at the T5 vertebral level in cadaver 1 and at the T8 vertebral level in cadaver 2. Both cadavers were preterm stillborn. Cadaver 1 weighed 1.6 kg and was 370 mm long, cadaver 2 weighed 0.6 kg and was only 350 mm long. An Edge™ Ultrasound machine (ref: P15000-11, SN-03P55Z) with a 6-13 MHz linear array probe (footprint size of 2.5 cm) was used in both procedures. The methylene blue mixture consisted of 10 mL of iodinated contrast material, diluted in 85 mL normal saline.

Cadavers were placed in the prone position, the spinous process and its corresponding transverse processes were identified with the aid of ultrasound. Subsequently, an ultrasound transducer was repositioned in both a transverse and parasagittal alignment to identify anatomical structures.

For the procedure, the transducer was placed parasagittally over the transverse process of T5 and T8, respectively, about 1 cm lateral to the spinous process. Using an in-plane approach a 21 mm needle was then directed in a cephalad to the caudal direction towards the transverse process. Once the tip of the needle contacted the transverse process, 0.05 mL of saline solution was injected to confirm the position of the needle tip. The erector spinae fascial plane space was further confirmed as the erector spinae muscle bundle was hydro dissected away from the transverse process. Methylene blue dye (0.5 mL for the first cadaver and 0.2 mL for the second cadaver) was then injected while observing the spread of the dye within the plane between the erector spinae muscle group and the transverse processes on the ultrasound screen. Dissections were then performed 30 min after the dye injection.

RESULTS

After exposure to the relevant tissue planes extensive dye spread was noted in a craniocaudal direction, both superficial and deep to the erector spinae fascial plane (figure 1). In the first cadaver, the dye was injected unilaterally (left side) at vertebral level T5 to determine the spread in the thoracic region.



© American Society of Regional Anesthesia & Pain Medicine 2020. No commercial re-use. See rights and permissions. Published by BMJ.

To cite: Govender S, Mohr D, Bosenberg A, et al. *Reg Anesth Pain Med* 2020;**45**:386–388.



Figure 1 Photographic image showing the superficial staining of the erector spinae muscle as well as the spread of dye deep to it.

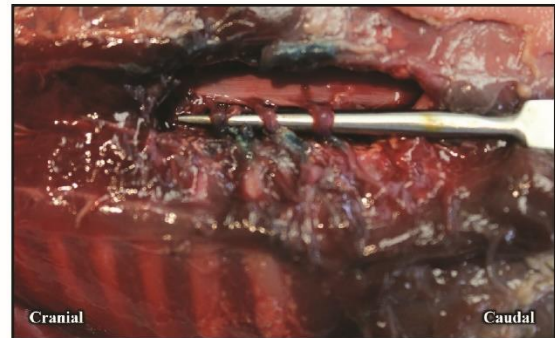


Figure 3 Photographic image revealing the staining of the rami of spinal nerves.

Based on surface staining, the dye spread from vertebral levels T2 to T12. Superficially, the trapezius, rhomboids, latissimus dorsi, and erector spinae muscles were stained by the methylene blue dye. Deeper, the dye was located over the posterior aspect of the transverse process, near the costotransverse ligament (foramen) (figure 2). Staining spread from T3 to T6 at the ventral and dorsal roots/ganglion level (figures 3 and 4). In the second cadaver, the dye was also injected on the left side but at the T8 level to determine the spread over the abdominal dermatomes. Based on superficial staining, the dye spread from vertebral levels T7 to L1, that is, superficial to the trapezius, latissimus dorsi, and erector spinae muscles. The ventral and dorsal roots/ganglion were stained from T7 to T11. (figures 3 and 4). In both cases, methylene blue dye was seen in the paravertebral and epidural spaces. The dura mater surrounding the spinal cord was found to be stained before the spinal cord was then cut and removed to expose the ventral and dorsal rami.

DISCUSSION

The ESP block is a novel technique that can be used as an alternative block for truncal procedures. We found that in fresh neonatal cadavers, injecting 0.2 and 0.5 mL of dye into the erector spinae fascial plane space at vertebral level T5 and T8 spreads 4–5 levels for the thoracic and abdominal regions, respectively. Although the exact dose for neonates, infants, or children has yet to be established, the spread in this small study suggests that 0.1 mL/kg per dermatome may be a useful guide.¹⁵

As dye was injected in close proximity to the costotransverse foramen, we found that the dye penetrates anteriorly through the intertransverse connective tissue, into the paravertebral, epidural, and intercostal spaces to stain the ventral and dorsal rami of the spinal nerves.¹⁶

Hamilton and Manickam suggested that the erector sheath is the reason for the success of the ESP block.¹⁷ They suggested that the sheath is intermittently tethered anteromedially to the bony structures along its course, resulting in multiple varied apertures or perforations.¹⁷

Supporting both Hamilton and Manikam, we believe that the erector sheath and the thoracolumbar fascia combine to form a continuous tissue plane over multiple vertebral levels, allowing for the craniocaudal spread of dye. Furthermore, the anterior perforations within the sheath explain the mechanism of anterior spread into the paravertebral, epidural, and intercostal spaces as seen in this study. We hypothesize that the anterior perforations may be attributed to the porous tissue found around the superior costotransverse ligament. Additionally, the spread could have been further facilitated through the costotransverse foramen that acts as a bony gap. The findings in this study are similar to that of other authors who suggest that the success of this block is due to the diffusion of local anesthetic through soft tissue gaps.^{3,18}

At dissection, some staining was also noted in the overlying muscular structures—the trapezius and rhomboid muscles—posterior to the erector spinae muscle at vertebral level T5.



Figure 2 Photographic image displaying the cleaned lamina, transverse process, and parts of the ribs.



Figure 4 Photographic image showing the dye staining of the intercostal nerves as the dye partially spread into the intercostal spaces.

Brief technical report

Barker and Briggs, concluded in their study, that a layer of the thoracolumbar fascia fuses with the muscular fascia of the trapezius and rhomboid muscles, which may account for the posterior staining seen in this study.¹⁹

Technical difficulties in the application of this block could result from the thinner muscle layers, sliding fascial planes and loose connective tissues in neonates and children.^{18,20} Therefore, a finer needle, for example, 27 G facilitates needle tip placement within these thin layers.

The spread of ESP block has been determined in adults. Ivanusic and co-workers reported on the lack of spread to the ventral rami.¹ Adhikary and others, not only reported a ventral and dorsal rami spread but also an epidural and intercostal space spread.³ Takata and colleagues reported that although the ESP block provided tolerable anesthesia for thoracoscopic lobectomy, it also provided weak dermatomal spread towards the anterior cutaneous region.³ Several authors, including Chin and co-workers, confirmed analgesic spread for the thoracic and abdominal regions when performing the block at vertebral levels T4/T5 and T7/T8, respectively.^{21,22}

The question of anatomical differences between age groups arises because of the contradicting results from various cadaveric studies performed predominantly in adults.^{16,17,19–21} Apart from the demographics such as weight, height and body shape, anatomical differences between neonates, infants children, and adults do exist. Factors such as the developmental formation of the vertebral curvature may contribute to the differences in paravertebral tissue and muscle thickness seen between age groups. Furthermore, given the more elastic pediatric spine,¹⁸ together with the less dense ligaments and cartilaginous laminae could allow for a more favorable spread in neonates and infants.²³ This would also affect the depth at which the ESP block is performed. Incomplete myelination of nerve fibers in neonates and infants allows lower concentration and volume of anesthetic required to perform the block.¹⁴

CONCLUSIONS

In two fresh neonatal cadavers, small amounts of dye injected into the ESP spread to the paravertebral, epidural, and intercostal spaces. Additionally, the dye was found to spread over multiple dermatomal levels while targeting the ventral and dorsal rami from T2 to T12. Clinical studies will be needed to identify if ESP blocks offer advantages over paravertebral or epidural injections in children and neonates.

Acknowledgements The authors gratefully acknowledge the donated cadaveric specimens, without which this research would not have been possible.

Contributors SG: conception and design of the study, acquisition of data, analysis and interpretation of data, drafting the article, revising it critically for important intellectual content, final approval of the version to be submitted. DM: acquisition of data and revising it critically for important intellectual content. AB: revising it critically for important intellectual content. ANVS: conception and design of the study, revising it critically for important intellectual content and final approval of the version to be submitted.

Funding This study was funded by National Research Foundation (NRF).

Competing interests None declared.

Patient consent for publication Not required.

Provenance and peer review Not commissioned; externally peer reviewed.

ORCID iDs

Sabashnee Govender <http://orcid.org/0000-0001-6738-9071>

Albert Neels Van Schoor <http://orcid.org/0000-0001-9813-0441>

REFERENCES

- Ivanusic J, Konishi Y, Barrington MJ. A cadaveric study investigating the mechanism of action of erector spinae blockade. *Reg Anesth Pain Med* 2018;43:567–71.
- Forero M, Adhikary SD, Lopez H, et al. The erector spinae plane block: a novel analgesic technique in thoracic neuropathic pain. *Reg Anaesth Pain Med* 2016;41:621–7.
- López MB, Cadórniga Álvaro Gasalla, González JML, et al. Erector spinae block. A narrative review. *Eur J Med Res* 2018;1:28–39.
- Vidal E, Giménez H, Forero M, et al. Erector spinae plane block: a cadaver study to determine its mechanism of action. *Rev Esp Anaesthesiol Reanim(English Edition)* 2018;65:514–9.
- Elkoundi A, Benthalha A, Kettani SE-CE, et al. Erector spinae plane block for pediatric hip surgery - A case report-. *Korean J Anesthesiol* 2019;72:68–71.
- Aksu C, Gurkan Y. Defining the indications and levels of erector spinae plane block in pediatric patients: a retrospective study of our current experience. *Cureus* 2019.
- Balaban O, Koçulu R, Aydın T. Ultrasound-Guided lumbar erector spinae plane block for postoperative analgesia in femur fracture: a pediatric case report. *Cureus* 2019.
- Gaio-Lima C, Costa CC, Moreira JB, et al. Continuous erector spinae plane block for analgesia in pediatric thoracic surgery: a case report. *Rev Esp Anaesthesiol Reanim* 2018;65:287–90.
- Aksu C, Gürkan Y. Do we still need central blocks while we have erector spinae plane block? case of 2.5 month old infant. *Brazilian Journal of Anesthesiology* 2019;69:417–9.
- Altıparmak B, Korkmaz Toker M, Uysal Ali İhsan, et al. Erector spinae plane block for pain management of esophageal atresia in a preterm neonate. *J Clin Anesth* 2019;56:115–6.
- Karaca O, Pinar HU. Efficacy of ultrasound-guided bilateral erector spinae plane block in pediatric laparoscopic cholecystectomy: case series. *Agri* 2019;31:209–213.
- Mostafa SF, Abdelghany MS, Abdelraheem TM, et al. Ultrasound-guided erector spinae plane block for postoperative analgesia in pediatric patients undergoing splenectomy: a prospective randomized controlled trial. *Pediatr Anaesth* 2019;29:1201–7.
- Tulgar S, Ahiskalioglu A, De Cassai A, et al. Efficacy of bilateral erector spinae plane block in the management of pain: current insights. *JPR* 2019;12:2597–613.
- Ponde V. Recent trends in paediatric regional anaesthesia. *Indian J Anaesth* 2019;63:746.
- Holland EL, Bosenberg AT. Early experience with erector spinae plane blocks in children. *Paediatr Anaesth* 2019. doi:10.1111/pan.13804. [Epub ahead of print: 28 Dec 2019].
- Schwartzmann A, Peng P, Maciel MA, et al. Mechanism of the erector spinae plane block: insights from a magnetic resonance imaging study. *Can J Anesth/Can Anesth* 2018;65:1165–6.
- Hamilton DL, Manickam BP. Is the erector spinae plane (ESP) block a sheath block? *Anaesthesia* 2017;72:915–6.
- Basu S. Spinal injuries in children. *Front Neurol* 2012;3.
- Willard FH, Vleeming A, Schuenke MD, et al. The thoracolumbar fascia: anatomy, function and clinical considerations: the thoracolumbar fascia. *J Anat* 2012;221:507–36.
- Aksu C, Gürkan Y. Aksu approach for lumbar erector spinae plane block for pediatric surgeries. *J Clin Anesth* 2019;54:74–5.
- Chin KJ, Adhikary S, Sarwani N, et al. The analgesic efficacy of pre-operative bilateral erector spinae plane (ESP) blocks in patients having ventral hernia repair. *Anaesthesia* 2017;72:452–60.
- Luftig J, Mantuani D, Herring AA, et al. Successful emergency pain control for posterior rib fractures with ultrasound-guided erector spinae plane block. *Am Journal Emerg Med* 2017.
- Gupta A, Usha U. Spinal anesthesia in children: a review. *J Anaesthesiol Clin Pharmacol* 2014;30:10.



The extent of cranio-caudal spread within the erector spinae fascial plane space using computed tomography scanning in a neonatal cadaver

Sabashnee Govender^{1,2} | Dwayne Mohr² | Albert Neels Van Schoor² |
Adrian Bosenberg³

¹Department of Anatomy, School of Medicine, Sefako Makgatho Health Sciences University, Ga-Rankuwa, South Africa

²Department of Anatomy, Section of Clinical Anatomy, School of Medicine, Faculty of Health Sciences, University of Pretoria, Gauteng, South Africa

³Department Anaesthesiology and Pain Management, University Washington and Seattle Children's Hospital, Seattle, WA, USA

Correspondence

Sabashnee Govender, Department of Anatomy, School of Medicine, Sefako Makgatho Health Sciences University, Ga-Rankuwa, South Africa.
Email: g.sabashnee@yahoo.com

Funding information

National Research Foundation (NRF), Grant/Award Number: NGAP_RDG180420323223

Section Editor: David Polaner

Abstract

Background: The erector spinae plane block (ESP) is a novel approach for blockade of the spinal nerves in infants, children, and adults. Until recently, the gold standard for truncal procedures includes the paravertebral and epidural blocks. However, the exact mechanism by which this blockade is achieved is subject to debate.

Methods: 2.3 mL (1 mL/kg) of iodinated contrast dye was injected bilaterally into the erector spinae fascial plane of a fresh unembalmed preterm neonatal cadaver (weighing 2.3 kg), to replicate the erector spinae plane block and to track the cranio-caudal spread of the contrast dye using computed tomography. The "block" was performed at vertebral level T8 on the right-hand side and at vertebral level T10 on the left-hand side.

Results: Contrast dye was spread over three dermatomal levels from T6 to T9 on the right-hand side, while on the left-hand side, the spread was seen over four dermatomal levels from T9 to T11/12. Contrast dye also spread over the costotransverse ligament, into the paravertebral space and further lateral from the lateral border of the erector spinae muscle into the intercostal space. However, no spread was seen in the epidural space.

Conclusion: The erector spinae plane block is a versatile technique that can be part of the multimodal postoperative analgesic strategy for truncal surgery. In this study, contrast material dye was tracked over four vertebral levels in the paravertebral space (suggesting an approximate volume of 0.5–0.6 mL per dermatome).

KEYWORDS

cranio-caudal, dermatomal spread, erector spinae plane block, neonates, paravertebral spread

1 | INTRODUCTION

Erector spinae plane (ESP) block is a novel approach to blockade of the spinal nerves in infants, children, and adults. Until recently, the gold standard for truncal procedures includes the paravertebral and epidural blocks.^{1,2} The ESP block serves as a "paravertebral by proxy" and is an alternative approach, targeting similar nerves as the

paravertebral and epidural blocks.³ The exact mechanism by which the ESP blockade is achieved is subject to debate.

The mechanism of analgesia is thought to result from blockade of the ventral and dorsal rami of spinal nerves.⁴ The ESP block is performed with deposition of local anesthetic deep to the erector spinae muscle, yet superficial and lateral to the tip of the transverse process. Authors have suggested the ESP block is safer than

epidural blocks as the local anesthetic is administered distant from the neuraxial structures within a fascial plane.⁵⁻⁸

The objective of this report is to determine the degree of cranio-caudal spread of contrast medium while replicating the ESP block in a fresh neonatal cadaver. Contrast material was injected into the erector spinae fascial plane with the aim of tracking the cranio-caudal spread within the fascial plane. The spread was confirmed using computed tomography (CT).

2 | MATERIALS AND METHODS

The study was approved by the PhD and Research Ethics Committee (94/2019), University of Pretoria, Gauteng, South Africa. Permission was also obtained from the Radiology Department, Steve Biko Academic Hospital to utilize their CT scanning equipment. A fresh unembalmed preterm neonatal cadaver (weighing 2.3 kg) subject to cryopreservation was obtained through the National Tissue Bank from the University of Pretoria under the regulations specified in the South African National Health Act 61 of 2003. Iodinated contrast dye was injected into the erector spinae fascial plane space by an experienced anesthesiologist to replicate the ESP block and to determine the cranio-caudal spread of the contrast using computed tomography.

Prior to placing, the ESP block test injections were done on the lower limb to determine the concentration of the contrast material that could be used. This depended on the amount of scatter—a combination of dark and light streaks between objects such as bone—on the Philips CT machine (parameters: 100 Kvp, 75 mAs, 7.2 scan time). Two milliliters of pure concentrated contrast dye was injected into the right leg, while two milliliters of diluted contrast dye was injected into the left leg. Upon scanning, the right side was difficult to interpret as the quality of the image was distorted by scatter artifacts. Therefore, we decided to use 30 mL of 30% urografin (cot 85588036) diluted in 200 mL of 0.9% sodium chloride (cot 9030801) as the contrast medium.

With the cadaver in a prone position, the procedure began by palpating the spinous process of the seventh cervical vertebra. This was further confirmed under ultrasound guidance by using an Edge ultrasound system machine (ref: P15000-11, SN-03P55Z) with a high-frequency (6-13 MHz) linear array transducer (footprint size of 2.5 cm) covered with a protective plastic sheath. Once the seventh cervical vertebra level was confirmed, the spinous process and the corresponding transverse process of vertebrae T8 and T10 were identified by counting inferiorly from the seventh cervical vertebrae. The transducer was placed perpendicular to the transverse process of T8, 1 cm lateral to the spinous process (on the right-hand side), to obtain a short-axis view of the bony landmarks and the surrounding musculoskeletal structures. The transducer was then rotated 90 degrees into a longitudinal parasagittal orientation, to establish a long axis view for the same structures. A 16 mm 21 g needle was then inserted in a cranio-caudal direction toward the lateral tip of the transverse process using the in-plane approach. Once contact was made

What is known about the topic

- The erector spinae plane block (ESP) is an interfascial block, in which local anesthetic travels deep to the erector spinae muscle targeting the ventral and dorsal rami of spinal nerves.

What new information this study adds

- The route of access for an ESP block follows a paravertebral spread into the paravertebral space covering 3-4 vertebral levels, suggesting an approximate volume of 0.5-0.6 mL per dermatome in the neonate.

with the transverse process, 2.3 mL (1 mL/kg) of contrast dye material was injected into the erector spinae fascial plane between the transverse process and the erector spinae muscle. As the contrast dye was injected, the erector spinae muscle was hydro-dissected away from the underlying bony landmarks. The procedure was then repeated on the left-hand side at vertebral level T10. The dye was



FIGURE 1 Lateral view of a three-dimensional volume rendered CT reconstruction of contrast injectate spread in a fresh neonate. Green arrows—represent the cranio-caudal spread within the erector spinae fascial plane space at vertebral level T8. Yellow arrows—represent the cranio-caudal spread within the erector spinae fascial plane space and posterior to the erector spinae muscle at vertebral level T10 [Colour figure can be viewed at wileyonlinelibrary.com]

allowed to spread for 20 minutes prior to turning the cadaver in a supine position for CT scanning. The images were reconstructed to provide a three-dimensional (3D) view of the trunk in an attempt to fully delineate the spread of the contrast dye.

3 | RESULTS

Using the multi-slice CT and 3D volume rendering function on Radiant DICOM viewer, we were able to determine the cranio-caudal spread over multiple vertebral levels. On the right-hand side, spread over three dermatomal levels from T6 to T9 was seen, while on the left-hand side, there was spread over four dermatomal levels from T9 to T11/12. (Figure 1). The contrast dye was observed over the costotransverse ligament and further lateral from the lateral border of the erector spinae muscle into the intercostal space. Contrast dye spread was also seen in the paravertebral space; however, no spread was seen in the epidural space. Additionally, contrast dye was seen anterior to the erector spinae muscle from vertebral levels T6 to T11/12, yet posterior to the muscle from vertebral levels T9 to T11/12 (Figure 1).

4 | DISCUSSION

Since its inception, the indications and clinical use of the ESP block for various surgical strategies have been increasing.⁹ The ESP block is a novel regional technique that could be used as an alternative to neuraxial blocks for truncal surgery.⁹⁻¹¹ The aim of this report was to determine the cranio-caudal spread of contrast material within the fascial plane space and subsequently infer the dermatomal coverage when replicating the procedure in a fresh neonatal cadaver.

The mechanism of spread for the ESP block is attributed to the anterior perforations in the sheath of the erector spinae muscle and the soft tissue gaps.^{12,13} It is hypothesized that the ESP block targets the ventral and dorsal rami of spinal nerves as the local anesthetic penetrates into the paravertebral and epidural spaces.^{14,15} However, this was not entirely the case in this study. Contrast dye was seen over the posterior aspect of the lamina, the posterior aspect of the transverse process, the costotransverse ligament and in the paravertebral space. Anatomically, based on this study and various other supporting studies the ESP block could be a possible alternative to a paravertebral block as the spread of local anesthetic solution is similar.^{6,16,17}

The lack of spread to the epidural space could be a result of *in vivo* factors such as intrathoracic pressure changes, as well as absence of muscle tone and tissue tension that may effect the spread of the contrast material in a cadaver.^{18,19} Volume may also be a factor, and using larger volumes may have led to epidural spread. In this study, 1 mL/kg was used, as the focus was on the spread of contrast rather than procedure simulation.

Various studies using alternative imaging techniques reported results similar to this study. Adhikary and colleagues, as well as

Schwartzmann and co-worker, used magnetic resonance imaging to display diffusion into paravertebral and epidural space, after performing an ESP block.^{20,21} Jadon and others reported cranio-caudal spread to the dorsal rami, ventral rami and lateral cutaneous branches of the intercostal nerves after an ESP block was placed under fluoroscopic guidance.²² Although these studies show more favorable results, including an epidural spread, it is important to note that certain imaging techniques offer a higher spatial resolution than others. Furthermore, the type of contrast material used may also result in discrepancies in the spread between soft tissue gaps.²³ Contrast also has different physicochemical properties than local anesthetic agents.

De Cassai and colleagues demonstrated that the median volume to cover one dermatome is equivalent 3.4 mL when performing the ESP block.²⁴ However, this is only applicable to adults. The volume to dermatome ratio in infants and children is yet to be determined. Several authors hypothesise that the a volume of 0.3-0.5 mL/kg should be enough to provide adequate spread in children.^{9,13,25} In this cadaver, we noted the contrast material spread approximately one dermatome cranially and two to three dermatomes caudally.

ESP block has been used as an alternative to neuraxial blocks for a wide range of procedures.^{5,6,8,17,25-32} Further investigations are needed to be performed in a larger sample size to determine whether 0.3-0.5 mL/kg provides adequate dermatomal spread in infants and children; whether "in-plane" or "out-of-plane" improves spread; or whether needle insertion over the lateral tip of the transverse process affects the cranio-caudal spread as opposed to needle placement deep to the erector spinae muscle between the transverse processes.

5 | CONCLUSION

The ESP block is a versatile technique that can be part of the multimodal postoperative analgesic strategy for truncal surgery. ESP block has become popular because of the ease of placement and potential safety as compared to other neuraxial techniques. In this study, a single neonatal cadaver, contrast dye spread over 3-4 vertebral levels in the paravertebral space (suggesting a volume of 0.5-0.6 mL per dermatome level).

ACKNOWLEDGMENTS

The authors of this article will like to thank everyone who has played a role in carrying out this research.

CONFLICTS OF INTERESTS

The authors report no conflict of interest.

AUTHOR CONTRIBUTIONS

S Govender: involved in the conception and design of the study, acquisition of data, analysis and interpretation of data, drafting the article, revising it critically for important intellectual content, final approval of the version to be submitted; D Mohr: involved in acquisition of data and revising it critically for important intellectual content; AN Van Schoor: involved in the conception and design of

the study, revising it critically for important intellectual content and final approval of the version to be submitted. Prof AT Bosenberg: involved in the concept and design of the study, revising it critically for important intellectual content and final approval of the version to be submitted.


DISCLOSURES

Author Adrian Bosenberg is a section editor of Pediatric Anesthesia.

ORCID

Sabashnee Govender  <https://orcid.org/0000-0001-6738-9071>

Dwayne Mohr  <https://orcid.org/0000-0002-1396-7427>

Albert Neels Van Schoor  <https://orcid.org/0000-0001-9813-0441>

Adrian Bosenberg  <https://orcid.org/0000-0002-1911-2681>

REFERENCES

- Godlewski C. Erector spinae plane block provides complete perioperative analgesia for chronic scapulothoracic pain. *J Anaesthesiol Clin Pharmacol*. 2019;35(3):424.
- Magoon R, Makhija N, Sarkar S. Erector spinae plane block and cardiac surgery: 'A closer look'. *J Clin Anesth*. 2020;60:8.
- Costache I, Pawa A, Abdallah FW. Paravertebral by proxy – time to redefine the paravertebral block. *Anaesthesia*. 2018;73(10):1185-1188.
- Balaban O, Koçulu R, Aydın T. Ultrasound-guided lumbar erector spinae plane block for postoperative analgesia in femur fracture: a pediatric case report. *Cureus*. 2019;11:e5148.
- Aksu C, Şen MC, Akay MA, Baydemir C, Gürkan Y. Erector spinae plane block vs quadratus lumborum block for pediatric lower abdominal surgery: a double blinded, prospective, and randomized trial. *J Clin Anesth*. 2019;57:24-28.
- Aksu C, Gürkan Y. Do we still need central blocks while we have erector spinae plane block? Case of 2.5 month old infant. *Can J Anesth*. 2019;66(5):607-608.
- Onishi E, Toda N, Kameyama Y, Yamauchi M. Comparison of clinical efficacy and anatomical investigation between retrolaminar block and erector spinae plane block. *BioMed Res Int*. 2019;2019:1-8.
- Elkoundi A, Bentalha A, Kettani SE-CE, Mosadik A, Koraichi AE. Erector spinae plane block for pediatric hip surgery -a case report. *Korean J Anaesthesiol*. 2019;72(1):68-71.
- Holland EL, Bosenberg AT. Early experience with erector spinae plane blocks in children. *Pediatr Anesth*. 2020;30(2):96-107.
- El-Emam E-S, El motilb EA. Ultrasound-guided erector spinae versus ilioinguinal/iliohypogastric block for postoperative analgesia in children undergoing inguinal surgeries. *Anesth Essays Res*. 2019;13(2):274.
- Altıparmak B, Korkmaz Toker M, Uysal Aİ, Özcan M, Gümüş DS. Erector spinae plane block for pain management of esophageal atresia in a preterm neonate. *J Clin Anesth*. 2019;56:115-116.
- Hamilton DL, Manickam BP. Is the erector spinae plane (ESP) block a sheath block? *Anaesthesia*. 2017;72(7):915-916.
- Govender S, Mohr D, Bosenberg A, Van Schoor AN. A cadaveric study of the erector spinae plane block in a neonatal sample. *Reg Anesth Pain Med*. 2020;2019:100985.
- Bang S, Chung K, Chung J, Yoo S, Baek S, Lee SM. The erector spinae plane block for effective analgesia after lung lobectomy: three cases report. *Medicine*. 2019;98(29):e16262.
- Hernandez MA, Palazzi L, Lapalma J, Forero M, Chin KJ. Erector spinae plane block for surgery of the posterior thoracic wall in a pediatric patient. *Reg Anesth Pain Med*. 2018;43:217-219.
- Moore R, Kaplan I, Jiao Y, Oster A. The use of continuous erector spinae plane blockade for analgesia following major abdominal surgery in a one-day old neonate. *J Clin Anesth*. 2018;49:17-18.
- Hernandez MA, Palazzi L, Lapalma J, Cravero J. Erector spinae plane block for inguinal hernia repair in preterm infants. *Pediatr Anesth*. 2018;28(3):298-299.
- Ivanusic J, Konishi Y, Barrington MJ. A cadaveric study investigating the mechanism of action of erector spinae blockade. *Reg Anesth Pain Med*. 2018;43(6):567-571.
- Vidal E, Giménez H, Forero M, Fajardo M. Erector spinae plane block: a cadaver study to determine its mechanism of action. *Revi Esp Anestesiol Reanim*. 2018;65(9):514-519.
- Adhikary SD, Liu WM, Fuller E, Cruz-Eng H, Chin KJ. The effect of erector spinae plane block on respiratory and analgesic outcomes in multiple rib fractures: a retrospective cohort study. *Anaesthesia*. 2019;74(5):585-593.
- Schwartzmann A, Peng P, Maciel MA, Forero M. Mechanism of the erector spinae plane block: insights from a magnetic resonance imaging study. *Can J Anesth*. 2018;65(10):1165-1166.
- Jadon A, Swarupa C, Amir M. Fluoroscopic-guided erector spinae plane block: a feasible option. *Indian J Anaesth*. 2018;62(10):806.
- López MB, Cadórniga ÁG, González JML, Suárez ED, Carballo CL, Sobrino FP. Erector spinae block. A narrative review. *Central Eur J Clin Res*. 2018;1(1):28-39.
- De Cassai A, Bonvicini D, Correale C, Sandei L, Tulgar S, Tonetti T. Erector spinae plane block: a systematic qualitative review. *Minerva Anestesiol*. 2019;85(3):308-319.
- Wong J, Navaratnam M, Boltz G, Maeda K, Ramamurthy RJ, Tsui BCH. Bilateral continuous erector spinae plane blocks for sternotomy in a pediatric cardiac patient. *J Clin Anesth*. 2018;47:82-83.
- Mostafa SF, Abdelghany MS, Abdelraheem TM, Abu Elyazed MM. Ultrasound-guided erector spinae plane block for postoperative analgesia in pediatric patients undergoing splenectomy: a prospective randomized controlled trial. *Pediatr Anesth*. 2019;29(12):1201-1207.
- Karaca Ö, Pınar HU. Efficacy of ultrasound-guided bilateral erector spinae plane block in pediatric laparoscopic cholecystectomy: case series. *Agri*. 2019;31(4):209-213.
- Munshay F, Rodriguez S, Diaz E, Tsui B. Continuous erector spinae plane block for an open pyeloplasty in an infant. *J Clin Anesth*. 2018;47:47-49.
- Tulgar S, Ahiskalioglu A, De Cassai A, Gurkan Y. Efficacy of bilateral erector spinae plane block in the management of pain: current insights. *JPR*. 2019;12:2597-2613.
- De la Cuadra-Fontaine JC, Concha M, Vuletin F, Arancibia H. Continuous erector spinae plane block for thoracic surgery in a pediatric patient. *Pediatr Anesth*. 2018;28(1):74-75.
- Ueshima H, Hiroshi O. Spread of local anesthetic solution in the erector spinae plane block. *J Clin Anesth*. 2018;45:23.
- Thomas DT, Tulgar S. Ultrasound-guided erector spinae plane block in a child undergoing laparoscopic cholecystectomy. *Cureus*. 2018;10(2):e2241.

How to cite this article: Govender S, Mohr D, Van Schoor AN, Bosenberg A. The extent of cranio-caudal spread within the erector spinae fascial plane space using computed tomography scanning in a neonatal cadaver. *Pediatr Anesth*. 2020;30:667-670. <https://doi.org/10.1111/pan.13864>



The anatomical features of an ultrasound-guided erector spinae fascial plane block in a cadaveric neonatal sample

Sabashnee Govender^{1,2} | Dwayne Mohr² | Adrian Bosenberg³ |
Albert Neels Van Schoor²

¹Department of Anatomy, School of Medicine, Sefako Makgatho Health Sciences University, Ga-Rankuwa, South Africa

²Department of Anatomy, Section of Clinical Anatomy, School of Medicine, Faculty of Health Sciences, University of Pretoria, Gauteng, South Africa

³Department Anaesthesiology and Pain Management, University Washington and Seattle Children's Hospital, Seattle, Wash, USA

Correspondence

Sabashnee Govender, Department of Anatomy, School of Medicine, Sefako Makgatho Health Sciences University, Ga-Rankuwa, South Africa.
Email: g.sabashnee@yahoo.com

Funding information

The financial assistance of the National Research Foundation (NRF) toward this research is hereby acknowledged. Opinions expressed and conclusions arrived at are those of the authors and are not necessarily attributed to the NRF.

Section Editor: Thomas Engelhardt

Abstract

Background: Since its inception, the erector spinae plane block has been used for a variety of truncal surgeries with success in both adults and children. However, the anatomical features, route of spread, and dermatomal coverage are still not fully understood in a pediatric population.

Objectives: To identify the anatomical features of the erector spinae fascial plane space by replicating an erector spinae plane block in a fresh neonatal cadaveric sample. The primary aim was to determine the spread of the dye within the fascial plane, while the secondary aims were to determine whether the needle direction or entry site affected the spread.

Methods: The block was replicated bilaterally using 0.1 mL/kg of iodinated contrast dye in nine fresh unembalmed preterm neonatal cadavers. The dye was introduced under ultrasound guidance at vertebral level T5 and T8. Additionally, the needle was oriented cranial-caudal vs caudal-cranial to determine if the needle orientation influenced the spread of dye. The block was also replicated midway between the adjacent transverse processes as opposed to the lateral tip of the transverse process to determine the spread.

Results: From the total sample size, 14 "blocks" were successfully replicated, while 4 "blocks" were either incomplete or failed blocks. Contrast dye was found in the paravertebral, intercostal, and epidural spaces, including posteriorly over the neural foramina. Results revealed that the needle direction or entry site did not influence the spread within the fascial plane.

Conclusion: Contrast material was found in the paravertebral, epidural, and intercostal spaces over an average of 5 vertebral levels when using 0.1 mL/kg.

KEY WORDS

anatomical features, dermatomal spread, erector spinae plane block, interfascial block, neonates

1 | INTRODUCTION

The erector spinae plane block is a novel interfascial regional anesthetic technique initially described for management of acute and chronic thoracic pain.¹ Since its inception, the erector spinae plane

block has been used for various truncal surgeries with success in both adults and children.² The therapeutic effect is attributed to the craniocaudal spread of local anesthetic over multiple vertebral levels within the tissue plane deep to the erector spinae muscle. It is also hypothesized that the interfascial spread blocks the ventral

and dorsal rami of the spinal nerves providing visceral and somatic analgesia in the targeted area.³⁻⁶ To our knowledge, this is the only cadaveric study reporting on the spread and dermatomal coverage in a neonatal sample.

1.1 | Aim and objectives

To identify the anatomical features of the erector spinae fascial plane space by replicating an erector spinae plane block in a fresh neonatal cadaveric sample. We hypothesize that the contrast material will spread into the neighboring spaces, accounting for its mechanism of action. The primary aim was to determine the spread of the dye within the fascial plane and determine the number of levels of spread by dissection of the relevant area after injection. The secondary aims were to determine whether cephalad or caudad directed injections made a difference to the spread, or whether needle placement at the transverse process or between the transverse processes affected the spread.

2 | BACKGROUND

The erector spinae plane block is performed deep (anterior) to the erector spinae muscle, which consists of three vertical muscle bands—the spinalis, longissimus, and iliocostalis. These muscles lie posterolateral to the vertebral column between the spinous processes medially and the angle of the ribs laterally. Located between adjacent transverse processes is an intertransverse connective tissue complex, which consists of a series of ligamentous structures and small muscles. It is formed by two ligaments—the superior costotransverse and intertransverse ligaments—together with the levator costarum, rotator costarum, and external and internal intercostal muscles.

Depending on the level at which the block is performed, various musculoskeletal and neurovascular structures can be found overlying the posterior aspect of the erector spinae muscle. Structures from superficial to deep between vertebral levels T2 to T6 include the following: the trapezius, rhomboids, serratus posterior, erector spinae, external and internal intercostal muscles, intercostal neurovascular bundle and the parietal pleura. Structures from superficial to deep from vertebral levels T7 to T12 include the same structures, except for the rhomboid muscles. The rhomboid muscles terminate at T7 that is, the inferior border of the scapula in adults.

The erector spinae fascial plane space is sandwiched (superiorly and inferiorly) between the head and neck of the adjacent ribs. It is bordered anteriorly by the transverse process of the relevant vertebrae and the superior costotransverse ligament, posteriorly by the deep fascia of the erector spinae muscle, medially by the lamina and spinous process of the relevant vertebrae and laterally by the distal part of the costotransverse ligament and the rib (Figure 1).

What is known about the topic?

The Erector Spinae plane block is an interfascial block that is hypothesized to block the ventral and dorsal rami of spinal nerves. However, the anatomical borders and route of spread are still debatable.

What new information this study adds

By using 0.1 mL/kg of injectate, contrast material was found in the paravertebral, intercostal and epidural spaces, as well as posteriorly over the neural foramina. Allowing us to conclude that the erector spinal fascial plane space has multiple connections with the surrounding fascial planes allowing for extensive spread over multiple vertebral levels.



FIGURE 1 Illustration of the erector spinae fascial plane space and the structures that form its borders (posterior view). Key: A, spinal nerve, B, ventral rami, C, dorsal rami, D, transverse process, E, lamina, F, spinous process, G, superior costotransverse process, H, intertransverse ligament, I, erector spinae fascial plane space, green arrows, represent the direction of spread

2.1 | Ultrasound anatomy

For superficial procedures—such as the erector spinae plane block—a high-frequency linear array probe is preferred as it provides better image resolution. Depending on the orientation of the transducer—transverse or parasagittal—over the mid-thoracic area, the on-screen image of the anatomy may vary. If the transducer is positioned transversely (perpendicular to the vertebral column), the anatomical structures will appear as follows: the transverse process of the vertebra can be identified as an obliquely elongated, oval, hyperechoic structure. Following the transverse process medially, the spinous process can be identified as a triangular, hyperechoic structure connected to the transverse process by the hyperechoic arch-shaped lamina. Immediately superior to the transverse process and

lateral to the spinous process, the erector spinae muscle appears as hypoechoic bands in direct contact with the bony structures. Filling the arch-shaped space lateral to the spinous process, covering part of the transverse process, is the spinalis muscle. Lateral to that, superior to the remainder of the transverse process, is the longissimus thoracis muscle. Superior to the longissimus thoracis muscles is another band-like muscular structure, the rhomboid major muscle. Superior to the rhomboid major muscle, extending from the tip of the spinous process laterally over the muscle is another band-like muscular structure, the trapezius muscle (Figure 2). The rhomboid muscle extends from 7th cervical vertebrae to 6th thoracic vertebrae. The rhomboids are not seen below the 6th vertebral level (T6).

If the transducer is positioned parasagittal (parallel to the vertebral column), the anatomical structures will appear as follows: The transverse processes of the adjacent vertebra can be identified as a rhomboid-shaped hyperechoic structure in a vertical line. Immediately inferior to each transverse process, the corresponding rib can be identified as an oval hyperechoic structure. Running from the superior border of the transverse process to the superior border of the adjacent transverse process is the intertransverse ligament, which can be identified as a hyperechoic line. Filling the spaces between the transverse processes of the adjacent vertebrae is a hypoechoic mass that is formed by a collection of structures. Running from the superior border of the transverse process to the inferior border of the adjacent rib in a cranial to caudal direction is the superior costotransverse ligament. This obliquely arranged ligament divides this space into a superior and inferior triangle.

The superior triangle is bordered laterally by the intertransverse ligament, medially by the superior costotransverse ligament, and caudally by the transverse process of the adjacent transverse process. The superior triangular space is occupied by a group of muscles, namely the levator costarum, rotator costarum, and the external and internal intercostal muscles.

The inferior triangle is bordered laterally by the superior costotransverse ligament, cranially by the transverse process and its corresponding rib and medially by the pleura. This triangular space is known as the paravertebral space. Superior to the intertransverse ligaments are three distinct hypoechoic muscular bands—the erector spinae, rhomboid major, and trapezius muscles—which are equal in size and can be traced cranially and caudally. Superficial to these

muscles is a layer of fat, which appears hyperechoic on the ultrasound screen (Figure 3).

3 | MATERIALS AND METHODS

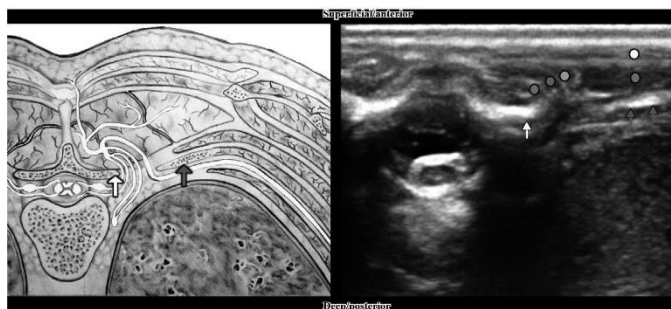
This study was approved by the Research Ethics Committee (94/2019), University of Pretoria, South Africa. Nine fresh unembalmed preterm neonatal cadavers subject to cryopreservation were obtained through the National Tissue Bank from the University of Pretoria and Sefako Makgatho Health Science University. The erector spinae plane block was replicated bilaterally—at vertebral level T5 on the right-hand side and T8 on the left-hand side—in all neonates under ultrasound guidance. An EdgeTM Ultrasound machine (ref: P15000-11, SN-03P55Z) with a 6 - 13MHz linear array probe (footprint size of 2.5cm) covered with a protective plastic sheath was used in all procedures. The methylene blue mixture consisted of 10 mL of iodinated contrast material, diluted in 85 mL of 0.9% sodium chloride.

The spinous process and its corresponding transverse processes were identified while the cadavers were in prone position. The transducer was placed sagittal over the spinous process in the neck region to identify C1. The spinous process and transverse process of T5 and T8 were identified by counting inferiorly from C1.

When replicating the erector spinae plane block, the transducer was placed parallel to the vertebral column over the transverse process of T5 and T8—approximately 1cm lateral to the spinous process. Using the in-plane approach, a 32 mm 21 gauge needle was directed in a cephalad to caudal (or vice versa) toward the superficial lateral tip of the transverse process. Once the tip of the needle contacted the transverse process, 0.05 mL of saline solution was injected to confirm the position of the needle tip. The erector spinae fascial plane was confirmed as the erector spinae muscle bundle was hydro dissected off the underlying bony structures.

Methylene blue dye solution (0.1 mL/kg) was then injected while observing the spread of the dye within the deep fascial plane. In an attempt to determine the extent of the dermatomal spread, we aimed to limit the injectate to 0.1 mL/kg in each instance. The needle was oriented cranial-caudal vs caudal-cranial needle insertion in a few cadavers ($n = 2$) to determine whether this influenced the spread. In addition, the “block” was performed midway between the adjacent

FIGURE 2 A diagram and transverse ultrasound image of neonatal anatomy at T5. Key: green—spinalis muscles, pink—longissimus muscle, blue—iliocostalis muscle, orange—rhomboid muscle, yellow—trapezius muscle, white arrow—transverse process of T5, red arrow(s)—rib



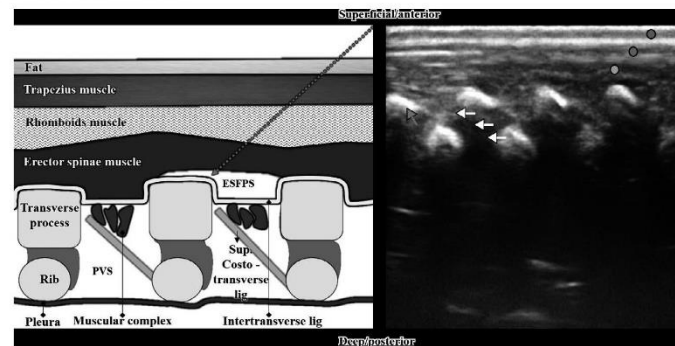


FIGURE 3 A diagram and ultrasound image of a parasagittal scan taken at T5. The hypoechoic muscular complex consists of the levator costarum, rotator costarum, and external intercostal muscles. Key: green arrow on the ultrasound scan—the transverse process of T5, green arrow on the diagram—needle insertion, white arrows—superior costotransverse ligament, orange circle—trapezius muscle, pink circle—rhomboids muscle, blue circle—erector spinae muscle, ESFPS—erector spinae fascial plane space, PVS—paravertebral space

transverse processes as opposed to the lateral tip of the transverse process ($n = 2$) to determine whether this influenced the spread. The dissections were all done 30 minutes after the dye injection.

Dissection proceeded to expose the fascial tissue plane, exposing the extensive craniocaudal spread both superficial and deep to the erector spinae muscle. A vertical skin incision was made along the midline over the spinous processes of C7 to L1, followed by horizontal incisions from the spinous process of T1 toward the acromion of the scapula. Horizontal incisions were also made at vertebral level T10 laterally toward the midaxillary line. The skin was then reflected laterally, to expose the posterior aspect of the scapular, thoracic, and lumbar regions. The surface staining of the methylene blue dye on the muscular structures was noted before further dissection.

The trapezius, rhomboids, and latissimus dorsi muscles were individually identified and reflected laterally to reveal the serratus posterior (which was removed) and the erector spinae muscles.

Again, surface staining of the muscles was noted before further dissection. Each band of the erector spinae (including the multifidus and rotatores) was cut and reflected from its insertion sites to reveal the bony structures deep to them. The lamina, transverse process, as well as the head, neck and tubercle of the corresponding rib, were cleaned to further view the spread of dye. The bony structures were then cut and removed to expose the ventral and dorsal rami of the spinal nerves within the intercostal space to determine whether they were stained by the dye. The craniocaudal and lateral spread across vertebral levels were noted and counted in all procedures. The spread was described in relation from the 1st to 12th thoracic vertebra.

4 | RESULTS

The erector spinae plane block was replicated bilaterally in nine fresh cadavers ($n = 18$ "blocks"), all were dissected after performing the block. From the total sample size, 14 of the "blocks" were successfully

placed. The remaining injections were either incomplete ($n = 1$) or failed blocks ($n = 3$). An incomplete block was defined as a block in which contrast material was only seen at the vertebral level in which the dye was introduced, with no craniocaudal spread. Whereas, a failed block was defined as a block with the complete absence of contrast material infiltration. The failed "blocks" were then excluded from the results. We discovered two cadavers had been frozen prior to performing the block and thus affected the spread (failed "blocks"). Upon dissection, surface staining was noticed on the trapezius, rhomboids, latissimus dorsi, and erector spinae muscles in all cadavers (Figure 4A). Methylene blue dye was found over the posterior aspect of the transverse process, in close proximity to the costotransverse ligament/foramen as well as around the neural foramina in 7 cadavers ($n = 14$). Deeper staining was also found at the level of the dorsal and ventral roots/ganglions of the spinal nerves in the paravertebral gutters in most cadavers ($n = 15$) (Figure 4B,C).

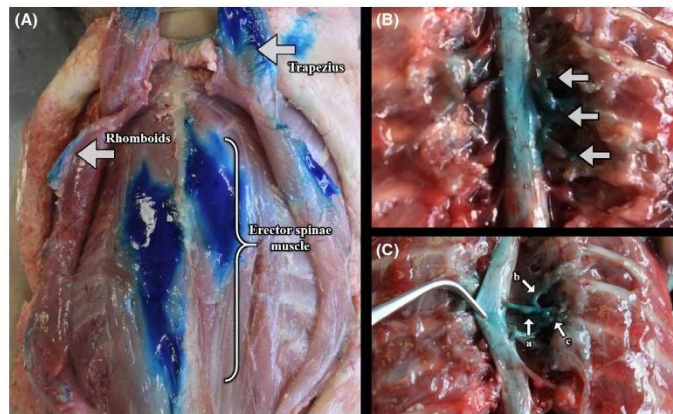
Paravertebral and neural foramina spread was noted in 15 "blocks" as the dye spread to the spinal roots, intercostal spread was seen in 14, whereas, epidural spread was only noted in nine. Table 1 below provides a detailed summary of the "blocks" replicated including the volume used, spread and dermatomal coverage.

The average spread of dye was 5 (range 3-7) vertebral levels in the thorax and the abdomen. While the dose per kilogram per dermatome ranged from 0.02 to 0.1 mL (Table 1). We also determined that inserting the needle cranial to caudal ($n = 2$) vs caudal to cranial ($n = 13$) did not alter the distribution of dye within the fascial space. Similarly, introducing the dye between adjacent transverse process ($n = 2$) as opposed to at the angle of the transverse process ($n = 13$) did not affect the spread.

5 | DISCUSSION

The erector spinae plane block is a novel technique that has been used for a variety of surgical procedures in neonates, children, and

FIGURE 4 A, Image displaying the surface staining of the trapezius, rhomboid, and erector spinae muscles before being reflected for deeper dissecting. B, Image revealing the deeper staining of the spinal nerves as it originates from the spinal cord. C, Image displaying the staining of methylene blue dye around the spinal nerve roots, trunk, and branches. Key a, ganglion, b, dorsal ramus, c, ventral ramus



adults. The mechanism of action is believed to be by anterior spread of local anesthetic through the intertransverse connective tissue into the paravertebral, epidural, and intercostal spaces as seen in this study.^{7,8} The erector spinae muscle sheath and the thoracolumbar fascia facilitate extensive multi-dermatomal spread of the erector spinae plane block.⁹ Since tissue plane blocks are volume dependent, the dermatomal coverage should be related to the volume used.¹⁰

Based on previous studies, authors suggested that 0.1 mL/kg would be sufficient to cover a single dermatome in a younger pediatric group.² Therefore, in this study, we used approximately 0.1 mL/kg to determine the extent of the dermatomal spread. Despite the small volume dose, the average spread of dye was 5 vertebral levels (range 3-7) in the thoracic and abdominal regions. Similar vertebral spread was noted by various authors who used larger volume doses (0.2-0.4 mL/kg), ranging from 3 to 8 segments.^{8,11}

In this study, methylene blue staining was found overlying the trapezius and rhomboid muscles posterior to the erector spinae muscle between vertebral levels T2 to T6. This could be a result of the fusion of the thoracolumbar fascia and the fascia of the trapezius and rhomboid muscles as indicated in a study conducted by Barker and Briggs.⁷ Muscular staining was also noted in the erector spinae muscle between vertebral levels T1 to L2. Additionally, contrast spread was found in the paravertebral space and neural foramen in all cadavers that had a successful placement in the erector spinae fascial plane. Epidural and intercostal spread was seen in the majority of the cadavers ($n = 14$ and 9 respectively); however, the vertebral level spread did not match the intercostal space spread in three cases. These findings support the existing literature, suggesting that the spread is facilitated by the soft tissue gaps, apertures, or perforations found in the erector spinae fascial sheath, allowing for spread to the neighboring tissue planes and spaces.^{7,12}

Adult anatomical studies that included both cadaveric dissection and imaging modalities reported dissimilarities with regards to the spread of injectate.¹³⁻¹⁷ Ivanusic and co-workers reported extensive craniocaudal spread to the dorsal rami of spinal nerves, but limited anterior spread to the ventral rami of spinal nerves.¹³ In contrast to

Ivanusic and co-workers, results from our study revealed spread to the ventral rami of spinal nerves, with spread well into the intercostal spaces. Adhikary et al¹⁴ demonstrated anterior spread into the paravertebral space, medial spread into the neural foramina as well as spread to the epidural space and ipsilateral sympathetic chain. Similar results were described by Yang and colleagues.¹⁵ Although the spread to the sympathetic chain was not assessed in our study, results are in accord with both authors. Vidal and co-workers reported evident spread posterior to the transverse process as well as in the paravertebral and intercostal spaces. However, no spread was assessed in the neural foramina or epidural space.¹⁶ In a magnetic resonance imaging study, Schwartzman and colleagues¹⁷ reported anterior spread into the paravertebral, epidural, and intercostal space as well as the neural foramina as seen in our study.

The spread of the erector spinae plane block has also been determined clinically in pediatric patients.^{2,18-20} Holland and Bosenberg performed the erector spinae plane block on numerous neonatal patients for both thoracic and abdominal procedures. Unilateral thoracotomies and thorascopies, laparoscopic or open gastrostomies, subcostal incisions, and peritoneal dialysis catheter placement, were among some of the documented procedures. The authors commented on the longer duration of action as compared to other truncal blocks. Moreover, they suggested using the erector spinae plane block when alternative neuraxial techniques such as epidurals are contraindicated due to patients being on anticoagulants or when the anesthesiologist has lack of experience.² Munoz and co-workers noticed an extensive multi-dermatomal sensory block of the anterior, posterior and lateral thoracic wall in a patient undergoing oncological thoracic surgery. Injectate was spreading into the paravertebral space as the anesthetic was inserted.¹⁸ Similar spread was also noted by Ueshima and Hiroshi.¹⁹ Thomas and Tuglal reported somatic and visceral analgesia when performing the erector spinae plane block in a child having a laparoscopic cholecystectomy.²⁰ In more recent studies, positive results were reported when performing the erector spinae plane block for the chest wall tumors and distal hypospadias repair. Authors also concluded that the erector spinae plane block

TABLE 1 Summary of the results obtained when replicating the erector spinae plane block in the neonatal cadavers

n	Weight (kg)	Volume (mL)	Injection level	Injectate spread				Dose/kg/dermatome (mL)	Paravertebral space	Epidural space	Intercostal space	Neural foramina
				Vertebral levels	Number of dermatomes	Paravertebral space	Epidural space					
1*	2.95	0.3	T8	T6-T9	4	✓	✓	✓	-	✓	✓	
			T10	T6-T12	7	✓	0.04	✓	-	T9-T11	✓	
2*	2.60	0.3	T5	T4-T8	5	✓	0.06	✓	✓	✓	✓	
			T8	T7-T11	5	✓	0.06	✓	✓	✓	✓	
3	1.7	0.2	T8	T5-T9	5	✓	0.04	✓	✓	✓	✓	
			T10	T11-L2	4	✓	0.05	✓	✓	✓	✓	
4	1.35	0.3	T5	T2-T7	6	✓	0.05	✓	-	T4-T6	✓	
			T8	T6-T11	6	✓	0.05	✓	✓	✓	✓	
5	2	0.3	T5	T2-T5	4	✓	0.08	✓	✓	✓	✓	
			T8*	Incomplete	-	✓	-	✓	-	-	-	
6	0.7	0.1	T5	T2-T6	5	✓	0.02	✓	✓	T4-T6	✓	
			T8	T7-T9	3	✓	0.03	✓	✓	✓	✓	
7	1.2	0.2	T5	T2-T7	6	✓	0.03	✓	✓	✓	✓	
			T8	T6-T10	5	✓	0.04	✓	-	✓	✓	
8	3.4	0.3	T8	T7-T9	3	✓	0.1	✓	-	-	✓	
			T10	Failed spread							“Blocks” were replicated; however, upon dissection, the dye was not found/seen. These cadavers were discovered to have been frozen prior to replicating the block.	
9	1.8	0.2	T5	Failed spread								
			T8	Failed spread								

Note: * Needle was inserted cranial to caudal.

• Needle was insertion midway between adjacent transverse processes.

★ Contrast material was only found at the vertebral level in which the injection was inserted.

can be used as part of a multimodal analgesic treatment for post-operative analgesia management in pediatric patients.²¹

Discrepancies in the spread between populations could be explained by the developmental differences in the anatomy. Authors have suggested that the more elastic pediatric spine, coupled with the less dense ligaments and cartilaginous vertebra, allow for a more favorable spread in infants and children.^{7,22}

Technically the erector spinae plane block is relatively easy and quick to perform with less risk compared to epidural or paravertebral blocks.¹¹ In neonates and infants, a fine needle is needed to ease the passage through the thinner muscle layers, sliding fascial planes and loose connective tissue.²³ Ultrasound guidance is essential to identify these superficial structures. The local anesthetic spread can be tracked, and the volume administered can be minimized while achieving the desired coverage thereby reducing the risk of toxicity.²⁴

6 | LIMITATIONS

A major limitation of this study was the difficulty in obtaining neonatal cadavers due to the sensitive nature of neonatal specimen procurement. The number of cadavers dissected in this study is small making it difficult to draw absolute conclusions. The use of cadavers to replicate spread in a live patient may introduce several confounders. The absence of intrathoracic pressure changes, muscle tone, or tissue tension in live patients may limit or enhance the spread of dye in cadavers.⁷ Moreover, the weight of the neonatal cadavers used in this study was variable, ranging from 0.7 to 3.4 kg, which could have influenced the spread. Partly frozen cadavers had a significant impact on the spread of dye in our "failures." Additionally, the lack of demographic information such as gestational age and preparation state made it difficult to fully evaluate the anatomical factors that may affect the spread of dye. Furthermore, the physicochemical properties of the dye solution used differ from local anesthetics and may impact the spread.²⁵

7 | CONCLUSION

This study aimed to evaluate the spread of local anesthetic when replicating an erector spinae plane block in neonatal cadavers. The spread occurred in the paravertebral, epidural, and intercostal spaces over an average of 5 dermatomal levels. There was little difference between cephalad or caudally directed needle insertion or whether the dye was injected between the transverse processes. Due to the anatomical and physiological differences between adult and pediatric populations, it is inappropriate to extrapolate data from an adult sample to a pediatric population. Therefore, this study is valuable as there is little literature reporting on the anatomy of this block in a neonatal sample. Results from this study mirror the clinical experience as seen in other studies.²

ACKNOWLEDGEMENTS

The authors of this article will like to thank everyone who has played a role in carrying out this research, specifically to Ms Jade Naicker and

Mr Niel van Tonder. The authors gratefully acknowledge the donated cadaver specimens, without which this research would not have been possible.

CONFLICTS OF INTERESTS

Author Adrian Bosenberg is a section editor of *PediatricAnesthesia*.

AUTHOR CONTRIBUTIONS

S Govender involved in the conception and design of the study, acquisition of data, analysis and interpretation of data, drafting the article, revising it critically for important intellectual content, final approval of the version to be submitted; D Mohr involved in acquisition of data, and revising it critically for important intellectual content; AN Van Schoor involved in the conception and design of the study, revising it critically for important intellectual content, and final approval of the version to be submitted. Prof AT Bosenberg involved in the concept and design of the study, revising it critically for important intellectual content, and final approval of the version to be submitted.

ORCID

Sabashnee Govender  <https://orcid.org/0000-0001-6738-9071>

Adrian Bosenberg  <https://orcid.org/0000-0002-1911-2681>

Albert Neels Van Schoor  <https://orcid.org/0000-0001-9813-0441>

REFERENCES

- Forero M, Adhikary SD, Lopez H, Tsui C, Chin KJ. The erector spinae plane block: a novel analgesic technique in thoracic neuropathic pain. *Reg Anesth Pain Med*. 2016;41(5):621-627.
- Holland EL, Bosenberg AT. Early experience with erector spinae plane blocks in children. *Pediatr Anesth*. 2020;30(2):96-107.
- Balaban O, Koçulu R, Aydın T. Ultrasound-guided lumbar erector spinae plane block for postoperative analgesia in femur fracture: a pediatric case report. *Cureus*. 2019;11(7):e5148.
- Aksu C, Gürkan Y. Ultrasound-guided bilateral erector spinae plane block could provide effective postoperative analgesia in laparoscopic cholecystectomy in paediatric patients. *Anaesth Crit Care & Pain Med*. 2019;38(1):87-88.
- Godlewski C. Erector spinae plane block provides complete perioperative analgesia for chronic scapulothoracic pain. *J Anaesthesiol Clin Pharmacol*. 2019;35(3):424.
- Bang S, Chung K, Chung J, Yoo S, Baek S, Lee SM. The erector spinae plane block for effective analgesia after lung lobectomy: three cases report. *Medicine*. 2019;98(29):e16262.
- Govender S, Mohr D, Bosenberg A, Van Schoor AN. A cadaveric study of the erector spinae plane block in a neonatal sample. *Reg Anesth Pain Med*. 2020;45(5):386-388.
- Elkoundi A, Bentalha A, Kettani SE-CE, Mosadik A, Koraichi AE. Erector spinae plane block for pediatric hip surgery - a case report. *Korean J Anesthesiol*. 2019;72(1):68-71.
- Hamilton DL, Manickam BP. Is the erector spinae plane (ESP) block a sheath block? *Anesthesia*. 2017;72(7):915-916.
- Tulgar S, Ahiskalioglu A, De Cassai A, Gurkan Y. Efficacy of bilateral erector spinae plane block in the management of pain: current insights. *JPR*. 2019;12:2597-2613.
- Hernandez MA, Palazzi L, Lapalma J, Forero M, Chin KJ. Erector spinae plane block for surgery of the posterior thoracic wall in a pediatric patient. *Pediatr Anesth*. 2018;28(3):298-299.

12. López MB, Cadórniga ÁG, González JML, Suárez ED, Carballo CL, Sobrino FP. Erector spinae block. A narrative review. *Central Eur J Clinical Res.* 2018;1(1):28-39.
13. Ivanusic J, Konishi Y, Barrington MJ. A cadaveric study investigating the mechanism of action of erector spinae blockade. *Reg Anesth Pain Med.* 2018;43(6):567-571.
14. Adhikary SD, Bernard S, Lopez H, Chin KJ. Erector spinae plane block versus retrolaminar block: a magnetic resonance imaging and anatomical study. *Reg Anesth Pain Med.* 2018;43(7):756-762.
15. Yang H-M, Choi YJ, Kwon H-J, O J, Cho TH, Kim SH. Comparison of injectate spread and nerve involvement between retrolaminar and erector spinae plane blocks in the thoracic region: a cadaveric study. *Anesthesia.* 2018;73(10):1244-1250.
16. Vidal E, Giménez H, Forero M, Fajardo M. Erector spinae plane block: a cadaver study to determine its mechanism of action. *REDAR(English Edition).* 2018;65(9):514-519.
17. Schwartzmann A, Peng P, Maciel MA, Forero M. Mechanism of the erector spinae plane block: insights from a magnetic resonance imaging study. *Can J Anesth.* 2018;65(10):1165-1166.
18. Muñoz F, Cubillos J, Bonilla AJ, Chin KJ. Erector spinae plane block for postoperative analgesia in pediatric oncological thoracic surgery. *Can J Anesth.* 2017;64(8):880-882.
19. Ueshima H, Hiroshi O. Spread of local anesthetic solution in the erector spinae plane block. *J Clin Anesth.* 2018;45:23.
20. Thomas DT, Tulgar S. Ultrasound-guided erector spinae plane block in a child undergoing laparoscopic cholecystectomy. *Cureus.* 2018;10(2):e2241.
21. Aksu C, Gürkan Y. Sacral erector spinae plane block with longitudinal midline approach: could it be the new era for pediatric postoperative analgesia? *J Clin Anesth.* 2020;59:38-39.
22. Gupta A, Usha U. Spinal anesthesia in children: a review. *Ann Card Anesth.* 2020;23(2):221.
23. Aksu C, Gürkan Y. Aksu approach for lumbar erector spinae plane block for pediatric surgeries. *J Clin Anesth.* 2019;54:74-75.
24. De Cassai A, Andreatta G, Bonvicini D, Boscolo A, Munari M, Navalesi P. Injectate spread in ESP block: a review of anatomical investigations. *J J Clin Anesth.* 2020;61:109669.
25. Greenhalgh K, Womack J, Marcangelo S. Injectate spread in erector spinae plane block. *Anesthesia.* 2019;74(1):126-127.

How to cite this article: Govender S, Mohr D, Bosenberg A, Van Schoor AN. The anatomical features of an ultrasound-guided erector spinae fascial plane block in a cadaveric neonatal sample. *Pediatr Anaesth.* 2020;00:1-8. <https://doi.org/10.1111/pan.14009>

Appendix D



UNIVERSITEIT VAN PRETORIA
UNIVERSITY OF PRETORIA
YUNIBESITHI YA PRETORIA

Faculty of Health Sciences

19 February 2019

Prof AN van Schoor
Department of Anatomy
Faculty of Health Sciences

Dear Prof AN van Schoor

STUDENT: GOVENDER S (PhD ANATOMY)

TITLE: The anatomical description of the erector spinae, paravertebral and epidural block for post-operative pain management in paediatric care

The above-mentioned student's protocol has been approved by the PhD committee.

We wish the student all the best with her studies.

Kind regards

A handwritten signature in black ink, appearing to read 'V Steenkamp'.

PROF V STEENKAMP
CHAIR: PhD COMMITTEE

Pharmacology Dept., BMS Building
University of Pretoria, Private Bag X323
Arcadia 0007, South Africa
Tel +27 (0)12 319 2254
Email: vanessa.steenkamp@up.ac.za

Fakulteit Gesondheidswetenskappe
Lefapha la Disaense tša Maphelo

Appendix E



Faculty of Health Sciences

The Research Ethics Committee, Faculty Health Sciences, University of Pretoria complies with ICH-GCP guidelines and has US Federal wide Assurance.

- FWA 00002567, Approved dd 22 May 2002 and Expires 03/20/2022.
- IRB 0000 2235 IORG0001762 Approved dd 22/04/2014 and Expires 03/14/2020.

28 March 2019

Approval Certificate New Application

Ethics Reference No.: 94/2019

Title: The anatomical description of the erector spinae, paravertebral and epidural block for post-operative pain management in paediatric care.

Dear Miss S Govender

The **New Application** as supported by documents received between 2019-02-27 and 2019-03-27 for your research, was approved by the Faculty of Health Sciences Research Ethics Committee on its quorate meeting of 2019-03-27.

Please note the following about your ethics approval:

- Ethics Approval is valid for 1 year and needs to be renewed annually by 2020-03-28.
- Please remember to use your protocol number (94/2019) on any documents or correspondence with the Research Ethics Committee regarding your research.
- Please note that the Research Ethics Committee may ask further questions, seek additional information, require further modification, monitor the conduct of your research, or suspend or withdraw ethics approval.

Ethics approval is subject to the following:

- The ethics approval is conditional on the research being conducted as stipulated by the details of all documents submitted to the Committee. In the event that a further need arises to change who the investigators are, the methods or any other aspect, such changes must be submitted as an Amendment for approval by the Committee.

We wish you the best with your research.

Yours sincerely



Dr R Sommers

MBChB MMed (Int) MPharmMed PhD

Deputy Chairperson of the Faculty of Health Sciences Research Ethics Committee, University of Pretoria

The Faculty of Health Sciences Research Ethics Committee complies with the SA National Act 61 of 2003 as it pertains to health research and the United States Code of Federal Regulations Title 45 and 46. This committee abides by the ethical norms and principles for research, established by the Declaration of Helsinki, the South African Medical Research Council Guidelines as well as the Guidelines for Ethical Research: Principles Structures and Processes, Second Edition 2015 (Department of Health)

Research Ethics Committee
Room 4-60, Level 4, Tswelopele Building
University of Pretoria, Private Bag X323
Arcadia 0007, South Africa
Tel +27 (0)12 356 3084
Email deepeka.behari@up.ac.za
www.up.ac.za

Fakulteit Gesondheidswetenskappe
Lefapha la Disaense tša Maphelo

Appendix F



Faculty of Health Sciences

Institution: The Research Ethics Committee, Faculty Health Sciences, University of Pretoria complies with ICH-GCP guidelines and has US Federal wide Assurance.

- FWA 00002567, Approved dd 22 May 2002 and Expires 03/20/2022.
- IORG #: IORG0001762 OMB No. 0990-0279 Approved for use through February 28, 2022 and Expires: 03/04/2023.

20 July 2020

Approval Certificate Annual Renewal

Ethics Reference No.: 94/2019

Title: The anatomical description of the erector spinae, paravertebral and epidural block for post-operative pain management in paediatric care.

Dear Miss S Govender

The **Annual Renewal** as supported by documents received between 2020-06-30 and 2020-07-15 for your research, was approved by the Faculty of Health Sciences Research Ethics Committee on its quorate meeting of 2020-07-15.

Please note the following about your ethics approval:

- Renewal of ethics approval is valid for 1 year, subsequent annual renewal will become due on 2021-07-20.
- Please remember to use your protocol number (94/2019) on any documents or correspondence with the Research Ethics Committee regarding your research.
- Please note that the Research Ethics Committee may ask further questions, seek additional information, require further modification, monitor the conduct of your research, or suspend or withdraw ethics approval.

Ethics approval is subject to the following:

- The ethics approval is conditional on the research being conducted as stipulated by the details of all documents submitted to the Committee. In the event that a further need arises to change who the investigators are, the methods or any other aspect, such changes must be submitted as an Amendment for approval by the Committee.

We wish you the best with your research.

Yours sincerely

Dr R Sommers

MBChB MMed (Int) MPharmMed PhD

Deputy Chairperson of the Faculty of Health Sciences Research Ethics Committee, University of Pretoria

* The Faculty of Health Sciences Research Ethics Committee complies with the SA National Act 61 of 2003 as it pertains to health research and the United States Code of Federal Regulations Title 45 and 46. This committee abides by the ethical norms and principles for research, established by the Declaration of Helsinki, the South African Medical Research Council Guidelines as well as the Guidelines for Ethical Research: Principles Structures and Processes, Second Edition 2015 (Department of Health)

Research Ethics Committee
Room 4-80, Level 4, Tswelopele Building
University of Pretoria, Private Bag x323
Gezina 0031, South Africa
Tel +27 (0)12 356 3084
Email: deepika.bhani@up.ac.za
www.up.ac.za

Fakulteit Gesondheidswetenskappe
Lefapha la Disaense tsa Maphelo

Appendix G

Date: 18 / 09 /2018

LETTER OF CLEARANCE FROM THE BIOSTATISTICIAN

This letter is to confirm that the student,

with the Name: Sabashnee Govender student number: 11083647

Studying at the University of Pretoria discussed the Project with the title:

“The anatomical description of the erector spinae, paravertebral and epidural block for post-operative pain management in paediatric care” with me.

I hereby confirm that I am aware of the project and also undertake to assist with the Statistical analysis of the data generated from the project.

The analytical tool that will be used will be:

For descriptive statistics, means and SDs if bell-shaped distributions: means, medians and IQRs for skewed or irregular distributions. Proportions will be used to summarise categorical variables. Multiple linear regression models will be developed to predict the outcomes of interest. A sample size of 50 is recommended where possible. This will result in a power of 79% to detect significant model predictors provided the individual univariate coefficient of determination is at least 0.16 (corresponding to a correlation coefficient of 0.4 or greater). It is recommended that predictors with statistically NS coefficients be retained in the model if there is existing evidence of their relevance. If smaller samples are all that is possible (for example 30) the power to detect $R^2 \geq 0.16$ will be lower (55.5% for a sample size of 30) and caution should be exercised when deciding whether to exclude an explanatory variable. It may, in such circumstances, be preferable to leave all plausible predictors in the regression model irrespective of their t-test p-values.

to achieve the objective(s) of the study.

Name: BV Girdler-Brown Date: 18 September 2018

Signature



Tel: 012 356 3287

Department or Unit: SHSPH

Official Stamp of
Biostatistician